FLOOD CONTROL RESERVOIR OPERATIONS FOR CONDITIONS OF LIMITED STORAGE CAPACITY

A Dissertation

by

HECTOR DAVID RIVERA RAMIREZ

Submitted to the Office of Graduate Studies of
Texas A&M University
in partial fulfillment of the requirements for the degree of

DOCTOR OF PHILOSOPHY

December 2004

Major Subject: Civil Engineering

FLOOD CONTROL RESERVOIR OPERATIONS FOR CONDITIONS

OF LIMITED STORAGE CAPACITY

A Dissertation

by

HECTOR DAVID RIVERA RAMIREZ

Submitted to Texas A&M University
in partial fulfillment of the requirements
for the degree of

DOCTOR OF PHILOSOPHY

Approved as to style and content by:

Ralph Wurbs (Chair of Committee)	Anthony Cahill (Member)
Francisco Olivera (Member)	Patricia Haan (Member)
David Rosowsky (Head of Department)	

December 2004

Major Subject: Civil Engineering

ABSTRACT

Flood Control Reservoir Operations for Conditions of Limited Storage Capacity.

(December 2004)

Héctor David Rivera Ramírez, B.S., Universidad de Puerto Rico;

M.S., University of Connecticut

Chair of Advisory Committee: Dr. Ralph Wurbs

The main objective of this research is to devise a risk-based methodology for developing emergency operation schedules (EOS). EOS are decision tools that provide guidance to reservoir operators in charge of making real-time release decisions during major flood events. A computer program named REOS was created to perform the computations to develop risk-based EOS. The computational algorithm in REOS is divided in three major components: (1) synthetic streamflow generation, (2) mass balance computations, and (3) frequency analysis. The methodology computes the required releases to limit storage to the capacity available based on the probabilistic properties of future flows, conditional to current streamflow conditions. The final product is a series of alternative risk-based EOS in which releases, specified as a function of reservoir storage level, current and past inflows, and time of year, are associated with a certain risk of failing to attain the emergency operations objectives. The assumption is that once emergency operations are triggered by a flood event, the risk associated with a particular EOS reflects the probability of exceeding a pre-established critical storage level given that the same EOS is followed throughout the event. This provides reservoir operators with a mechanism for evaluating the tradeoffs and potential consequences of release decisions.

The methodology was applied and tested using the Addicks and Barker Reservoir system in Houston, TX as a case study. Upstream flooding is also a major concern for these reservoirs. Modifications to the current emergency policies that would allow

emergency releases based on the probability of upstream flooding are evaluated. Risk-based EOS were tested through a series of flood control simulations. The simulations were performed using the HEC-ResSim reservoir simulation model. Rainfall data recorded from Tropical Storm Allison was transposed over the Addicks and Barker watersheds to compute hypothetical hydrographs using HEC-HMS. Repeated runs of the HEC-ResSim model were made using different flooding and residual storage scenarios to compare regulation of the floods under alternative operating policies. An alternative application of the risk-based EOS in which their associated risk was used to help quantify the actual probability of upstream flooding in Addicks and Barker was also presented.

To my wife Debbie,
my parents Nery and Tito,
and all those who believed in me

ACKNOWLEDGMENTS

I would like to express my appreciation and gratitude to all those individuals and institutions that supported me during my doctoral studies and helped make this project a reality. The expertise, support, and commitment of Dr. Ralph Wurbs, Chair of my Advisory Committee, were essential in all stages of this project. His professionalism and availability allowed for an excellent graduate school experience, and for that I am deeply grateful. I would also like to thank Dr. Francisco Olivera, Dr. Anthony Cahill, and Dr. Patricia Haan, members of my Advisory Committee, for their willingness to be a part of this project and for their contributions.

Thanks to the efforts of Dr. Robert Lytton, this project was funded for 4 years by the National Science Foundation through a project entitled "NSF Traineeships in Civil Infrastructure for the Colonias" (Grant No. 9454025). I am deeply thankful to Dr. Lytton for giving me the opportunity to be a part of this project. The Civil Engineering Department at Texas A&M University also provided funds to help defray my educational costs. I also owe gratitude to the U.S. Army Corps of Engineers, Galveston District, in particular Karl Brown and Charles Scheffler, and to the Planning Department Manager of the Harris County Flood Control District, Burton L. Johnson. These persons contributed greatly to this project by providing their invaluable expertise, ideas, data, and documentation.

I would also like to give special thanks to other people who supported and encouraged me throughout my doctoral studies. First of all, my wife Déborah M. Santos-Román, who always trusted in me and gave me her unconditional love and full support. My parents Héctor L. Rivera and Nereida Ramírez, who constantly showed me their love and encouraged me to finish strong. The people at Grace Bible Church, who helped me to keep focused on the really important things in life and who constantly prayed for me. And finally, to the members of the International Christian Fellowship, especially Andriy Nemchenko, Sujan Dan, and Kent and Judy Marshall, you guys made my latter years at Texas A&M very special.

TABLE OF CONTENTS

CHAPTER Page

LIST OF FIGURES

FIGURE Page

FIGURE Page

LIST OF TABLES

TABLE Page

CHAPTER I

INTRODUCTION

1.1. BACKGROUND

Throughout history, human societies have exhibited a tendency to occupy the lowlands adjacent to river systems as they provide numerous benefits that are fundamental to human society or that can help to enhance it. These lands, however, are also part of the river's natural floodplain, and thus human settlements in these areas are also susceptible to periodic flooding during storm events. Nonetheless, people have typically accepted the tradeoffs between flooding risks and the potential benefits of occupying such lands. Floodplains are prosperous lands for agriculture and their relatively flat topography makes them highly desirable for construction associated with urban development. In addition, they provide aesthetic open spaces that can be used for many recreational activities. History has demonstrated that despite the potential flooding risks, floodplain occupation will continue as long as those areas represent a source of economic benefits. The Federal Emergency Management Agency (FEMA) estimates that 10 million households in the United States are located in areas of significant flood risk. Consequently, a paramount issue in the field of water resources planning and management is to develop effective strategies to prevent or to reduce flood damages in the occupied floodplains.

In the United States, floodplain management is a joint effort of local communities and FEMA. Stormwater management and drainage is a local responsibility. The United States Army Corps of Engineers (USACE) is the primary federal agency responsible for major flood control reservoirs, levees, and other river control structures.

This dissertation follows the style and format of the *Journal of Water Resources Planning and Management*.

Federal flood control activities took definite form with the establishment of the Mississippi River Commission in 1879. The early flood control projects were mainly structural remedies such as dams and reservoirs, levees and dikes, channel modifications, etc. In 1936, the U.S. Congress created the Flood Control Act, which authorized nearly 300 flood control projects at a cost of $370 million (Arnold 1988). Section 1 of this act declared flood control to be a proper federal activity and that the federal government should improve or participate in the improvement of navigable waters or their tributaries for flood control if the benefits to whomsoever they may accrue are in excess of the estimated costs, and if the lives and social security of people are otherwise adversely affected (USACE 1987). This legislation marked the beginning of the USACE construction and responsibility for federal flood control projects. Most of the reservoir projects were constructed between 1900 and 1970, which has been called the construction era of water resources development. Since the 1970's water resources management policy and practice have shifted to a greater reliance on managing floodplain land use and optimizing the operation of existing facilities (Wurbs 1996).

The method of operation of a reservoir is the most important factor in insuring the realization of the benefits that justified the construction of the project (USACE 1959). The key variables governing the operation of flood control reservoirs are: (1) the available (or residual) storage capacity, and (2) the expected volume of inflow from an incoming flood. Although the residual storage is always known, the uncertainty regarding future inflows makes flood regulation a challenging task, especially for conditions of limited storage capacity. The operation of a flood control reservoir is normally accomplished using specific operating policies, or operating rules, which set forth the guidelines for making release decisions under various hydrologic conditions. These operating rules are also referred to as the reservoir regulation schedule. A reservoir regulation schedule actually consists of two distinct operational schemes that are used interchangeably depending upon whether or not the reservoir storage capacity is expected to be exceeded. The *normal operations* scheme is followed as long as sufficient storage capacity is available to regulate a flood without having to deal with the

risk of exceeding the storage capacity. Alternatively, when inflows are expected to exceed the residual storage capacity the *emergency operations* scheme is implemented. The normal operations schedule is followed as long as the indicated releases are greater than those specified by the emergency operations schedule (EOS).

The primary objective under normal operations is to prevent flood damages downstream from the reservoir. Accordingly, releases are restricted by the maximum allowable non-damaging channel capacity at downstream control points. On the other hand, the top priority under emergency conditions is ensuring that the dam is never overtopped. Therefore, reservoir releases would be made even if that entails exceeding channel capacities at downstream locations so that the reservoir will not be completely filled before the entire flood has passed. The basis for this approach is that moderately high damaging releases beginning before the flood control storage is full are considered preferable to waiting until a full reservoir necessitates much higher releases to avoid overtopping. Although there is good logic behind this preventive approach, emergency releases are still a function of future inflows which is a highly uncertain variable. Therefore, inherent to the EOS is the risk of making insufficient releases that could result in dam overtopping or excessive releases resulting in unnecessary damages downstream.

1.2. MOTIVATION FOR THE STUDY

The water resources research literature contains a myriad of studies where mathematical optimization and simulation models have been developed in order to determine, test, and improve reservoir operating policies (Wurbs et al. 1985; Yeh 1985; Wurbs 1993). However, the majority of those that specifically address flood control operations emphasize normal rather than emergency operations. One of the reasons for the lack of research related to emergency operations may be that, in general, federal flood control reservoirs are able to contain at least the 50-year recurrence interval flood, and in many cases, they have the capacity to contain floods greater than the 100-year flood without making any releases that would contribute to downstream flooding (Wurbs

1996). Therefore, if the entire flood control capacity of a reservoir is available, only an extremely severe flood event would require the implementation of the EOS for most reservoir projects, and thus the bulk of the research has been focused on how to manage the more frequent low-magnitude floods.

In this study, it is recognized that an extreme flood event is not the only scenario in which emergency releases would be required. When a reservoir's flood control pool has been partially filled by previous floods, a future flood (not necessarily of a large magnitude) occurring before the entire flood control capacity has been recuperated may produce an inflow volume large enough to deplete the residual storage and emergency releases would be required to accommodate the excess volume. Although the probability of facing flooding conditions requiring emergency releases is still relatively small, it is critical to be prepared to operate a reservoir efficiently under such conditions when the consequences of committing an operational error could be very serious. For instance, if an operator makes emergency releases during a storm event and later learns that the flood control pool never filled, then the operator would have unnecessarily aggravated downstream flooding conditions. Conversely, if emergency releases are not made and the storage capacity is then exceeded, flood damages could occur both upstream and downstream of the reservoir. Moreover, dam overtopping may result in a catastrophic dam break that would cause extensive damages to the protected regions and may even result in the loss of human life. In recognition of these ever present risks, this study addresses several aspects of emergency operating practices; particularly the development and implementation of the EOS.

The standard methodology that has been used to develop the EOS for most USACE reservoir projects dates to the 1950's. This method is based on a deterministic estimate of the minimum inflow volume that can be expected during the remainder of a flood event which is assumed to have just crested and that it will continue a rapid receding trend. These simplifying assumptions regarding future flows result in conservatively low flood volume estimates. Once the minimum inflow volume is estimated for a given initial inflow rate, the outflow required to limit the storage to the

capacity available is determined by mass balance computations. This conservative approach was adopted in an attempt to minimize the risk of committing an operational error in terms of excessive releases (USACE 1959). Excessive releases are of great concern to reservoir operators due to the strong public opposition to the release of stored water as long as downstream flooding continues. On the other hand, following this conservative approach, irrespective of the flood magnitude and the reservoir's storage level, is also risky. In reality, streamflows are highly uncertain, thus the actual inflow volume may be considerably larger than expected. Although reservoir releases would be increased in an attempt to accommodate the larger flood, the possibility exists that the releases cannot be increased to the required rate quickly enough and the resulting increase in storage may be sufficiently large to cause dam overtopping.

In designing the major flood control reservoirs nationwide, the USACE's emergency operating policies could be conservative in the sense of erring on the side of more storage/higher dam. However, the focus is now on operating existing dams with storage fixed and limited by upstream and downstream urban encroachment. Urban encroachment along the downstream channel limits its ability to convey water, forcing reservoir releases to be reduced accordingly. Reduced releases result in higher storage levels and retention of stored water for periods longer than originally intended. This presents a serious problem for reservoir projects in which much of the land within the flood control pool is not in federal ownership and has been subject to urban development. Minimizing the risks and consequences of storage backwater effects contributing to flooding upstream of the dam is evidently an important tradeoff consideration for such reservoir projects (Wurbs 1996).

The current EOS for most reservoir projects were developed based on the hydrologic conditions of the river basin prior to construction of the projects. These conditions, however, may change significantly over time rendering the EOS obsolete. This creates a need for periodically revising the existing emergency operating policies to make them applicable to current conditions. This is particularly important for reservoirs that have experienced intense urban development in their river basins as this may

drastically alter non-damaging channel capacities, critical storage levels, regulation goals, etc. Furthermore, updating the existing EOS is warranted since most of them were prepared with an outdated method and with limited hydrologic data. The sophisticated computer modeling capabilities and data analysis techniques currently available together with the additional inflow data that have been recorded since the construction of the projects could allow for significant improvements in the EOS development and implementation procedures.

One of the most significant limitations of an EOS developed with the standard method is that they do not provide a mechanism for evaluating and balancing the potential risks associated with release decisions. These schedules only provide a rigid and conservative set of rules that are assumed to be appropriate under all flooding conditions. The same EOS is followed for conditions in which ample storage is available and there is a relatively small risk for overtopping, as for conditions in which the reservoir storage is at critical levels and there is a greater risk for overtopping and/or upstream flooding. The primary purpose of this study is to devise an alternative methodology for developing EOS in which emergency releases would be based on the probability or risk that the expected flows would exceed the reservoir's maximum storage capacity or any other critical storage level. As opposed to the USACE approach, the proposed methodology deals with uncertainties regarding future inflows by considering them as a stochastic process. Stochastic streamflow generation models provide the capability of analyzing statistical probabilities of the expected inflow volumes. This analysis allows formulating a series of alternative risk-based EOS (REOS) in which the reservoir releases, specified as a function of the reservoir storage level, current and past inflows, and time of year, are associated with certain risk of failing to attain the emergency operations objectives. In other words, the REOS provide a set of rules that reflect the risk of flooding upstream as well as downstream of the dams. The USACE and other reservoir management agencies may use the methodology proposed in this study for redesigning/refining/updating their regulation schedules. Reservoir operators may use the risk parameter as a means to evaluate the tradeoffs and

the potential consequences of their release decisions. It is envisioned that the risk-based schedules will provide a wider and more flexible decision framework for reservoir operators in which the risks of committing an operational error may be taken explicitly into account.

1.3. RESEARCH SCOPE

The objectives of this research are as follows:

(1) Devise a methodology for developing risk-based EOS.

(2) Compare the methods and establish the advantages and disadvantages of the standard and the risk-based EOS.

(3) Test and evaluate the performance of both types of EOS in meeting the emergency operations objectives using the Addicks and Barker Reservoir system, located in the Buffalo Bayou watershed in Houston, Texas, as the case study.

(4) Identify, investigate, and assess potential modifications to the current emergency operation policies/practices of the Addicks and Barker Reservoir system in order to reduce the risks of upstream flooding.

(5) Provide a measure of the risk of upstream flooding at Addicks and Barker Reservoirs.

The flood regulation problem that will be investigated in this study is how to determine reservoir releases under emergency conditions that will result in the best use of the available storage. The optimum release rate is that which if held constant during the remainder of a flood will exactly fill the residual flood control storage. Determining this optimum rate is of course nearly impossible as future inflows are highly uncertain. The standard method for developing EOS deals with this uncertainty by taking a conservative approach in which a deterministic estimate of the minimum inflow volume that can be expected is used to determine the required outflow rates. This research is directed toward developing emergency operating rules that establish the required releases based on the probabilistic properties of the expected inflows, rather than on one

deterministic estimate, and assessing how the inclusion of probability considerations can enhance the release decision process.

The probabilistic method developed in this study allows, to a certain extent, quantifying the risks associated with implementing a particular EOS. Having a series of alternative risk-based schedules allows management agencies to select the schedule that is in accordance with a certain level of risk that is considered acceptable. The decision as to what will be considered as acceptable level of risk largely depends on engineering judgment and the particular characteristics of the project.

Once the appropriate schedule has been selected, the actual release decisions are made as a function of certain parameters that provide an indication about the potential inflow volumes. The parameters incorporated in the EOS may be regarded as predictor variables of the expected inflow volume and the scheduled releases are a function of the residual storage capacity and the information associated with these parameters. The only parameter incorporated in the standard EOS is the current inflow rate. Besides this, the risk-based EOS incorporate the antecedent streamflow conditions (i.e. rising or receding inflows) and the time of year as parameters in the schedules. This research assesses how the inclusion of these parameters can provide an improved basis for decision making.

The Addicks and Barker Reservoir system was selected as the case study for this research project. These reservoirs were constructed during the 1940's and are operated as a system by the USACE, Galveston District, to prevent downstream flooding along Buffalo Bayou through the city of Houston. This system provides an excellent case study for various reasons. First, the current EOS for these reservoirs are outdated. Significant changes have occurred since the original emergency schedules in the 1962 reservoir regulation manual were developed. Some of these changes include urban development along the channel below the dams and adjacent to the reservoir Government Owned Lands (GOL), addition of gates to the outlet structures, and restrictions on downstream channel capacities. In addition, several of the supplementary projects in the original flood management plan for Buffalo Bayou were not completed thereby forcing a more restrictive operation of the reservoirs. Due to these changed

conditions, the current operational procedures of the reservoirs are significantly different from those established in the original project design. A reevaluation of the emergency operating policies is thus warranted. Second, these reservoirs now present the operational challenge of having to manage the tradeoffs between flooding risks upstream and downstream from the dams. One of the main features of the risk-based EOS is that they provide a means for considering these risks in the release decision process. This reservoir system provides an opportunity for testing the effectiveness of the proposed approach. The potential for upstream flooding has become a major concern among flood management agencies due to the growing development adjacent to the GOL. The GOL limit is the storage level above which residential and commercial properties are susceptible to flooding, however, the occurrence of upstream flooding does not justify making emergency releases under the current policy. Potential modifications to the current operating policies that would allow making emergency releases based on the probability of upstream flooding are evaluated in this study. Third, although extreme flood events are infrequent, the historical rainfall events that have occurred in the Buffalo Bayou watershed have demonstrated that there is a realistic threat for flooding conditions involving stages that could approach or exceed the GOL limits. This fact supports the preventive efforts conducted in this study for redefining the original regulation schedules to make them applicable to the current flooding hazards. Finally, there is a relatively long record of daily flows currently available for both reservoirs providing a reliable data set for the development of the stochastic streamflow generation models which are essential in the development of the risk-based EOS.

The EOS for the reservoirs were developed using both the standard and the risk-based methods. An existing model of the reservoirs developed for the *HEC-5 Simulation of Flood Control and Conservation Systems* (1998) computer program was updated to a *HEC-ResSim Reservoir System Simulation* (2003) model in order to perform the flood control simulations with the latest modeling capabilities. HEC-ResSim is the USACE Hydrologic Engineering Center (HEC) next generation reservoir simulation program that will eventually replace HEC-5. HEC-ResSim provided the capabilities for applying the

risk-based EOS and for testing and evaluating the proposed operating policies. The emergency schedules were tested through a series of flood control simulations using hypothetical flood events occurring under different initial storage conditions. The occurrence of extremely high pool levels in these reservoirs, however, is typically attributed to the accumulation of water in storage over rainy periods rather than from a single rainfall event. In order to consider this cumulative effect, long-term simulations using historical data were used to establish the initial storage conditions at the reservoirs before the beginning of the hypothetical flood events.

1.4. ORGANIZATION OF THE DISSERTATION

This dissertation is comprised of eight chapters. Chapter II provides a review of the published literature addressing the problem of developing and testing reservoir operating rules for flood regulation. A review of some of the existing stochastic streamflow generation techniques is also presented. Both the standard and risk-based methodologies for developing EOS are fully described and compared in Chapter III. A detailed description of the Addicks and Barker Reservoir system is provided in Chapter IV. Chapter V presents the application of the methodologies described in Chapter III to the Addicks and Barker Reservoir system. The existing EOS for the reservoirs along with three newly developed risk-based EOS are tested and evaluated in Chapter VI. An alternative application of the risk-based EOS in which their risk parameter is used to help quantify the actual probability of upstream flooding in Addicks and Barker Reservoirs is presented in Chapter VII. The research summary and conclusions are presented in Chapter VIII.

CHAPTER II

LITERATURE REVIEW

Most of the water resources research literature addressing the problem of developing and testing reservoir operating rules for flood regulation involves the use of mathematical simulation and optimization models. Wurbs et al. (1985) and Yeh (1985) presented extensive lists of references and in-depth reviews on the use of these models for various reservoir system analyses. Wurbs (1993) inventories several models and compares them from a general overview perspective, with emphasis on practical applications. Labadie (1997) presented a detailed discussion and formulation of reservoir simulation models and optimization techniques including the emerging heuristic programming methods that utilize fuzzy logic, neural networks, and genetic algorithms.

A simulation model is a mathematical representation of a system that is able to predict the behavior of the system under a given set of conditions (Wurbs 1993). Simulation models allow for a detailed and realistic representation of the complex physical and hydrologic characteristics of a river/reservoir system. In general, a river/reservoir simulation model computes storage levels and discharges at pertinent locations for a given set of hydrologic inputs, system demands, and operating rules. Although a pure simulation model contains no algorithm for defining an optimum solution directly, a typical approach is to make numerous runs with alternative operational rules in a trial-and-error search for an optimal or near optimal solution (Wurbs et al. 1985). Simulation models have been routinely applied for many years by water resources development agencies responsible for planning, construction, and operation of reservoir projects (Wurbs 1993). The USACE Hydrologic Engineering Center (HEC) has historically used mathematical simulations as their principal systems analysis technique (Feldman 1992). The *HEC-5 Simulation of Flood Control and Conservation Systems* (USACE 1998) computer program is probably the most versatile model available in the sense being applicable to a wide range of both flood control and

conservation operation problems (Wurbs 1996). HEC-5, however, will be eventually replaced by the next generation *HEC-ResSim Reservoir System Simulation* (USACE 2003) model, which will continue to provide all the capabilities of HEC-5 as well as some additional capabilities.

Optimization is a mathematical formulation in which a formal algorithm computes a set of decision variable values that minimize or maximize an objective function subject to constraints (Wurbs 1996). Most optimization applications to reservoir system analysis involve linear, non-linear, or dynamic programming, or some variation of these techniques. Each technique can be applied using deterministic or stochastic hydrologic inputs. A deterministic model implicitly assumes that future streamflows are known with certainty, and thus it can compute the decision variable optimum values for all periods simultaneously. Implicit stochastic optimization methods, also known as Monte Carlo optimization, optimize over long continuous series of historical or synthetically generated inflow time series, or several shorter equally likely sequences. This allows the stochastic nature of the problem to be implicitly included and deterministic methods can be directly applied. Alternatively, explicit stochastic optimization procedures attempt to operate directly on probabilistic descriptions of random streamflow processes rather than deterministic hydrologic sequences. Optimization is thus performed without perfect knowledge of future events.

The research summaries provided in the following sections will serve to illustrate how the aforementioned techniques have been applied to develop and/or implement flood control operating rules. The general strategy behind the development of operating rules is to establish a functional relationship between the controlled releases and any data on the state of the system available at the time when the release is determined. Section 2.1 includes studies where the system state data consists of a combination of known and forecasted hydrologic quantities, while section 2.2 presents studies where only known quantities are used to determine releases. Methodologies that incorporate probability considerations in the formulation of operating rules are described in section 2.3. Finally, a number of stochastic streamflow generation techniques are presented in section 2.4.

2.1. FLOOD CONTROL OPERATIONS USING KNOWN AND FORECASTED HYDROLOGIC QUANTITIES

Windsor (1973) formulated a methodology employing recursive linear programming (LP) to establish the optimal real-time operation of a network of flood control reservoirs. This study shows how releases may be adjusted to incorporate the latest forecast information and thus ensure maximum flexibility under actual operating conditions. The LP model objective was to minimize during each flood the peak discharge at all locations being protected. The procedure is divided in two steps. First, flood hydrographs are simulated at all pertinent locations based on the latest hydrometeorological data. Second, the hydrographs and current storage levels are input to the LP model to determine the optimum short-term releases for each reservoir. These steps are repeated each time step so that releases are continually modified during the flood in response to the changing conditions. Therefore, regulation of the entire system is accomplished strictly on a foresight basis in a manner similar to what would occur under actual operating conditions. The author recognized, however, that since forecasts are not entirely accurate the resulting releases may not be optimal in actual operations.

Wasimi and Kitanidis (1983) described a methodology for solving the combined problem of real-time forecasting and short-term (daily) operation of a multi-reservoir system during floods. State-space mathematical models were used for short-term forecasting of inflows and to simulate the reservoir system. The optimization problem was solved using a discrete-time linear quadratic Gaussian control model. A set of desirable states (storage level) and some quantitative measures of cost for deviations from the target states were defined. The objective was to use all available real-time information to regulate a reservoir system so that the expected value of flood damage during a short operating horizon is minimized and to do so consistently with the long-term operational strategy. In this approach, releases are given as a function of the current and the expected values of the state variables which are updated at each time step. Thus complete use of available information is made in determining the optimal flood

regulation policy. The method, however, was found to be valid only under moderate flood conditions (normal operations) when capacity constraints are not likely to become binding.

Jain et al. (1998) adopted the simulation approach to derive operating rules for a multipurpose reservoir system in India. Monthly storage targets for conservation purposes were first defined for all reservoirs. These storage targets also define the available flood control capacity. For the major flood control reservoir in the system, an analysis of flood regulation simulations (one-hour time step) was performed using the reservoir's design flood hydrograph (DFH) in order to define an emergency level within the flood control pool and to develop the operating rules. Through several simulations, using different normal and emergency rules and various scenarios of safe channel capacities and initial reservoir storage, the investigators found the emergency level and safe channel capacity that resulted in the best protection of downstream areas from the DFH while keeping the storage below the maximum capacity. Software was developed to determine safe releases from the reservoir during normal flooding conditions considering the uncontrolled runoff expected to reach the damage centers. For emergency conditions, the rules do not specify how much water to release but simply indicate that releases should be made to drawdown the reservoir to a safer level as soon as possible.

Heuristic programming (HP) models have also been used to assist reservoir operations. Popular HP models in reservoir system management include: fuzzy rule-based models (FRB), artificial neural networks (ANN), and genetic algorithms (GA). Fuzzy sets provide a means of translating linguistic rules, typically obtained from experienced operators, into usable numerical form (Labadie 1997). The FRB model operates on an "if-then" principle, where the "if" is a vector of fuzzy premises (storage level, estimated inflows, demands). The "then" is a fuzzy consequence such as the actual volume released from a reservoir. Cheng and Chau (2001) used an FRB model along with a decision support system (DSS) to facilitate real-time flood control operations. For large magnitude floods, the DSS automatically sets the maximum and minimum release based on the flood's frequency. According to flow forecasts and other data, the DSS produces a list of feasible flood operation alternatives and the FRB model

evaluates them in order to make a recommendation to the operator. Shrestha et al. (1996) also used a FRB model to derive operation rules for a multipurpose reservoir in Oklahoma.

One of the primary uses of ANN in reservoir system optimization may be for determining optimal rules from implicit stochastic optimization (Labadie 1997). Hasebe and Nagayama (2002) develop a reservoir operation support system based on fuzzy and neural network systems. The ANN system was composed of three layers, sensory layer, associate layer, and reaction layer. Each layer consists of "neurons" which capture specific data. The combination of network connections of sensory to association layers was decided based on operation rules and experience of skilled operators. Neurons in the input layer capture precipitation, forecasted inflows, reservoir water level, etc. Neurons in the associate layer respond to these hydrological data leading to the selection of the operation policy; reservoir release or store water. Then, the actual quantity (outflow or target storage) is determined using the FRB model based on certain antecedent and/or forecasted conditions.

2.2. FLOOD CONTROL OPERATIONS USING KNOWN HYDROLOGIC QUANTITIES

Although release decisions are typically determined at a reservoir control center, which has access to real-time hydrologic information systems, these systems may fail or have considerable forecasting errors during emergency conditions. Rule curves may be developed to guide real-time operations without the need for forecasts or running computer models during an extreme flood. For example, the emergency operation schedules (EOS) developed with the standard USACE method specify emergency releases as a function of the current reservoir inflows and storage level (USACE 1987). These schedules do not depend on rainfall and runoff forecasts, downstream flooding conditions, or any other data external to the reservoir itself. These types of "blind" decision curves can be used by operators in complete isolation at the dam, a common situation under emergency conditions. Furthermore, in small basins, when response and

forecasting lead times are very short, information collected at the dam site is the most important and reliable (Valdes and Marco 1995).

Beard and Chang (1979) presented a methodology to formulate flood control operating rules taking into account the value of flood warning time and increased damage due to duration of flooding, in addition to the traditional considerations. The procedure assumes that floods (historic or synthetic) following a particular system state are representative of all floods expected to follow that class of system state. The system state was defined based on the initial reservoir storage, current inflow, and rate of change of inflow. For each flood in a given system state a number of discrete outflows are selected for the first time step. Then, an optimum operation for the remainder of the flood is computed with a dynamic programming (DP) model based on knowledge of future inflows. This is repeated for each system state of interest. The optimum initial outflow is selected as that which results in the minimum total damage for all floods starting at a given system state and not necessarily that which causes minimum damage in each individual flood. The final operation rules specify the release to be made during the current time interval solely as a function of system state. The assumption is that the target flow established for each system state will result in minimum expected damages if applied consistently to the first period of all floods following that system state. Thus, the release criterion based on minimum expected damages is not dependent on perfect forecasts. As it will be seen in subsequent chapters, several of the strategies used by Beard and Chang (1979) are parallel to those adopted in this study.

HP models have also been developed to determine reservoir releases using only known data. Chang and Chen (1998) utilized GA's to optimize the parameters in the fuzzy inference rules of a flood control reservoir model. GA's perform optimization by producing populations of solutions whose offspring display increasing levels of fitness (Labadie 1997). The model was implemented in a computerized fuzzy expert system that suggests reservoir releases based on the current storage and inflow. The fuzzy structure included four basic flood control rules each containing one parameter to determine the magnitude of water release. The GA was used to select these parameters

so that the reservoir could best achieve its designated goal. The authors compared two types of GA's and a random search method and found that the GA's were more efficient and robust the random search method.

2.3. PROBABILISTIC METHODS FOR DEVELOPING OPERATING RULES

Probabilistic or risk-based methods aim at incorporating the real-world uncertainties of not knowing future inflows into the operating rules. Willis et al. (1984) developed a method for determining probabilistic release rules using Monte Carlo optimization. A large number of synthetic inflow sequences are generated and an LP model determines the optimal releases for all periods in each sequence. The resulting ensemble of optimal releases is used to develop operating rules by conditioning its probability density function (*pdf*) on observable hydrologic conditions. The conditional *pdf* can be used to determine releases when knowledge about the system is limited to some key hydrologic conditions. This approach allows associating the operating policies with an exceedence probability (E). Releases for a given policy will be at least E percent of the optimal releases under the same key conditions. The method was applied to the Mad River Basin in California to develop monthly release rules. For several test cases, releases determined by the probabilistic rules (E = 75%, 95%) were nearly identical to the optimal releases. This indicates very good performance, since only the current inflow and previous month storage were available to the probabilistic rules, while the optimal release model had perfect knowledge of past and future system states.

Jain et al. (1992) proposed a methodology to determine reservoir operation policies based on explicit risk consideration. The risk of dam overflow was included as a constraint in a stochastic DP formulation that maximizes storage at the end of the flood season while ensuring that the risk of an overflow in each period is within acceptable limits. Two state variables were used in the formulation: storage and an information variable (V). V represents the level of information available (current inflows, forecasts, etc.) which can be used to infer about the probabilistic properties of the expected inflows. The *pdf* for inflows conditioned on V was derived from historical data. The DP

uses this *pdf* to calculate the probability that the expected inflow volume will exceed the residual storage in each period. The developed operation policy specifies, for each period and for different combinations of the state variables, the optimal release according to the allowable risk for that period. The performance of a policy derived for the Dharoi Reservoir in India was evaluated through simulation using historic and synthetic data and was found to be satisfactory. Levin (1969) utilized the same approach to develop operating rules for a water-supply reservoir during floods.

Marien et al. (1994) formulated an implicit stochastic optimization model for building seasonal rule curves for multipurpose multi-reservoir systems. The objective was to determine how much empty storage should be available in a reservoir system to control a future flood. A stochastic streamflow generation model is used to generate a large set (Ω) of equally likely inflow sequences (s). The minimum needed empty storage as a function of time for each sequence (ES_t^s) is determined with a mass balance backwards recursion formula. Computations start with $ES_t^s = 0$ in the last time step and releases are always restricted by the safe channel capacity. Thus, the ES_t^s values form a rule curve which protects downstream areas from flooding if sequence s occurs. To develop rule curves for a specified recurrence interval (RI) of flooding the k most severe sequences are eliminated from Ω, where k is the largest integer smaller than N/RI (N = # of sequences). The envelope rule curve given by the maximum ES_t^s sequence from the remaining set represents that which would protect downstream areas from floods up to the selected RI. The authors recognized, however, that the derived rule curves only correspond to RI when an efficient real-time regulation of the system during flood events is used.

Cruise and Singh (1996) presented an atypical flood regulation approach. A stochastic streamflow model was used to develop a risk methodology for real-time reservoir flood operation. The stochastic model allows for the calculation of flood volumes corresponding to any desired RI. The result of the methodology is not a storage trace serving as a target level, but rather a set of risk evaluation curves that provide

information on making release decisions in an easily accessible form without the necessity of running computer models. The curves give the probabilities of certain flood events occurring within a certain time interval and release decisions may be adjusted based on these probabilities. This information gives some idea of the risk assumed by the operator in choosing whether or not to empty the reservoir rapidly after an event or to pre-release in anticipation of a larger incoming event. For example, if there is a high probability of a flood event whose volume will exceed the remaining storage, then pre-releases can be made to create more storage. Probabilities of sequences of specified events can also be calculated and thus consequences of possible actions can be evaluated by the operator. This aids reservoir operators in making the difficult real-time decisions which they frequently face in practical situations.

2.4. STOCHASTIC STREAMFLOW GENERATION MODELS

Some of the studies described in the previous sections utilized stochastic streamflow generation models as part of their methodologies for developing reservoir regulation policies. These models are an integral component of the methodology developed in this dissertation to formulate risk-based EOS (REOS). The REOS methodology is based on the probability that the expected inflow volume of an incoming flood would exceed the residual storage capacity in a reservoir given an initial streamflow condition and a constant reservoir release rate. Although the probability analysis may be based on the historical streamflow record, it is unlikely that a sufficient number of streamflow sequences will be available for each initial condition of interest. Nonetheless, the historical record provides a sample from the population of possible streamflow sequences and its statistical properties may be considered as an estimate of the true population parameters. The basis of synthetic streamflow generation models is to reproduce streamflow sequences that will be statistically similar to the historical record and thus, they may be considered as equally likely realizations from the same population. Yet, these models only preserve certain statistical parameters of the observed data (mean, standard deviation, autocorrelation), and they do not provide

additional information regarding the statistical characteristics of the streamflow that is not already contained in the historical record. In this context, the generated flows are not a prediction of future flows but only a representation of likely flows in a stream succeeding a given initial condition.

Stochastic models are frequently applied to generate the streamflow sequences required by many reservoir system analysis exercises. Generally, in these models streamflow is regarded as a stochastic process with a random chance component as well as a certain degree of correlation between successive flows. A considerable diversity exists among stochastic hydrology techniques to synthesize daily flows and no universality is given here to any one of them.

2.4.1. Disaggregration Models

One of the earliest methods to generate daily streamflows was developed by Beard (1967). Essentially, the procedure is based on generation of monthly streamflows and subsequent allocation of the monthly total amount to each day. Valencia and Schaake (1973) also presented a technique that combines a model that generates annual events with a disaggregation model for generating seasonal, monthly, or daily events. In Beard (1967), the monthly model consisted of a simple autoregressive lag-1 model AR(1), also known as a first-order Markov chain, with each flow consisting of a random component correlated with the preceding month's flow. The daily streamflow generator consisted of a 2-pass generation by use of a second-order Markov chain applied to standardized variates derived from a logarithmic Pearson Type III distribution. The model was applied to the Kern River in California, and it was found that the model produced reasonable results insofar as high flows are concerned. However, Green (1973) pointed out that this statistical model was not able to reproduce such characteristics as storm hydrograph shape or baseflow recessions.

2.4.2. Interpolation Models

Another approach to the generation of daily flows is to interpolate pentad data to form daily units (Kottegoda 1972; Green 1973). The model presented by Green (1973)

was based on a linear interpolation of the logarithms of 5-day average flows. The 5-day average flows were produced using an existing statistical model (Kottegoda 1970). These flows are then split into daily average flows using a method of linear interpolation. The 5-day model preserves the long-term characteristics of the daily data, while the short-term characteristics such as hydrograph shape are superimposed by the interpolation method. A stochastic error term is superimposed on the interpolated daily flows to model the non-deterministic nature of the daily time series. The model was applied to three rivers in Great Britain and it was found that it was unable to reproduce extreme flows for flashy rivers but it still met most of the requirements needed for a daily flow model. Masking the short-term fluctuations of daily streamflows, however, is considered a significant limitation since this is one of the most important features in daily streamflow (Xu et al. 2003).

2.4.3. Dual Models

Dual models aim at simulating the rising and recession limbs of a hydrograph separately under the premise that they result from different physical processes. Kelman (1980) developed a model in which the watershed is represented as two linear reservoirs. Runoff was considered to be the sum of three components: (1) groundwater storage (reservoir 1), (2) the lumped storages of surface detention storage, bank storage, and channel storage (reservoir 2), and (3) direct runoff. Direct runoff (rising limb) was modeled using a stochastic precipitation model developed by Kelman (1977). The recession limbs were generated based on the exponential recession curve equation and they are the result of emptying the two reservoirs. Visual assessment of 40 years of generated daily flows for the Powell River in Tennessee showed that the generated hydrographs looked like the historic hydrographs in a general hydrologic sense. Tests of statistical equality of samples for the maximum daily discharge and mean daily discharge for each particular month were also favorable.

Aksoy (2003) proposed an algorithm for the stochastic generation of daily intermittent streamflow data. Two two-state Markov chains or alternatively one

three-state Markov chain are first used for determining the state of the stream (i.e. rising, receding, or zero flow). The rising limb was modeled based on a two-parameter gamma distribution which describes its probability distribution. The model splits the recession limb into an upper and a lower part and they are simulated by the typical exponential decay function with two parameters. Both techniques were applied on two intermittent streamflows in Turkey and it was found that the models preserved long-term statistics such as mean, variance, skewness, and correlation, and also short-term features such as the shape of the daily streamflow hydrograph.

2.4.4. Shot Noise Models

Shot noise (SN) models aim at reproducing short term characteristics (rising and recession limbs) of the daily streamflow hydrographs as well as the long term characteristics. SN models were first applied by Weiss (1977). SN models are characterized by a series of instantaneous pulses that occur along the time scale according to a simple Poisson process (Weiss 1977). These pulses are routed through one or more linear reservoirs to create a response. The responses are then aggregated to obtain streamflow sequences. A similar model was developed by Treiber and Plate (1977). This model consisted of a stochastic component of pulses and a deterministic part that transforms pulses into streamflow. The height of the pulses was generated from a AR(1) model with Weibull distribution residual (Kron et al. 1990). The pulses are then transformed into streamflow by convolution with a system function determined from the observed streamflow processes. Other examples of SN models are presented by Cowpertwait and O'Connell (1992) and Murrone et al. (1997).

Merits of these models include that pulses may be regarded as quantities similar to effective daily rainfall and that the stochastic properties of the pulses are much simpler and easily to be simulated than those of streamflows (Kron et al. 1990). These features make the SN models especially suitable for the generation of daily streamflow (Xu et al. 2003). Although SN models are capable of properly generating the rising and recession limbs of the hydrographs, their performance in reproducing low flows has been

found weak (Aksoy 2003). In addition, the recessions decay too fast to zero and too many rises and recessions are generated (Cowpertwait and O'Connell 1992).

2.4.5. Multi-site Models

For many water resources systems planning and operational studies concurrent sequences of flows are necessary at more than one site. The series of studies presented by Xu et al. (2001a, 2001b, 2003) were directed toward developing models that could perform simulation of flows at various locations simultaneously. Initially, Xu et al. (2001a) proposed the Markov autocorrelation pulse (MACP) model to generate streamflows at two sites. Xu et al. (2001b) proposed a chain-dependent Markov correlation pulse (CDMCP) model for the temporal and spatial description of daily streamflow at multiple sites. Finally, Xu et al. (2003) presented a Markov cross-correlation pulse (MCCP) model, which was an extension of the two previous models.

In essence, all of these models consist of four components: (1) simulation of wet/dry spells, (2) generation of pulse height for a wet day at one site, (3) generation of cross-correlated pulses at different sites, and (4) use of a response function to transform the pulses into streamflow sequences. In the MACP model, the pulse occurrence or non-occurrence (wet/dry spell) on a given day is described by a Bernoulli process, the pulse height is determined using a lag-1 Markov model, a cross-correlation model is used to generate pulses at the other site, and the streamflow sequences are obtained using a polynomial equation response function proposed by Treiber and Plate (1977). The occurrence of pulse is simulated in the CDMCP model by means of a two-state (wet/dry) first-order Markov chain. A random "spatial intensity process" determines the spatial occurrence of pulses. A lag-1 Markov model is then used to determine pulse height. The response function is the same as in the MACP model.

The results of the model applications for both the MACP and CDMCP models were satisfactory. However, the main limitation of both models is that the cross-correlation of pulses among different sites was not represented well. The MCCP model (Xu et al. 2003) combined a multi-site autoregressive moving average (ARMA) model,

proposed by Matalas (1967), with the SN models developed by Weiss (1977) and Treiber and Plate (1977). The inclusion of the multi-site ARMA model provided a simpler and efficient framework for the cross-correlation of pulses at different sites which improved the performance of the previous models. Another distinction of the MCCP model is that the response function has periodic parameters representing the 12 calendar months of the year in order to explicitly incorporate the seasonal dependence of streamflows. The statistical analysis of the model results showed that the MCCP model provided a better representation of the observed daily streamflow.

2.4.6. FARIMA Models

Many of the traditional stochastic models for streamflow generation are statistical ones, including the well known autoregressive moving average (ARMA) models and their variants (ARIMA, periodic ARMA, fractional Gaussian noise model, broken line model, etc.). Kottegoda (1980) provides theoretical descriptions of these types of models. These models are typically fitted to the observed series by matching the autocorrelation function (ACF) of the model with the ACF of the observed series. The ACF is a measure of the degree of dependence between observations as a function of their separation (lag) along the time axis (Brockwell and Davis 1996). The ACF of daily streamflows is usually characterized by a slow decay, due to the strong persistence that affects streamflows observed at fine time scales (Montanari et al. 1999). Persistence is the presence in a time series of significant dependence between observations a long time span apart (Hosking 1984). Persistence can also be seen as the tendency for high flows to be followed by high flows, and low flows to be followed by low flows. A process showing strong persistence, it is said to have “long memory”.

The widely used autoregressive integrated moving average models (ARIMA), fully described by Box and Jenkins (1976) and Brockwell and Davis (1987), can reproduce the ACF of a time series exhibiting long memory if a high number of autoregressive parameters is introduced in the model. However, such model would not satisfy the principle of parsimony, which refers to fitting a model using the smallest

possible number of parameters that can adequately represent the process (Box and Jenkins 1976). A noteworthy solution to this problem is the use the fractional ARIMA (FARIMA) models. These models, first introduced by Granger and Joyeux (1980) and Hosking (1981), are an extension of the classic ARIMA models that allows fitting long memory ACF structures parsimoniously.

The FARIMA approach was adopted in this study to generate the daily average streamflow sequences required to develop the REOS. The general form of a FARIMA (p, d, q) model can be expressed in Box and Jenkins (1976) notation as

$$\phi_p(B)(1-B)^d X_t = \theta_q(B) Z_t \tag{2.1}$$

where X_t is the observed (zero mean) time series, B is the backward shift operator which is defined by $BX_t = X_{t-1}$; hence $B^m X_t = X_{t-m}$, $\phi_p(B)$ is the p-order autoregressive polynomial, $\theta_q(B)$ is the q-order moving average polynomial, Z_t is the noise term, which is assumed to be uncorrelated and with zero mean, and d is the differencing order, allowed to take nonintegral values. The values for p, q, and the corresponding parameters in $\phi_p(B)$ and $\theta_q(B)$ allow for the modeling of short-term properties. The parameter d determines the long-term behavior and indicates the degree of persistence in the series, the higher d the higher the persistence. Thus, a FARIMA model may be considered as a mixed model consisting of an ARMA part, which accounts for the short-term properties of an observed series, together with a fractional differencing of an appropriate order to explain any persistent long-term behavior in the series (Hosking 1984). The mathematical foundations of FARIMA models are fully described by Beran (1994) and by Samorodnitsky and Taqqu (1994).

Montanari et al. (1997) provided a framework for the identification and estimation of FARIMA models along with some applications. The authors pointed out that the lack of flexibility in representing the combined effect of short and long memory has been the major limitation of the typical stochastic models used to analyze hydrologic time series. The FARIMA models were presented as an alternative approach capable of

reproducing the autocorrelation structure of natural processes displaying both short and long memory. One of the applications consisted of fitting four ARIMA models and one FARIMA model to the historical mean daily inflows for Lake Maggiore in Italy. The FARIMA model performed consistently better than the ARIMA models based on several statistical tests, proving that the FARIMA approach provides a better representation of the observed data than traditional ARIMA models.

One important condition that has to be met before the FARIMA models can be applied is that the observed data must be stationary. The statistical properties of a stationary time series do not change over time. It is difficult to satisfy this condition when dealing with daily flows, whose statistical properties change with the season or even with the month (Levin 1969; Montanari et al. 1999). Although a FARIMA model may be fitted to the entire historical data assuming that it is stationary (Giraitis and Leipus 1995; Montanari et al. 1997), an alternative approach is to fit a FARIMA model to the data corresponding to each month of the year. In this manner, the data may be considered stationary within each month. In an extension of their previous work, Montanari et al. (1999) adopted this approach and introduced a non-stationary FARIMA model. The final model is a composition of 12 models with periodical parameters. Accordingly, the proposed formulation allows one to vary the model structure and the parameter values with the season, so as to fit separately the autocorrelation structure of each month. The model was applied on the series of daily flows of the Po River in Italy. The similarity of the sample ACF and probability density of the observed and simulated data and other statistical tests demonstrated the capability of the model to reproduce long memory effects and seasonal variations in streamflow. This non-stationary approach was also adopted in this study as it allows for a more detailed representation of the streamflow processes that would result in a more reliable and robust set of REOS.

CHAPTER III

DESCRIPTION OF METHODS FOR DEVELOPING EMERGENCY RESERVOIR OPERATION SCHEDULES

3.1. INTRODUCTION

3.1.1. Overview

Flood control reservoirs are a principal structural remedy in flood management projects. The basis of their operation is to obtain the maximum beneficial use of the available storage during flood events. In general, federal flood control reservoirs are able to contain at least the 50-year recurrence interval flood, and in many cases, they have the capacity to contain floods greater than the 100-year flood without making any releases that would contribute to downstream flooding (Wurbs 1996). Although reservoirs are not designed to provide complete protection against all possible floods, an efficient use of their storage capacity can reduce flood levels and prevent major flood disasters.

The main objective of flood control reservoir operations is to minimize flood damages at downstream locations, while ensuring that the maximum flood control storage capacity of the reservoir is never exceeded. Two distinct operational schemes are used interchangeably to accomplish this objective, depending upon whether or not the reservoir storage capacity is expected to be exceeded. The *normal operations* scheme is followed as long as sufficient storage capacity is available to regulate a flood without having to deal with the risk of exceeding the storage capacity. Alternatively, when the storage capacity is limited and inflows are expected to exceed the residual storage capacity, the *emergency operations* scheme is implemented. The scheme that requires the greatest release, for a given inflow and storage condition, has precedence over the other.

Under normal operations, the primary objective is to minimize flood damages downstream from the reservoir. Therefore, release decisions are contingent upon

downstream flow conditions. As previously stated, the storage capacity of federal flood control reservoirs is sufficient to accommodate the more frequent low-magnitude flood events; hence, normal operations are predominant. However, the possibility of a major flood that would require emergency releases is a major concern in reservoir operations. Extreme flood events, although rare, can result in storages that could exceed the capacity of a reservoir and threaten the integrity of the embankment. Excessive storages can also result from multiple flood events of lesser magnitude occurring over a relatively short period. The accumulated storage limits the capacity of the reservoir to accommodate a subsequent flood. Following the normal operations scheme during a major flood event could result in exceeding the storage capacity of a reservoir, which in turn could result in flooding upstream structures, dam overtopping, and in the worst case, a dam break. Due to this dangerous situation, the primary objective under emergency operations is the protection of the dam. Nevertheless, maximizing the use of the available storage is an important secondary objective, as damaging releases should not be made if not all of the flood space is utilized.

A common practice in reservoir operations is to develop emergency operation schedules (EOS). These schedules are decision tools that provide guidance to reservoir operators in charge of making real-time release decisions during major flood events. Optimum release decisions would result in full use of the available storage while ensuring that the storage capacity is not exceeded. Such a theoretical optimum is only possible with perfect knowledge of future inflows. Although forecasting technology is currently able to reduce considerably the uncertainty about future inflows, still, for many events, especially for heavy rain storms and floods, forecasts remain far from perfect (Krzysztofowicz 2001). Due to this limitation, EOS may result in either insufficient or excessive releases.

The methodology currently used by the U.S. Army Corps of Engineers (USACE) for developing EOS dates back to 1959 (USACE 1959). This methodology, although theoretically sound, is based on a series of simplifying assumptions regarding future flows. The required releases to limit the storage to the capacity available are determined

based on estimating the minimum inflow volume expected during the remainder of a flood. This volume is obtained by assuming that the inflow hydrograph has just crested and computing the volume under the recession limb of the hydrograph. For conservatively low inflow volume estimates, the assumed recession is made somewhat steeper than the average observed recession.

The primary objective of this study is to devise an alternative methodology for developing EOS. As opposed to the USACE approach, the proposed methodology deals with uncertainties regarding future inflows by considering them as a stochastic process. Stochastic streamflow generation models provide the capability of analyzing statistical probabilities of the expected inflow volumes conditional to the current streamflow conditions and time of year. This analysis allows formulating a series of alternative risk-based EOS in which the reservoir releases, specified as a function of reservoir levels, inflows, and time of year, are associated with a certain risk of failing to attain the emergency operations objectives. It is envisioned that this series of schedules will provide a wider and more flexible decision framework for reservoir operators in which risk may be taken explicitly into account.

3.1.2. Flood Control Reservoir Operations

The key variables governing the operation of flood control reservoirs are: (1) the available (or residual) storage capacity, and (2) the expected volume of inflow from an incoming flood. Although the residual storage is always known, the uncertainty regarding the expected inflow volumes makes reservoir regulation a challenging task. The method of operation of a reservoir is the most important factor in insuring the realization of the benefits that justified construction of the project (USACE 1959). As stated by Beard (1963), proper reservoir regulation depends as much on the ability to release without damage as it does on the ability to store. An efficient combination of the normal and emergency operation schemes often results in the most appropriate flood regulation (USACE 1987).

3.1.2.1. Normal Operations

The normal operations scheme is based on the concept of reducing damaging stages at downstream control points during a single flood event with the currently available storage capacity (USACE 1987). This approach disregards the possibility of having a substantial portion of the flood control storage filled upon the occurrence of a large subsequent flood. Provided that the expected inflow volume will not exceed the available storage capacity, releases are based on the maximum allowable non-damaging channel capacity at downstream control points. This maximum channel capacity is associated with bankfull stream capacities, stages at which considerable damages occur, environmental considerations, and constraints such as inundation of valuable infrastructure among others (Wurbs 1996). Every effort must be made in actual operations to use the full channel capacity in order to attain maximum flood control benefits (Beard 1963).

During normal non-flooding conditions, the outlet works are set to pass the inflows in order to maintain an empty reservoir. Whenever significant rainfall occurs or it is expected to occur, the outlet works are closed and they remain closed until it is evident that the flood has crested and downstream conditions are below non-damaging levels. The traditional approach of the post-flood evacuation process is to make releases that will empty the reservoir as quickly as possible without contributing to flows at downstream control points exceeding the channel capacity.

For systems of flood control reservoirs protecting a joint downstream location, their combined releases should not exceed the established maximum channel capacity at common control points. Release decisions are based on maintaining equal available flood storage in each reservoir. Thus, releases are made from the reservoir with the greatest percentage of used storage. Other balancing configurations are possible, however, depending on the characteristics of the system.

Another important consideration when making release decisions is the runoff contribution from uncontrolled areas. If control points are located at relatively far distances, allowance must be made for any runoff from the uncontrolled watershed areas

below the dam. This runoff could account for a significant portion of the allowable channel capacity. If rainfall occurs after a release has been made but within the water travel time to a control point, reservoir releases may combine with the uncontrolled runoff and cause downstream flooding. This runoff must be forecasted, a possible forecast error added, and the resulting quantity deducted from the allowable channel capacity in order to determine appropriate reservoir releases (Beard 1963). Accurate rainfall and runoff forecasts are essential for this aspect of reservoir operations.

Following the normal operation scheme typically results in maximizing the use of the available flood storage. However, it may also result in prolonged retention times of the stored volume if releases are controlled by stringent downstream constraints. Furthermore, reservoir releases may be reduced by extraneous circumstances that interfere with normal operations. For instance, delays in releases to allow removal and/or protection of infrastructure downstream, or to facilitate evacuation and rescue operations, will increase retention times. Prolonged retention times can give rise to a phenomenon referred to as the ratcheting effect (Costello 2000). If a reservoir experiences multiple flood events over periods which are not long enough to drain the reservoir to safe levels, the reservoir stage can gradually increase to critical levels due to the cumulative effect of the multiple floods, even though no single large flood event may have occurred. This ratcheting effect gradually limits the capacity of a reservoir to accommodate subsequent flood events. Cruise and Singh (1996) considered this phenomenon in their work and were able to develop release curves that incorporated the probability that a subsequent flood event would be large enough to fill the residual storage capacity in a reservoir given the magnitude of the preceding flood. This information would aid a reservoir operator to decide if it is necessary to make pre-releases from the reservoir in order to accommodate the incoming flood.

In any event, if a major flood occurs while there is a limited amount of flood control storage capacity, operation is switched over to emergency operations, wherein a fixed schedule of releases is followed to assure greater control of the flood event (USACE 1987).

3.1.2.2. Emergency Operations

EOS are decision tools typically in the form of a family of regulation curves that expresses reservoir releases as a function of reservoir state (i.e. reservoir inflows and storage level). These schedules do not depend on rainfall and runoff forecasts, downstream flooding conditions, or any other data external to the reservoir itself. These schedules are considered as guides to be used by reservoir operators during critical floods with variation therefrom to be based on additional hydrologic information, if advisable.

Although release decisions are typically determined at a reservoir control center, which has access to real-time hydrologic information systems, these systems may fail or have considerable forecasting errors during emergency conditions. Moreover, communications between the reservoir operator and the control center may be interrupted during emergency conditions. Thus, emergency schedules are convenient as they can be used in complete isolation at the dam site. Furthermore, in small basins, when response and forecasting lead times are very short, information collected at the dam site is the most important and reliable (Valdes and Marco 1995).

The top priority under emergency operations is ensuring that the embankment is never overtopped. As opposed to normal operations, release decisions are based on the current reservoir state, not on downstream conditions. Therefore, flood stages may be exceeded at some locations so that the reservoir will not be completely filled before the entire flood has passed. The basis for this approach is that moderately high damaging releases beginning before the flood control storage is full are considered preferable to waiting until a full reservoir necessitates much higher releases to avoid overtopping. It is highly important that the necessary releases are made as soon as possible because even a minor delay in releases can result in a major increase in storage requirement (Beard 1963). However, reservoir releases must be increased gradually in order to prevent undue damage downstream. Abrupt gate openings causing a flood wave with rapid changes in river stage are dangerous from the perspective of downstream hazards to public safety (Wurbs 1996).

The consequences of exceeding the storage capacity of a reservoir are typically far worse than making pre-releases early in a flood event to provide the additional storage required to accommodate the remainder of the flood. Pre-releases are critical when operating reservoirs with a limited amount of flood control storage capacity. If the storage capacity is exceeded, flood damages will occur both upstream and downstream of the reservoir. The excessive water elevation in the reservoir will cause upstream flooding, and uncontrolled releases through emergency spillways will aggravate downstream flooding. Furthermore, the reservoir operator needs to consider that the dam itself represents an additional risk, although small, to dam break by overtopping. A dam break would cause damages to the protected region that would greatly exceed those produced by the flood alone under natural conditions. If a dam is located upstream from urbanized regions, it is very likely that a dam break would even involve the loss of human life.

An important conflict of objectives emerges during emergency operations. Although the primary objective is the protection of the dam, maximizing the use of the flood control storage is also desired. This secondary objective aims for the maximum possible protection of downstream regions, which is typically the primary reason that justified construction of the project. Ideally, the required emergency release rate for a given reservoir state is that which, if held constant during the remainder of the flood, will exactly fill the residual flood control storage, thereby fully satisfying both objectives. In actual operations, however, future inflows are unknown, and therefore, this uncertainty poses a serious conflict to the reservoir operator. If emergency releases are not made assuming that the storage capacity will not be exceeded and later inflows continue increasing, even larger releases will be needed to avoid overtopping and damages downstream will be greater than if moderate releases were made earlier. On the other hand, if emergency releases are made but the actual inflow volume was smaller than expected, the excessive releases will result in a portion of the flood control storage not being used during the flood. This situation could bring several complaints or even lawsuits from downstream dwellers since damaging releases were made even though the

reservoir never reached its full capacity. Nonetheless, the risk of such situation during emergency conditions needs to be accepted to some extent considering the adverse consequences of dam overtopping.

3.2. DEVELOPMENT OF EMERGENCY OPERATION SCHEDULES – USACE STANDARD METHOD

3.2.1. General Framework

The standard methodology currently used by the USACE for developing EOS is based on a prediction of the minimum inflow volume that can be expected during the remainder of a single flood event (USACE 1959). This volume is estimated under the premise that the inflow hydrograph has just crested and then computing the volume under the recession limb of the hydrograph. The hydrograph recession is computed based on a conservatively rapid recession rate. Once a minimum inflow volume is determined for a given initial inflow and constant outflow rate, this volume is subtracted from the maximum storage capacity of the reservoir to obtain the initial storage level at the beginning of the recession. The initial reservoir stage is then determined based on the reservoir's storage-elevation relationship. The complete family of regulation curves forming the emergency operations schedule can be obtained by repeating this procedure for various assumed inflow and constant outflow rates. The regulation curves specify the required outflow rate that will limit the storage to the capacity available as a function of the current reservoir state. The following section presents a description of this methodology based on the USACE manuals on reservoir regulation (USACE 1959; USACE 1987).

3.2.2. Description of the Standard Methodology

The first step in the procedure is to perform a recession analysis to obtain the recession constant that will be used to derive the recession limb of the inflow hydrographs. The recession limb is a representation of how streamflow diminishes after

a rainfall event. The most common mathematical function to describe this process is the simple exponential decay function:

$$Q_t = Q_0 \, k^{\,t} \tag{3.1}$$

where Q_0 = initial discharge at any time; Q_t = discharge t time units after Q_0; and k = recession constant.

A large k value indicates that drainage is very slow, while a smaller k indicates rapid drainage and little storage. Several graphical and analytical techniques are available to calculate an average k value (Rivera-Ramírez et al. 2002). Recessions that follow Equation (3.1) would form three straight lines on a semi-logarithmic plot (discharge at the log y-axis). The slope of each line represents the recession constant from three different streamflow components, overland flow, interflow, and baseflow. The recession constant of interest for this particular application is the one associated with overland flow, which represents the initial segment of the recession limb. The recession characteristics of this segment may vary considerably depending on the magnitude of the flood. Thus, for conservative results, the assumed recession constant should be determined from a large flood caused by a short period of intense rain. The spillway-design flood is typically used for this calculation (USACE 1987).

If a recession is assumed to follow Equation (3.1), then integrating this function with respect to time, between limits $T = t$ and $T = \infty$, gives storage (S):

$$S = - Q_0 \, k^{\,t} / ln\,(k) = - Q_t / ln\,(k) \tag{3.2}$$

Rearranging Equation (3.2) gives:

$$S / Q_t = -1 / ln\,(k) \tag{3.3}$$

Since k is a constant, it can be seen from Equation (3.3) that storage and flow are proportional and that the ratio between their rates of change is constant. Defining this constant as T_s, Equation (3.3) can be expressed as:

$$T_s = -1 / ln\,(k) \tag{3.4}$$

where T_s has the dimension of time. Since T_s is a function of k, it can also be regarded as a parameter that describes the recession limb of a hydrograph. T_s is an essential parameter in the actual computation of the emergency operations schedules using this method.

An alternative approach for calculating T_s is based on the following considerations. If t is the time required for the discharge to decrease from Q_1 at time T_1 to Q_2 at time T_2, then, based on Equation (3.1), $k = (Q_2/Q_1)^{1/t}$. Substituting for k in Equation (3.4) gives:

$$T_S = \frac{-t}{\ln(Q_2 / Q_1)} \tag{3.5}$$

and by definition, Equation (3.5) can also be expressed as:

$$T_2 - T_1 = t = -T_S \ln(Q_2 / Q_1) \tag{3.6}$$

From Equation (3.6) it follows that $T_s = T_2 - T_1$ when $\ln(Q_2 / Q_1) = -1$. Note that $\ln(Q_2 / Q_1)$ equals –1 when $(Q_2 / Q_1) = (1/e) \approx (1/2.7)$. Therefore, T_s is equal to the time required in a recession for the discharge to decrease from a discharge Q_1, to Q_2, where Q_2 equals $Q_1/2.7$ (Figure 3.1).

Once the value for T_s is obtained, a relationship to calculate the volume of inflow resulting from a recession starting at an initial inflow Q_1 and decreasing up to a value equal to a constant outflow Q_2, can be derived from mass balance considerations. The change in storage as a flood progresses in time is given by the continuity equation:

$$\frac{dS(t)}{dt} = I(t) - O(t) \tag{3.7}$$

where I is the inflow rate and O is the outflow rate. Integrating this function with respect to time gives cumulative storage. The S_{min} value in Figures 3.1 and 3.2 represent the total inflow volume that would be stored during the remainder of a flood given that the outflow rate remains constant. In other words, S_{min} is the accumulated storage from

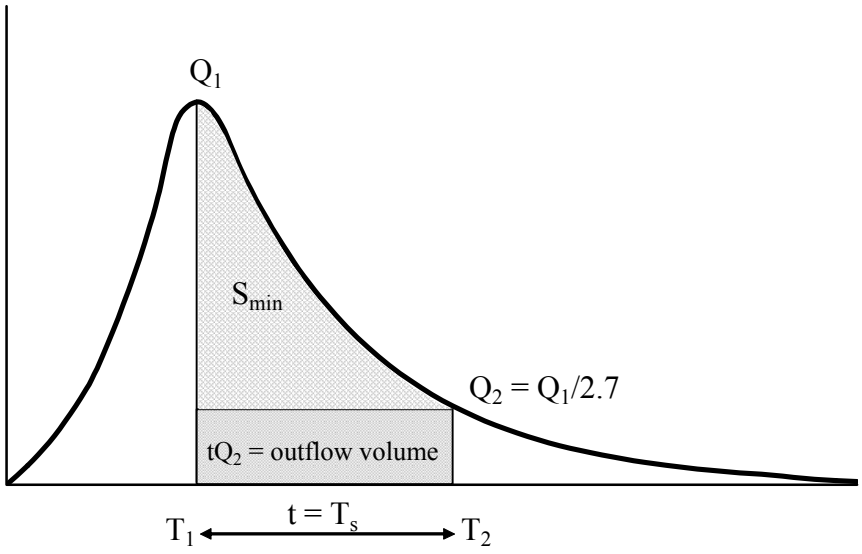

FIGURE 3.1. Schematic Hydrograph

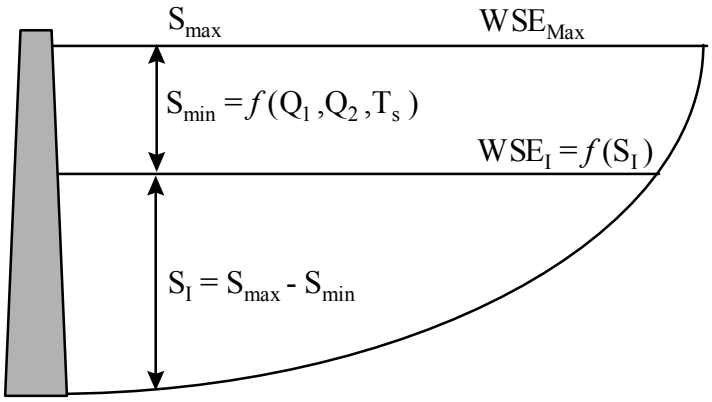

FIGURE 3.2. Schematic Reservoir

T_1 to T_2. S_{min} is related to T_s by the following equation:

$$T_S = \frac{(S_{\min}/2) + Q_2 t}{Q_1 - Q_2} = \frac{S_{\min} + 2Q_2 t}{2(Q_1 - Q_2)} \tag{3.8}$$

By substituting the value of t from Equation (3.6) in Equation (3.8), and solving for S_{min} we obtain:

$$S_{\min} = 2T_S\left[Q_1 - Q_2\left(1 + \ln(Q_1/Q_2)\right)\right] \tag{3.9}$$

The second step in the procedure is solving Equation (3.9) for a series of assumed inflow and outflow rates. Then, the initial storage level (S_I) at the beginning of the recession may be determined by:

$$S_I = S_{max} - S_{min} \tag{3.10}$$

where S_{max} is the maximum storage capacity (Figure 3.2). S_{max} is the storage associated with the maximum water surface elevation (WSE_{max}) permitted in a reservoir. These computations allow linking S_I with a unique combination of initial inflow and the required outflow to limit the storage to the capacity available. In other words, the storage that is available between S_I and S_{max} at the beginning of the recession will be exactly filled by the S_{min} calculated for the given initial inflow and constant outflow rate.

The third step is to use the reservoir's storage-elevation relationship to determine the initial water surface elevation (WSE_I) corresponding to each S_I. The complete regulation schedule is obtained by plotting the WSE_I corresponding to various outflows using inflow as a parameter. Finally, the regulation curves are adjusted according to the reservoir's outflow-elevation relationship if necessary. This relationship expresses the outflow rate limits of the outlet facilities as a function of reservoir stage. Since these computations do not include this relationship explicitly, each point in the curves should be verified to ensure that the indicated outflow rate does not exceed the limit for that particular stage. If at a given point in the curve the outflow rate exceeds this limit, then that outflow rate is reduced to the maximum possible rate for that stage. Sample

computations for a portion of a standard emergency operations schedule are illustrated in the following section.

3.2.3. Sample Computations

The application of the methodology is presented here for a hypothetical reservoir. The minimum and maximum water surface elevations in the reservoir are 0 and 100 ft, respectively. For simplicity, the following linear functions are assumed to describe the reservoir elevation versus storage and outflow relationships:

$$\text{Storage (ac-ft)} = 1{,}000\ \text{(ac)} \times \text{Elevation (ft)} \tag{3.11}$$

$$\text{Outflow limit (cfs)} = 100\ (\text{ft}^2/\text{s}) \times \text{Elevation (ft)} \tag{3.12}$$

The reservoir maximum storage capacity (S_{max}) is 100,000 ac-ft. The adopted value for T_s is 0.63 days. This value was determined by assuming that the hypothetical hydrograph depicted in Figure 3.3 represents the spillway-design flood hydrograph for this reservoir. The value for T_s is read from the hydrograph as the time required for the

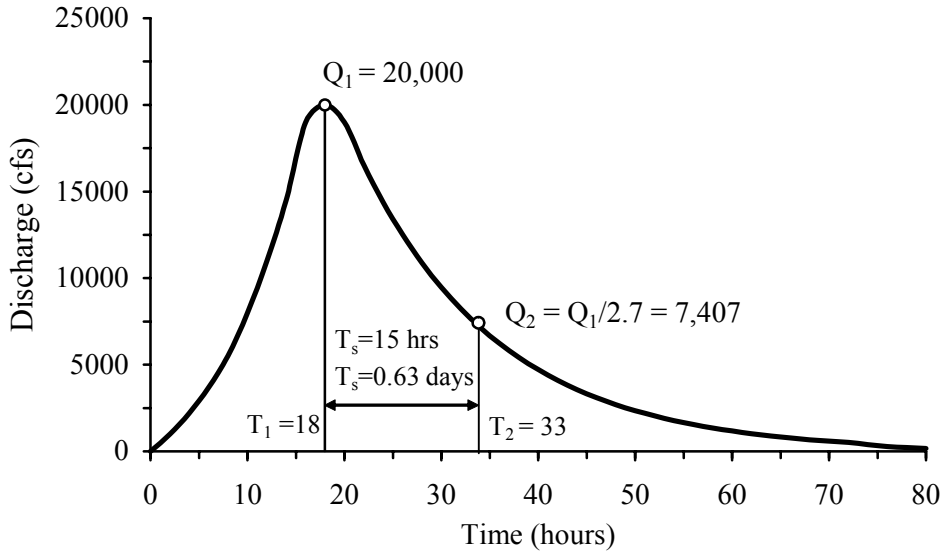

FIGURE 3.3. Hypothetical Hydrograph for Sample Computations

recession to decrease from 20,000 cfs (Q_1) to 7,407 cfs ($Q_2 = Q_1/2.7$). A set of four regulation curves will be developed for this example. The parameter values represent the average inflow to the reservoir during the preceding hour. The computations for the regulation curves corresponding to parameter values of 10,000 and 20,000 cfs are shown in Table 3.1. Column (1) corresponds to the assumed constant outflow rates (Q_2), which range from 0 to 10,000 cfs. These rates should not exceed the inflow rate of the corresponding curve. In other words, reservoir release rates during a flood should not be greater than those produced by the flood alone if the reservoir was not in place. For every value in column (1), the corresponding values for S_{min} (columns 2 and 5) and S_I (columns 3 and 6) are determined using Equations (3.9) and (3.10), respectively. The initial water surface elevation (WSE_1) is determined in columns (4) and (7) based on Equation (3.11). Columns (1) and (4) are then used to plot the regulation curves (Figure 3.4a). Notice that a portion of the 20, 30, and 40 thousand cfs curves exceeds the outflow limits curve. These portions are invalid and should be adjusted accordingly. The adjusted curves are shown in Figure 3.4b.

The shape of the regulation curves show how the required releases increase with the initial reservoir stage. Also, for a given reservoir stage, the required releases increase as the inflow increases. In this example, if the initial reservoir stage is 90 ft, the outflow required for an inflow of 10,000 cfs is approximately 500 cfs, whereas for an inflow of 20,000 cfs this value increases to about 5,000 cfs. This increasing pattern continues until the required releases are restricted by the outflow limits of the reservoir. For instance, for initial inflows of 30,000 and 40,000 cfs, the required releases exceed the outflow limits at 90 ft (Figure 3.4a). For this critical condition the reservoir outlet facilities would have to be completely opened to attain the maximum possible outflow rate at that stage (9,000 cfs). Therefore, the same outflow rate would result for both initial inflow conditions despite their different magnitudes (Figure 3.4b).

Notice that at relatively low reservoir stages, when there is ample storage available, there is no need to make emergency releases for the inflow rates considered in the example. The reservoir stage associated with the zero outflow point in the curves is

TABLE 3.1. Sample Calculations for Developing an Emergency Operation Schedule Using the USACE Standard Method

	Initial Inflow Q_1 in cfs					
	10,000			20,000		
Q_2 (cfs) (1)	S_{min} (ac-ft) (2)	S_I (ac-ft) (3)	WSE_I (ft) (4)	S_{min} (ac-ft) (5)	S_I (ac-ft) (6)	WSE_I (ft) (7)
0	12,600	87,400	87.40	25,200	74,800	74.80
500	10,083	89,917	89.92	22,246	77,754	77.75
1,000	8,439	91,561	91.56	20,165	79,835	79.83
1,500	7,124	92,876	92.88	18,414	81,586	81.59
2,000	6,024	93,976	93.98	16,877	83,123	83.12
2,500	5,083	94,917	94.92	15,500	84,500	84.50
3,000	4,269	95,731	95.73	14,249	85,751	85.75
3,500	3,560	96,440	96.44	13,104	86,896	86.90
4,000	2,942	97,058	97.06	12,048	87,952	87.95
4,500	2,402	97,598	97.60	11,072	88,928	88.93
5,000	1,933	98,067	98.07	10,166	89,834	89.83
5,500	1,527	98,473	98.47	9,323	90,677	90.68
6,000	1,178	98,822	98.82	8,538	91,462	91.46
6,500	882	99,118	99.12	7,805	92,195	92.19
7,000	634	99,366	99.37	7,121	92,879	92.88
7,500	431	99,569	99.57	6,481	93,519	93.52
8,000	271	99,729	99.73	5,884	94,116	94.12
8,500	149	99,851	99.85	5,326	94,674	94.67
9,000	65	99,935	99.93	4,805	95,195	95.20
9,500	16	99,984	99.98	4,319	95,681	95.68
10,000	0	100,000	100.00	3,866	96,134	**96.13**

NOTES: $T_S = 0.63$ days

$S_{max} = 100{,}000$ ac-ft

Col. (2) and (5) = $2T_S[Q_1-Q_2(1+\ln(Q_1/Q_2))]$; except for $Q_2 = 0$, where Col.(2) and (5) = $2T_S$

Col. (3) and (6) = $S_{max} - S_{min}$

Col. (4) and (7) = Col. (3) or (6)/1000; from storage-elevation relationship

Values in bold in Col. (7) indicate an elevation for which Q_2 exceeds the outflow limit as given by the reservoir's outflow-elevation relationship

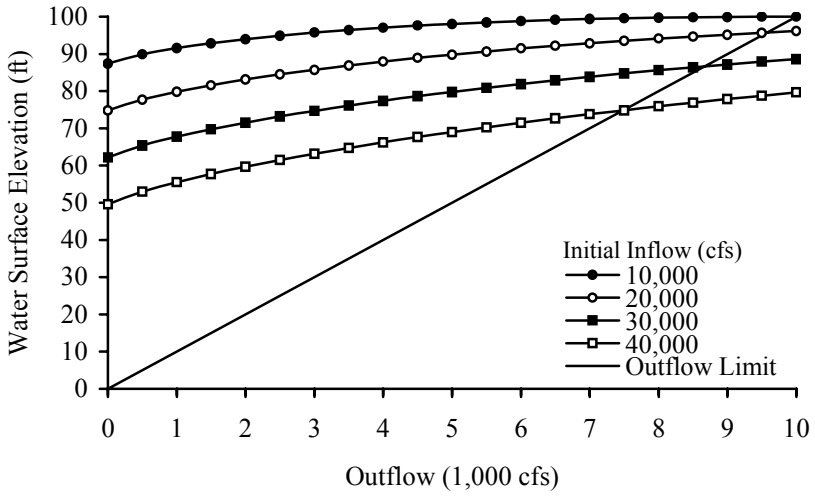

(a)

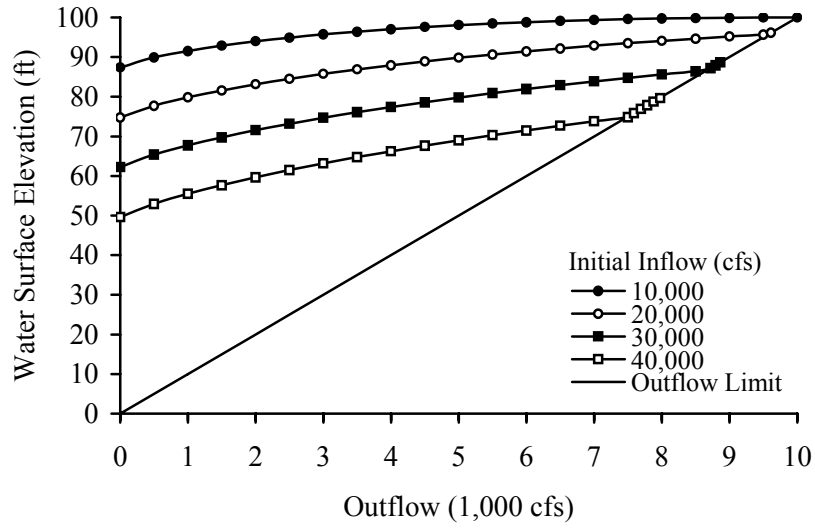

(b)

FIGURE 3.4. Sample Emergency Operations Schedule. (a) Prior to Outflow Limits Adjustment; (b) After Outflow Limits Adjustment

thus of special interest. This stage represents the maximum initial stage (MIS) at which the reservoir outlet facilities can remain closed and yet the reservoir would still be able to accommodate the remainder of the flood. Conversely, if the reservoir stage were greater than the MIS for a particular inflow rate, then this would indicate that the residual storage is insufficient to accommodate the remainder of the flood and emergency releases would be required to provide the necessary additional storage to avoid dam overtopping. Thus, the MIS values may be considered as triggers that indicate the transition from normal to emergency operations.

3.3. DEVELOPMENT OF RISK-BASED EMERGENCY OPERATION SCHEDULES – REOS METHOD

3.3.1. General Framework

The methodology for developing risk-based EOS presented in this study is based on the probability that the expected inflow volume would exceed the residual storage capacity in a reservoir given an initial streamflow condition and a constant reservoir release rate. This exceedance probability, or exceedance frequency, is incorporated as a parameter for developing a series of alternative regulation schedules. The exceedance frequency is interpreted as the risk of dam overtopping associated with a given regulation schedule. The complementary non-exceedance frequency is interpreted as the risk that the regulation schedule will result in excessive releases. For instance, if release decisions are based on the 1% exceedance frequency schedule, there is a 1% risk that the releases will not be able to provide an adequate amount of storage to fully accommodate the incoming flood. Conversely, there is a 99% risk that the schedules will dictate releases that would result in a portion of the flood control storage not being used during the flood and thus, the releases would unnecessarily contribute to downstream damages. This series of alternative schedules provides a management tool that enables reservoir operators to take explicitly into account the risks of failing to accomplish the emergency operations objectives.

A computer program named REOS was coded in FORTRAN to perform the necessary computations to develop Risk-based Emergency Operation Schedules. REOS defines the regulation schedules based on the probabilistic properties of the expected inflows, rather than on one particular inflow sequence. In order to develop adequate schedules using this method, a large number of sufficiently long inflow sequences, which are assumed to represent a wide range of the infinite number of possible outcomes given an initial streamflow condition, needs to be analyzed. Typically, the historical streamflow record does not provide an adequate number of inflow sequences to obtain confident results from a probability analysis. Therefore, REOS relies upon synthetic streamflow generation models to simulate the necessary inflow sequences. These models have the capability to simulate any number of inflow sequences that are equally likely with respect to the historical streamflow record. An ensemble of 10,000 inflow sequences is generated in REOS for every combination of initial inflow rate (Q_0) and streamflow state (*SS*). The streamflow state refers to the antecedent streamflow conditions and it is classified in two categories, rising and receding. This information is valuable to the release decision process because of the strong tendency of streamflows to continue their current trend (Beard 1967; Gan and Beard 1980; Philbrick and Kitanidis 1999). Thus, the streamflow state is also incorporated as a parameter in the schedules.

REOS determines the required storage to precisely accommodate a given inflow sequence using a simple mass balance equation that relates cumulative inflows and outflows to storage changes. The maximum cumulative storage change (SC_{max}) represents the maximum volume to be stored in a reservoir for a given inflow sequence and constant outflow rate (O_c). SC_{max} values are determined for each of the 10,000 daily average inflow sequences using various O_c values. This computation is repeated for various Q_0 of interest and both *SS* categories. The result is an array of equally likely SC_{max} realizations for a given system condition. The system condition is composed by Q_0, O_c, and *SS*. The SC_{max} array is then ranked in order of magnitude and a relative exceedance frequency (*EF*) is assigned to each value. Notice that these are conditional exceedance frequencies, and they only pertain to repetitions of occasions having the

same system condition. Therefore, SC_{max} may be expressed as a function of the system condition and *EF*, where *EF* denotes the percentage of the total observations that resulted in a value equal or greater than the specified SC_{max} value. Alternative regulation schedules may be developed based on the SC_{max} values corresponding to a specific *EF*. The initial reservoir storage is determined by subtracting SC_{max} from the maximum storage capacity of the reservoir. This initial storage is then expressed as the initial water surface elevation (WSE_I). Consequently, each WSE_I value is linked with specific values of the system condition and *EF*. The family of regulation curves forming the emergency operations schedule for a selected *EF* and *SS* are developed by plotting the WSE_I corresponding to a continuous set of O_c values using Q_0 as a parameter.

3.3.2. Synthetic Streamflow Generation Models

Proper evaluation of the statistical properties of future flows requires an adequate number of streamflow sequences representing a wide range of possible outcomes. Although this analysis may be based on the historical streamflow record, it is unlikely that a sufficient number of streamflow sequences will be available for each initial condition of interest. Nonetheless, the historical record provides a sample from the population of possible streamflow sequences and its statistical properties may be considered as an estimate of the true population parameters. The basis of synthetic streamflow generation models is to reproduce streamflow sequences that will be statistically similar to the historical record and thus, they may be considered as equally likely realizations from the same population. Notice, however, that these models only preserve certain statistical parameters of the observed data (mean, standard deviation, autocorrelation), and they do not provide additional information regarding the statistical characteristics of the streamflow that is not already contained in the historical record. In this context, the generated flows are not a prediction of future flows but only a representation of likely flows in a stream succeeding a given initial condition.

Stochastic models are frequently applied to generate the streamflow sequences required by many reservoir system analysis exercises. In these models, streamflow is

considered a stochastic process with a random chance component as well as a certain degree of correlation between successive flows. Several stochastic hydrology techniques are available to synthesize daily flows (see Chapter II). Selection of an appropriate technique or type of model depends upon the streamflow characteristics of the river/reservoir system for which the analysis will be conducted. Although the choice of a particular technique is inconsequential regarding the overall methodology presented in this study, the robustness of the results is dependent upon the ability of the models to generate realistic sequences. Hence, a comprehensive analysis of the performance of various potential techniques is always recommended.

3.3.2.1. Considering Stationarity in Daily Streamflow Generation

Stationarity implies that the statistical properties of a time series do not change over time. Typically, the stationarity condition is not met when dealing with daily flows, whose statistical properties may change with the season or even with the month (Levin 1969; Montanari et al. 1999). Some forms of stochastic models may be fitted to the entire historical record assuming that the data is stationary (Giraitis and Leipus 1995; Montanari et al. 1997). An alternative approach is to divide the year in an arbitrary number of seasons and fit a model to each season (Beard 1967; Montanari et al. 1999; Xu et al. 2001; Aksoy 2003; Xu et al. 2003). Montanari et al. (1999) found that when dealing with daily flows, 12 seasons, each representing a calendar month, are often needed to meet the stationarity condition. This approach allows one to vary the model structure and the parameter values in order to fit separately the autocorrelation structure of the streamflows for each month. The final model is a composition of 12 different models having periodical parameters.

The latter approach was adopted in this study as it allows for a more detailed representation of the streamflow processes and it brings greater flexibility in developing the EOS. For instance, a single annual regulation schedule may be developed based on the expected flows succeeding an initial condition that is evaluated at different times of the year. Consequently, this schedule may be implemented along the year.

Alternatively, monthly regulation schedules may be defined if the initial condition is always evaluated in the same month. In this case, the result is a set of 12 monthly schedules and the appropriate schedule is implemented accordingly.

3.3.2.2. Effects of the Initial Streamflow Conditions

Streamflow generation models require, as a minimum, one assumed value to initialize their recursive computations. These values are typically set to the average of the observed series (Beard 1967; Salas 1993; Gupta 1995; Viessman and Lewis 1996). Since these initial values will introduce a certain degree of bias at the beginning of a simulation, the first portion of a generated sequence is usually discarded. In this study, however, capturing the effects of the initial conditions on the generated sequences is of utmost importance. The goal here is to analyze the statistical probabilities of future flows given a recurrent initial streamflow condition, which is defined by Q_0 and its preceding values.

Due to the strong correlation between succeeding flows, the values preceding Q_0 should not be selected arbitrarily. A backward generation process may be used to estimate these values (for details see Box and Jenkins 1976). This process allows the preceding values to be correlated with Q_0, and thus, both past and future inflows are affected by Q_0. A simple autoregressive lag-1 model AR(1), also known as a first-order Markov process, is well suited for this particular application since in this type of model the value to be predicted is only correlated to the value of the previous time step. The typical AR(1) model has the form

$$X_t = \phi_1 X_{t-1} + Z_t \tag{3.13}$$

where X_t represents a time series, ϕ_1 is the autoregressive coefficient, and Z_t is a white noise process (random term) with zero mean and constant variance σ_Z^2 [WN(0, σ_Z^2)]. Equation 3.13 may also be expressed as

$$(1 - \phi_1 B) X_t = Z_t \tag{3.14}$$

where B is the backward shift operator, which is defined by $BX_t = X_{t-1}$; hence $B^m X_t = X_{t-m}$. The probability structure of a time series is equally explained by the forward model (3.13, 3.14), or by the backward model

$$(1 - \phi_1 F)X_t = W_t \tag{3.15}$$

where F is the forward shift operator, which is defined by $FX_t = X_{t+1}$; hence $F^m X_t = X_{t+m}$, and $W_t \sim$ WN(0, $\sigma_W{}^2 = \sigma_Z{}^2$). This backward model may be used to estimate values that have occurred before the first observation. If a particular streamflow generation model requires *n* preceding values (Q_{-1}, Q_{-2}, …, Q_{-n}) to initiate a simulation, these values may be "back forecasted" recursively using Q_0 as the initial input in the backward model.

3.3.3. REOS Computational Algorithm

A general outline of the REOS computational algorithm is depicted in Figure 3.5. The first step in the procedure is to read the required input data. These data include the reservoir storage-elevation relationship (*RS*), the outlet works rating curves (*RQ*), the streamflow generation models data (*SG*), the maximum water surface elevation (WSE_{max}) and the maximum initial inflow rate (Q_{max}) that will be included in the regulation schedules. REOS reads the *RS* and *RQ* data from an input file that follows the format used for the HEC-5 computer program (USACE 1998). The *SG* data is provided in a separate file that specifies model coefficients and all other pertinent statistical data corresponding to each month. The values for WSE_{max} and Q_{max} are selected by the user in the main screen of the program. WSE_{max} is used to determine the reservoir maximum storage capacity based on the provided *RS* relationship. Once the input data is read, REOS performs the following steps:

Step 1: Establish the Initial Inflow Rate

The initial inflow rate Q_0 is the principal parameter for developing EOS. Each curve forming the regulation schedule is based on an assumed value for Q_0. This value

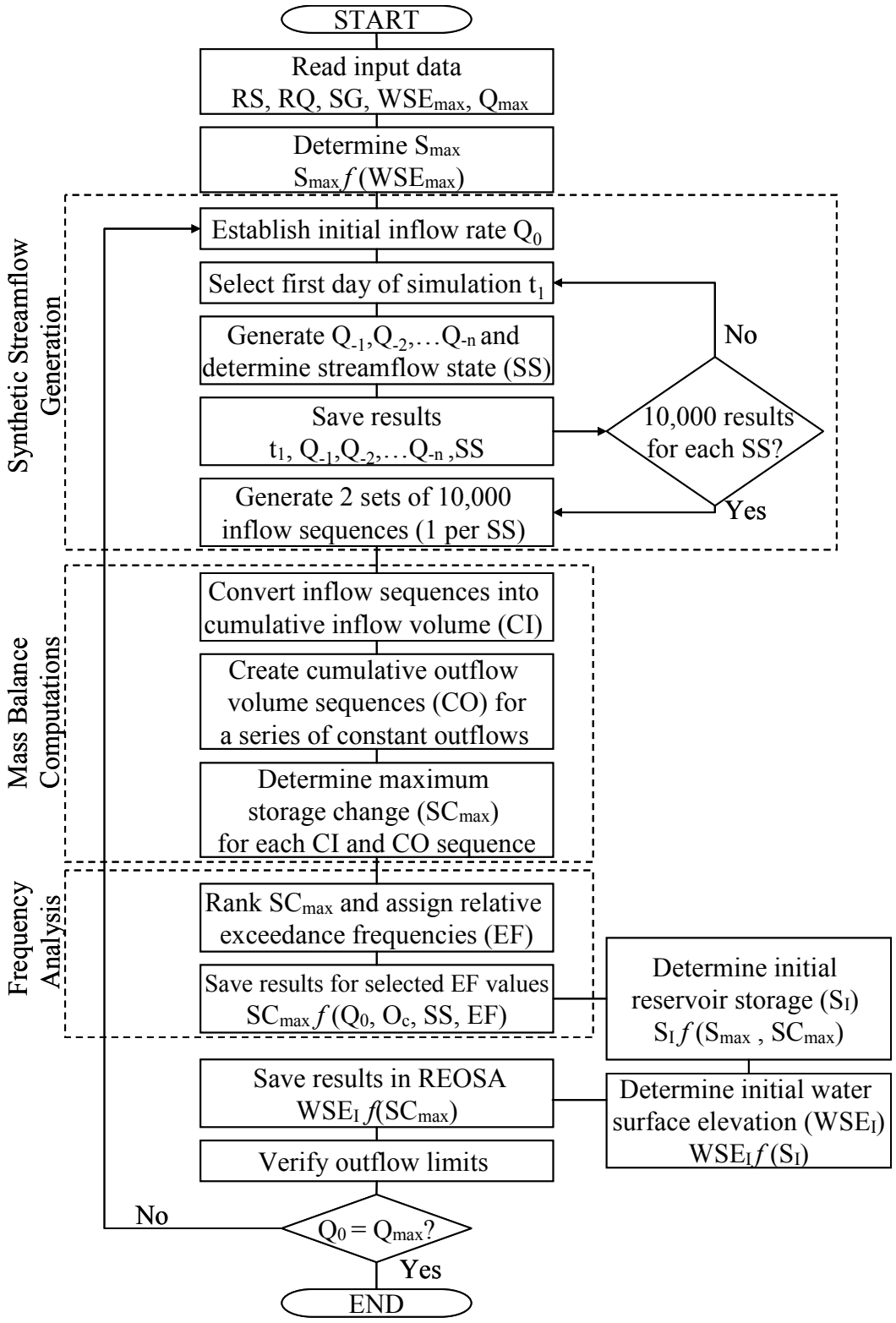

FIGURE 3.5. Flow Chart of the REOS Computational Algorithm

represents the average inflow rate observed in the 24-hour period prior to the actual release decision. Q_0 is the initial value in every inflow sequence, and is used as input to determine the preceding inflow values and the streamflow state. The generated inflow sequences are representative of the expected flows succeeding Q_0. Therefore, both past and future inflows are initially dependent upon Q_0. A series of Q_0 values is automatically generated in REOS in increments of 1,000 cfs up to the selected value for Q_{max}.

Step 2: Select First Day of Simulation

In order to develop the annual regulation schedules, a random selection of the first day for each inflow sequence is required. Although Q_0 is the initial discharge in every simulation, the first day (t_1) of the generated sequence may be any day of the year. Based on t_1, the appropriate streamflow generation model and its corresponding parameters are selected to start each simulation. The annual schedules are developed under the premise that the generated sequences have the same probability of occurring in any day of the year regardless of the selected t_1. Since this analysis is based on a large number of inflow sequences, it is expected that enough variation will result in terms of t_1 and thus, the resulting schedules may be implemented any time of the year.

This step is slightly modified for developing monthly regulation schedules. In this case, every inflow sequence starts in the same month and t_1 is randomly selected within that month. This type of schedule is only valid for the particular month for which it was developed.

Step 3: Generate Preceding Inflows and Determine the Streamflow State

Q_0 is used as the initial input to a backward AR(1) model to generate the n preceding discharge values (Q_{-1}, Q_{-2},…, Q_{-n}) required to initiate the streamflow simulations (see Section 3.3.2.2). The streamflow state (*SS*) is classified as rising or receding based on Q_0 and Q_{-1}. Once *SS* is determined, the corresponding array of n preceding values is stored aside. This process is repeated until 10,000 arrays have been stored for each *SS* category.

Step 4: Generate Synthetic Inflow Sequences

The streamflow generation models are used to generate two sets (one for each *SS* category) of 10,000 synthetic daily average inflow sequences using the discharge values computed in Step 3 (Q_{-1}, Q_{-2},…, Q_{-n}) and Q_0 as initial conditions. Each sequence starts at a random day t_1, which was selected in Step 2. Based on t_1, the corresponding model is selected to start the simulation. When t reaches the end of the month, the next model is used to continue the simulation. This process continues until a one-year inflow sequence (Q_t: t = 1, …, 365) is completed. This length was chosen to ensure that the sequences would be suitable for the storage change computations performed in Step 7. In addition, generating long inflow sequences allows incorporating the possibility of multiple consecutive events that could result in significant increases in storage content over periods of several weeks (ratcheting effect).

Step 5: Create Cumulative Inflow Sequences

The cumulative inflow (*CI*) sequences are obtained by accumulating the generated inflow sequences over time from Q_1 onwards. The *CI* sequences start from Q_1, as these values represent the expected inflow volume following the assumed value for Q_0. The *CI* sequences are then multiplied by a conversion factor to convert them to an inflow volume sequence.

Step 6: Create Cumulative Outflow Sequences

A series of constant outflow rates (O_c) is used to create cumulative outflow (*CO*) volume sequences. The O_c values range from zero to an upper limit that is set by either the maximum discharge rate specified in the *RQ* data, or by Q_0, whichever is smaller. The latter upper limit implies that reservoir outflows should not be greater than the current inflow rate. The series of O_c values is generated in REOS using a fixed increment of 100 cfs, which is assumed sufficiently small to obtain a well-defined regulation curve.

Step 7: Determine the Maximum Cumulative Storage Change

The maximum cumulative storage change (SC_{max}) for every *CI* and *CO* sequence is determined in this step. SC_{max} is the maximum volume to be stored in a reservoir for a

given CI and CO sequence. SC_{max} is determined by the following mass balance equation:

$$SC_{max} = \max [(CI_t - CO_t)] \tag{3.16}$$

The time domain for Equation 3.16 ranges from $t = 0$ to some future time whereupon the cumulative storage change equals zero. For example, consider the hypothetical CI and CO sequences in Figure 3.6a. The slope of the CI curve for a given period reflects the inflow rate during that period. Similarly, the slope of the CO curve reflects the constant outflow rate O_c. At t_{end}, CI and CO are equal, and thus the cumulative storage change equals zero. Therefore, SC_{max} is determined by solving Equation 3.16 for the time interval $t \in [0, t_{end}]$. The time at which SC_{max} occurs will be referred to as t_{max}. Consider now Figure 3.6b, which shows the fluctuations in storage volume (SV) produced by the sequences in Figure 3.6a. If at $t = 0$ a reservoir is at some initial storage S_I, then SV for each time step is given by:

$$SV_t = S_I + SC_t = S_I + (CI_t - CO_t) \tag{3.17}$$

Observe that from $t = 0$ to t_{max}, SV is increasing. This indicates that during this period, the inflows were greater than O_c and the surplus volume was accumulated in the reservoir. After t_{max}, the opposite takes place. O_c is greater than the inflows, and thus SV is decreasing. Notice that the maximum storage volume (SV_{max}) in the reservoir is equal to $S_I + SC_{max}$. Therefore, SC_{max} represents the minimum flood control storage that must be available between S_I and the maximum storage capacity of a reservoir in order to accommodate a given inflow sequence if reservoir releases are kept constant at O_c. Alternatively, O_c may be regarded as the minimum outflow rate required to accommodate a given inflow sequence when the initial reservoir storage is S_I.

The SC_{max} computations performed in this step are valid as long as a suitable time domain for Equation 3.16 is available. Therefore, the CI and CO sequences should be sufficiently long to allow the cumulative storage change to reach a maximum and then return to zero. However, if $O_c = 0$ the cumulative storage change becomes a sole

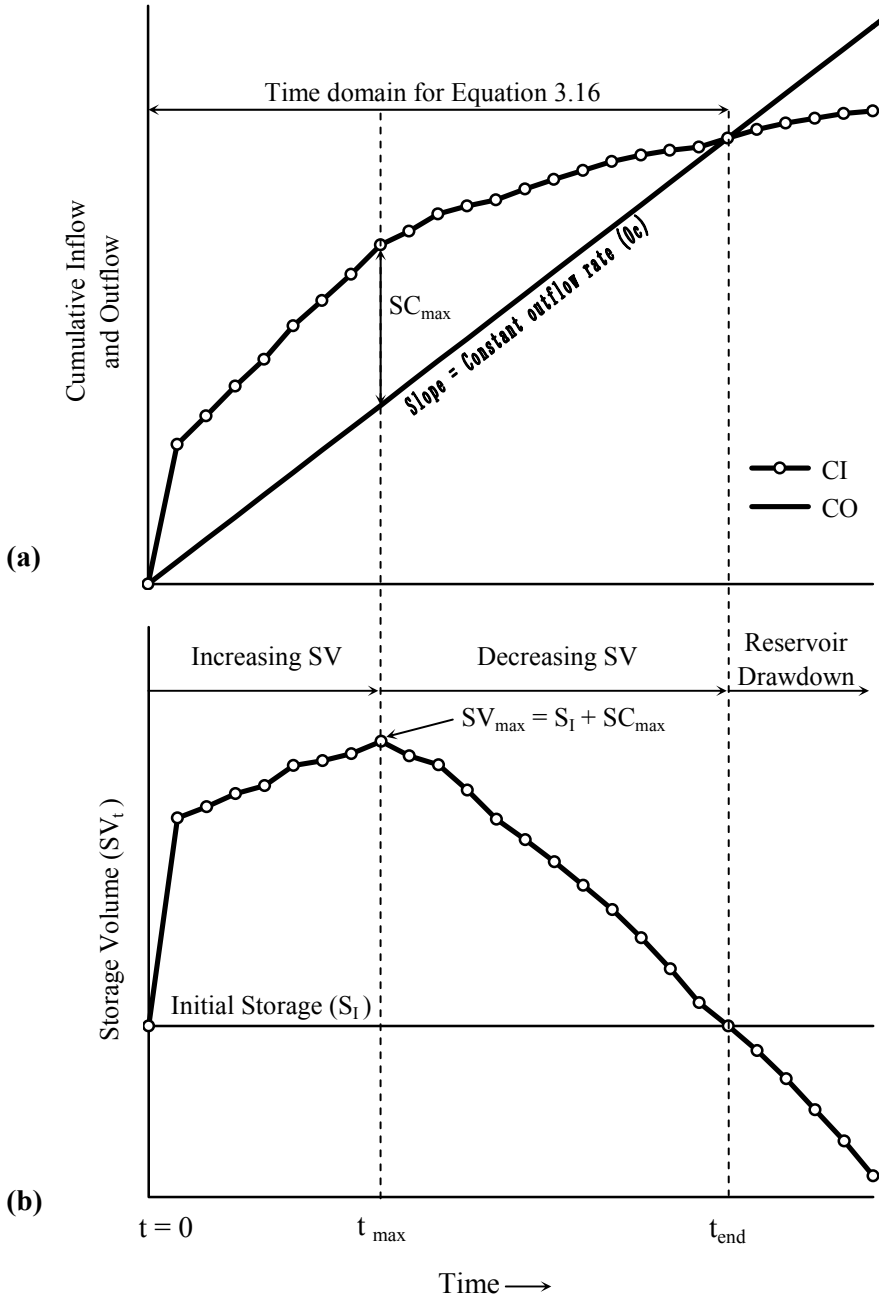

FIGURE 3.6. Example of Maximum Cumulative Storage Change Computations. (a) Cumulative Inflow and Outflow; (b) Storage Volume ($SV_t = SI + CI_t - CO_t$)

function of the *CI* sequence. In this case, *SV* will either increase or remain constant, and thus, the reservoir would not return to its initial storage condition (*SC* = 0). Consequently, an alternative approach was devised to compute SC_{max} for the zero outflow case. In this approach, it is assumed that SC_{max} is the accumulated inflow volume from the beginning of a flood event up to the period in which the reservoir storage volume ceases to increase significantly. An example of the computations performed in this approach is presented in Table 3.2. A graphical illustration of the results is shown in Figure 3.7. Given that $O_c = 0$, the cumulative storage change in the reservoir is equal to *CI* (column 2). The increase in *SV* is evaluated by calculating the cumulative storage change ratio (SC_R) for successive periods (column 3). Ratios greater than one indicate an increase in storage during that period. Similarly, ratios equal to one indicate that the storage remained constant. Due to the possibility of multiple flood events, *SV* should remain relatively constant for a significant period before SC_{max} is determined. This period is identified based on a moving average value of SC_R over a specific number of preceding periods (column 4). A 3-day period was arbitrarily selected in this example. A value equal to one in column 4 indicates that the flood has receded and that the reservoir storage remained constant, or nearly so, over the specified period. Notice that at $t = 23$, the 3-day SC_R moving average value is equal to one for the first time. Thus, SC_{max} is equal to 3,334 acre-ft, which is the accumulated storage hitherto.

Step 8: Determine Exceedance Frequencies

Exceedance frequencies are assigned to each SC_{max} value based on an empirical relative frequency relation. The array of SC_{max} observations is ranked in descending order of magnitude with a rank *m* of 1 assigned to the highest value. The probability P_m that the observation with rank *m* is equaled or exceeded may be approximated by

$$P_m = \frac{m}{N} \tag{3.18}$$

where *N* is the number of observations (sample size). Evidently, the accuracy of this estimate depends upon the sample size. It is assumed that the sample size adopted for this study ($N = 10{,}000$) is sufficiently large so that Equation 3.18 will provide a reliable

TABLE 3.2. Example of the SC_{max} Computations for the Zero Outflow Case

Time (days) (1)	CI = SC (ac-ft) (2)	SC_R (3)	SC_R 3d-MA (4)	Time (days) (1)	CI = SC (ac-ft) (2)	SC_R (3)	SC_R 3d-MA (4)
1	1,000	--	--	14	2,303	1.01	1.02
2	1,052	1.05	--	15	2,716	1.18	1.06
3	1,253	1.19	--	16	2,967	1.09	1.09
4	1,283	1.02	1.09	17	3,082	1.04	1.10
5	1,293	1.01	1.07	18	3,098	1.01	1.05
6	1,419	1.10	1.04	19	3,241	1.05	1.03
7	1,519	1.07	1.06	20	3,301	1.02	1.02
8	2,039	1.34	1.17	21	3,315	1.00	1.02
9	2,143	1.05	1.15	22	3,325	1.00	1.01
10	2,143	1.00	1.13	23	3,334	1.00	1.00
11	2,168	1.01	1.02	24	3,336	1.00	1.00
12	2,268	1.05	1.02	25	3,337	1.00	1.00
13	2,288	1.01	1.02				

NOTES: Col. (3) SCR = (CI_{t+1}/CI_t)

Col. (4) SC_R 3d-MA =3-day moving average value for SC_R

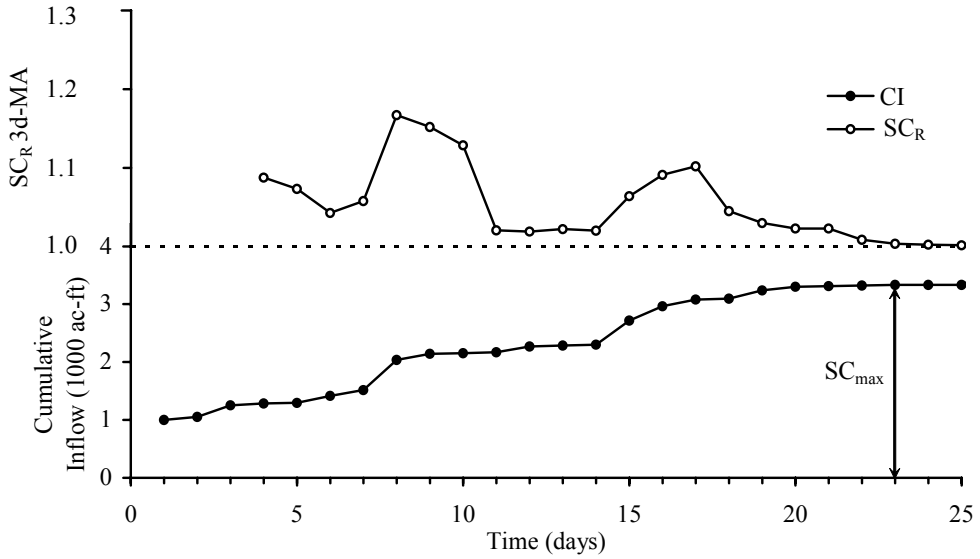

FIGURE 3.7. Graphical Illustration of the SC_{max} Computations for the Zero Outflow Case

estimate of the true probability. The exceedance probability is expressed as an exceedance frequency (*EF*) in percent by multiplying P_m by 100 percent. Notice, however, that *EF* is conditional upon a specific combination of values of Q_0, O_c, and *SS* (the system condition). Therefore, *EF* is interpreted as the probability that an SC_{max} observation with rank *m* will be equaled or exceeded in any given occurrence of a specific system condition.

The results for a selected set of exceedance frequencies are recorded aside in a 4-dimensional array that stores SC_{max} as a function of the system condition and *EF*. This array is the basis for the final computations of the procedure in which the calculated storage changes are associated with actual reservoir storages and water surface elevations to form the regulation schedules. The *EF* associated with a given schedule may be interpreted as the probability or risk that an incoming flood will equal or exceed the residual storage capacity of a reservoir given a specific system condition. Likewise, the complementary non-exceedance frequency (*NEF*) defined as

$$NEF = (100\% - EF) \tag{3.19}$$

may be interpreted as the probability that an incoming flood will only fill a portion of the residual storage capacity given the same system condition.

Step 9: Determine Initial Reservoir Storage and Water Surface Elevation

The initial reservoir storage S_I is determined by subtracting SC_{max} from the maximum storage capacity (S_{max}) of the reservoir:

$$S_I = S_{max} - SC_{max} \tag{3.20}$$

The S_I values may be used to define the regulation schedules in terms of storage. However, it is convenient to convert these values to initial water surface elevations (WSE_I) so that the schedules can be used more directly in actual operations. The *RS* relationship is used to solve for WSE_I given S_I. Note then that for a given S_{max}, WSE_I becomes a sole function of SC_{max}. Therefore, the SC_{max} values from the 4-dimensional array developed in Step 8 can be replaced with the corresponding WSE_I value. This

updated array, which will be referred to herein as REOSA (i.e. REOS Array), contains all the required information to define the regulation schedules.

Step 10: Verify Outflow Limits

This final step is required to ensure that the outflow rates associated with each WSE_I value in REOSA are consistent with the reservoir outlet works outflow limits. The feasible domain of reservoir releases lies between 0 and the maximum outflow capacity at any given WSE_I, denoted here by $O_{max}(WSE_I)$. REOS compares every O_c value in REOSA with the corresponding $O_{max}(WSE_I)$. If O_c is greater than $O_{max}(WSE_I)$, then O_c is set equal to $O_{max}(WSE_I)$.

As the entire process is repeated for each Q_0 value, the WSE_I corresponding to each combination of Q_0, O_c, *SS*, and *EF* is stored in REOSA. The family of curves forming the regulation schedules for a selected *EF* and *SS* are developed by reading from REOSA the WSE_I corresponding to a continuous set of outflows and plotting these values using Q_0 as a parameter. The final product is a series of alternative schedules that represent the required releases as a function of the reservoir water surface elevation, current and past inflows, time of year, and the risk of exceeding the residual storage capacity.

3.4. COMPARISON OF THE METHODOLOGIES

Both of the methodologies presented herein are based on the same general principle; namely, determining the release rate that will limit storage to the capacity available. Each method adopts a distinct computational approach to determine these values; however, both are based on mass balance considerations. Although the methods hold these basic similarities, they do differ in three major aspects: (1) the method for estimating the expected inflow volumes, (2) the parameters that are incorporated in the regulation schedules, and (3) the actual implementation of the schedules.

3.4.1. Estimation of the Expected Inflow Volume

The estimation of the expected inflow volume is one of the major contrasts between the methodologies. Ultimately, the regulation schedules are defined based on this volume, and thus, the adopted procedure for its estimation has great influence over the results.

The USACE standard method is a deterministic procedure that defines the regulation schedules based on one conservative estimate of the expected inflow volume for each reservoir inflow and outflow combination. A series of simplifying assumptions regarding future flows are adopted in this method in order to obtain this estimate. First, it is assumed that the current inflow rate corresponds to the peak discharge of the flood event and that inflows will follow a receding trend for the remainder of the event. The inflow volume computations only reflect the input of this single event, disregarding the possibility that inflows may continue to increase or that the recession may be interrupted by a subsequent event that could result in additional volumes. Second, it is assumed that all hydrograph recessions may be computed using the same recession constant, regardless of the initial inflow rate. This recession constant is derived from a large flood with a relatively steep recession. Since the initial segment of a hydrograph recession varies considerably depending on the magnitude of the flood, the adopted recession constant will generally result in conservatively low inflow volume estimates. These estimates are regarded as the minimum volume that can be expected from a flood. The reservoir outflows required to accommodate this minimum volume under various initial storage conditions form the basis for the regulation schedules.

Due to the inherent variability of streamflows, infinite possibilities exist for sequencing of future flows. Therefore, formulating an emergency operation schedule assuming that a single sequence of streamflows is adequate to describe all future conditions is rather limited. Several investigators have acknowledged that deterministic methods are inadequate to identify appropriate release decisions and have used probabilistic methods instead (Beard and Chang 1979; Willis et al. 1984; Jain et al. 1992; Cruise and Singh 1996; Philbrick and Kitanidis 1999; Andrade et al. 2001).

Probabilistic methods allow, to a certain extent, the quantification of the risks associated with a particular release decision.

The REOS method is a risk-based approach that defines the regulation schedules based on the probability that the expected inflow volume would exceed the residual storage capacity in a reservoir for a given system condition. The assumptions of the standard method regarding future flows are removed in this method by using stochastic streamflow generation models to create the inflow sequences. Inflows may or may not continue in their current trend, so it is unknown whether the inflow hydrograph has already peaked. Furthermore, even if the current inflow is indeed the peak discharge, the hydrograph will not necessarily continue a receding trend, for it may start rising again due to a subsequent rainfall event. The introduction of these uncertainties concerning future flows implies that, in all likelihood, the estimated inflow volume for a given system condition will result in a different value every time it is evaluated. Hence, each system condition is evaluated multiple times, thereby providing the basis for the probability analysis in which exceedance frequencies are assigned to the resulting array of inflow volumes. The regulation schedules are formulated based on the inflow volumes that were equaled or exceeded in certain percentage of the realizations for each system condition.

3.4.2. Regulation Schedule Parameters

One of the major limitations that hinder effective operation of a reservoir under emergency conditions is the lack of a reliable forecast of the incoming flood upon which apposite release decisions may be taken. Hence, release decisions under such conditions have to be based on certain parameters that can provide an indication about the potential inflow volumes. The parameters incorporated in the EOS may be regarded as predictor variables of the expected inflow volume. The scheduled releases are a function of the residual storage capacity and the information associated with these parameters.

The only parameter incorporated in the standard regulation schedules is the current inflow rate Q_0. The relationship among Q_0, the residual storage, and the required

releases is expressed in a single regulation schedule, which provides a general basis for regulation. Besides Q_0, the REOS method incorporates the streamflow state, and the time of year (if using monthly schedules) as parameters in the schedules. Considering the natural tendency of flows to remain in their current state and the seasonal differences in flood characteristics allows for the formulation of a series of regulation schedules that are more refined in the sense that they are tailored to the specific conditions described by the parameter values. The exceedance frequency is a supplementary parameter that is incorporated but not as a predictor variable per se. As previously explained, the exceedance frequency and the complementary non-exceedance frequency associated with each schedule represent, respectively, the risk that the specified release rates will be insufficient to avoid dam overtopping and the risk that they will be excessive thereby causing unnecessary damages downstream. Reservoir operators may use this parameter as a means to evaluate the tradeoffs and the potential consequences of their release decisions.

3.4.3. Implementation of the Regulation Schedules

Reservoir releases are made according to normal operation procedures until it becomes apparent from the current reservoir state that the residual storage capacity may be exceeded, whereupon operations switch to emergency procedures. The same general strategy for making emergency releases applies for both of the regulation schedules discussed herein. Essentially, once emergency operations are in effect, release decisions are reevaluated each hour and outflows are adjusted in accordance to the current parameter values and reservoir stage. The rating curves of the outlet facilities are used to set gate openings for the scheduled release rates. After a peak reservoir stage is attained and inflows and stage start decreasing, the post-flood evacuation process is initiated. The maximum gate opening attained during regulation is maintained until the reservoir stage reaches a designated safe level. Then, if current reservoir outflows when combined with runoff from uncontrolled areas below the dam are greater than the allowable channel capacity at downstream control points, outflows are adjusted to pass

the inflows (reservoir level remains constant) until the combined discharge does not exceed the channel capacity. At this time, normal operations resume and releases are made according to the allowable non-damaging channel capacity until the reservoir is empty.

The standard emergency operations schedules offer a straightforward set of rules to be followed by reservoir operators. The parameter values classifying each curve represent the average inflow to the reservoir in the preceding hour. The value for this parameter may be provided by the reservoir control center, which has access to real-time streamflow measurements, or if real-time data is unavailable or undependable, it can be measured at the dam site based on the changes in reservoir stage. Once this value is determined, the required release rate is read off the corresponding curve as a function of the current reservoir stage. This operation continues until the required conditions to initiate the post-flood evacuation process are met.

As previously discussed, these regulation schedules are formulated based on a conservative estimate of the expected inflow volumes. This conservative approach is adopted in an attempt to minimize the risk of committing an operational error in terms of excessive releases (USACE 1959). This error is of great concern to reservoir operators due to the strong public opposition to the release of stored water as long as downstream flooding continues. According to the assumptions adopted in this method, the scheduled releases should provide enough storage to accommodate the remainder of a flood if flows continue a receding trend as described by the adopted recession constant. If, however, inflows continue increasing or if they recede less rapidly than expected, even greater releases than those initially specified will be required. Consequently, there should be no reluctance to set releases to those specified because even larger releases will probably be required and because it would be virtually impossible to operate the reservoir for the remainder of the flood with lesser releases (Beard 1963). An important assumption here is that there will always be sufficient time to increase releases in a manner that is in accordance with the maximum allowable rate of change of release rates. This assumption becomes less reasonable if the reservoir storage is close to its

maximum capacity. Under this condition, if an increase in reservoir releases is required but the specified rate cannot be attained quickly enough, the resulting increase in storage may be sufficiently large to cause dam overtopping. Hence, reservoir operators need to exercise proper judgment when implementing this type of schedule since their effectiveness in avoiding dam overtopping may lessen as the reservoir storage reaches its maximum capacity.

Implementing the risk-based EOS involves the determination of up to four parameter values before a release decision is made. Disregarding the risk parameter for the moment, releases are based on the current inflow rate (Q_0), the streamflow state, and the time of year if using the monthly schedules. Once these parameters are determined, the matching schedule is selected and the required release rate is read off the corresponding curve as a function of the current reservoir stage. Notice that in contrast to the USACE standard method, Q_0 is the average inflow rate over the past 24-hour period instead of the past hour. The streamflow state is classified as rising or receding based on Q_0 and the average inflow rate in the 24-hour period before Q_0. Release decisions are reevaluated every hour based on this 48-hour period of analysis.

The risk parameter associated with each regulation schedule may be regarded as a measure of the degree of protection that the schedules provide against dam overtopping. In addition, this parameter provides a means to evaluate the tradeoffs between the emergency operation objectives and the potential consequences of the scheduled releases. Essentially, a low-risk schedule provides great protection against dam overtopping at the expense of a high probability of making excessive releases resulting in unused storage and unnecessary damages downstream. Conversely, a high-risk schedule decreases the probability of making excessive releases at the expense of a high probability of making insufficient releases that could result in dam overtopping. If the dam is overtopped, uncontrolled spills at high flow rates may occur and they would typically be more damaging than those that were initially avoided.

As previously stated, the REOS method allows, to a certain extent, quantifying the risks associated with implementing a particular EOS. Having a series of alternative

risk-based schedules allows reservoir management agencies to select the schedule that is in accordance with a certain level of risk that is considered acceptable. The decision as to what will be considered as acceptable level of risk largely depends on engineering judgment and the particular characteristics of the project.

CHAPTER IV

DESCRIPTION OF THE ADDICKS AND BARKER RESERVOIR SYSTEM

4.1. PROJECT HISTORY

The Addicks and Barker Reservoir system is located in the Buffalo Bayou watershed of the San Jacinto River basin west of the city of Houston, TX (Figure 4.1). The Addicks and Barker dams and reservoirs were constructed during 1946-1948 and 1942-1945, respectively, at a cost of $5,248,000 and $4,530,000. The reservoirs are located in parallel and are operated as a system by the USACE, Galveston District, to prevent downstream flooding of Buffalo Bayou through Houston. Barker Reservoir is located on the headwaters of Buffalo Bayou and Addicks Reservoir is situated on South Mayde Creek and several other creeks that are tributaries of Buffalo Bayou. The reservoirs remain dry most of the time. Consequently, most of the federal lands acquired for flood detention have been leased for recreational development and public use. When the reservoirs were completed, they were approximately 15 miles west of the Houston city boundaries. Both reservoirs now lie entirely within the Houston boundaries. Although large sections of the reservoirs remain undeveloped, considerable urban development has occurred adjacent to the federal reservoir lands, along the channel below the dams, and throughout the Buffalo Bayou watershed (Wurbs 2002). In 1970, the Addicks Reservoir watershed contained 554 residential structures and grew to more than 25,119 residential structures by 1990, for an average annual growth rate of 21%. During the same period, residential structures in the Barker Reservoir watershed grew from 1,330 to 14,903, for an annual growth rate of 12.8% (USACE 1995).

The Buffalo Bayou project was authorized by the River and Harbor Act of June 20, 1938, in response to the devastating floods that occurred in the Houston area in 1929 and 1935. The project was subsequently modified by the Flood Control Acts of August 11, 1939; September 3, 1954; and October 27, 1965. The project plan for improvement of Buffalo Bayou is contained in House Document 250, 83rd Congress, 2nd Session. The

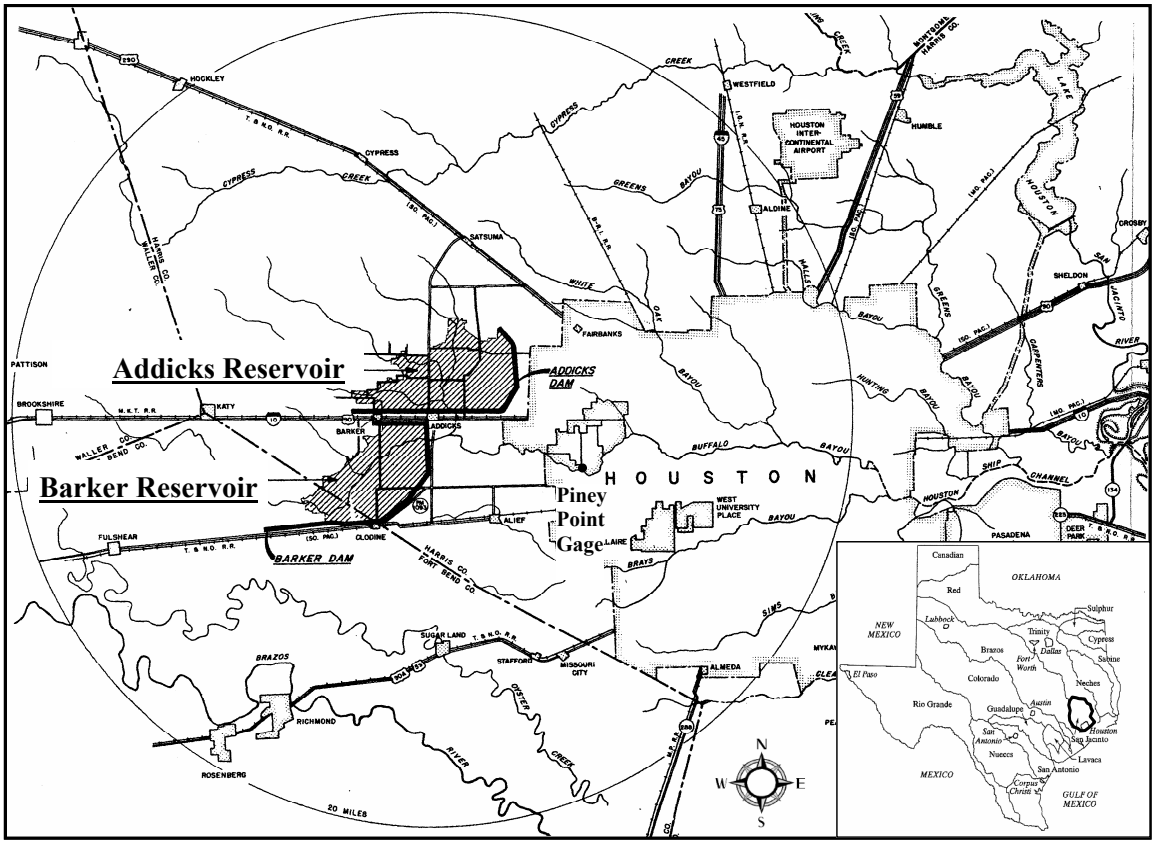

FIGURE 4.1. Location of the Addicks and Barker Reservoir System (Source: USACE 1977)

original flood management plan provided for a series of structural measures including three reservoirs (Addicks, Barker, and White Oak), a system of canals to convey releases from Addicks and Barker Reservoirs south of Houston to Galveston Bay, and a levee along the Cypress Creek divide to prevent overflows from entering into Addicks Reservoir. For various reasons, the original plan was not fully implemented. During the pre-construction planning for Addicks Dam it was determined to be more economical to increase the capacity of the reservoir to accommodate the Cypress Creek overflow and eliminate the diversion levee. The required additional storage was obtained through the purchase of lands up to 3.6 ft above the elevation of the previously purchased lands (Costello 2000). A review of reports completed in 1952 concluded that rising land costs

and rapid urban development made construction of White Oak Reservoir impractical and recommended channel rectification and enlargement of Buffalo, Brays and White Oak Bayous (USACE 1977). These projects were authorized in the 1954 Flood Control Act and included channel enlargement of 29.3 miles of Buffalo Bayou through the city to the Houston Ship Channel turning basin, and enlargement of 10.4 miles of White Oak Bayou and 25.4 miles of Brays Bayou above their confluence with Buffalo Bayou. Since Addicks and Barker provided a measure of protection to Buffalo Bayou, priority was given to the Brays and White Oak projects, which have been substantially completed, and only 7.4 miles of the authorized channel rectification for Buffalo Bayou were completed just downstream of the dams. The only other downstream improvements completed were the construction of four retaining walls near the downtown area. Further construction of the Buffalo Bayou authorized improvements have been deferred due to encroachment along the stream, limited financial resources, and environmental and aesthetic concerns (USACE 1977; USACE 1995).

4.2. PROJECT STRUCTURAL DESCRIPTION AND MODIFICATIONS

Addicks and Barker Reservoirs are similar structures formed by rolled earthen dams with lengths of 61,166 and 71,900 ft, respectively, and a maximum height of 49.6 and 38.7 ft above the streambed. The outlet works for both dams consist of five conduits controlled with vertical slide gates, and emergency spillways over the natural ground at the end of the dams. Reservoir releases pass through a spillway into a stilling basin, thence through riprap lined outlet channel emptying into the improved channels below the dams. A detailed description of the dams and outlet works is presented in Plates 2-3 of the Addicks and Barker reservoir regulation manual (USACE 1962). A summary of relevant data describing the reservoirs is presented in Table 4.1.

Originally, four of the five conduits in each structure were ungated, permitting an uncontrolled discharge of about 15,700 cfs into Buffalo Bayou. Since the channel improvements on Buffalo Bayou were not fully implemented, the downstream channel

TABLE 4.1. Addicks and Barker Reservoirs Project Data

	Addicks	Barker
Drainage area (squared miles)	136	130
Dam		
Type	Rolled earth embankment	Rolled earth embankment
Length (ft)	61,166	71,900
Height above streambed (ft)	49.6	38.7
Outlet works		
5 Gated concrete conduits		
Conduits dimensions (ft)	8 W x 6 H x 252 L	9 W x 7 H x 190.5 L
Spillway length (ft)	43.5	55.5
Stilling basin dimensions (ft)	40 L x 60 W	50 L x 60 W
Outlet channel length (ft)	150	160
Elevations (ft above MSL)		
Top of dam	122.7	114.7
Maximum design water surface	112.7	105.0
Natural ground at ends of dam	112.0	106.0
Standard project flood	110.6	100.4
100-yr flood	104.1	97.8
Limits of government-owned land	106.1	97.3
Outlet invert	71.1	73.2
March 1992 flood of record	100.6	95.9
Storage capacity (acre-feet)		
Maximum storage capacity	200,800	209,000
Standard project flood	178,556	123,653
100-yr flood	92,572	89,498
Limits of government-owned land	116,263	83,410
March 1992 flood of record	57,956	66,910
Surface area (acres)		
Natural ground at ends of dam	16,423	16,739
Standard project flood	15,402	13,889
100-yr flood	11,213	12,293
Limits of government-owned land	12,460	12,060

Sources: USACE 1977; USACE 1995

capacity is much less than envisioned in the original design of the reservoirs. Thus, two additional gates were installed in 1948 to reduce reservoir releases. Uncontrolled releases were reduced to 7,900 cfs, which was considered the channel capacity at that time (USACE 1986). Increasing urban growth adjacent to Buffalo Bayou during the 1940's and 1950's caused a potential flood threat by the uncontrolled releases from the reservoirs, and thus, the remaining two conduits were gated in 1963. The embankment material (compacted random earthen fill) was considered adequate for detention type facilities where ponded water would be discharged relatively quickly following flood events. However, the installation of additional gates and the need to control outflows resulted in prolonged ponding in the reservoirs, which was not intended in the original design. Prolonged ponding after some floods in the 1970's caused seepage through and under the dam embankments. Emergency seepage control measures were required for both dams in 1977 and were completed in 1982 at a cost of $15 million. The measures consisted of construction of a soil bentonite slurry trench through the embankments and pervious foundations, placement of a downstream berm to enhance slope stability, and placement of clay blankets to thicken the impervious cover over pervious foundation materials (USACE 1995). Additional modifications were made to the dams during 1986-1989 to comply with Dam Safety Assurance Program. These modifications included raising the crest elevations of the dams to comply with the freeboard requirements for wind-generated wave runup, and erosion protection to the lower ends of the dams so the ends can serve as overflow spillways during major storms greater than the Standard Project Flood, up to and including the Probable Maximum Flood (USACE 1995).

4.3. RESERVOIRS POOL ELEVATIONS

Table 4.1 includes water surface elevations and associated storages pertinent to the Addicks and Barker Reservoir system. The storage versus elevation curve for the reservoirs is depicted in Figure 4.2. The maximum storage capacities of the reservoirs are 200,800 and 209,000 acre-ft, respectively, for Addicks and Barker. These storage

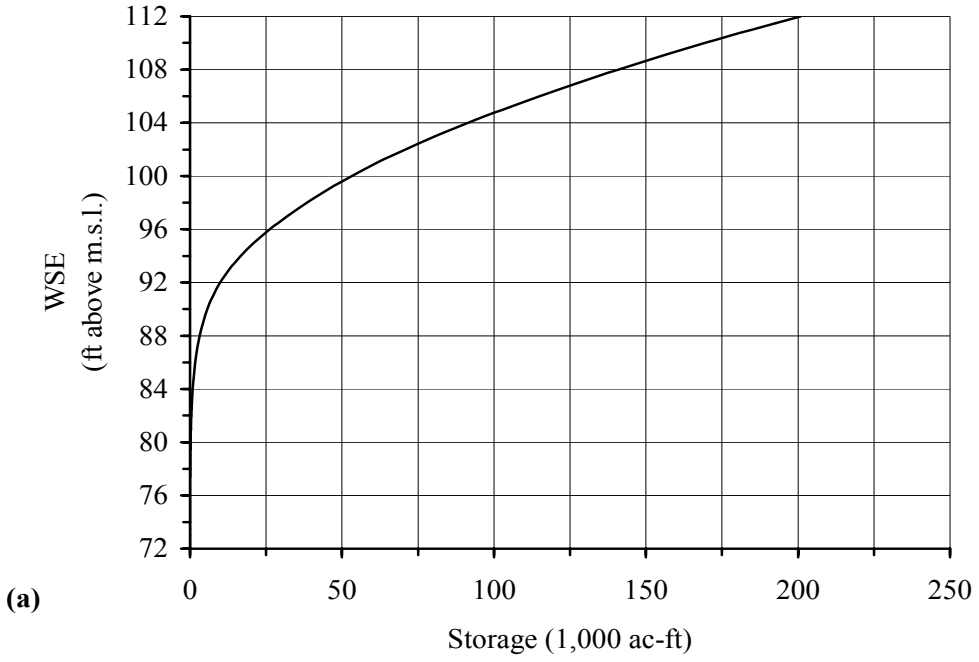

(a)

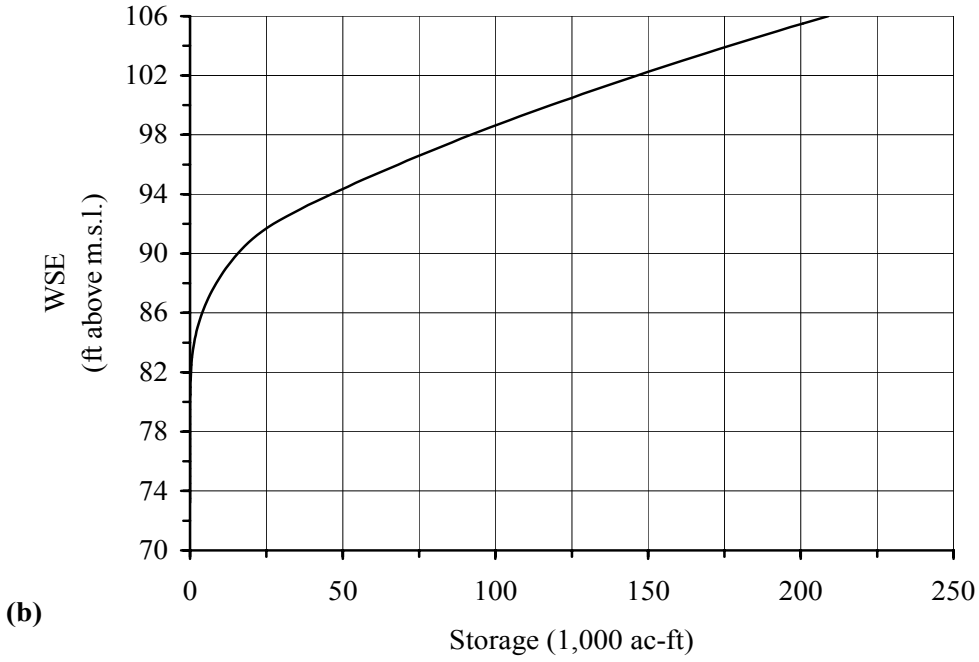

(b)

FIGURE 4.2 Reservoir Storage versus Water Surface Elevation Relationship. (a) Addicks; and (b) Barker

capacities are set by the elevation of the natural ground at the end of the dams, which is 112.0 and 106.0 ft above mean sea level. At these elevations, the maximum release rate through the outlet works is 7,785 cfs for Addicks and 8,814 cfs for Barker. The outlet works rating curves for the reservoirs are shown in Figure 4.3.

If water levels exceed the elevation at the end of the dams, uncontrolled discharges would occur over the natural ground overflow spillways. Flood damages, however, would occur within the reservoir pools at much lower elevations. The federal government purchased reservoir lands for flood detention purposes up to an elevation 3 ft above the predicted stage that would have been produced by the 1935 flood centered over each of the reservoir watersheds. This resulted in the acquisition of land 5.9 and 8.7 ft below the natural ground at the ends of the dams at Addicks and Barker, respectively (USACE 1995). This government-owned land (GOL) constitutes about 76 and 72% of the total land area within the reservoir pools. It has been estimated that Addicks and Barker Reservoirs have sufficient GOL to contain floods up to the 250-year and 70-year flood events, respectively (USACE 1995). Although urban development is restricted within the GOL, extensive urban development has occurred in the fringe areas between the upper limits of the GOL and the maximum pool levels. Thus, the GOL upper limits of 106.1 and 97.3 ft indicate the elevation above which residential and commercial properties are susceptible to flooding. The fringe areas comprise 3,963 acres in Addicks and 4,679 acres in Barker. These areas are depicted in Figure 4.4.

Other significant elevations used as hydrological design criteria are those that would result from hypothetical events such as the Standard Project Flood (SPF), the Probable Maximum Flood (PMF), and the worse case scenario of having the PMF occurring right after the SPF. The SPF is approximately equivalent to the 1,000-year flood for Addicks Reservoir and to the 500-year flood for Barker Reservoir. The PMF is greater than the 10,000-year flood for both reservoirs (USACE 1995). The SPF is predicted to result from 21 inches of rain occurring over a 72-hour period. This flood would result in water surface elevations of 110.6 and 100.4 ft, respectively, for Addicks and Barker, and accumulated storages of 193,956 and 125,061 acre-ft (USACE 1977).

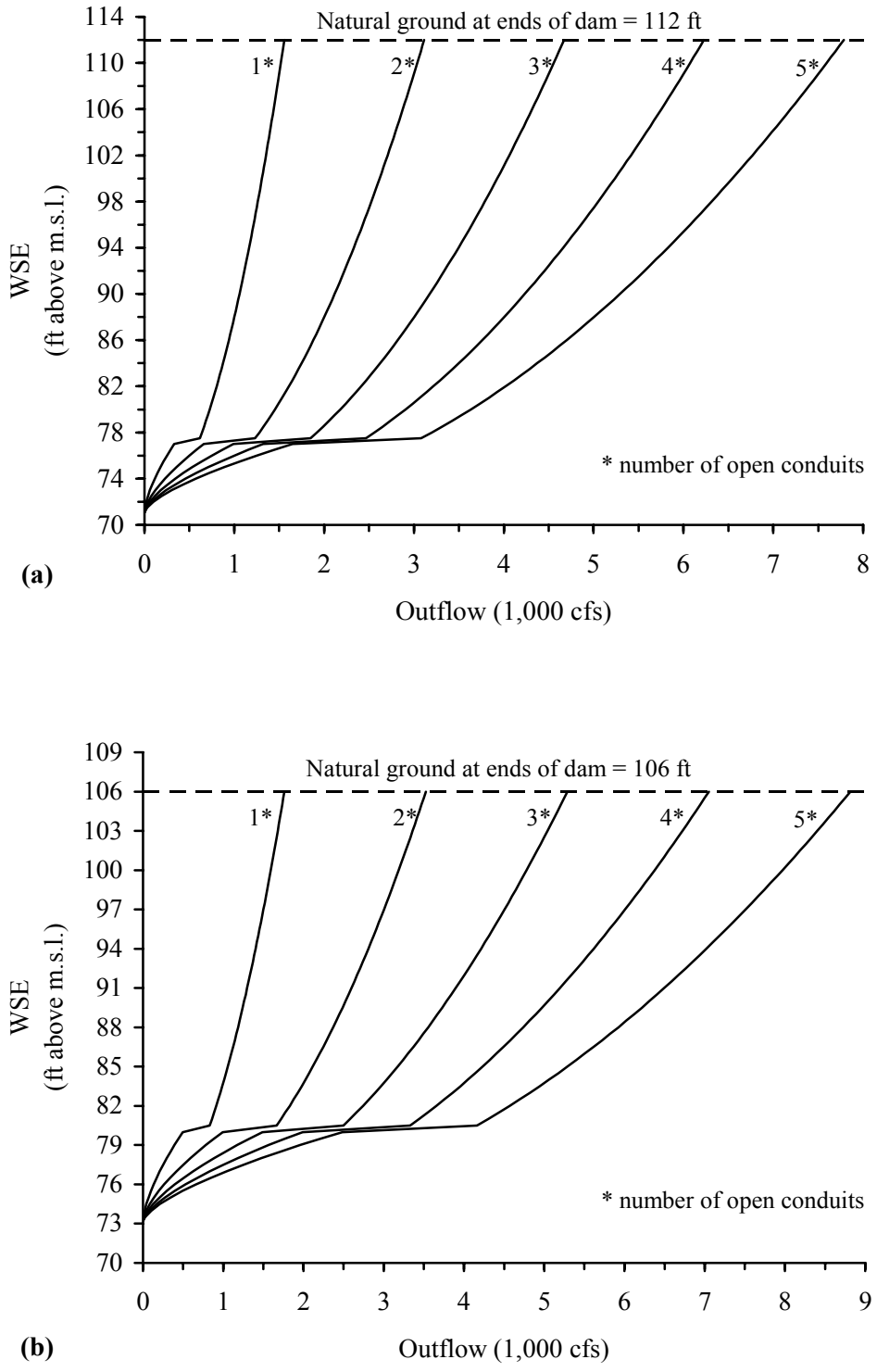

FIGURE 4.3. Outlet Works Rating Curves. (a) Addicks; and (b) Barker

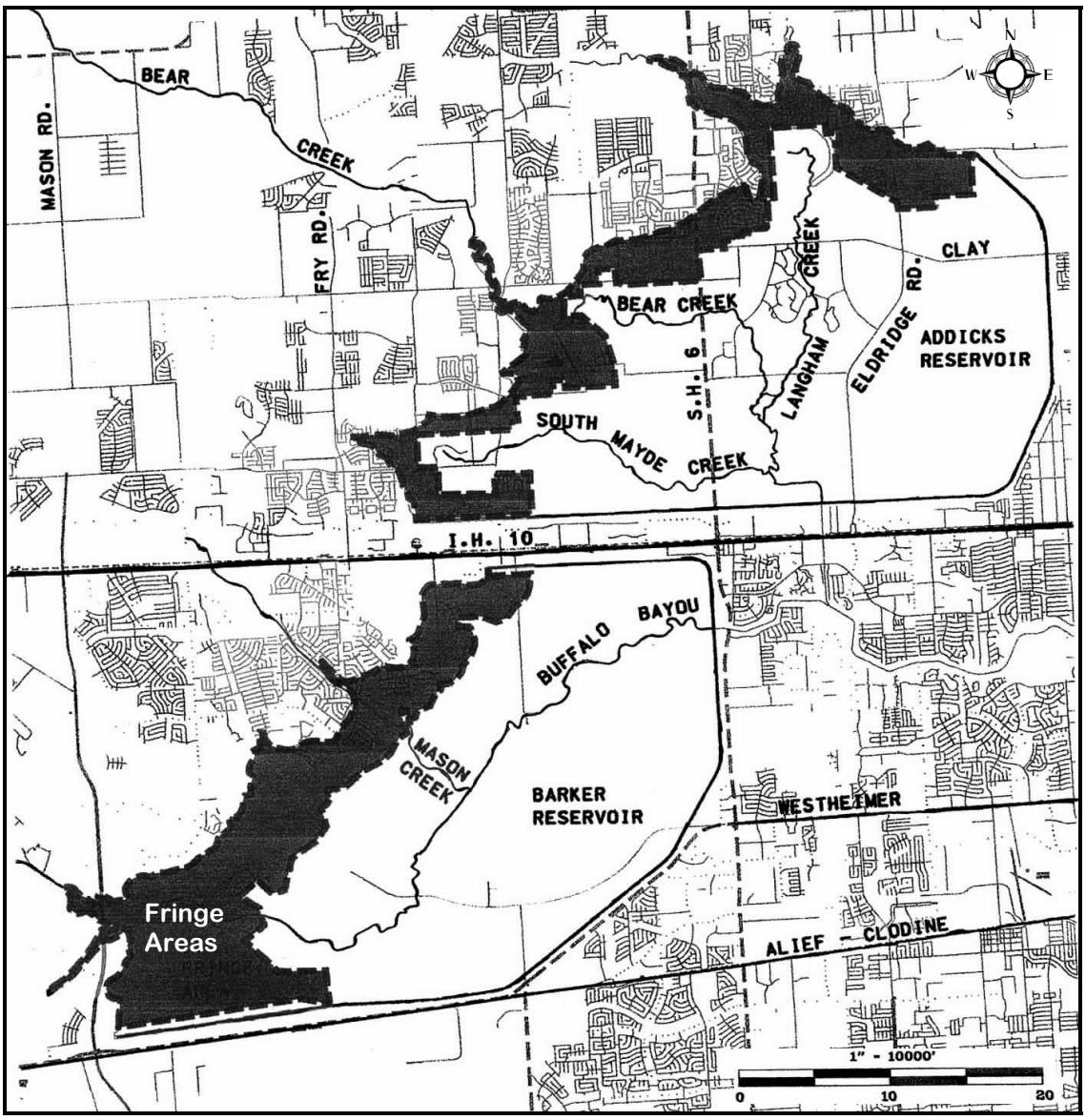

FIGURE 4.4. Fringe Areas Between the Upper Limit of the GOL and the Maximum Pool Elevations in the Addicks and Barker Reservoir System (Source: Costello 2000)

These storages are smaller than the maximum capacity at each reservoir, and thus, the SPF can be contained within the reservoirs without releases. The PMF reflects the runoff produced by approximately 43 inches of rain in 72 hours. This flood would result in accumulated storages of 462,145 and 279,072 acre-ft, which are much greater than the

maximum capacity of the reservoirs. Thus, emergency releases would be necessary during this hypothetical flood. Routing of the PMF through the reservoirs based on the regulation policies prescribed in the 1962 regulation manual for the reservoirs resulted in elevations of 114.6 ft for Addicks and 106.4 ft for Barker (USACE 1962). These values were updated to 112.7 and 105.0 ft, respectively, in accordance to the 1973 datum adjustment (USACE 1995). These elevations are referred to as the maximum design water surface in Table 4.1. The upper extreme of the worst flooding conditions was predicted from the occurrence of the SPF followed approximately 5 days later by the PMF. Routing of this extreme event resulted in reservoir stages of 118.1 and 110.3 ft, respectively, for Addicks and Barker. Clearly, uncontrolled outflows through the natural ground spillways would occur long before the reservoirs reach such high stages.

4.4. RESERVOIR REGULATION PROCEDURES

The primary objective of the Addicks and Barker Reservoir system is to prevent or reduce damaging stages along Buffalo Bayou as much as possible during floods with the currently available storage space. The current normal operation procedures are based on a maximum allowable non-damaging flow rate of 2,000 cfs at the Piney Point gaging station located in Buffalo Bayou about eleven miles downstream of the dams (Figure 4.1). Since the channel improvements on Buffalo Bayou were never completed, the maximum allowable channel capacity of 6,000 cfs specified in the 1962 regulation manual (USACE 1962) had to be reduced to 2,000 cfs to preclude damages on downstream properties. Stage-damage investigations have shown that flow rates higher than 2,000 cfs at the Piney Point station would result in flood damages in some reaches along Buffalo Bayou (Bernard Johnson Inc. 1995).

Under non-flooding conditions, when there is negligible ponding in the reservoirs, two conduit gates are set at an opening of one foot in order to pass the normal low flows at the dam (300 – 500 cfs). When rains occur on the watershed, which are insufficient to cause downstream flooding, the reservoirs are operated so that their combined releases together with the runoff from the uncontrolled 51–mi^2 watershed

between the dams and the Piney Point station does not exceed 2,000 cfs. Release decisions are based on maintaining equal available flood storage in each reservoir. Conversely, when significant rainfall occurs and runoff is expected to be sufficient to produce downstream flooding, reservoir gates are closed and kept under hourly surveillance. The gates remain closed until flows at the Piney Point station peak and then recede to a level such that reservoir releases can be made without risk of contributing to flows exceeding the 2,000 cfs limit, or until reservoir pool levels rise to such an extent as to require emergency releases. Emergency releases are made until a peak reservoir stage is attained and inflows and stage start decreasing.

Under normal operations, the post-flood evacuation process consists of emptying the reservoirs as quickly as allowed by the downstream flow conditions at the Piney Point station. An important consideration in this process is that reservoir releases require approximately 12 hours to travel to the Piney Point station, and even longer to flow through the city. Thus, there is a potential for reservoir releases to combine with uncontrolled runoff produced by rainfall occurring hours after a release decision. This situation may result in flows that greatly exceed the maximum channel capacity. Accordingly, if rainfall in excess of one inch within 24-hours falls below the reservoirs during the evacuation period, the gates are closed again until the above operation can be resumed. If emergency operations were implemented, the maximum gate opening attained during regulation is maintained until the reservoir storage falls to about 75% of its total capacity (USACE 1962). The reservoir stages associated with this storage level are 108.7 ft at Addicks and 102.7 ft at Barker. Then, if reservoir releases, when combined with uncontrolled runoff and releases from the other reservoir, are greater than the channel capacity, the gates are adjusted to release inflow (reservoir level held constant) until discharge does not exceed channel capacity. At this time, normal operations resume and releases are made according to the allowable non-damaging channel capacity until the reservoir is empty.

4.5. OPERATIONAL COMPLEXITIES AND FLOODING HAZARDS

The current operational procedures of the Addicks and Barker Reservoir system are significantly different from those established in the original project design, and further changes and/or refinements may be warranted to cope with the current flooding hazards. Failure to complete the channel improvements below the dams coupled with extensive urban encroachment along the channel have limited the ability of the channel to convey releases from the reservoirs. In the original design, a combined discharge rate of 15,700 cfs was permitted into Buffalo Bayou, but this rate has been reduced over the years to its present rate of 2,000 cfs in order to mollify downstream flooding hazards. As a result, landowners have made significant investments in property closer to the channel in reliance on the restricted flows. Since the decisions to reduce the flow rates were made by the USACE without any apparent legal obligation to do so, any decision to reverse this would have to be well reasoned and designed to prevent extensive damages elsewhere (USACE 1995).

The limited ability of the channel to convey larger flows without causing damages has forced a severely compromised method of operation of the reservoirs. As previously explained, the reservoir gates are kept closed during flood events until flows at the Piney Point station have receded sufficiently to allow non-damaging releases from the reservoirs. Although the reservoirs have served their purpose well and have prevented millions of dollars in downstream damages, this method of operation results in higher storage levels and retention of stored water for periods approximately three times longer that would occur if the channel improvements downstream were complete (USACE 1986). Higher storages would not pose a significant flooding hazard if the fringe areas between the GOL limits and the maximum pool levels had remained undeveloped as they were in the 1940's when the project was completed. However, the potential for upstream flooding has become a major concern due to the continuing development within the fringe areas. Approximately 5,000 structures now exist in the Addicks Reservoir fringe area, approximately 1,000 structures within the Barker Reservoir fringe area, and the undeveloped areas are expected to develop in the near

future (Costello 2000). Furthermore, the development itself has contributed to the prospective flooding problem due to increase runoff rates into the reservoirs resulting in higher storage levels.

The occurrence of extremely high pool levels in these reservoirs is typically attributed to the accumulation of water in storage over rainy periods rather than from a single rainfall event (ratcheting effect). Consider for instance the flood of record of 1992. The record reservoir levels were produced by numerous rainfall events beginning in December 1991 and continuing through the spring of 1992. These events filled the reservoir pools in Barker to near record capacity and had already exceeded the previous record pool in Addicks by late February (Figure 4.5). On February 27, the storage levels were already at 39 and 60% of the total storage within the GOL in Addicks and Barker Reservoirs, respectively. The reservoirs reached peak stages after a major rain event that occurred in March 4; when up to 10 inches of rain fell in portions of western Houston. Addicks Reservoir reached its peak storage (57,956 ac-ft) on March 9 and Barker Reservoir (66,910 ac-ft) on March 7 (USACE 1995). The reservoirs were finally drained to safe levels in July 1992. The peak storage that occurred was approximately 50 and 80% of the total storage within the GOL at Addicks and Barker Reservoirs, respectively, and 29 and 32% of the maximum storage capacity. The annual exceedance frequency (recurrence interval) associated with peak stages in each of the reservoirs is estimated to be about 4% (25 years), and the annual exceedance frequency associated with the March 4 rainfall event is estimated to be between 3.3 and 2.5% (30 to 40 years) (USACE 1995; Wurbs 2002). If a higher intensity rainfall event had occurred and/or the rainfall events had continued without a chance for offsetting the reservoirs storage with some releases, flooding may have occurred within the fringe areas.

Further operational complexities arise when considering emergency procedures. As for most USACE reservoir projects, the emergency operation schedules for the Addicks and Barker Reservoir system were based on ensuring that the dams are never overtopped. If the maximum storage capacity of a reservoir is expected to be exceeded emergency releases are made even if they contribute to downstream flooding. Otherwise

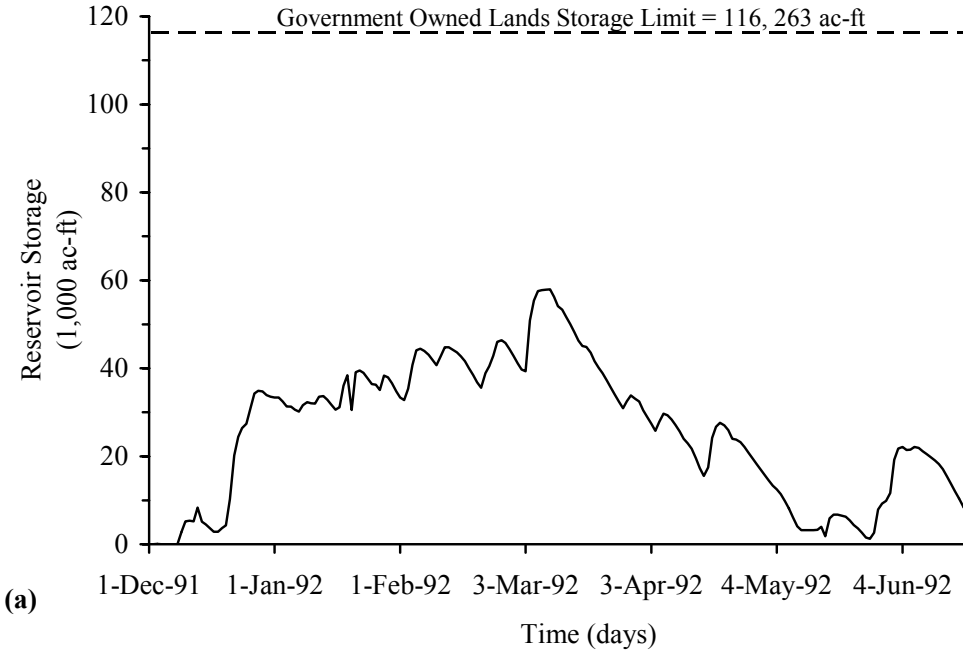

(a)

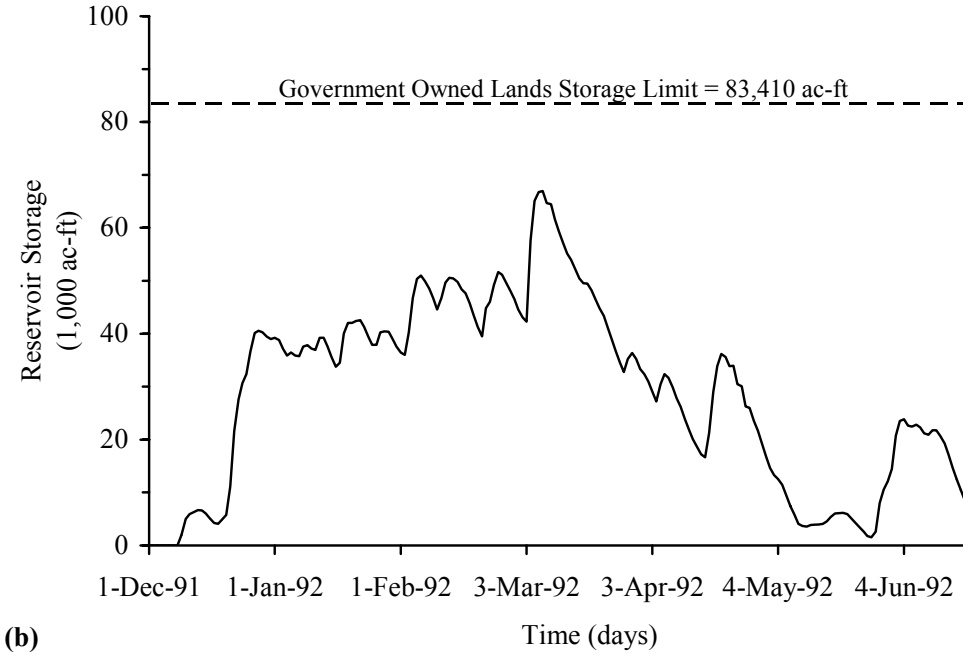

(b)

FIGURE 4.5. Daily Reservoir Storage During December 1991 - July 1992. (a) Addicks; and (b) Barker

the reservoir is operated based on normal regulation procedures wherein releases are restricted by downstream flow conditions. As stated earlier, the primary objective of this reservoir system is to prevent downstream flooding, and all lands within the project boundaries, including those above the GOL limits, were originally intended to provide flood storage. Since Addicks and Barker have, respectively, 42 and 60% of their total storage capacity above the GOL limits, the occurrence of emergency releases would be unlikely under most flooding conditions even if reservoir stages have already exceeded the GOL limits. In other words, under the current emergency operation policies the possible occurrence of upstream flooding does not justify making emergency releases.

Flooding properties above the GOL limits was not a major concern in the original design of the reservoirs and the operating plans. Evidently, the extensive urban development that occurred within the fringe areas was not expected. Although this reservoir system has not experienced a flood of sufficient magnitude to cause upstream flooding, the flood of record demonstrated that there is a realistic threat for flooding properties in the fringe areas, especially at Barker. Thus, an operational dilemma would emerge under extreme flooding conditions in terms of managing tradeoffs between flooding risks upstream and downstream from the dams. The current operation policies would provide a great measure of protection to downstream areas but at the expense of a high risk for upstream flooding. For this particular reservoir system, allowing upstream flooding in order to protect downstream areas may not result in minimization of overall damages given the nature of the expensive structures that would be flooded and other losses associated with traffic disruptions at major roadways within the reservoirs. In addition, flooding of upstream structures may last for a significant length of time due to the restrictions on reservoir releases. Therefore, emergency releases may be appropriate if reservoir levels are approaching or have exceeded the GOL limits. Changes in the current operational procedures that would allow making emergency releases based on the probability of upstream flooding will be explored in the following chapters.

CHAPTER V

APPLICATION OF THE METHODOLOGIES FOR DEVELOPING EMERGENCY RESERVOIR OPERATION SCHEDULES

The methodologies described in Chapter III are applied in this chapter in order to revamp the emergency operation schedules (EOS) for the Addicks and Barker Reservoir system. Both methods were used to develop two sets of EOS, one based on the Maximum Storage Capacity (MSC) of the reservoirs and one based on the storage capacity that is available within the Government Owned Land (GOL) limits. The original EOS were developed in the 1940's as part of the design process for the reservoirs and they are included in their 1962 reservoir regulation manual (USACE 1962). The latest information regarding the elevation-storage relationship and outlet works rating curve of the reservoirs, along with a revised recession constant (T_s) are used here to update the original EOS using the USACE standard method. A comparison of the original and updated EOS is also presented.

The application of the REOS methodology for developing a series of alternative risk-based EOS is presented in the second major section of this chapter. A critical aspect of this novel approach is the proper generation of synthetic streamflow data. The mathematical structure of the selected stochastic streamflow generation models is described followed by the identification, estimation, and validation of the models. Several sample results are then presented and compared in order to evaluate the variation in emergency release policies as a function of parameters like the antecedent streamflow conditions, time of year, and the risk of failing to attain the emergency operation objectives.

5.1. EMERGENCY OPERATION SCHEDULES BASED ON THE USACE STANDARD METHOD

The first step in the application of the standard method is to obtain the recession constant (T_s) that will be used in the expected inflow volume computations. The

spillway-design flood (SDF) recession is typically used to determine T_s. The SDF for Addicks and Barker Reservoirs is equivalent to their probable maximum flood. The SDF reflects the runoff resulting from the spillway-design storm centered over each watershed above the dams. This hypothetical storm would produce approximately 43 inches of rain in 72 hours (USACE 1977). The resulting SDF hydrographs are presented in Figure 5.1.

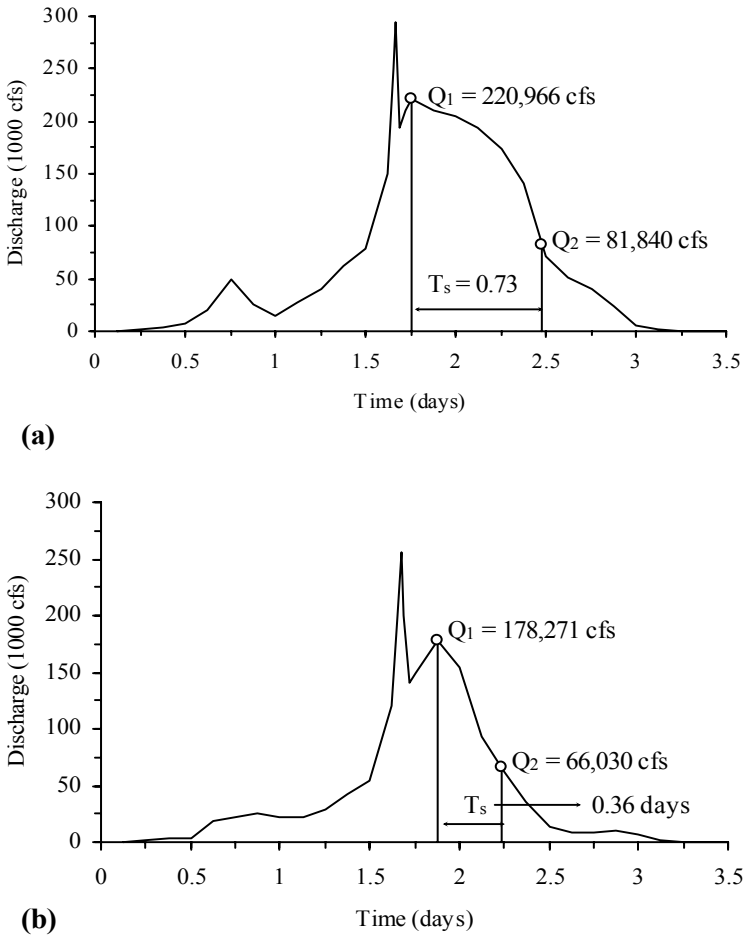

FIGURE 5.1. Spillway-Design Flood Hydrographs. (a) Addicks; and (b) Barker (Source: USACE 1977)

The SDF peak discharge values were not used as the initial value of the recession limb, since, in both cases, the recession was quickly interrupted, and a second peak was observed in the hydrographs. The value for T_s was read from the hydrographs as the time required for the recession to decrease from the second peak (Q_1) to a value Q_2 equal to $Q_1/2.7$ (see Chapter III, section 3.2.2). The values for Q_1 and Q_2 for Addicks are 220,966 and 81,840 cfs respectively, and 178,271 and 66,030 cfs for Barker. The adopted T_s values are 0.73 and 0.36 days for Addicks and Barker respectively (Figure 5.1). A computer program named SEOS (Standard Emergency Operation Schedules) was created to perform the necessary computations to develop the updated EOS for Addicks and Barker Reservoirs. The updated EOS were developed in tabular format for initial inflows of 1,000 to 300,000 cfs at increments of 1,000 cfs. Graphical EOS for selected initial inflows are presented in Figure 5.2. The upper limits of 112 and 106 ft in the EOS correspond to the MSC of the reservoirs, which is 200,800 acre-ft for Addicks and 209,000 acre-ft for Barker. Each curve forming the EOS indicates the required emergency releases as a function of the current water surface elevation (WSE) and inflow rate.

5.1.1. Sensitivity of the EOS to the T_s Value

Taking into account that the computations for T_s depend on an arbitrary selection of the initial value of the recession limb (Q_1), two additional T_s values were determined in order to compare the resulting EOS and evaluate their sensitivity to changes in T_s. These values were obtained by considering two of the subsequent inflow values after the second peak of the SDF as Q_1. The computations for all T_s values are reported in Table 5.1 and the resulting EOS based on the additional T_s values are presented in Figures 5.3 and 5.4. T_s may be seen as an indication of how fast inflows will recede after they have peaked. Smaller T_s values indicate a faster recession, and thus, less inflow volume would result for a given initial inflow rate. Notice then that as T_s decreases, the EOS curves shift upward. This shift indicates that there is a reduction in the required outflow rate for any given WSE and inflow rate. A comparison of the required outflow

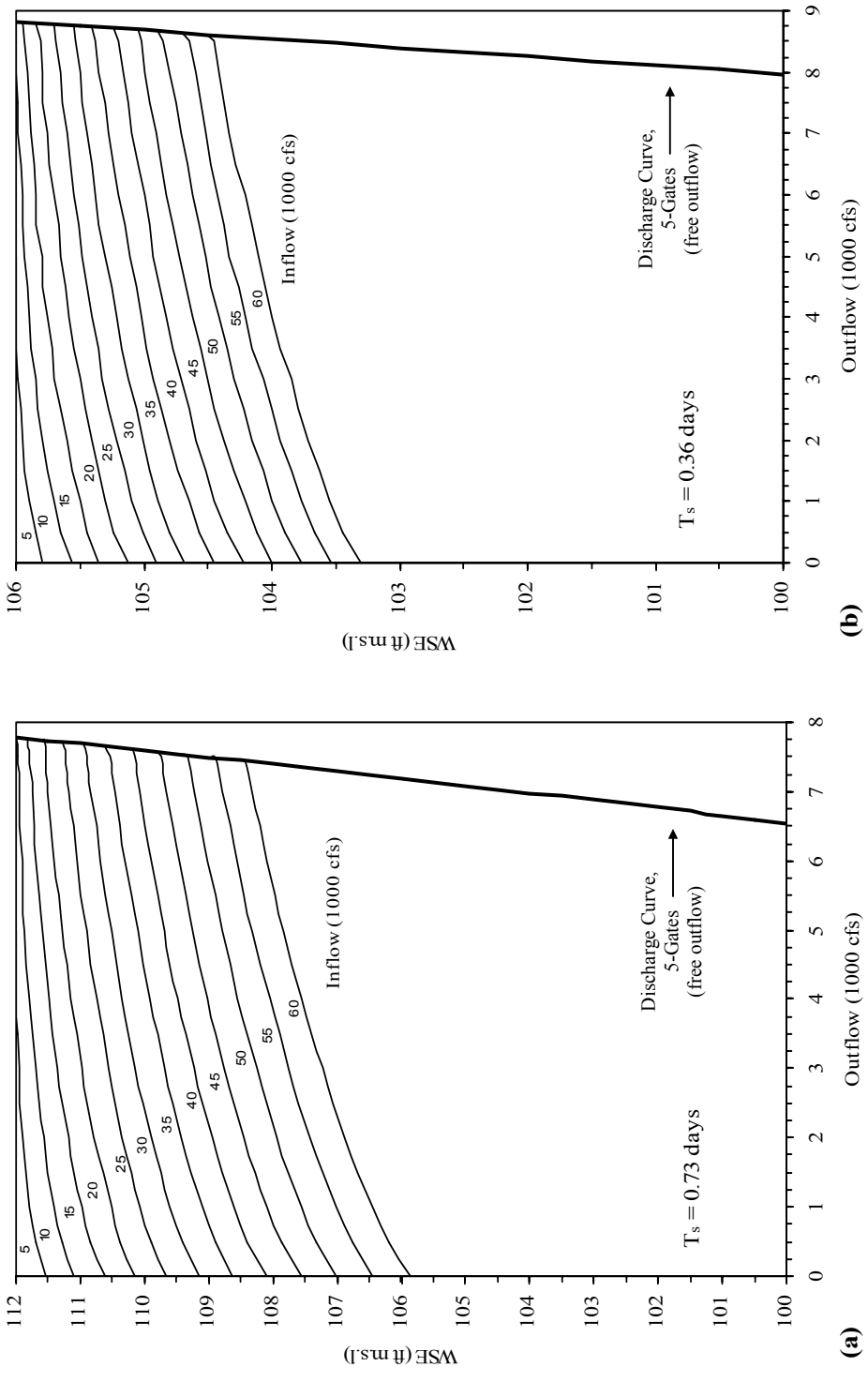

FIGURE 5.2. Standard Emergency Operation Schedules Based on the Maximum Storage Capacity of the Reservoirs. (a) Addicks: Ts = 0.73 Days; and (b) Barker: Ts = 0.36 Days

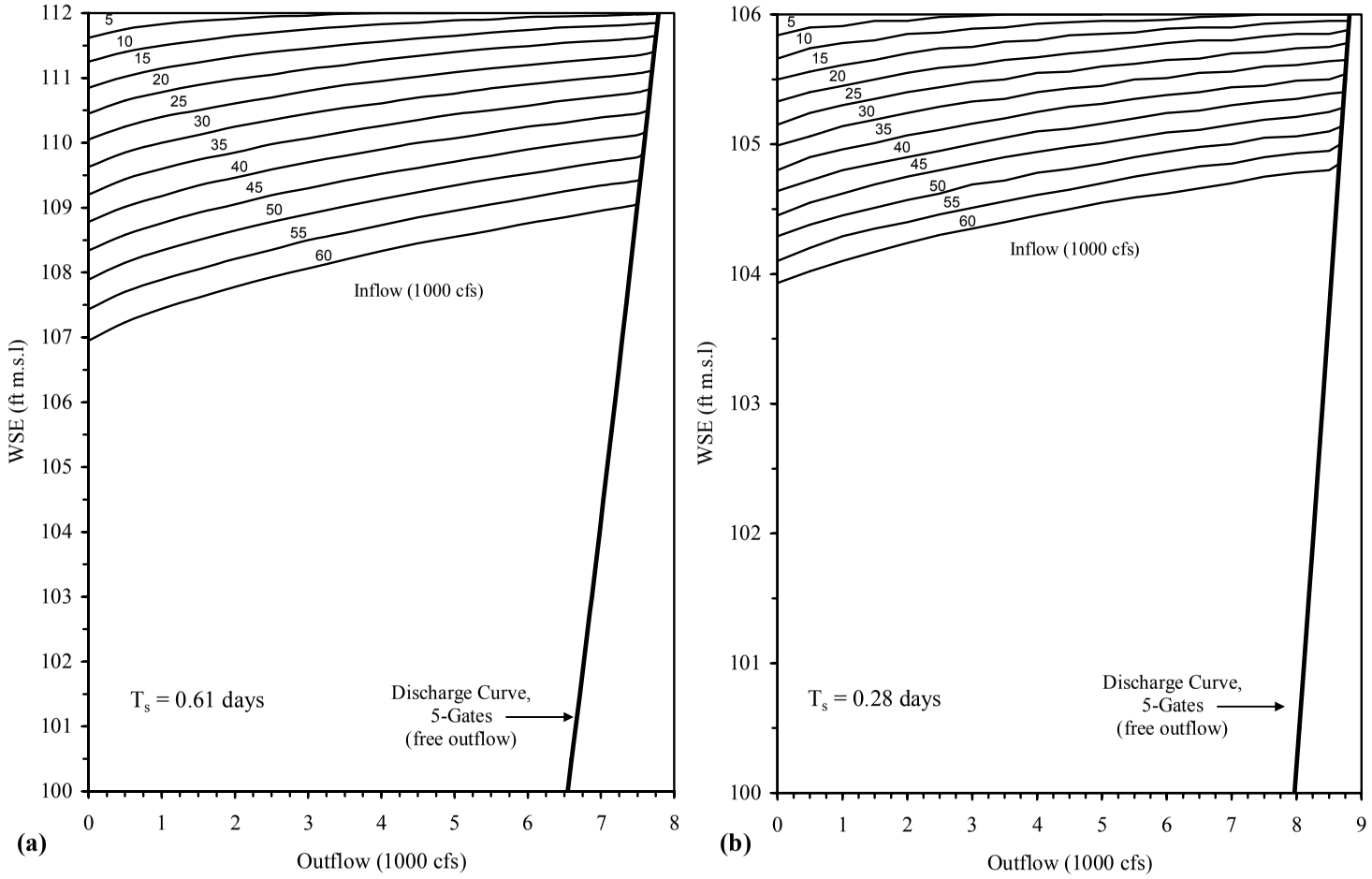

FIGURE 5.3. Standard Emergency Operation Schedules. (a) Addicks: T_s = 0.61 Days; and (b) Barker: T_s = 0.28 Days

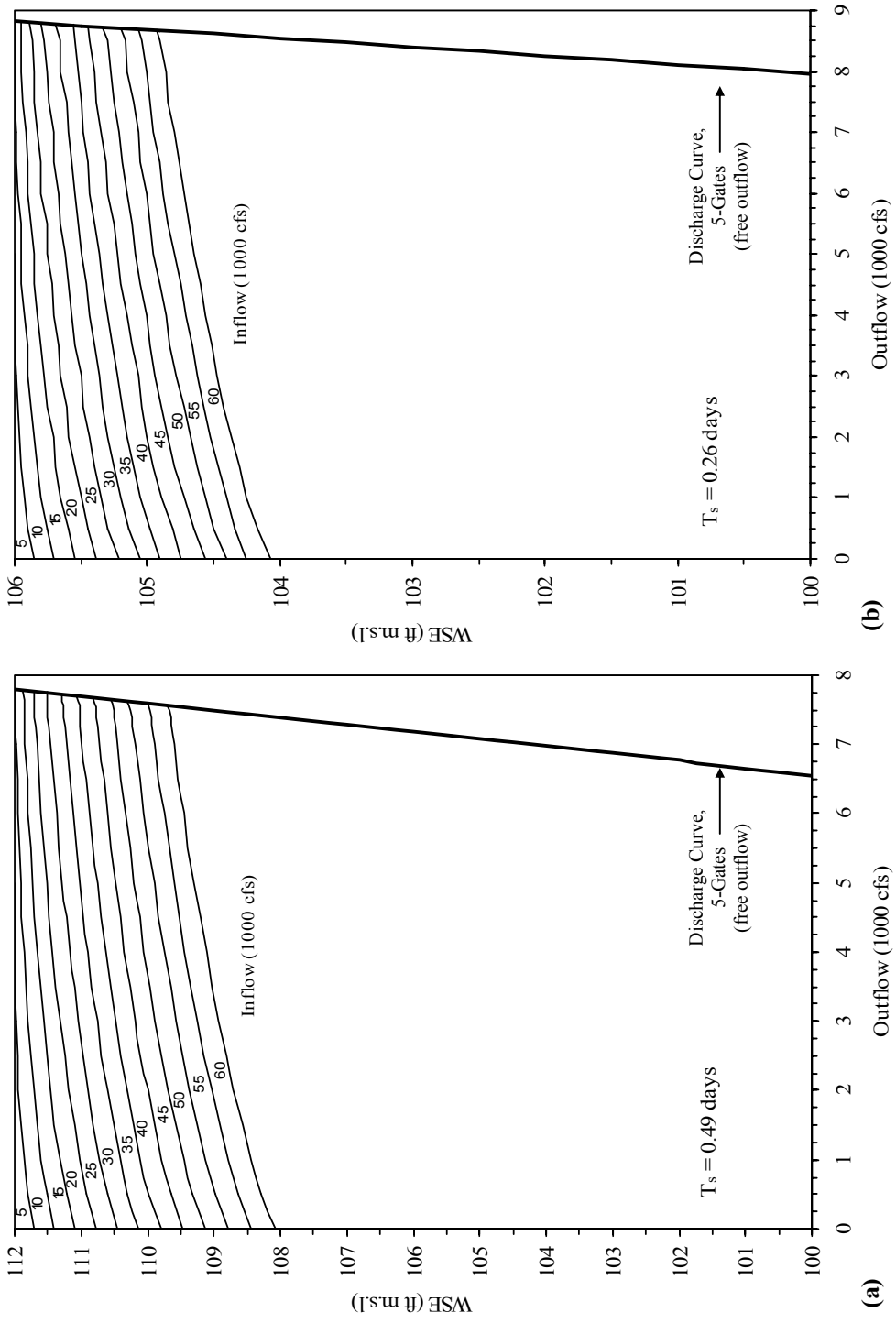

FIGURE 5.4. Standard Emergency Operation Schedules. (a) Addicks: T_s = 0.49 Days; and (b) Barker: T_s = 0.26 Days

TABLE 5.1. Recession Constant (T_s) Computations

Reservoir (1)	Q_1 (cfs) (2)	Q_2 (cfs) (3)	T_1 (days) (4)	T_2 (days) (5)	$T_s = T_2 - T_1$ (days) (6)
Addicks	220,966	81,839	1.75	2.48	0.73
	210,000	77,778	1.88	2.49	0.61
	205,000	75,926	2.00	2.49	0.49
Barker	178,271	66,026	1.88	2.24	0.36
	154,000	57,037	2.00	2.28	0.28
	94,000	34,815	2.13	2.39	0.26

NOTES: Col. (3) = Col. (1)/2.7
Col. (4) and (5) = Time corresponding to Q_1 and Q_2 respectively.

rates for selected WSE and inflow rates is presented in Tables 5.2 and 5.3 for Addicks and Barker respectively. The outflow rates in columns (3) through (5) were read off the EOS in Figures 5.2 – 5.4. Columns (6) and (7) show the difference between the outflow rates in column (3) and those in columns (4) and (5) respectively. Columns (8) and (9) express this difference as the percentage of outflow reduction relative to column (3).

Tables 5.2 and 5.3 show that, as stated above, the effect of reducing T_s is a reduction of the required outflow rate for any given initial condition. However, keynote here is the magnitude of this reduction. Notice that there is a significant change in outflow rates even if the difference in T_s is relatively small. For instance, the difference between the T_s values in columns (3) and (4) for Barker (Table 5.3) is only 0.08 days, yet the decrease in outflow rates ranges from 31.3 to 100% (column (8)). Observe also that there is a greater reduction in outflow rates (columns (6) and (7)) as the initial inflow increases for a given WSE, as well as when the WSE increases for a given initial inflow. An exception to this pattern however is observed in column (6) of Table 5.2 for WSE of 111 ft and initial inflow of 30,000 cfs. The unadjusted outflow rate for this reservoir

TABLE 5.2. Comparison of the Required Outflow Rates for Selected Initial Conditions for Addicks

WSE (ft above m.s.l.) (1)	Initial Inflow (1000 cfs) (2)	Outflow (cfs) for Ts (days) = 0.73 (3)	= 0.61 (4)	= 0.49 (5)	Reduction in Outflow (cfs) Col.(3) - Col.(4) (6)	Col.(3) - Col.(5) (7)	Reduction in Outflow (%) $\frac{\text{Col.(6)}}{\text{Col.(3)}} * 100$ (8)	$\frac{\text{Col.(7)}}{\text{Col.(3)}} * 100$ (9)
108	45	775	0	0	775	775	100.0	100.0
	50	2,136	182	0	1,955	2,136	91.5	100.0
	55	3,863	1,364	0	2,500	3,863	64.7	100.0
	60	5,637	2,750	0	2,887	5,637	51.2	100.0
109	35	775	0	0	775	775	100.0	100.0
	40	2,173	500	0	1,673	2,173	77.0	100.0
	45	4,000	1,818	0	2,182	4,000	54.5	100.0
	50	5,955	3,364	500	2,591	5,455	43.5	91.6
110	25	818	0	0	818	818	100.0	100.0
	30	2,500	1,000	0	1,500	2,500	60.0	100.0
	35	4,409	2,636	545	1,773	3,864	40.2	87.6
	40	6,500	4,500	2,000	2,000	4,500	30.8	69.2
111	15	1,091	455	0	636	1,091	58.3	100.0
	20	3,136	2,091	909	1,045	2,227	33.3	71.0
	25	5,500	4,364	2,636	1,136	2,864	20.7	52.1
	30	**7,689**	6,909	4,750	780	2,939	10.1	38.2

NOTES: Values in bold in Col.(3) indicate that the required outflow is limited by the capacity of the outlet works at that reservoir stage.

TABLE 5.3. Comparison of the Required Outflow Rates for Selected Initial Conditions for Barker

WSE (ft above m.s.l.) (1)	Initial Inflow (1000 cfs) (2)	Outflow (cfs) for Ts (days) = 0.36 (3)	= 0.28 (4)	= 0.26 (5)	Reduction in Outflow (cfs) Col.(3) - Col.(4) (6)	Col.(3) - Col.(5) (7)	Reduction in Outflow (%) $\frac{\text{Col.(6)}}{\text{Col.(3)}} * 100$ (8)	$\frac{\text{Col.(7)}}{\text{Col.(3)}} * 100$ (9)
104	45	0	0	0	0	0	--	--
	50	1,000	0	0	1,000	1,000	100.0	100.0
	55	2,500	0	0	2,500	2,500	100.0	100.0
	60	4,000	400	0	3,600	4,000	90.0	100.0
104.5	45	3,000	250	0	2,750	3,000	91.7	100.0
	50	4,750	1,400	500	3,350	4,250	70.5	89.5
	55	6,750	2,800	1,850	3,950	4,900	58.5	72.6
	60	8,600	4,500	3,250	4,100	5,350	47.7	62.2
105	25	500	0	0	500	500	100.0	100.0
	30	1,900	0	0	1,900	1,900	100.0	100.0
	35	3,750	1,400	600	2,350	3,150	62.7	84.0
	40	6,000	3,000	2,000	3,000	4,000	50.0	66.7
105.5	15	1,000	0	0	1,000	1,000	100.0	100.0
	20	3,000	1,500	1,000	1,500	2,000	50.0	66.7
	25	5,250	3,400	2,800	1,850	2,450	35.2	46.7
	30	8,000	5,500	5,000	2,500	3,000	31.3	37.5

condition is 8,326 cfs. This value was reduced to 7,689 cfs which is the maximum discharge at this reservoir stage, thereby reducing the value in column (6) from 1,417 cfs to 780 cfs. These results indicate that the EOS are fairly sensitive to T_s and that the effects of changing T_s are more pronounced as the reservoir conditions worsen (i.e. higher WSE and/or higher inflows).

Clearly, each of the EOS presented thus far recommends a significantly different operation of the reservoirs. For example, by comparing the outflow values in columns (3) through (5) we observe that there are various instances in which the EOS developed with the adopted T_s would require considerable reservoir releases in order to avoid dam overtopping, but the other EOS indicate that the reservoir would be able to accommodate the remainder of the flood without making any releases. Therefore, the critical decision of making emergency releases that would contribute to downstream flooding and the magnitude of such releases are greatly affected by the selection of T_s.

5.1.2. Reproducing the Original EOS

The original EOS were developed in the 1940's as part of the design process for the reservoirs and they were included as Plates 14 and 15 of the 1962 reservoir regulation manual (USACE 1962). Several unexpected difficulties were encountered in the process of reproducing these schedules. Inconsistencies were found in the data that is provided in the regulation manual concerning the adopted T_s values. The manual indicates that the T_s values used to develop the EOS were 0.5 and 1.1 days, for Addicks and Barker respectively. However, these values are not in accordance with those obtained by analyzing the original SDF hydrographs (Figure 5.5). Table 5.4 shows the T_s values computed from the original SDF using the peak discharge and two subsequent inflows after the peak as Q_1. None of these values match the ones in the regulation manual. Assuming then that the T_s values in the regulation manual were correct but that they were determined using a different hydrograph or a different method, the standard method was applied in order to find if the schedules could be reproduced. It was found that these values are not accurate, since the resulting schedules were significantly different

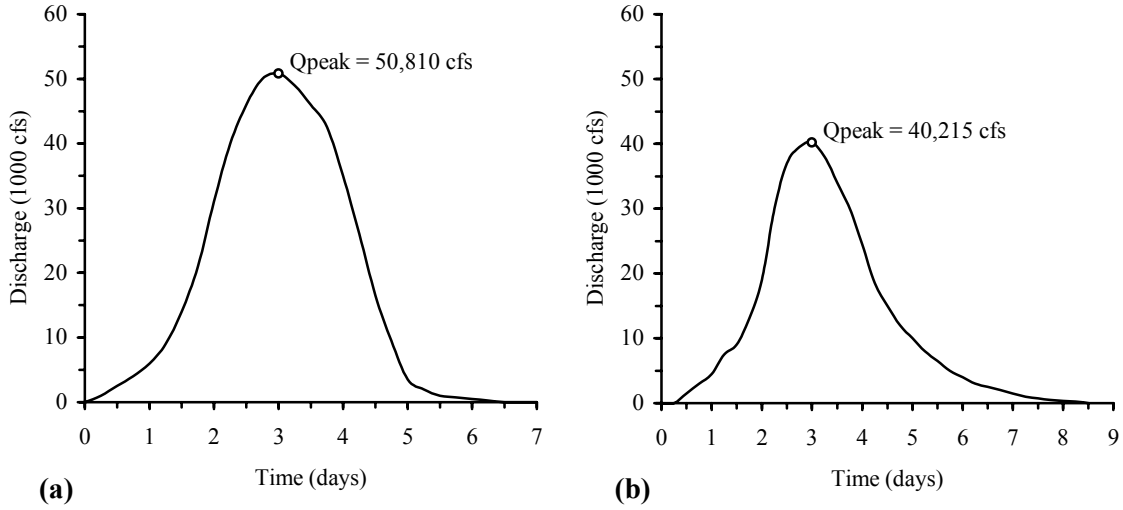

FIGURE 5.5. Original Spillway-Design Flood (SDF) Hydrographs. (a) Addicks; and (b) Barker (Source: USACE 1962)

TABLE 5.4. Recession Constant (T_s) Computations Based on the Original SDF

Reservoir (1)	Q_1 (cfs) (2)	Q_2 (cfs) (3)	T_1 (days) (4)	T_2 (days) (5)	$T_s = T_2 - T_1$ (days) (6)
Addicks	50,810	18,819	3.00	3.96	0.96
	49,000	18,148	3.25	4.12	0.87
	46,000	17,037	3.50	4.24	0.74
Barker	40,215	14,894	3.00	4.50	1.50
	38,000	14,074	3.25	4.59	1.34
	34,000	12,593	3.50	4.70	1.20

NOTES: Ts from 1962 Regulation Manual = 0.50 for Addicks and 1.10 for Barker
Col. (3) = Col. (1)/2.7
Col. (4) and (5) = Time corresponding to Q_1 and Q_2 respectively.

from those in the regulation manual. Subsequently, EOS were developed based on the T_s values in Table 5.4, but the results were also unsatisfactory. Since the schedules could not be reproduced based on these T_s values, a backwards procedure was adopted in which the WSE corresponding to several outflows were read off the original EOS for each inflow curve and they were used to solve for T_s by reversing the standard method computations. The results demonstrated that no particular T_s can be used to reproduce the entire EOS. Further investigation allowed to discover that if a different T_s value is used for each of the constant outflows being evaluated, then the schedules could be closely reproduced. Recall from Chapter III that the series of WSE forming the EOS are determined for each initial inflow rate given a constant outflow rate. This process was repeated for various outflow rates using the T_s that would result in WSE values for each initial inflow that would match those in the original EOS. The appropriate T_s values were found via optimization. The resulting EOS, along with the T_s for each outflow rate, are presented in Figure 5.6. Although these values can be used to develop EOS that closely resemble those in the regulation manual, it is not clear whether the original EOS were developed in this manner.

5.1.3. Comparison of the Original and Updated EOS

The original EOS were developed in the 1940's as part of the design process for the reservoirs and they were included as Plates 14 and 15 of the 1962 reservoir regulation manual (USACE 1962). The design of the reservoirs was based on historical rainfall data and the hydrologic characteristics of the watersheds at that time. The total rainfall produced by the original spillway design storm was approximately 30 inches of rain in 72 hours. The updated EOS presented herein were based on the spillway design storm developed in 1977, which produced 43 inches of rain in 72 hours (USACE 1977). For comparison purposes, both of the resulting SDF hydrographs are plotted in Figure 5.7. The vast difference between these hydrographs in terms of their magnitude and shape, accounts for the difference between the adopted T_s values and ultimately, between the original and the updated EOS.

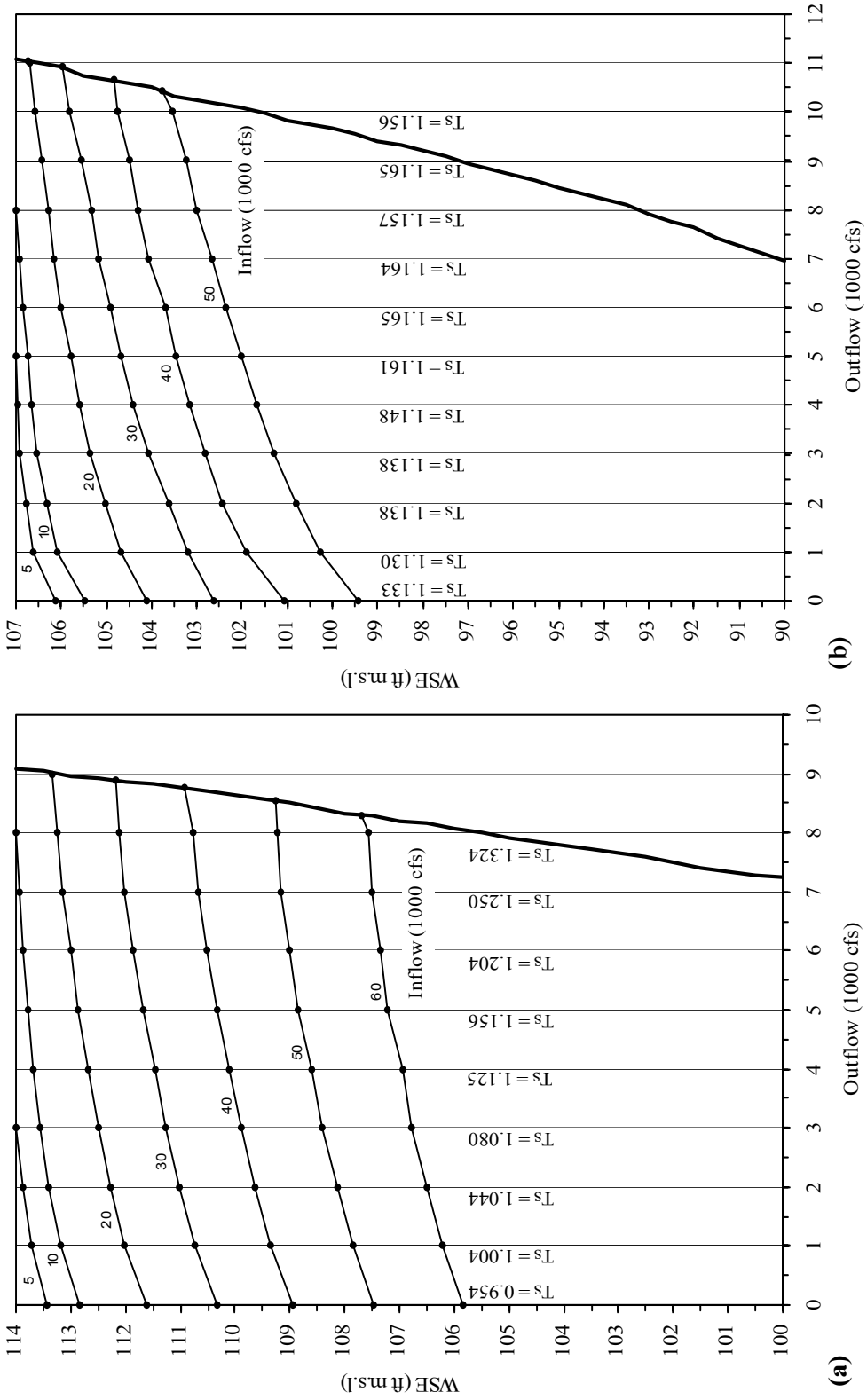

FIGURE 5.6. Reproduction of the Original Emergency Operation Schedules Using Various T_s Values. (a) Addicks; and (b) Barker

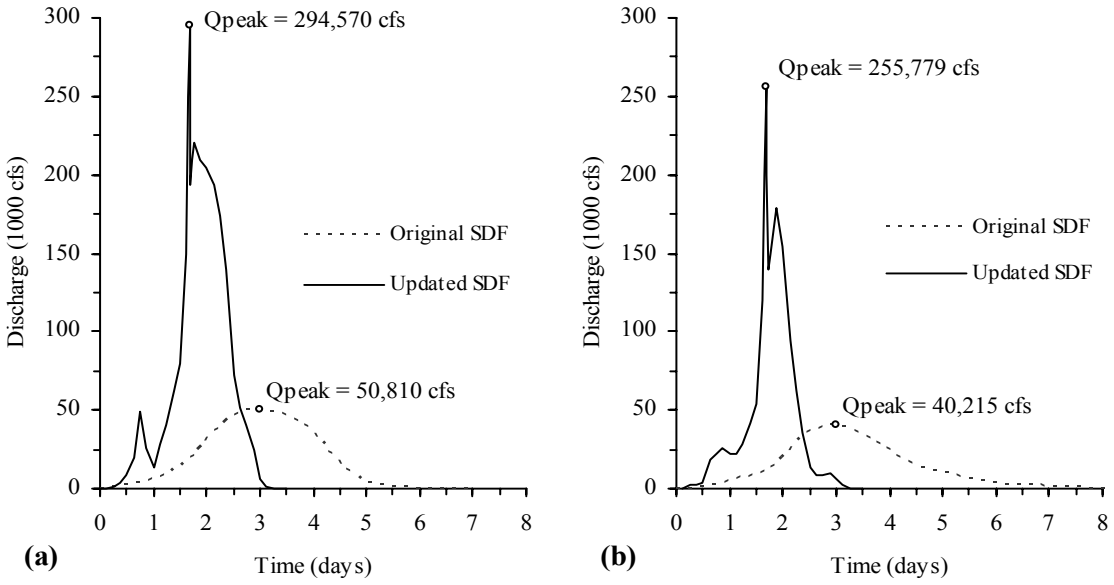

FIGURE 5.7. Original and Updated Spillway-Design Flood (SDF) Hydrographs. (a) Addicks; and (b) Barker (Source: USACE 1962; USACE 1977)

The original EOS presented in Figure 5.6 were modified according to the 1973 datum adjustment and were superimposed with the updated EOS (Figure 5.8). This figure reiterates what was stated in section 5.1.1, namely, that the effects of developing the EOS with a different T_s value are more evident as the reservoir initial conditions worsen. Notice that for Addicks the 5,000 and 10,000 cfs curves are very close to each other, but as the inflow increases the separation between the curves also increases. The much larger differences observed in the Barker EOS curves reflects the large disparity between the adopted T_s in the updated curves (0.36 days) and any of the values used to reproduce the original EOS (1.130 – 1.165 days). The adopted value indicates a much faster recession rate, and thus, the updated curves are much more conservative than the original curves.

Evidently, the operating rules suggested by these schedules would result in considerably different release decisions for a given reservoir condition. For instance, consider the reservoir stages associated with the zero outflow points in the curves.

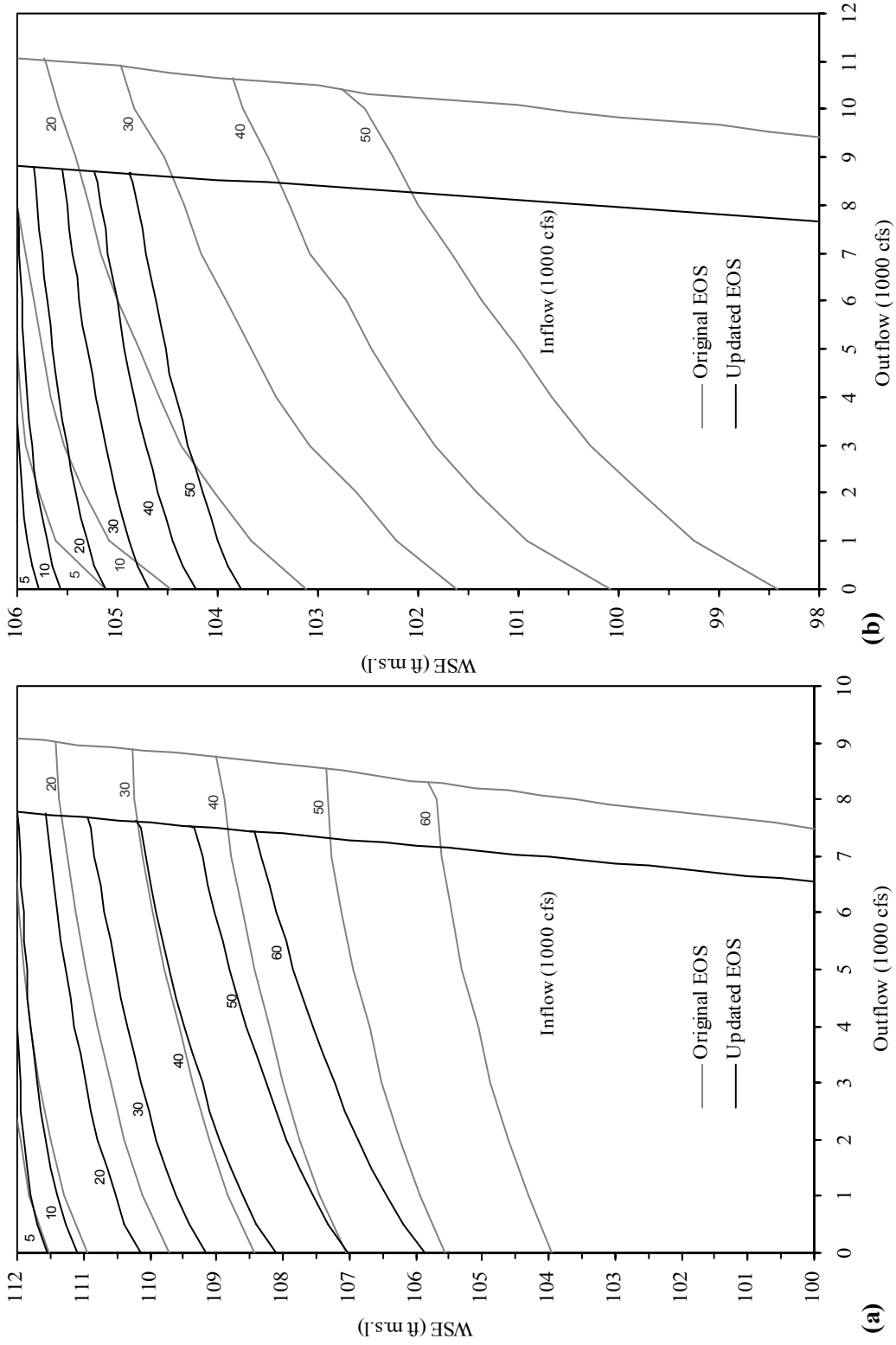

FIGURE 5.8. Original and Updated Emergency Operation Schedules. (a) Addicks; and (b) Barker

These stages represent the maximum initial stage (MIS) at which the reservoir outlet gates can remain closed and yet the reservoir would still be able to accommodate the remainder of the flood. The MIS is a critical component of the EOS since it can be considered as a trigger that indicates the transition from normal to emergency operations. A comparison of these values is presented in Tables 5.5 and 5.6 for Addicks and Barker respectively. These tables show that the transition from normal to emergency operations would occur at lower stages with the original EOS. In other words, the updated EOS allows higher reservoir stages before any emergency releases are made. For example, based on the original EOS, if the current inflow rate is 50,000 cfs, emergency releases would be necessary if the WSE at Addicks is above 105.6 ft and above 98.4 ft at Barker (the reservoirs have been filled to 54.6 and 46.5% of the MSC, respectively (column (7)). On the other hand, the updated EOS indicates that for the same inflow, emergency releases would only be necessary if the WSE at Addicks is above 107 ft (1.4 ft higher) and above 103.8 ft (5.4 ft higher) at Barker (63.7 and 82.8% of the MSC, respectively (column (8)).

To further explore the differences between these schedules, a comparison of the required outflow rates for selected WSE and inflow rates is presented in Tables 5.7 and 5.8 for Addicks and Barker respectively. The outflow rates in columns (3) and (4) were read off the EOS in Figure 5.8. Column (5) shows the difference between the outflow rates required by the original and the updated EOS. Column (6) expresses this difference as the percentage of outflow reduction relative to column (3). These tables demonstrate that the actual operation of the reservoirs would be drastically different depending on which EOS is implemented. For instance, for a WSE at Addicks of 106 ft and an inflow rate is 60,000 cfs, the original EOS requires a release of 7,192 cfs, while the updated EOS only requires 216 cfs, a difference of 6,976 cfs. Even greater differences are observed for Barker. Notice that there are two conditions (WSE = 104 ft and inflow = 40,000 cfs; WSE = 104.5 ft and inflow = 30,000 cfs) for which the original EOS indicates that the reservoir outlet works should be completely opened while the updated EOS indicates that no releases are necessary. Clearly, such operational differences

TABLE 5.5. Comparison of the Maximum Initial Stage (MIS) for the Original and Updated EOS for Addicks

Inflow	MIS (ft above m.s.l.)			MIS (acre-ft)		Percent of MSC[†]	
(1000 cfs)	Original	Updated	Difference[‡]	Original	Updated	Original	Updated
(1)	(2)	(3)	(4)	(5)	(6)	(7)	(8)
5	111.5	111.6	0.1	193,201	193,523	96.2	96.4
10	110.9	111.1	0.2	183,836	186,351	91.6	92.8
20	109.7	110.2	0.5	165,291	171,701	82.3	85.5
30	108.4	109.2	0.8	146,720	157,003	73.1	78.2
40	107.0	108.1	1.1	128,217	142,322	63.9	70.9
50	105.6	107.0	1.6	109,621	127,828	54.6	63.7
60	104.0	105.9	1.9	90,897	113,166	45.3	56.4

NOTES: Stage values in Col. (2,3) are given in feet above mean sea level.

[‡]Col. (4) = Col.(3) - Col.(2)

[†]MSC = Maximum Storage Capacity = 200,800 acre-ft.

TABLE 5.6. Comparison of the Maximum Initial Stage (MIS) for the Original and Updated EOS for Barker

Inflow	MIS (ft above m.s.l.)			MIS (acre-ft)		Percent of MSC[†]	
(1000 cfs)	Original	Updated	Difference[‡]	Original	Updated	Original	Updated
(1)	(2)	(3)	(4)	(5)	(6)	(7)	(8)
5	105.1	105.8	0.7	194,655	205,510	93.1	98.3
10	104.5	105.6	1.1	183,878	201,700	88.0	96.5
20	103.1	105.1	2.0	163,219	194,492	78.1	93.1
30	101.6	104.8	3.2	141,086	189,155	67.5	90.5
40	100.1	104.2	4.1	119,234	180,078	57.0	86.2
50	98.4	103.8	5.4	97,234	173,038	46.5	82.8

NOTES: Stage values in Col. (2,3) are given in feet above mean sea level.

[‡]Col. (4) = Col.(3) - Col.(2)

[†]MSC = Maximum Storage Capacity = 209,000 acre-ft.

TABLE 5.7. Comparison of the Required Outflow Rates for Selected Initial Conditions Based on the Original and Updated EOS for Addicks

WSE (ft above m.s.l.) (1)	Initial Inflow (1000 cfs) (2)	Outflow (cfs)		Reduction in Outflow (cfs)	Reduction in Outflow (%)
		Original EOS (3)	Updated EOS (4)	Col.(3) - Col.(4) (5)	$\frac{\text{Col.(5)}}{\text{Col.(3)}} * 100$ (6)
106	50	1,182	0	1,182	100.0
	60	**7,192**	216	6,976	97.0
107	50	5,324	0	5,324	100.0
	60	**7,294**	2,324	4,970	68.1
108	40	3,000	0	3,000	100.0
	50	**7,395**	2,162	5,233	70.8
	60	**7,395**	5,649	1,746	23.6
109	30	1,649	0	1,649	100.0
	40	**7,494**	2,162	5,332	71.2
	50	**7,494**	5,919	1,575	21.0
110	20	703	0	703	100.0
	30	6,324	2,487	3,837	60.7
	40	**7,593**	6,649	944	12.4
111	10	190	0	190	100.0
	20	5,216	3,162	2,054	39.4

NOTES: Values in bold in Col.(3) indicate that the required outflows are limited by the capacity of the outlet works at that water surface elevation.

would have a substantial impact in terms of the potential for contributing to downstream flooding considering that the downstream channel capacity at Piney Point is only 2,000 cfs. The tradeoff here is that although the updated EOS would provide a much larger degree of protection to downstream areas, this conservative schedule could be rather risky from the perspective of dam overtopping. The smaller releases would only be appropriate if the flood recedes as quickly as is indicated by the adopted T_s. If this is not the case, the residual storage capacity may not be sufficient to accommodate the remainder of the flood and avoid dam overtopping. This comparison highlights one of the major limitations of the standard method, namely, developing the EOS assuming that one T_s value is appropriate to describe the recession characteristics of every inflow hydrograph.

TABLE 5.8. Comparison of the Required Outflow Rates for Selected Initial Conditions Based on the Original and Updated EOS for Barker

WSE (ft above m.s.l.) (1)	Initial Inflow (1000 cfs) (2)	Outflow (cfs)		Reduction in Outflow (cfs)	Reduction in Outflow (%) $\frac{\text{Col.(5)}}{\text{Col.(3)}} * 100$
		Original EOS (3)	Updated EOS (4)	Col.(3) - Col.(4) (5)	(6)
103	30	2,813	0	2,813	100.0
	40	6,750	0	6,750	100.0
103.5	20	688	0	688	100.0
	30	4,313	0	4,313	100.0
104	40	**8,542**	0	8,542	100.0
	50	**8,542**	1,000	7,542	88.3
104.5	30	**8,616**	0	8,616	100.0
	40	**8,616**	1,375	7,241	84.0
	50	**8,616**	4,625	3,991	46.3
105	20	6,000	0	6,000	100.0
	30	**8,679**	1,875	6,804	78.4
	40	**8,679**	6,000	2,679	30.9
105.5	10	2,813	0	2,813	100.0
	20	**8,747**	3,000	5,747	65.7
	30	**8,747**	8,000	747	8.5

NOTES: Values in bold in Col.(3) indicate that the required outflows are limited by the capacity of the outlet works at that water surface elevation.

5.1.4. EOS Based on the Government Owned Land (GOL) Storage Limit

The Addicks and Barker Reservoir system is characterized by the peculiar situation of having urban development within their flood control pools (see Chapter IV, sections 4.3 and 4.5). The federal government purchased reservoir lands for flood detention purposes up to an elevation of 106.1 ft at Addicks and 97.3 ft at Barker. Although urban development is restricted within the GOL, extensive urban development has occurred in the fringe areas between the upper limits of the GOL and the maximum pool levels. Thus, the GOL upper limits indicate the elevation above which residential and commercial properties are susceptible to flooding. Although the storage levels in the reservoirs have never exceeded the GOL limits, the foreseeable socioeconomic impacts of upstream flooding are a major concern to the agencies responsible for flood

management in the Houston area and have prompted the evaluation of operational changes that would help prevent such a situation.

The EOS presented so far were developed based on the MSC of the reservoirs. Since Addicks and Barker have, respectively, 42 and 60% of their total storage capacity above the GOL limits, the occurrence of emergency releases would be unlikely under most flooding conditions even when reservoir stages have already exceeded the GOL limits. In other words, under the current emergency operation policies the possible occurrence of upstream flooding does not justify making emergency releases. An alternative policy which would allow emergency releases at reservoir stages below the GOL is presented in this section. In contrast to the typical emergency operations objective of avoiding dam overtopping, the objective of this policy is to prevent flood damages to upstream structures. In accordance with this objective, a new set of EOS were developed by setting the maximum allowable reservoir stage at the GOL limits (Figure 5.9). This modification results in a significant reduction of the available flood storage capacity of the reservoirs, and thus, emergency releases would be allowed at considerably lower stages. For instance, for an inflow rate of 50,000 cfs the EOS in Figure 5.2 would dictate emergency releases if the WSE at Addicks is above 105.6 ft and above 98.4 ft at Barker, while the EOS in Figure 5.9 would dictate emergency releases if the WSE at Addicks is above 98.7 ft and above 94.1 ft at Barker; a difference of 6.9 and 4.3 ft respectively. The operation of the reservoirs based on this alternative policy provides a greater degree of protection to upstream structures, but at the same time, it allows for a greater risk of making releases in excess of the downstream channel capacity. This tradeoff presents a potential conflict of interests in which serious complaints or even lawsuits from downstream dwellers may arise since the policy allows emergency releases even though the reservoirs still have a significant amount of available storage capacity. A more detailed evaluation of the operation of the reservoirs and the tradeoffs inherent to these policies will be presented in later chapters.

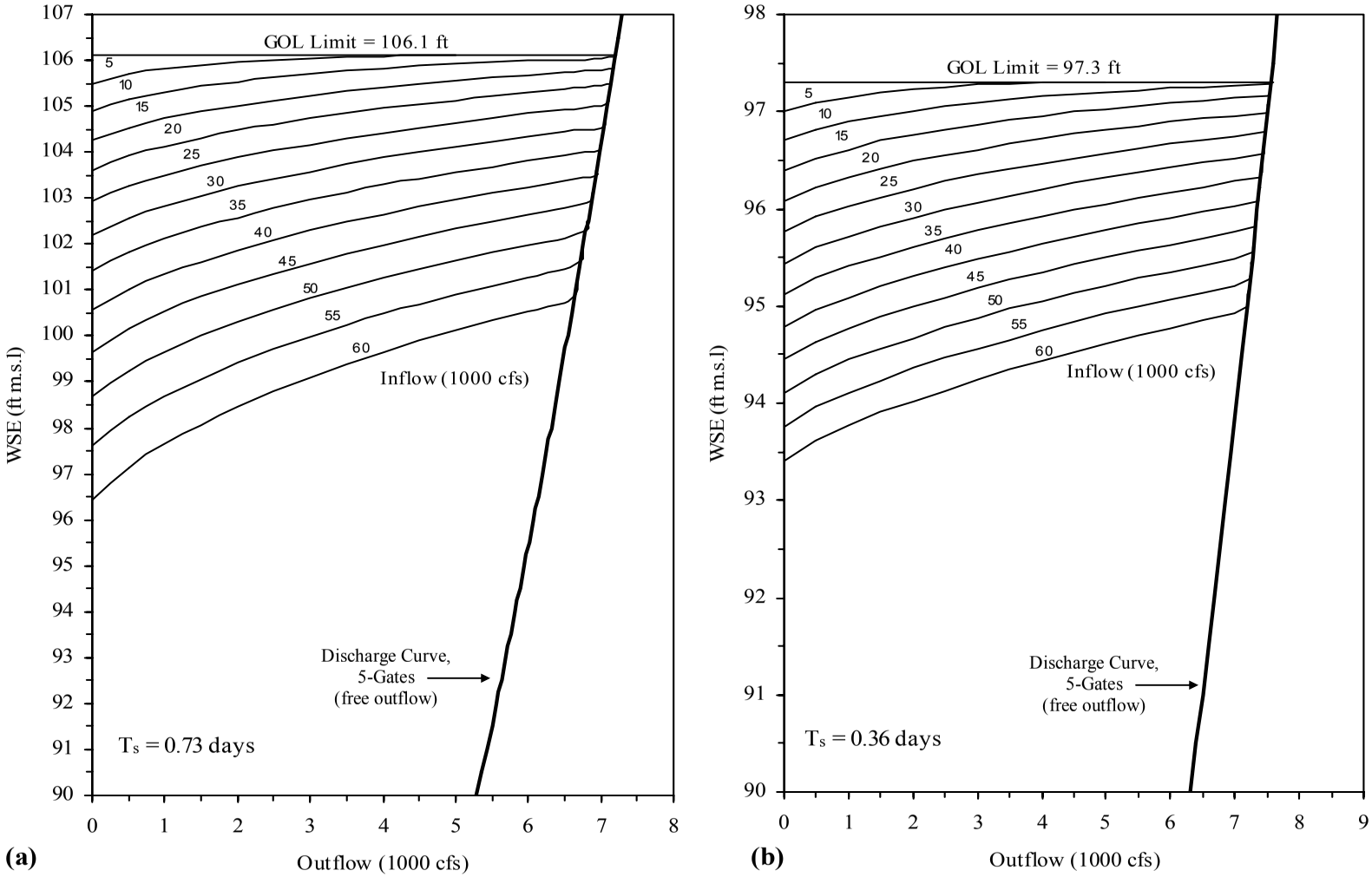

FIGURE 5.9. Standard Emergency Operation Schedules Based on the GOL Storage Capacity. (a) Addicks; and (b) Barker

5.2. RISK-BASED EMERGENCY OPERATION SCHEDULES (REOS)

One of the principal objectives of this study is to devise alternative methods for the operation of the Addicks and Barker Reservoir system under emergency conditions. The REOS method is a risk-based approach that defines the EOS based on the probability that the inflow volume that is expected to be produced by a flood would exceed the residual storage capacity in a reservoir. In contrast to the USACE standard method, the expected inflow volume is not determined based on a particular recession constant. Instead, stochastic streamflow models are used to generate a large number of inflow sequences which allows analysis of the statistical probabilities of the expected inflow volume following a given streamflow condition. Therefore, prior to the application of the REOS method a collection of streamflow generation models needs to be developed and their performance needs to be carefully evaluated in order to select the most appropriate models. The selected models are then input to the REOS computer program, which develops a series of alternative risk-based EOS that specify reservoir releases as a function of reservoir levels, inflows, and the time of year, and are associated with certain risk of failing to attain the emergency operations objectives (see Chapter III, section 3.3). Risk-based EOS will be developed based on both the MSC and GOL limits of the reservoirs.

5.2.1. Selection of the Stochastic Streamflow Generation Models

The basis of stochastic streamflow generation models is to reproduce streamflow sequences that will be statistically similar to the observed data so that they may be considered as equally likely realizations from the same population. These models are typically fitted to the observed series by matching the autocorrelation function (ACF) of the model with the ACF of the observed series. The ACF is a measure of the degree of dependence between observations as a function of their separation (lag) along the time axis (Brockwell and Davis 1996). The ACF of daily streamflows is usually characterized by a slow decay, due to the strong persistence that affects streamflows observed at fine time scales (Montanari et al. 1999). Persistence is the presence in a

time series of significant dependence between observations a long time span apart (Hosking 1984). Persistence can also be seen as the tendency for high flows to be followed by high flows, and low flows to be followed by low flows (Viessman and Lewis 1996). A process showing strong persistence, it is said to have "long memory" or "long-term dependence". The widely used autoregressive integrated moving average models (ARIMA), fully described by Box and Jenkins (1976) and Brockwell and Davis (1987), can reproduce the ACF of a time series exhibiting long memory if a high number of autoregressive parameters is introduced in the model. However, such a model would not satisfy the principle of parsimony, which refers to fitting a model using the smallest possible number of parameters that can adequately represent the process (Box and Jenkins 1976). A noteworthy solution to this problem is the use the fractional ARIMA (FARIMA) models. These models, first introduced by Granger and Joyeux (1980) and Hosking (1981), are an extension of the classic ARIMA models that allows fitting long memory ACF structures parsimoniously. The mathematical foundations of FARIMA models are fully described by Beran (1994) and by Samorodnitsky and Taqqu (1994).

The general form of a FARIMA (p, d, q) model can be expressed in Box and Jenkins (1976) notation as

$$\phi_p(B)(1-B)^d X_t = \theta_q(B) Z_t \tag{5.1}$$

where X_t is the observed (zero mean) time series, B is the backward shift operator which is defined by $BX_t = X_{t-1}$; hence $B^m X_t = X_{t-m}$, $\phi_p(B)$ is the p-order autoregressive polynomial, $\theta_q(B)$ is the q-order moving average polynomial, Z_t is the noise term, which is assumed to be uncorrelated and with zero mean, and d is the differencing order, allowed to take nonintegral values. The values for p, q, and the corresponding parameters in $\phi_p(B)$ and $\theta_q(B)$ allow for the modeling of short-term properties. The parameter d determines the long-term behavior and indicates the degree of persistence in the series, the higher d the higher the persistence. The range of interest for d in the context of long-memory processes is $0 \le d < 0.5$ (Beran 1994). If $d = 0$, the FARIMA

model reduces to a short-memory ARMA (p, q) process. Thus, a FARIMA model may be considered as a mixed model consisting of an ARMA part, which accounts for the short-term properties of an observed series, together with a fractional differencing of an appropriate order to explain any persistent long-term behavior in the series (Hosking 1984).

One important condition that has to be met before the FARIMA models can be applied is that the observed data must be stationary. The statistical properties of a stationary time series do not change over time. As stated in Section 3.3.2.1, it is difficult to satisfy this condition when dealing with daily flows, whose statistical properties change with the season or even with the month (Levin 1969; Montanari et al. 1999). Although a FARIMA model may be fitted to the entire historical data assuming that it is stationary (Montanari et al. 1997), an alternative approach is to fit a FARIMA model to the data corresponding to each month of the year (Montanari et al. 1999). In this manner, the data may be considered stationary within each month. The final model is a composition of 12 models with periodical parameters. Accordingly, the proposed formulation allows one to vary the model structure and the parameter values with the season, so as to fit separately the autocorrelation structure of each month (Montanari et al. 1999). The latter approach was adopted in this study as it allows for a more detailed representation of the streamflow processes and it brings greater flexibility in developing the EOS.

5.2.1.1. FARIMA Model Application

The FARIMA model was applied on the series of inflows of the Addicks and Barker Reservoir system. Mean daily reservoir inflows data for the period of August 22, 1945 to April 12, 1998 were included in the analysis. This data set counts 19,224 observations. Figure 5.10 shows the plots of these series. The first step in the FARIMA model application was to analyze the autocorrelation structure of the data for each month. The monthly data was collected together in chronological order and was input

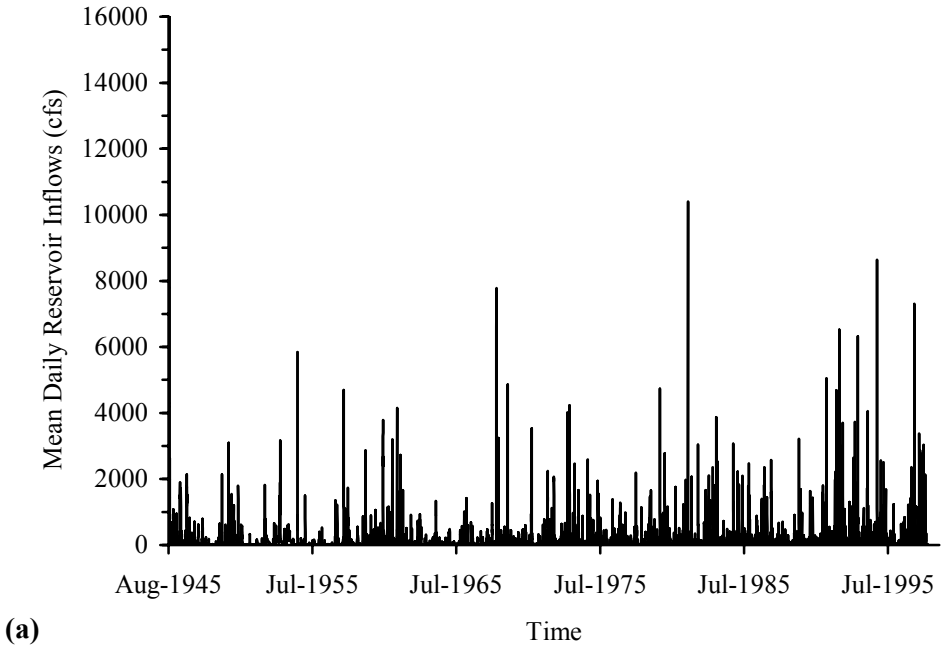

(a)

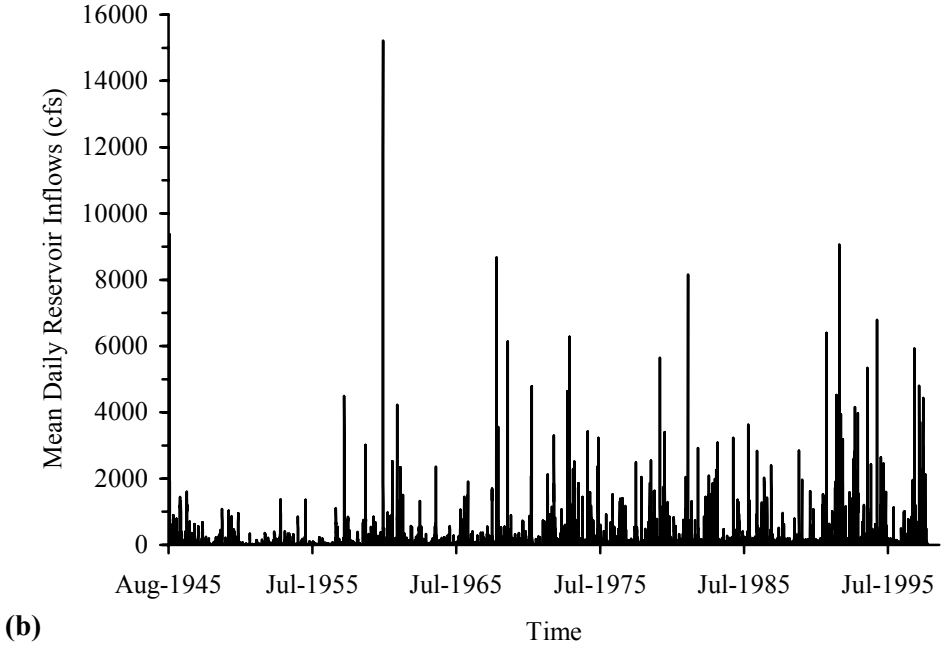

(b)

FIGURE 5.10. Mean Daily Reservoir Inflows During 1945-1998.
(a) Addicks; and (b) Barker

into the time series package ITSM2000 (Brockwell and Davis 1996). As expected, the ACF for each month were considerably different, yet they were all characterized by a slow decay suggesting the presence of long memory in the data. Developing 12 FARIMA models with periodical parameters is thus appropriate since they would be capable of fitting the different monthly slow-decaying autocorrelations.

The program ITSM2000 was used to identify the order of the autoregressive and moving average polynomials, to estimate the models parameters, and to perform goodness-of-fit tests to verify the appropriateness of the models. The program carries out the estimation of the parameters for a FARIMA model using the Whittle's approximation to the Gaussian maximum likelihood function. Details on the Whittle's approximation applied to FARIMA models are presented by Beran (1994). Daily streamflow data is typically non-Gaussian, but the estimation of FARIMA models using the Whittle estimator has been proven reliable for non-Gaussian data (Kokoszka and Taqqu 1996; Taqqu and Teverovsky 1998). Based on these findings, preliminary models were fitted to the data despite it being non-Gaussian. These models had to be discarded, however, since they were not able to reproduce streamflow sequences that were statistically similar to the observed data. In order to overcome this problem, the observed data was transformed using the Box-Cox transformation:

$$\begin{aligned} Y_t &= \left(X_t^{\lambda} - 1\right)/\lambda, & \lambda \neq 0 \\ &= \log\left(X_t\right), & \lambda = 0 \end{aligned} \tag{5.2}$$

where X_t is the original data and λ is the transformation parameter. The value for λ is selected so as to make Y_t as Gaussian as possible (Montanari et al. 1997). It was found that a transformation coefficient $\lambda = 0.5$ was satisfactory for all data sets.

The FARIMA model building procedure was applied to the transformed data for each month. The parameters for several candidate models having different p and q orders were estimated. If a model is appropriate for a given dataset, the sample and the model ACF should match closely and the model residuals should have properties consistent to

those of a white noise sequence (i.e. uncorrelated random variables). It was observed that, for the most part, only one model would satisfy these conditions; however, in the case of having more than one potential model, the model with the lowest Akaike's Information Criterion (AIC) was selected. If the model ACF matched the sample ACF closely, the next step was performing goodness-of-fit tests on the model residuals to verify whether the estimation was well-performed. The Ljung-Box test of correlation was used to evaluate the model residuals for each month (Ljung and Box 1978; Brockwell and Davis 1996). This test is a refinement of the Portmanteau test that allows one to test the null hypothesis that the residuals can be considered white noise. This test is performed by computing

$$Q_{LB} = n(n+2)\sum_{j=1}^{h} \hat{\rho}^2(j)/(n-j) \tag{5.3}$$

where Q_{LB} is the Ljung-Box statistic, n is the sample size, $\hat{\rho}(j)$ is the sample autocorrelation at lag j, and h is the degrees of freedom. The distribution for Q_{LB} is approximated by the chi-square distribution with h degrees of freedom. A large value of the Q_{LB} suggests that the sample autocorrelations of the residuals are too large for them to be considered white noise. The null hypothesis is thus rejected at significance level α if $Q_{LB} > \chi^2_{1-\alpha}(h)$, where $\chi^2_{1-\alpha}(h)$ is the $1 - \alpha$ quantile of the chi-squared distribution with h degrees of freedom ($\alpha = 0.05$ and $h = 20$ in this study). In ITSM2000, the value for Q_{LB} is given along with its corresponding p-value. The p-value is the probability that the test statistic would assume a value greater than or equal to the observed value strictly by chance. Therefore, a p-value less than α indicates rejection of the null hypothesis.

The parameters of the best fitting FARIMA models along with the corresponding p-value for the Ljung-Box test are presented in Tables 5.9 and 5.10 for Addicks and Barker, respectively. The most common models were the FARIMA(3,d,0) (12 models) and the FARIMA(2,d,0) (8 models). There are two FARIMA(3,d,1) models, both for Addicks, and one FARIMA(1,d,1) and FARIMA(2,d,1) models. The estimated values

TABLE 5.9. FARIMA Models Fitted to the Daily Streamflows for Addicks

Month (1)	Model Order (2)	φ_1 (3)	φ_2 (4)	φ_3 (5)	θ_1 (6)	d (7)	Ljung-Box test p-value (8)
Jan	(3,d,0)	0.743	-0.188	0.101	--	0.261	0.574
Feb	(3,d,0)	0.647	-0.180	0.068	--	0.266	0.122
Mar	(1,d,1)	0.486	--	--	0.018	0.270	0.292
Apr	(3,d,0)	0.734	-0.105	0.041	--	0.193	0.051
May	(2,d,0)	0.782	-0.102	--	--	0.185	0.665
Jun	(3,d,0)	0.832	-0.134	0.048	--	0.140	0.055
Jul	(2,d,0)	0.624	-0.040	--	--	0.272	0.274
Aug	(3,d,0)	0.806	-0.135	0.044	--	0.084	0.055
Sep	(3,d,0)	0.772	-0.159	0.004	--	0.250	0.655
Oct	(3,d,1)	0.907	-0.212	0.078	0.018	0.148	0.759
Nov	(3,d,1)	0.801	-0.208	0.108	-0.017	0.220	0.617
Dec	(2,d,0)	0.752	-0.130	--	--	0.250	0.063

NOTES: p-value < 0.05 indicates rejection of the null hypothesis of uncorrelated residuals at $\alpha = 0.05$.

TABLE 5.10. FARIMA Models Fitted to the Daily Streamflows for Barker

Month (1)	Model Order (2)	φ_1 (3)	φ_2 (4)	φ_3 (5)	θ_1 (6)	d (7)	Ljung-Box test p-value (8)
Jan	(2,d,0)	0.782	-0.161	--	--	0.290	0.095
Feb	(3,d,0)	0.758	-0.228	0.055	--	0.250	0.950
Mar	(3,d,0)	0.564	-0.056	0.030	--	0.267	0.077
Apr	(2,d,1)	0.950	-0.206	--	-0.094	0.137	0.025
May	(3,d,0)	0.862	-0.126	-0.043	--	0.166	0.252
Jun	(2,d,0)	0.934	-0.197	--	--	0.143	0.012
Jul	(2,d,0)	0.689	-0.108	--	--	0.280	0.891
Aug	(3,d,0)	0.919	-0.211	0.038	--	0.078	0.044
Sep	(2,d,0)	0.985	-0.259	--	--	0.096	0.667
Oct	(3,d,0)	0.981	-0.328	0.077	--	0.196	0.302
Nov	(2,d,0)	0.810	-0.129	--	--	0.206	0.616
Dec	(3,d,0)	0.752	-0.179	0.053	--	0.243	0.041

NOTES: p-value < 0.05 indicates rejection of the null hypothesis of uncorrelated residuals at $\alpha = 0.05$.

for *d* indicate a moderate degree of persistence in all models except for the August model for Addicks and the August and September models for Barker which showed a weaker degree of persistence. Short memory ARMA models were thus fitted to these months' data, but the FARIMA models still provided a better fit. Note that all models for Addicks pass the Ljung-Box test at $\alpha = 0.05$. This was not the case for Barker, however, for which four models (April, June, August, and December) have *p*-values smaller than α. Notice also that the models for Addicks corresponding to these same months have the lowest *p*-values amongst all models for Addicks and they barely passed the test. These results causes some suspicion of lack of fit of these models, yet, as it will be shown in the next section, they were able to reproduce streamflow sequences with statistical properties similar to those of the observed data.

5.2.1.2. FARIMA Model Validation

In order to evaluate the capability of the selected models to reproduce the statistical properties of the observed data, 50 series of synthetic data with sample size equal to that of the observed series (53 years), were generated. The FARIMA models were fitted to the observed daily streamflow sequences of each month so as to preserve the mean, standard deviation (SD), and the lag-1 autocorrelation coefficient ($\rho(1)$). The statistics for one of the generated series are compared to their observed series counterparts in Tables 5.11 and 5.12, for Addicks and Barker respectively. In order to test if the models were able to consistently reproduce the statistics of the observed data, the distribution of the computed statistics for the 50 generated series was compared to the observed statistics using box and whisker plots (Figures 5.11 and 5.12). The short line within the box represents the median of the given variable. The bottom and top edges of the box represent the 25^{th} and 75^{th} percentiles. Hence, 50% of the observations fall within the box, and 25% each above and below. The "whiskers" extend to the 5^{th} and 95^{th} percentiles. The minimum and maximum values in the sample are indicated with a '+' sign. These plots show that the models are capable of reproducing the mean and $\rho(1)$ of the observed data satisfactorily, but clearly, the models underestimate the

TABLE 5.11. Monthly Statistics for Daily Streamflows at Addicks

	Mean			SD			Lag-1 Autocorrelation		
Month	Obs.	Gen.	%Error	Obs.	Gen.	%Error	Obs.	Gen.	%Error
(1)	(2)	(3)	(4)	(5)	(6)	(7)	(8)	(9)	(10)
Jan	138.1	145.6	5.4	255.1	226.6	-11.2	0.737	0.745	1.1
Feb	156.5	127.3	-18.7	350.6	192.8	-45.0	0.633	0.633	0.0
Mar	83.8	82.2	-1.9	246.9	120.6	-51.2	0.554	0.540	-2.5
Apr	119.3	109.3	-8.4	344.2	164.9	-52.1	0.692	0.662	-4.3
May	154.4	141.4	-8.4	459.8	198.6	-56.8	0.707	0.676	-4.4
Jun	147.6	142.4	-3.5	426.1	211.4	-50.4	0.733	0.713	-2.8
Jul	74.4	74.7	0.4	141.7	109.6	-22.7	0.723	0.694	-4.0
Aug	114.2	122.1	6.9	593.1	165.6	-72.1	0.587	0.633	7.8
Sep	101.5	101.0	-0.5	266.3	136.1	-48.9	0.746	0.659	-11.6
Oct	127.6	126.8	-0.6	406.0	190.9	-53.0	0.745	0.743	-0.3
Nov	123.3	111.6	-9.5	269.2	165.5	-38.5	0.754	0.769	2.0
Dec	135.4	129.7	-4.2	259.4	185.6	-28.5	0.719	0.692	-3.8

TABLE 5.12. Monthly Statistics for Daily Streamflows at Barker

	Mean			SD			Lag-1 Autocorrelation		
Month	Obs.	Gen.	%Error	Obs.	Gen.	%Error	Obs.	Gen.	%Error
(1)	(2)	(3)	(4)	(5)	(6)	(7)	(8)	(9)	(10)
Jan	141.4	160.9	13.8	287.3	229.6	-20.1	0.767	0.774	1.0
Feb	171.3	164.4	-4.0	397.8	244.8	-38.5	0.667	0.700	5.0
Mar	85.4	90.7	6.2	204.7	141.8	-30.7	0.620	0.693	11.7
Apr	116.9	117.2	0.2	369.9	156.5	-57.7	0.781	0.709	-9.3
May	160.3	163.0	1.7	473.7	245.6	-48.2	0.749	0.734	-2.0
Jun	173.9	179.1	3.0	696.0	255.2	-63.3	0.791	0.733	-7.4
Jul	76.9	79.9	4.0	149.5	117.7	-21.3	0.756	0.757	0.1
Aug	81.9	76.8	-6.2	248.6	109.5	-56.0	0.703	0.637	-9.4
Sep	115.4	119.9	3.9	327.1	180.7	-44.8	0.733	0.703	-4.1
Oct	116.0	116.5	0.4	317.1	171.8	-45.8	0.764	0.784	2.6
Nov	116.2	118.9	2.3	253.5	187.3	-26.1	0.759	0.769	1.4
Dec	136.6	130.7	-4.3	285.8	170.4	-40.4	0.679	0.635	-6.5

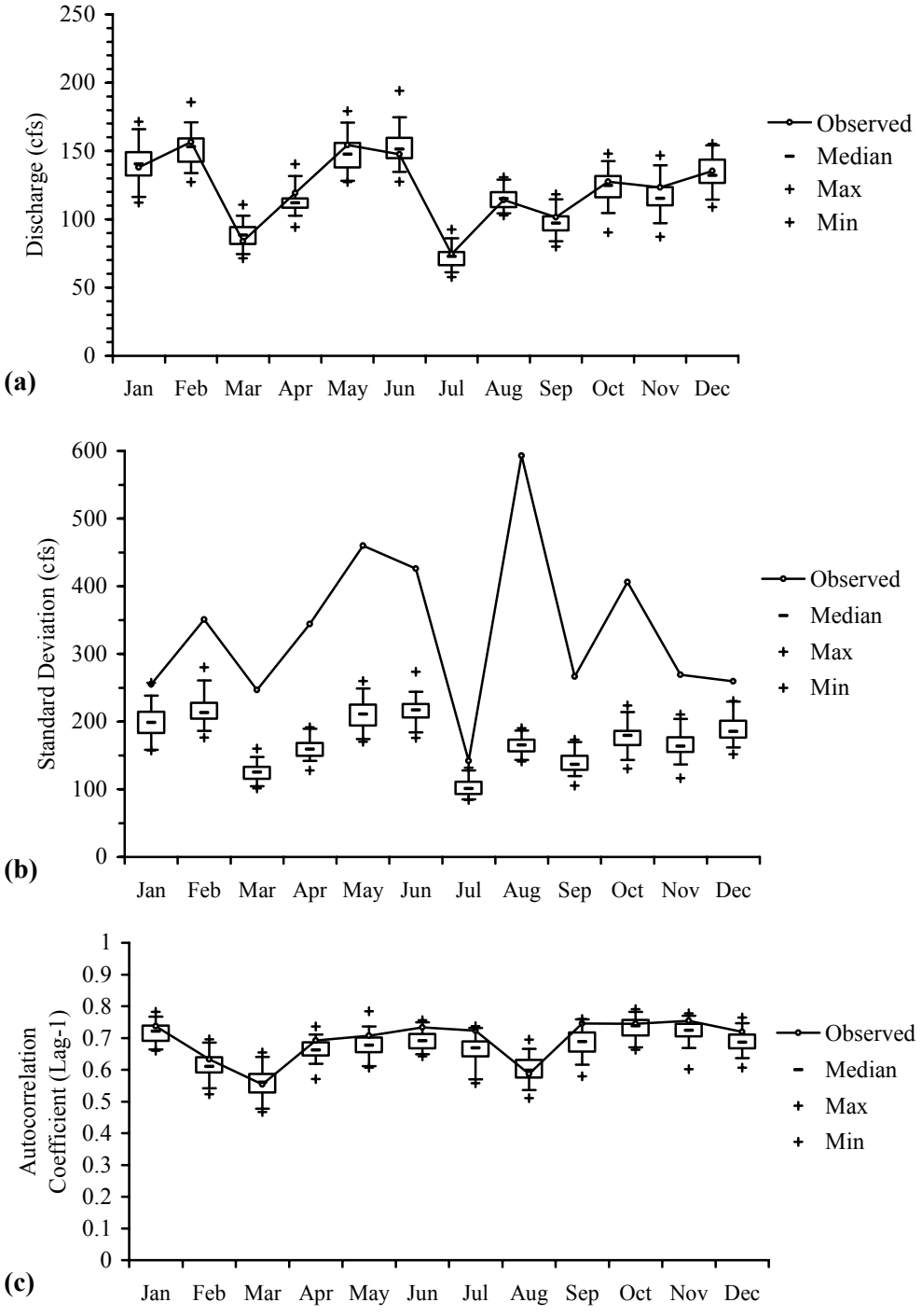

FIGURE 5.11. Box and Whisker Plots of the Distribution of the (a) Means, (b) Standard Deviations; and (c) Lag-1 Autocorrelation Coefficients of the Generated Sequences for Addicks

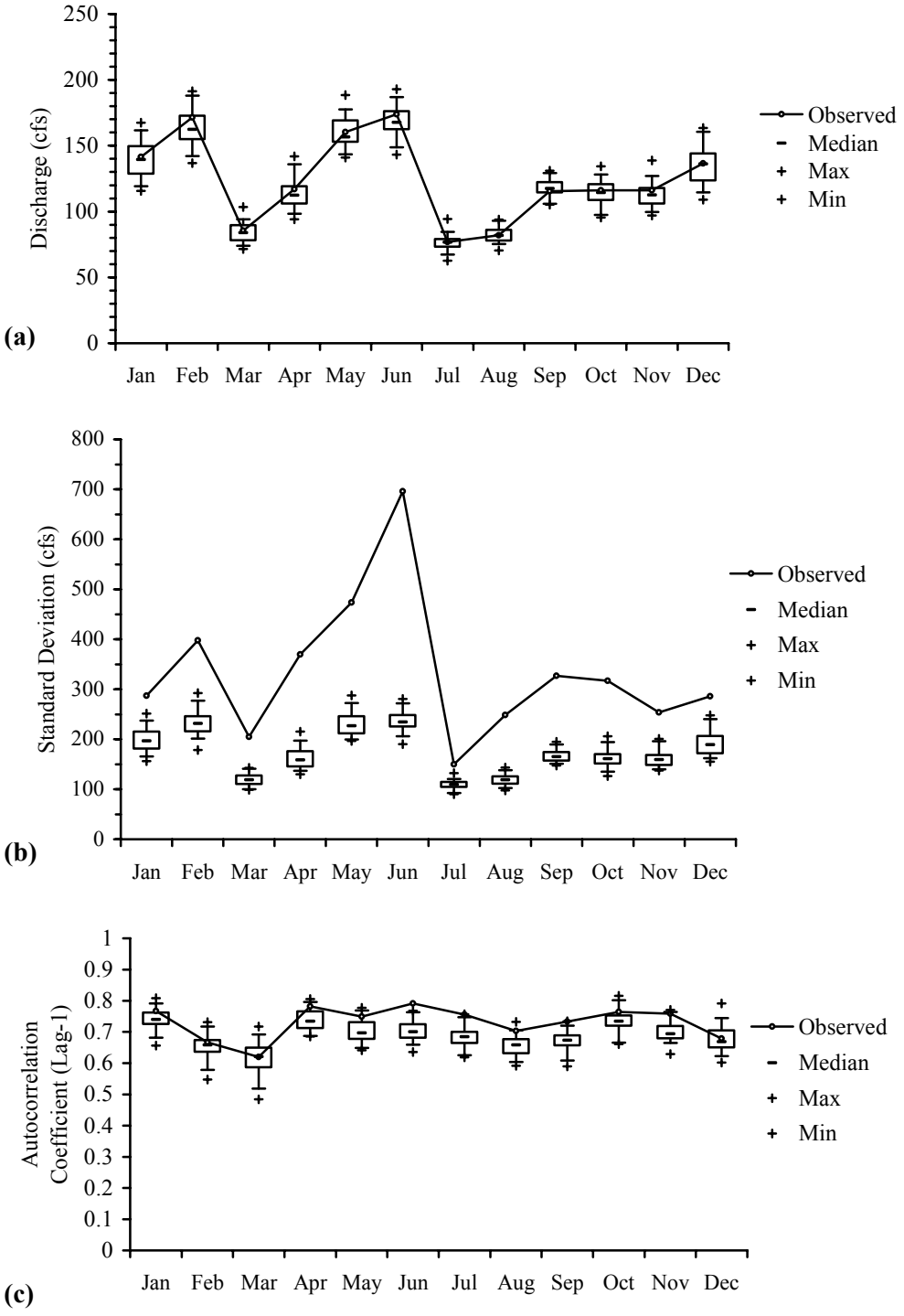

FIGURE 5.12. Box and Whisker Plots of the Distribution of the (a) Means, (b) Standard Deviations; and (c) Lag-1 Autocorrelation Coefficients of the Generated Sequences for Barker

SD, sometimes by as much as 50% or more. The SD of the observed data is greatly influenced by the peak discharge values, which account for a considerable amount of the variation in the data. For example, the SD for the August data for Addicks decreases from 593 to 421 cfs (29% decrease) if the peak discharge of the series is not considered. Similarly, the SD for the June data for Barker decreases from 696 to 583 cfs (16.3% decrease). The observed peak discharge values were not well reproduced by the FARIMA models, causing the SD of the synthetic series to be much lower than the SD of the observed series. This discrepancy was not considered a major limitation for this particular study since in the REOS methodology high flows are introduced into the streamflow sequences as a recurrent initial condition, and thus, the models need not to reproduce high flows in order to develop the EOS for such conditions. Therefore, the models can be considered adequate for the purpose at hand.

To further investigate the adequacy of the models, the cumulative frequency of the observed and the generated daily streamflows was compared. This comparison is presented graphically for each month in Figures 5.13 – 5.14. The generated data should provide good approximations of the cumulative frequency curves of the observed data. A visual inspection of these figures shows that, save for May and June for Addicks, and May, June, and November for Barker, the cumulative frequency curves are in good agreement. The two-sample Kolmogorov-Smirnov (K-S) test was then applied to formally test the hypothesis of statistical similarity between the observed and the generated data. The K-S test consists of calculating the maximum vertical deviation (D) between the cumulative frequency curves:

$$D = \max_{x} \left| F_O(x) - F_G(x) \right| \tag{5.4}$$

where $F_O(x)$ is the empirical cumulative frequency curve of the observed series and $F_G(x)$ is its counterpart for the generated series. Then, D is compared against the critical

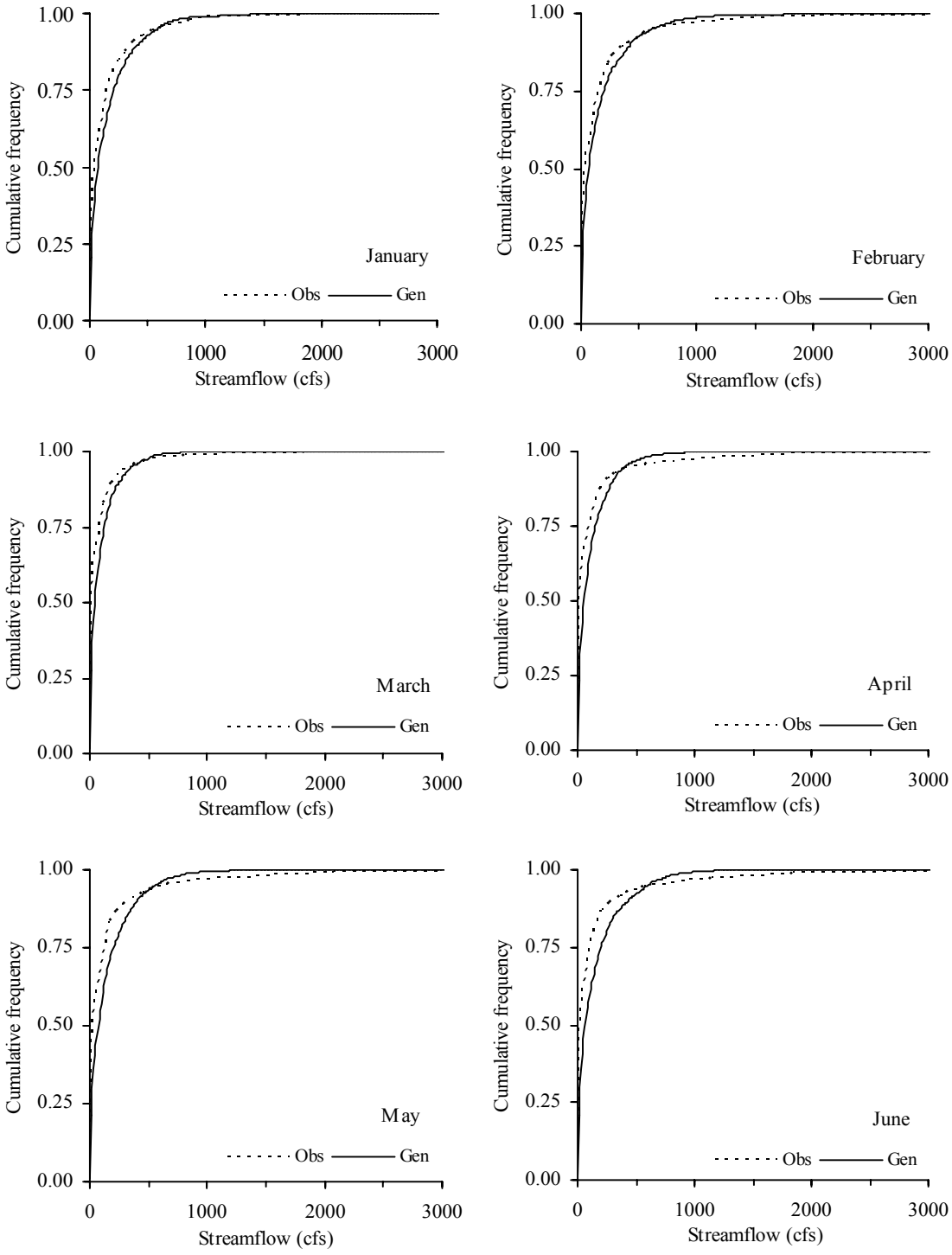

FIGURE 5.13. Comparison Between the Sample Frequency Distribution of Observed and Generated Daily Streamflows for Each Month at Addicks

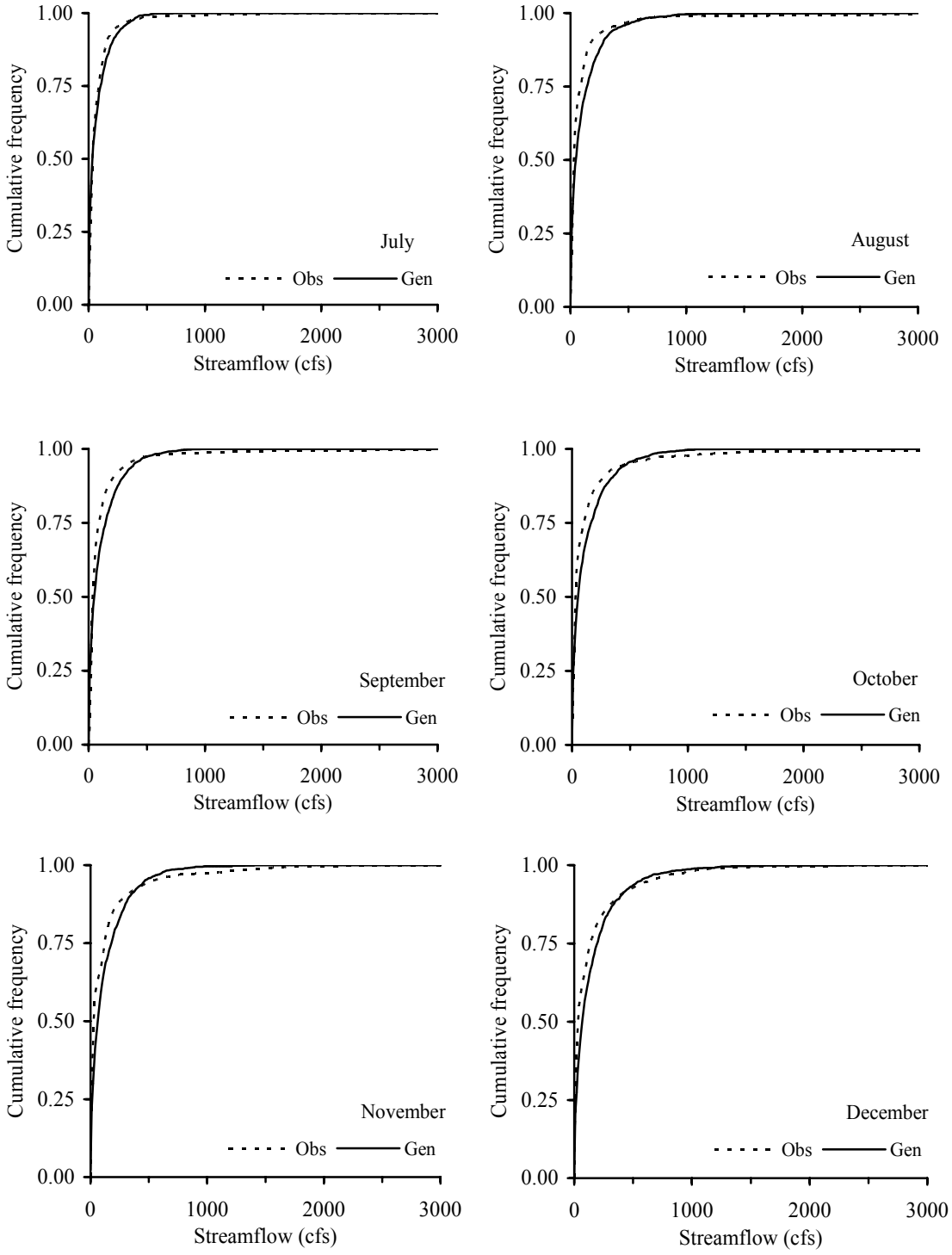

FIGURE 5.13. Continued

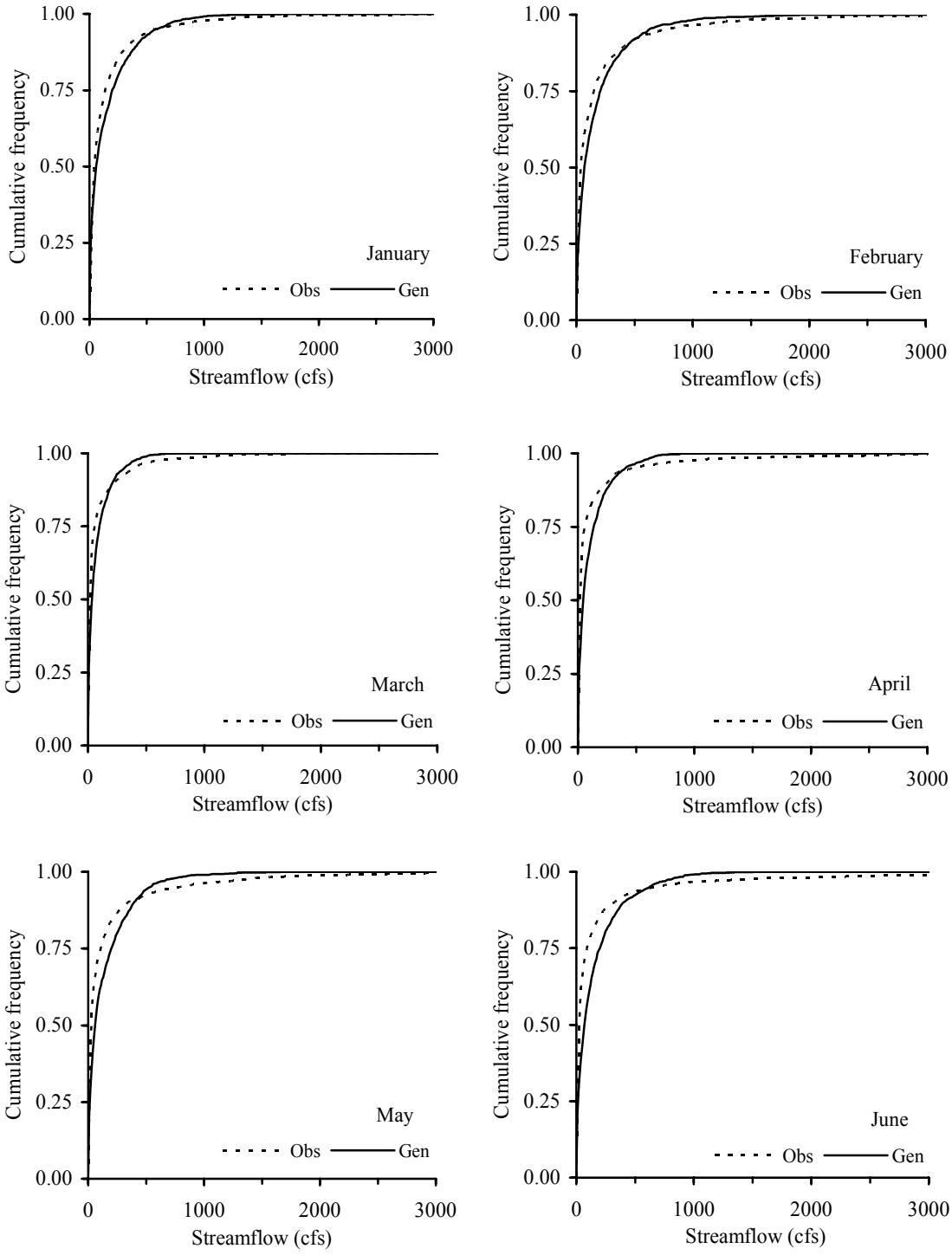

FIGURE 5.14. Comparison Between the Sample Frequency Distribution of Observed and Generated Daily Streamflows for Each Month at Barker

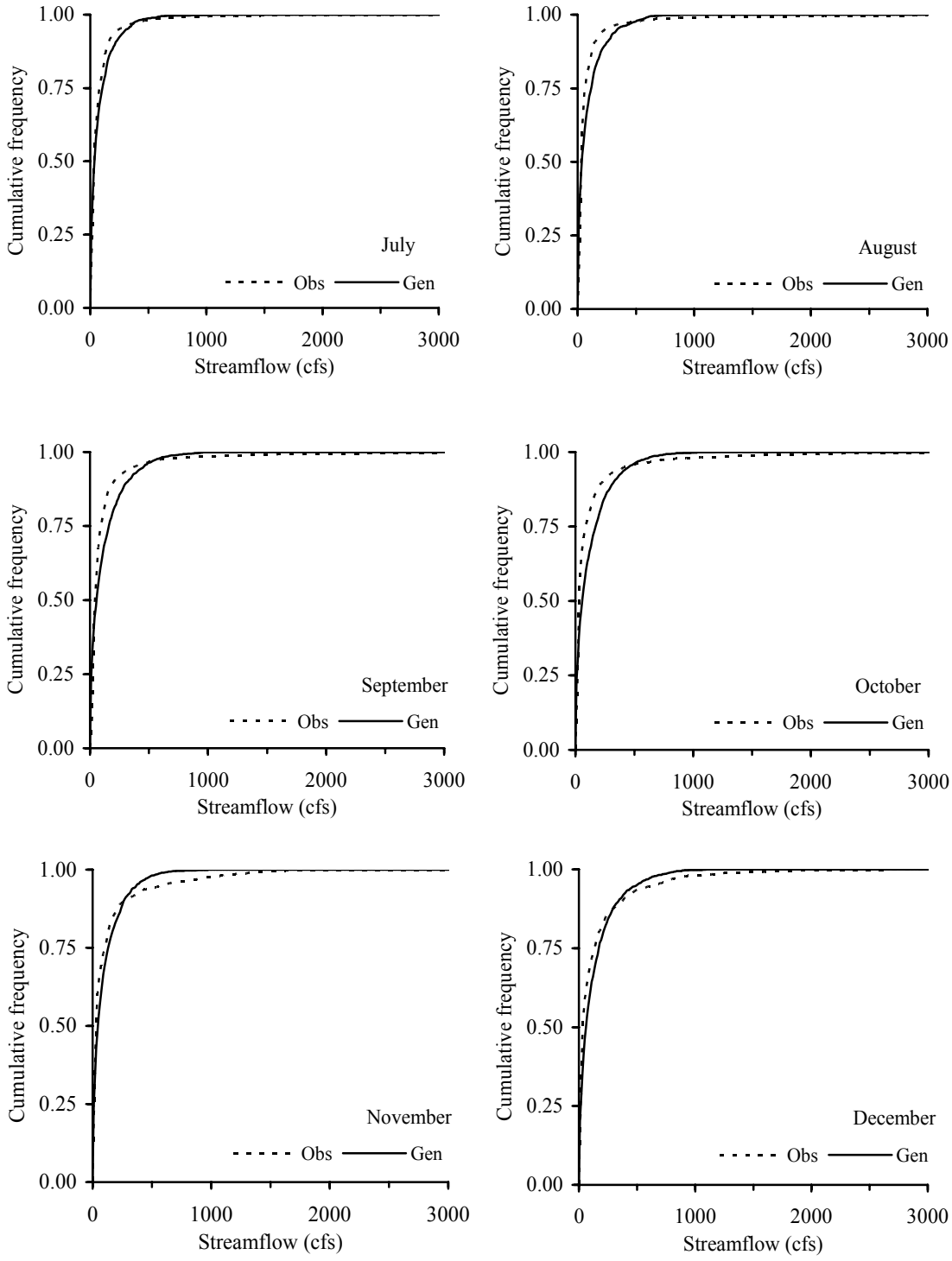

FIGURE 5.14. Continued

5% *D*-statistic (d_{95}), which is given approximately by:

$$d_{95} = 1.358\sqrt{\frac{n_1 + n_2}{n_1 n_2}} \tag{5.5}$$

where n_1 and n_2 are the sample sizes of the observed and generated data respectively. If D is greater than d_{95}, then the null hypothesis that the distributions are statistically similar is rejected at the 5% significance level. For $n_1 = n_2 = 53$, $d_{95} = 0.264$. The results for the K-S test are presented in Table 5.13. Notice that even though the models are not capable of reproducing peak discharges as large as those of the observed data, all deviations are smaller than d_{95}. This suggests that the peak values only account for a small fraction of the data, and that for the most part; every FARIMA model is capable of generating streamflows similar to those of the observed series.

TABLE 5.13 K-S Difference *D* for the Daily Streamflow Distribution for Each Month

	Reservoir	
Month	Addicks	Barker
(1)	(2)	(3)
Jan	0.109	0.101
Feb	0.120	0.140
Mar	0.178	0.171
Apr	0.220	0.238
May	0.161	0.184
Jun	0.195	0.232
Jul	0.134	0.102
Aug	0.140	0.194
Sep	0.168	0.199
Oct	0.152	0.177
Nov	0.175	0.115
Dec	0.157	0.132

Notes: Critical 5% value $d_{95} = 0.264$

So far, we have examined the performance of the models on a month-to-month basis. An additional means of evaluating the models is by comparing the generated monthly data, assembled together to compose the annual series, with the entire observed series. As with the individual models, the K-S test was applied. The resulting *D*-statistic was 0.137 for Addicks and 0.145 for Barker, both well below d_{95}. Finally, the ACF of the observed series was compared against the ACF of one of the generated annual series. This comparison is presented in Figure 5.15. It was expected that having 12 models, each fitting the autocorrelation structure of each month separately, would result in a generated series with an autocorrelation structure similar to that of the historical series as a whole. As it can be observed in Figure 5.15, the ACF's are fairly similar up to lag 40 for Addicks and at least up to lag 16 for Barker. These results also corroborate the adequacy of the seasonal FARIMA models for this particular application.

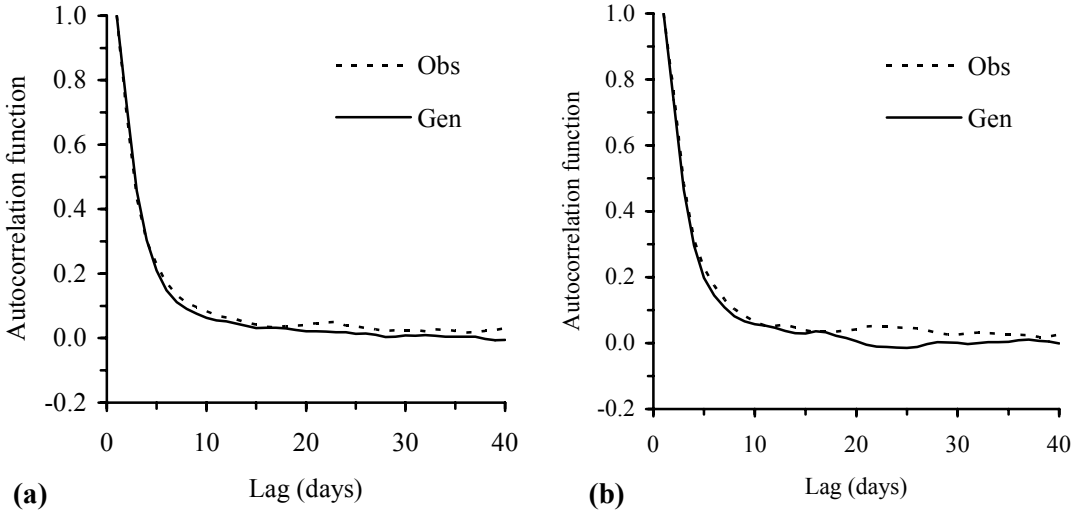

FIGURE 5.15. Comparison Between the Annual Sample Autocorrelation Function of the Observed and Generated Series. (a) Addicks; and (b) Barker

5.2.1.3. Establishing the Initial Streamflow Conditions: Q_0 and AR(1) models

In most stochastic hydrology applications, the staring values that are needed to initiate the recursive calculations in the streamflow generation model are set to the average value of the observed series (Beard 1967; Salas 1993; Gupta 1995; Viessman and Lewis 1996). This arbitrary selection of the starting values is irrelevant, since the first values in the simulation are typically discarded in order to neglect the effects of the initial conditions. In this study, however, capturing the effects of the initial conditions on the generated sequences is of utmost importance. The goal here is to analyze the statistical probabilities of future flows given a recurrent initial streamflow condition, which is defined by the initial inflow rate Q_0 and its preceding values. The estimated FARIMA models for this study require up to three assumed values to initialize their recursive computations. The first of these values is Q_0, which is the recurrent streamflow value in every simulation (see Chapter III, section 3.3.3). Due to the strong correlation between succeeding flows, the values preceding Q_0 should not be selected arbitrarily. A backward generation process is adopted in REOS to estimate these values using autoregressive lag-1 (AR(1)) models (see Chapter III, section 3.3.2.2 for details). Briefly, the backward AR(1) model is expressed as

$$(1-\phi_1 F)X_t = W_t \tag{5.6}$$

where X_t represents a time series, ϕ_1 is the autoregressive coefficient, F is the forward shift operator defined by $FX_t = X_{t+1}$, and W_t is a white noise process with zero mean and constant variance equal to that of the forward model. This process is useful in estimating values of the series that have occurred before the first observation was made. If a model requires n preceding values (Q_{-1}, Q_{-2}, …, Q_{-n}) to initiate a simulation, these values may be "back forecasted" recursively using Q_0 as the initial input in the model.

The estimation of the AR(1) model coefficients for the transformed series of each month was also carried out in ITSM2000. The results are reported on Table 5.14. These models were only tested in terms of their ability to reproduce $\rho(1)$ for each month given that $\rho(1)$ is the most relevant statistic for this particular application. A synthetic series

TABLE 5.14. Backward AR(1) Models Coefficients

	Reservoir	
	Addicks	Barker
Month	ϕ_1	ϕ_1
(1)	(2)	(3)
Jan	0.846	0.864
Feb	0.789	0.810
Mar	0.760	0.735
Apr	0.823	0.832
May	0.832	0.844
Jun	0.841	0.857
Jul	0.784	0.841
Aug	0.772	0.814
Sep	0.840	0.839
Oct	0.871	0.863
Nov	0.847	0.850
Dec	0.837	0.834

TABLE 5.15. Comparison Between the Lag-1 Autocorrelation Coefficients of the Observed and Generated With Backward AR(1) Models Series

	Reservoir					
	Addicks			Barker		
Month	Obs.	Gen.	%Error	Obs.	Gen.	%Error
(1)	(2)	(3)	(4)	(5)	(6)	(7)
Jan	0.737	0.756	2.6	0.767	0.722	-5.8
Feb	0.633	0.665	5.1	0.667	0.706	5.9
Mar	0.554	0.568	2.5	0.620	0.612	-1.3
Apr	0.692	0.650	-6.1	0.781	0.713	-8.8
May	0.707	0.693	-2.0	0.749	0.727	-2.9
Jun	0.733	0.699	-4.7	0.791	0.761	-3.9
Jul	0.723	0.684	-5.4	0.756	0.738	-2.3
Aug	0.587	0.614	4.6	0.703	0.705	0.3
Sep	0.746	0.715	-4.1	0.733	0.739	0.9
Oct	0.745	0.747	0.3	0.764	0.716	-6.3
Nov	0.754	0.714	-5.3	0.759	0.721	-5.0
Dec	0.719	0.682	-5.1	0.679	0.691	1.8

with sample size equal to that of the observed series (53 years) was generated and $\rho(1)$ was calculated for the aggregated data of each month (Table 5.15). The results in Table 5.15 indicate that the models were able to reproduce the observed $\rho(1)$ satisfactorily.

5.2.2. Risk-based Emergency Operation Schedules Sample Results

Once the necessary streamflow generation models are developed, the REOS computer program may be used to formulate the risk-based EOS. The REOS computational algorithm is fully described in Chapter III section 3.3.3. As opposed to the standard method, in which only one EOS is developed, REOS formulates a series of alternative EOS, each corresponding to a particular combination of hydrological and operational conditions. These conditions were classified as follows:

(1) Antecedent streamflow conditions or streamflow state: *SS* = rising or receding.

(2) Time of year: *TY* = annual or monthly schedules. A single annual EOS may be developed which is valid throughout the year; alternatively, monthly EOS may be defined and the appropriate schedule is implemented accordingly.

(3) Acceptable risk of failing to attain the emergency operations objectives expressed as an exceedance (*EF*) or non-exceedance (*NEF*) frequency. *EF* is interpreted as the risk of dam overtopping associated with a given EOS and its complementary *NEF* is interpreted as the risk that the EOS will result in unused storage: 21 *EF* values were selected ranging from 0.5 to 99%.

Each of the resulting 546 EOS represents an alternative operational scheme tailored to a specific set of conditions. The EOS were developed in tabular format for initial inflows of 1,000 cfs to 60,000 cfs at increments of 1,000 cfs. The comparisons of sample results presented hereafter illustrates how the EOS developed for various conditions differ in terms of the outflow rates that they require for a given initial condition (i.e. Q_0 and WSE). The zero outflow points in each EOS were computed according to the procedure explained in Section 3.3.3 (*Step 7*) using a five-day period of analysis.

5.2.2.1. Variation in Emergency Releases as a Function of Streamflow State

The following discussion focuses on how the streamflow state (*SS*) would affect the operation of the reservoirs under emergency conditions. Figure 5.16 depicts the EOS for *TY* = annual, *EF* = 1%, and for both *SS* conditions. Notice that the curves forming the EOS for *SS* = rising are below their counterparts for *SS* = receding. This indicates that for rising streamflow conditions the transition from normal to emergency operations would occur at lower stages and that a larger outflow rate would be required for any given initial condition. This was an expected result since streamflows usually exhibit a strong tendency to continue their current trend (i.e. rising inflows tend to continue increasing and receding inflows tend to continue decreasing). Due to this tendency, the inflow volume following Q_0 will typically be greater for rising conditions than for receding conditions, and thus, greater outflow rates would be needed to accommodate the remainder of the flood. Evidently, this streamflow tendency was well-reproduced by the stochastic streamflow generation models and its anticipated effects were reflected in the schedules. A comparison of the required outflow rates for selected initial conditions is presented in Tables 5.16 and 5.17 for Addicks and Barker, respectively. The values in column (3) correspond to the residual storage capacity as a percentage of the MSC of the reservoir. The outflow rates in columns (4) and (5) were read off the EOS in Figure 5.16. Column (6) shows the difference between the required outflow rates for rising and receding conditions. Observe that for a given Q_0 the values in column (6) increase as the residual storage capacity decreases and that the magnitude of the differences is greater for Barker than for Addicks. This indicates that as the residual storage capacity diminishes, the streamflow state becomes an increasingly significant factor in the release decision process, especially for Barker Reservoir.

5.2.2.2. Variation in Emergency Releases as a Function of Time of Year

One of the potential modifications to the current emergency operation policies for the Addicks and Barker system is to allow the operation of the reservoirs to be adjusted according to the time of year. The objective of this operational change is to

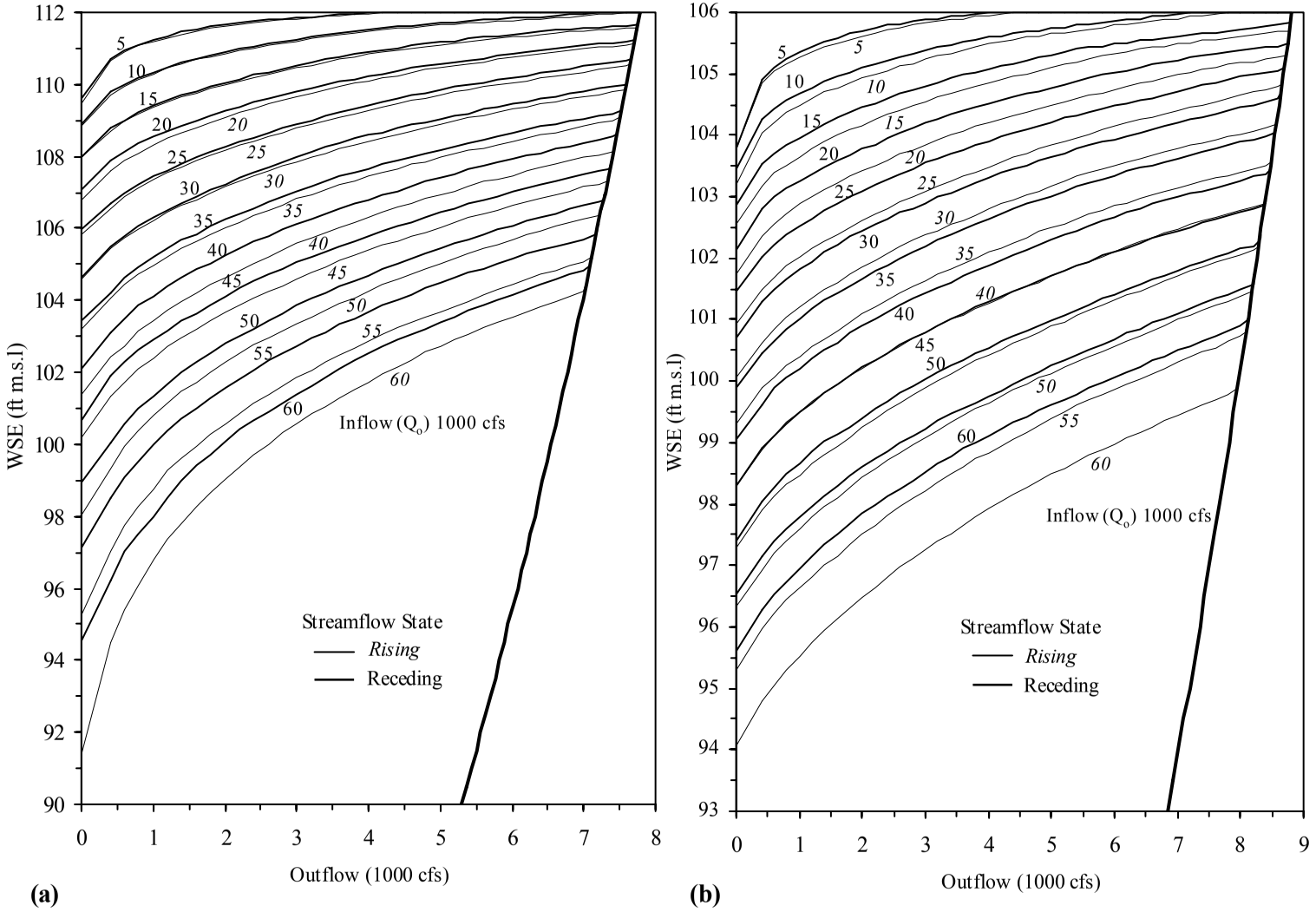

FIGURE 5.16. Risk-based EOS for TY = Annual, EF = 1%, and SS = Rising and Receding. (a) Addicks; and (b) Barker

TABLE 5.16. Comparison of the Required Outflow Rates for Selected Initial Conditions Based on the EOS Depicted in Figure 5.16 for Addicks

Q_o (1000 cfs) (1)	WSE (ft above m.s.l.) (2)	Residual Storage (% of MSC) (3)	Outflow (cfs)		Reduction in Outflow (cfs)
			SS = Rising (4)	*SS* = Receding (5)	Col.(4) - Col.(5) (6)
20	108	30	675	500	175
	109	23	1,833	1,583	250
	110	16	3,750	3,417	333
25	106	43	125	0	125
	108	30	1,667	1,500	167
	109	23	3,408	3,208	200
	110	16	5,833	5,417	416
30	106	43	792	750	42
	107	36	1,792	1,708	84
	108	30	3,250	3,000	250
	109	23	5,208	4,917	291
35	104	54	375	292	83
	106	43	2,000	1,750	250
	108	30	5,042	4,583	459
	109	23	7,375	6,833	542
40	104	54	1,417	875	542
	106	43	3,542	2,875	667
	107	36	5,158	4,333	825
	108	30	7,083	6,167	916
45	102	65	708	417	291
	104	54	2,375	1,917	458
	106	43	4,925	4,333	592
	107	36	6,708	6,000	708
50	100	74	625	375	250
	102	65	1,792	1,375	417
	104	54	3,667	3,167	500
	106	43	6,500	5,833	667
55	100	74	1625	1000	625
	102	65	3167	2333	834
	104	54	5417	4375	1,042
	105	49	6833	5750	1,083
60	99	77	1083	583	500
	100	74	2625	1958	667
	102	65	4250	3500	750
	104	54	6667	5833	834

TABLE 5.17. Comparison of the Required Outflow Rates for Selected Initial Conditions Based on the EOS Depicted in Figure 5.16 for Barker

Q_o (1000 cfs) (1)	WSE (ft above m.s.l.) (2)	Residual Storage (% of MSC) (3)	Outflow (cfs) *SS* = Rising (4)	Outflow (cfs) *SS* = Receding (5)	Reduction in Outflow (cfs) Col.(4) - Col.(5) (6)
10	104	15	390	290	100
	105	8	2,250	1,800	450
15	103	23	300	100	200
	104	15	1,600	1,050	550
	105	8	4,600	3,700	900
20	103	23	1,200	600	600
	104	15	3,400	2,500	900
	105	8	7,000	5,900	1,100
25	102	30	975	375	600
	103	23	3,800	2,800	1,000
	104	15	5,500	4,200	1,300
30	101	37	750	200	550
	102	30	2,300	1,250	1,050
	103	23	5,600	4,200	1,400
	104	15	7,800	6,225	1,575
35	100	43	550	100	450
	101	37	1,750	1,000	750
	102	30	3,800	2,600	1,200
	103	23	6,500	4,950	1,550
40	100	43	1,700	750	950
	101	37	3,400	2,200	1,200
	102	30	5,700	4,300	1,400
45	100	43	3,200	1,700	1,500
	101	37	5,300	3,400	1,900
	102	30	7,800	5,700	2,100
50	98	56	1,450	400	1,050
	99	50	2,900	1,400	1,500
	100	43	4,700	2,950	1,750
	101	37	7,000	5,000	2,000

capitalize on the information obtained from the historical streamflows for each month, particularly their autocorrelation structure. Recall that the required outflow rates in the risk-based EOS are essentially a function of the current WSE and the expected inflow volume for a given initial condition. The key to this approach lies in that this volume may be rather different in each month as it will tend to be larger for months that exhibit strong autocorrelation and smaller for months that exhibit weak autocorrelation. As previously expounded, the FARIMA models are capable of capturing the particular autocorrelation structure of each month and reflecting it in the generated sequences; thereby allowing the development of alternative EOS that vary according to the typical streamflow characteristics of each month.

A set of monthly EOS with *EF* = 1% and *SS* = rising is presented in Figures 5.17 and 5.18 for Addicks and Barker respectively. These figures clearly demonstrate that there is a significant variation in the release policies that resulted for each month. The position of the curves forming the EOS shifts downward or upward as a reflection of the magnitude of the typical inflow volumes that can be expected for each month according to the FARIMA models. That is, if the position of the curves for month "X" is lower than that of month "Y" it means that the computed inflow volumes in month "X" were usually larger than in month "Y", and thus, the EOS for month "X" would require larger outflow rates at any given WSE in order to offset the expected inflow volumes for that month and avoid dam overtopping. Based on the resulting EOS, the smallest inflow volumes can be expected in February, March, and July for both reservoirs, while the largest inflow volumes can be expected in June, August, and October for Addicks, and April, June, and August for Barker.

In order to better illustrate the variation in monthly release policies a comparison of the outflow rates required by each EOS for selected initial conditions is presented in Table 5.18. The standard deviation (SD) of the values was included as a measure of variability. The following observations were made:

(1) Emergency releases may be drastically different depending upon the time of year at which emergency conditions are encountered. For instance, notice that for

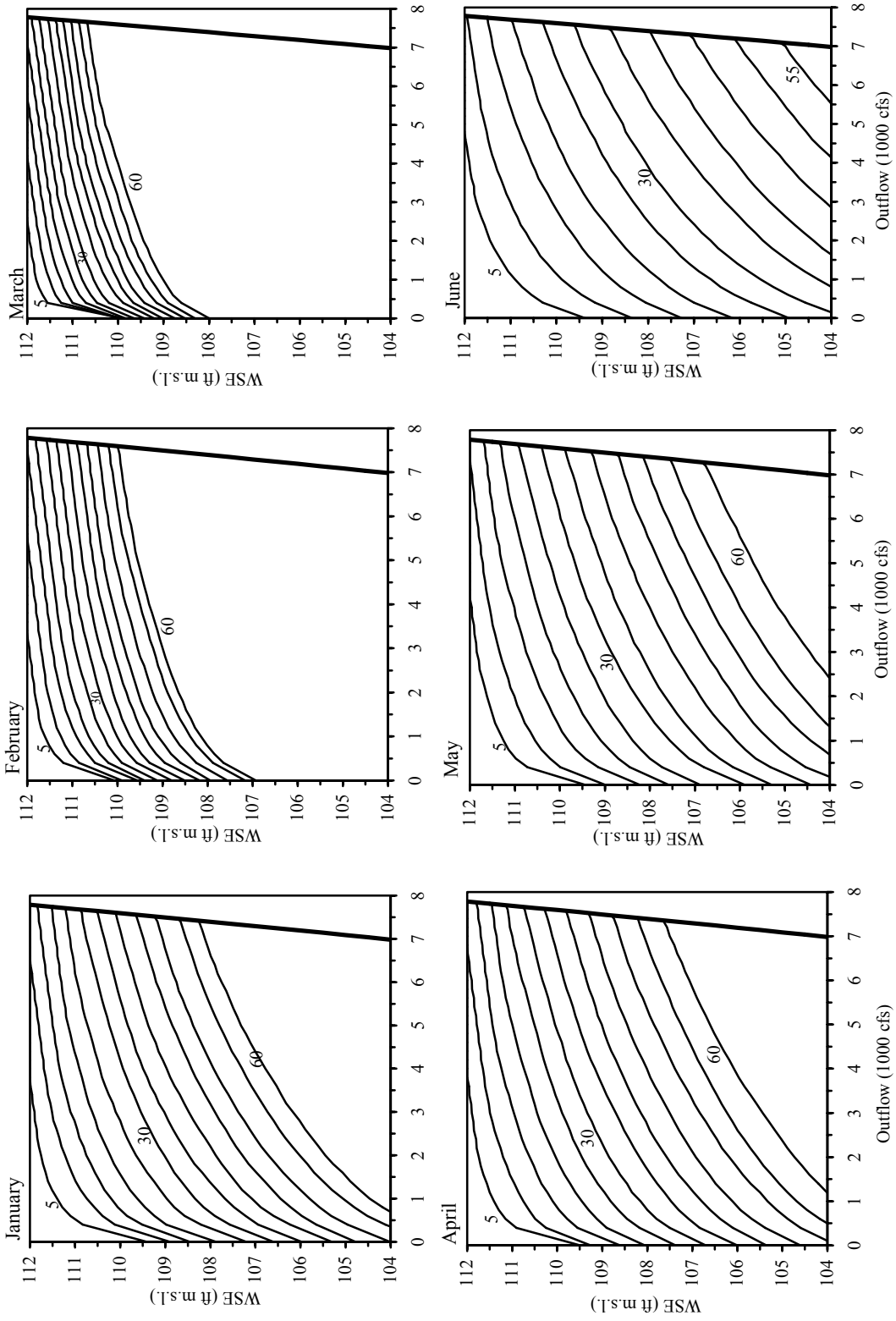

FIGURE 5.17. Monthly EOS for Addicks (EF = 1%, SS = Rising). Numbers on Curves Denote Initial Inflow in 1000 cfs

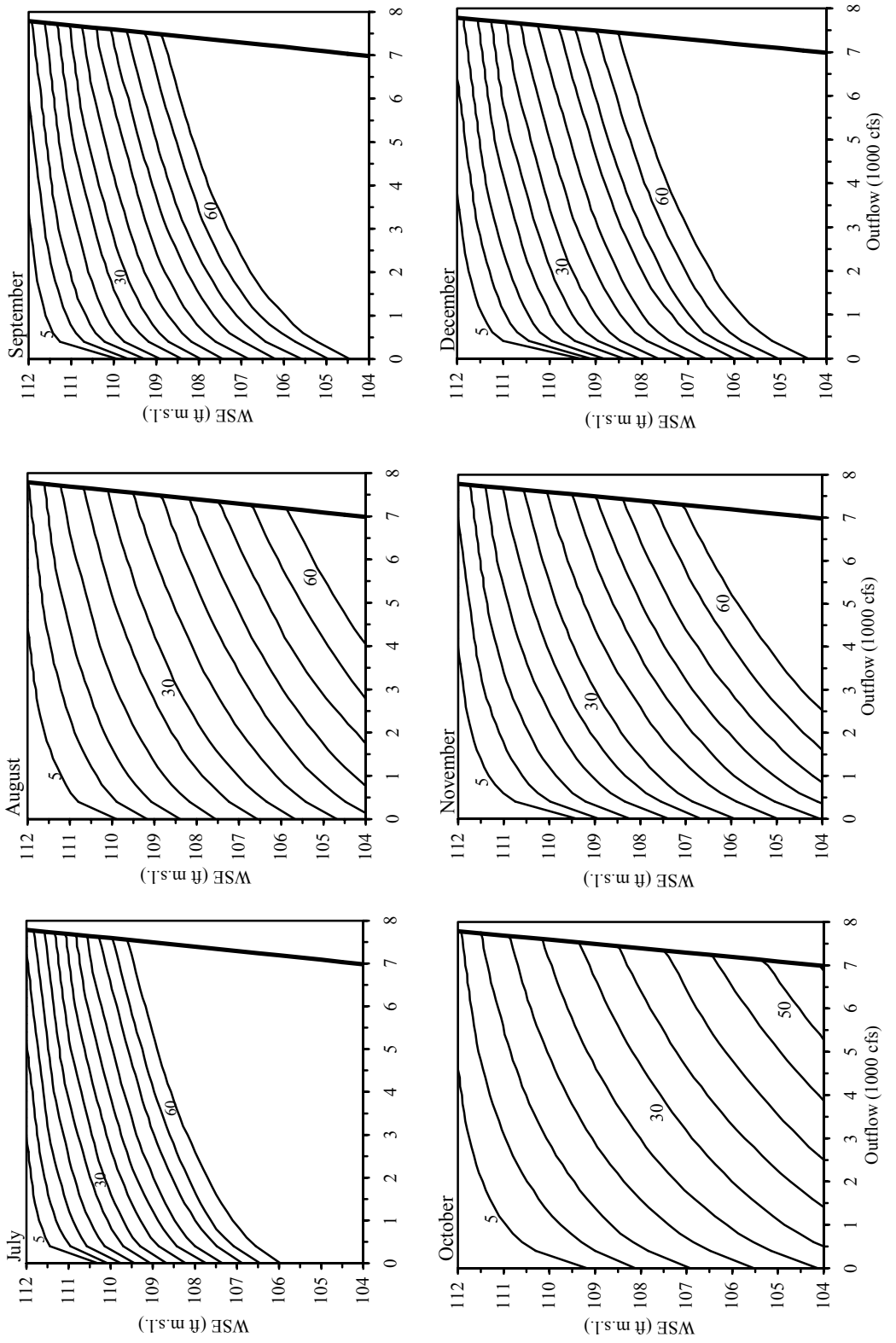

FIGURE 5.17. Continued

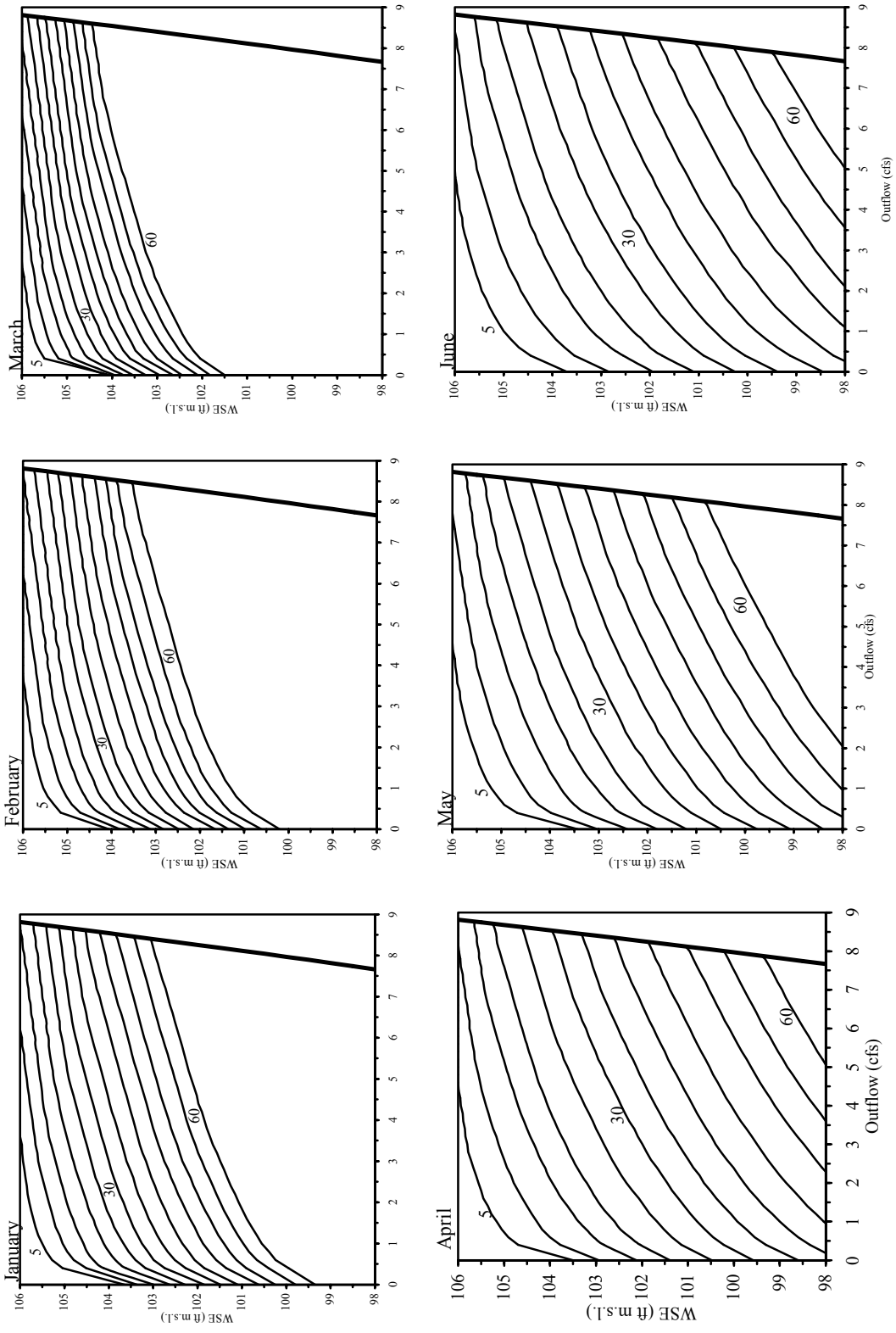

FIGURE 5.18. Monthly EOS for Barker (EF = 1%, SS = Rising). Numbers on Curves Denote Initial Inflow in 1000 cfs

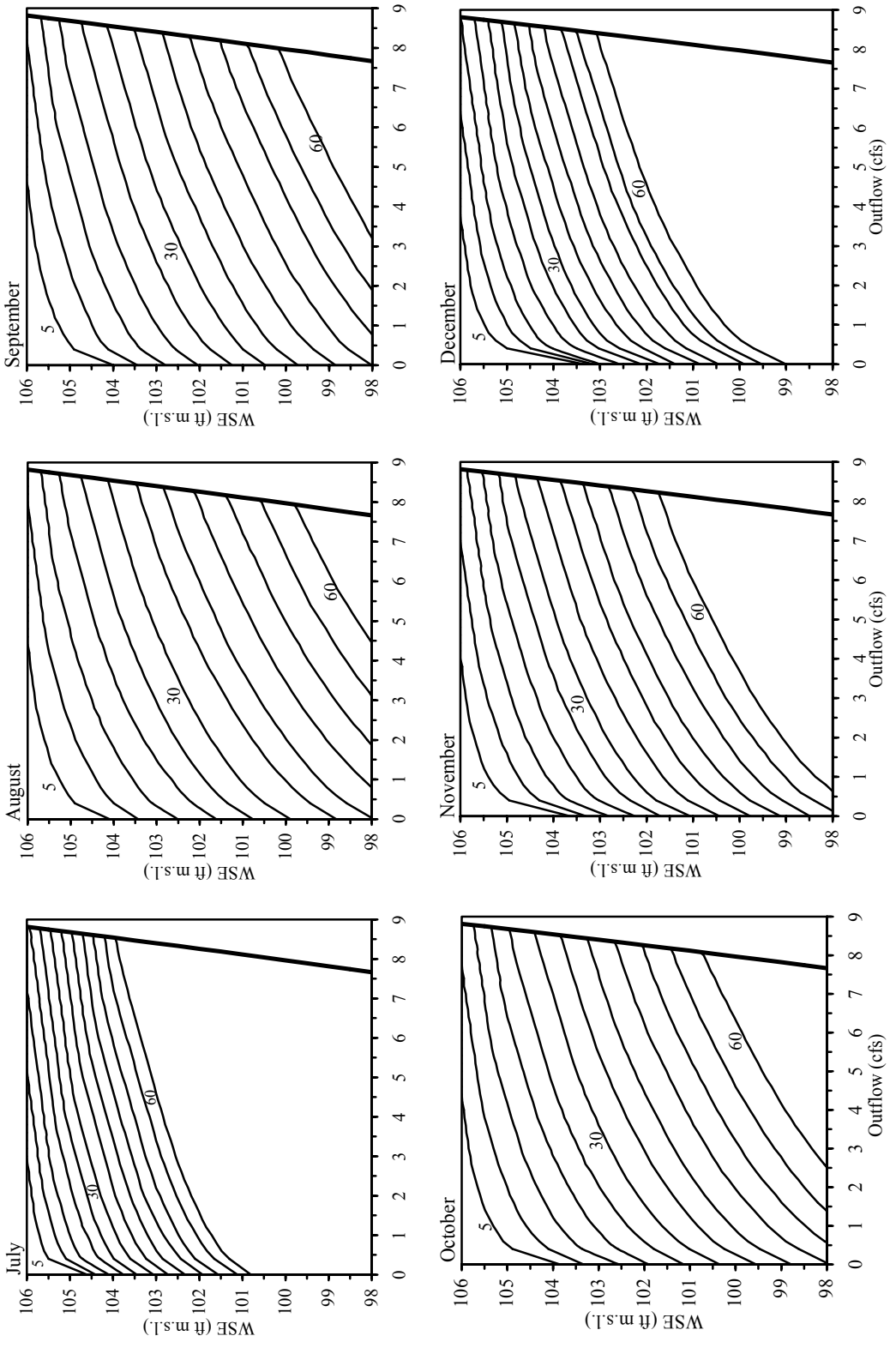

FIGURE 5.18. Continued

TABLE 5.18. Comparison of the Required Outflow Rates for Selected Initial Conditions Based on the Monthly EOS Depicted in Figures 5.17 and 5.18

Reservoir >>	Addicks					Barker				
WSE >>	109.5 (ft m.s.l.)					104 (ft m.s.l.)				
	Outflow (cfs) for Q_0 (1000 cfs) =					Outflow (cfs) for Q_0 (1000 cfs) =				
Month	5	15	30	45	60	5	15	30	45	60
(1)	(2)	(3)	(4)	(5)	(6)	(7)	(8)	(9)	(10)	(11)
Jan	50	400	2,800	7,100	**7,544**	100	350	3,000	7,600	**8,542**
Feb	0	0	365	1,900	4,800	0	250	2,000	6,000	**8,542**
Mar	0	0	0	500	2,200	0	0	525	2,700	5,900
Apr	0	400	3,400	**7,544**	**7,544**	150	2,100	**8,542**	**8,542**	**8,542**
May	25	650	4,500	**7,544**	**7,544**	200	1,400	7,000	**8,542**	**8,542**
Jun	50	1,900	7,200	**7,544**	**7,544**	150	2,500	**8,542**	**8,542**	**8,542**
Jul	0	0	600	3,400	7,200	0	0	1,200	4,700	8,540
Aug	0	900	5,600	**7,544**	**7,544**	0	1,800	8,000	**8,542**	**8,542**
Sep	0	100	1,500	5,400	**7,544**	0	1,600	8,000	**8,542**	**8,542**
Oct	100	2,100	**7,544**	**7,544**	**7,544**	50	1,200	7,000	**8,542**	**8,542**
Nov	25	600	4,100	**7,544**	**7,544**	100	800	5,200	**8,542**	**8,542**
Dec	25	250	2,000	6,400	**7,544**	150	400	3,100	7,500	**8,542**
SD	31.0	711.2	2,568.6	2,513.7	1,659.2	75.4	854.5	3,042.7	1,918.8	762.6

NOTE: Values in bold denote maximum outflow rate at the specified WSE.

Addicks an inflow of 30,000 cfs in March would not require emergency releases (i.e. outlet gates remain closed); while the same inflow in October would require an outflow rate of 7,544 cfs (i.e. outlet gates are completely open).

(2) As Q_0 increases, the variability (SD) of the outflow rates increases up to certain value and then decreases as the number of months requiring the maximum outflow rate increases. Although the presented values for Q_0 only reach 60,000 cfs, it is evident that as Q_0 continues increasing there will be one value for which all EOS will require the maximum outflow rate.

(3) The difference in outflow rates for successive months can be very significant.

The latter observation would present an operational challenge when regulating floods occurring near the end of a month that is followed by a month with a significantly different EOS. This situation would create a degree of uncertainty in terms of which EOS would be more appropriate to regulate the flood. A decision needs to be made as to which EOS to follow, considering that even if the flood started in a particular month the incoming streamflows may reflect the characteristics of the next month. This is a critical decision especially because each EOS may establish the transition from normal to emergency operations at significantly different reservoir stages. Consider for instance the March and April EOS for Barker, which show the greatest variation between successive months for this reservoir. The March EOS indicates that for Q_0 = 30,000 cfs emergency releases would be required if the WSE is above 103.3 ft (reservoir is at least 79% full), whereas the April EOS would dictate releases if the WSE is above 99.6 ft (reservoir is at least 54% full). Therefore, conditions that would trigger emergency releases in April would not do so in March. In fact, while the outlet gates would remain closed in March for reservoir stages between 99.6 and 103.3 ft, outflow rates of up to 6,200 cfs would have been required in April. Considering that an operational error may cause unnecessary flooding downstream and/or upstream of the dams, operational guidelines should be established beforehand to assist reservoir operators in selecting the apposite EOS so that potential conflicts can be avoided.

5.2.2.3. Variation in Emergency Releases as a Function of Risk

The principal feature of the risk-based EOS is that they provide a means for taking explicitly into account the risks of failing to accomplish the emergency operations objectives. As previously discussed, the *EF* and *NEF* associated with each EOS represent, respectively, the risk that the specified release rates may be insufficient to avoid dam overtopping and the risk that they may be excessive resulting in unused storage. *EF* may also be regarded as a measure of the level of protection that the schedules provide against dam overtopping, which is the primary objective during emergency conditions. Having a series of alternative risk-based EOS would allow adjusting the operation of the reservoirs in accordance with certain level of risk that has been deemed acceptable for the condition at hand.

The operation of the reservoirs can be rather different depending upon the level of protection that is desired. In order to evaluate the variation in release policies as a function of risk, a series of 21 risk-based EOS were developed for *EF* values ranging from 0.5 to 99% (*SS* = rising, *TY* = annual). The required outflow rates for selected initial conditions were read off these plots and then plotted as Figures 5.19 and 5.20 for Addicks and Barker respectively. Each curve shows the required outflow rates for a specific initial condition as a function of risk. The following observations were made:

(1) The required outflow rates increase as the desired level of protection increases (i.e. decreasing *EF*). Increasing levels of protection, however, would be attained at the expense of increasing risks of committing an operational error in terms of excessive outflows that would result in unused storage and cause unnecessary damages downstream (i.e. increasing *NEF*).

(2) In general, there is a significant change in the average slope of the curves around *EF* = 20%. Above *EF* = 20%, significant increases in the level of protection can be obtained with relatively small increases in outflow rates. However, the flatter slope observed for *EF* values below 20% indicates that greater changes in outflow rates are required in order to increase the level of protection by the same

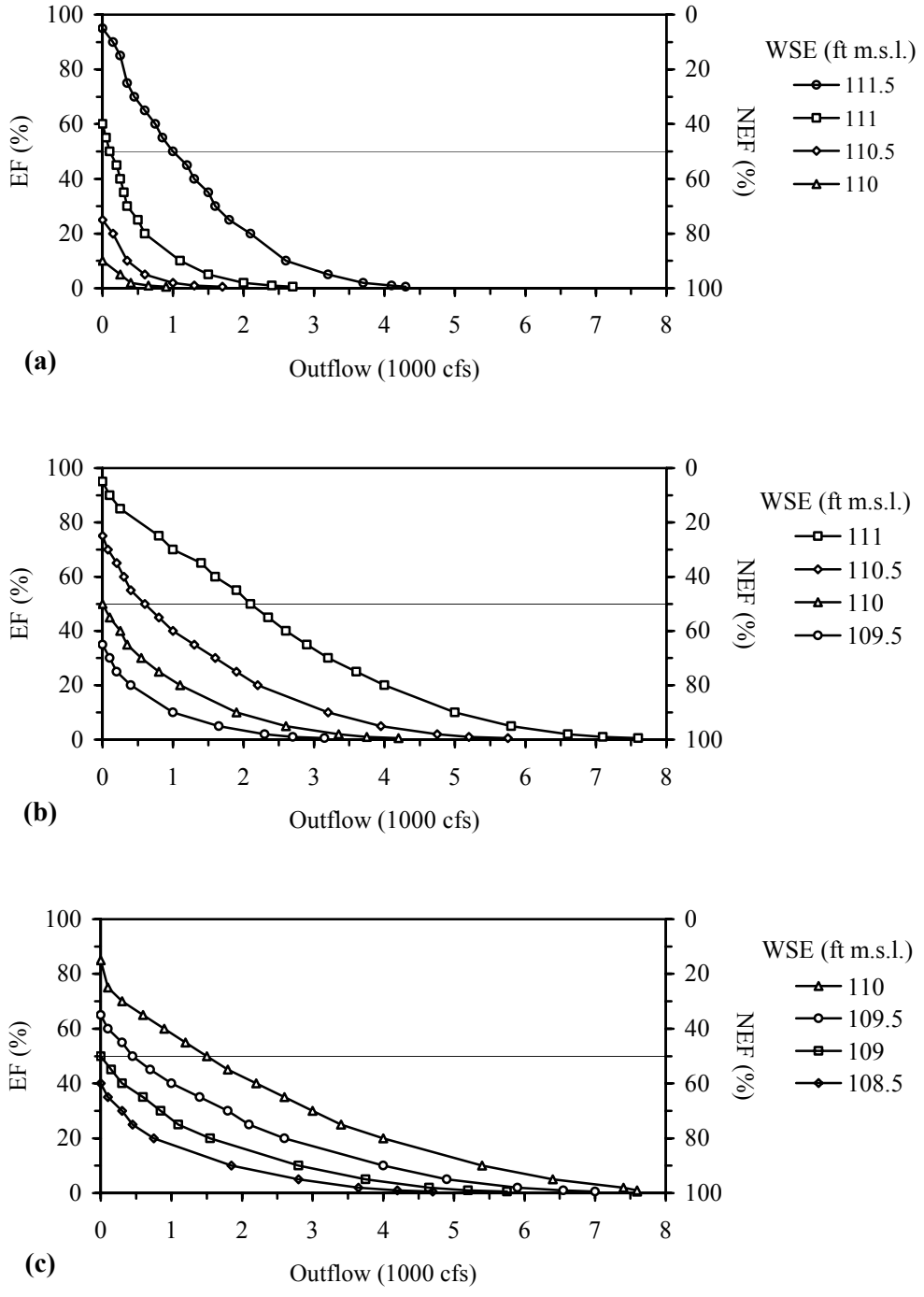

FIGURE 5.19. Variation in Outflow Rates as a Function of Risk for Selected Initial Conditions at Addicks. (a) Q_0 = 10,000 cfs (b) Q_0 = 20,000 cfs; and (c) Q_0 = 30,000 cfs

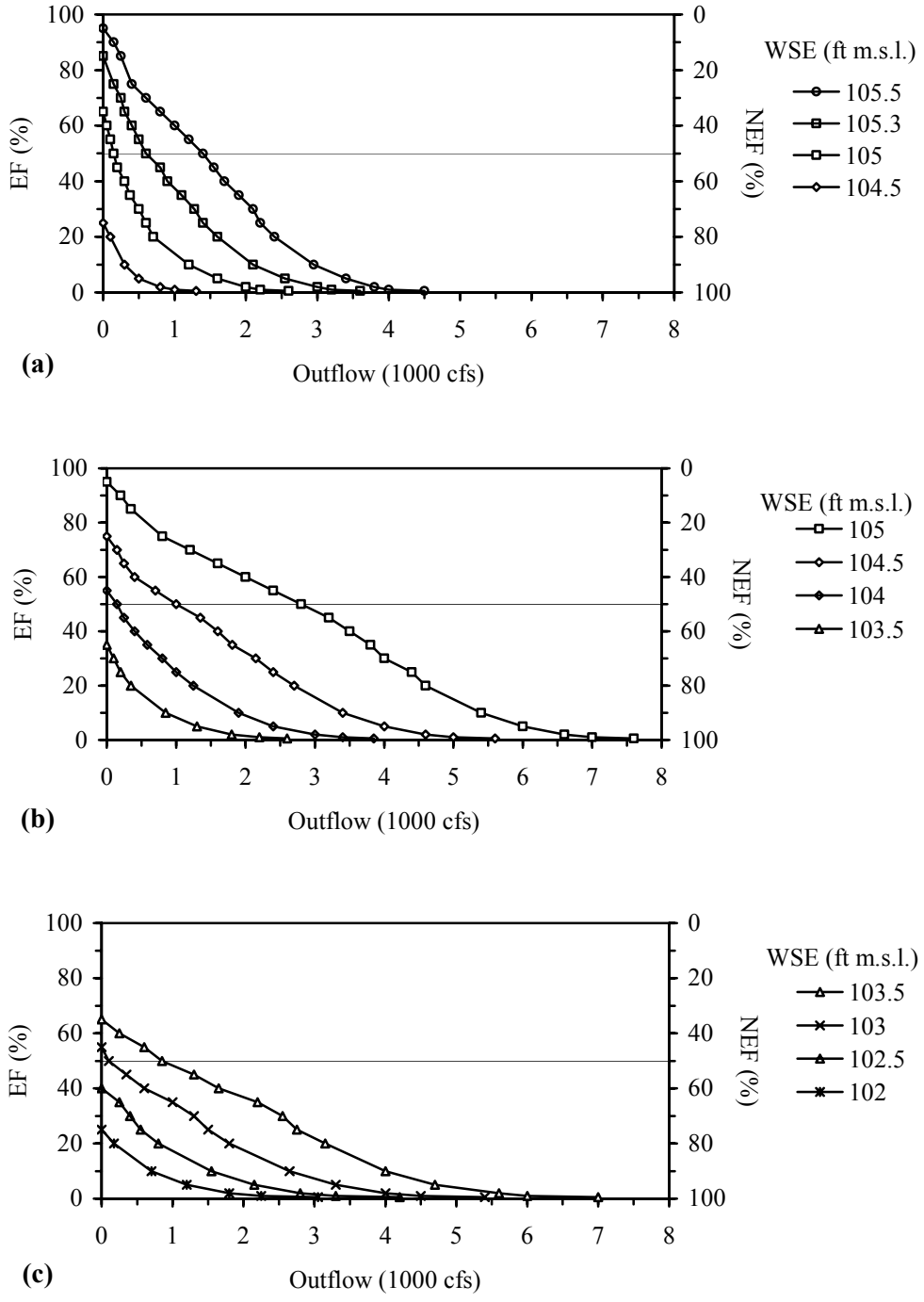

FIGURE 5.20. Variation in Outflow Rates as a Function of Risk for Selected Initial Conditions at Barker. (a) Q_0 = 10,000 cfs (b) Q_0 = 20,000 cfs; and (c) Q_0 = 30,000 cfs

amount. For example, if the initial conditions at Barker are: Q_0 = 10,000 cfs, WSE = 105 ft (Figure 5.20a), and *EF* is to be decreased from 60 to 50%, the outflow rate needs to be increased from 50 to 150 cfs. However, if *EF* is to be decreased from 20 to 10%, the outflow rate needs to be increased from 700 to 1,200 cfs.

(3) The *EF* value associated with the zero outflow point in each curve represents the risk of dam overtopping that would be taken if no releases are made. On the other hand, the corresponding *NEF* value represents the probability that the reservoir will be able to accommodate the remainder of the flood even if no releases are made. For example, if the initial conditions at Addicks are Q_0 = 10,000 cfs (Figure 5.19a) and WSE = 111 ft (residual storage = 16,023 acre-ft = 8% of MSC), there is a 60% risk (*EF*) that the residual storage will be exceeded if the outlet gates are kept closed during the remainder of the flood. Conversely, there is a 40% probability (*NEF*) that the residual storage will be sufficient to contain the entirety of the incoming flows.

(4) The separation between the curves for a given Q_0 implies that the outflow rate required to maintain the same level of protection (constant *EF*) increases considerably with relatively minor reductions in residual storage. For example, at Barker, the residual storage corresponding to WSE's of 102, 102.5, 103 and 103.5 ft are: 62,561; 55,225; 47,748; and 40,132 acre-ft (reductions in residual storage of 11.7, 13.5, and 16.0%, respectively). For Q_0 = 30,000 cfs (Figure 5.20c) and *EF* = 1%, the required outflows at these stages are: 2,250; 3,300; 4,500; and 6,000 cfs (increases of 31.8, 26.7, and 25.0% respectively). Greater increases in outflow rates (percentage wise) are observed as *EF* increases.

(5) The upward shift of the curves for a given WSE indicates that greater outflow rates are required in order to maintain the same level of protection as Q_0 increases. For instance, if the initial conditions at Addicks are WSE = 110 ft and Q_0 = 10,000 cfs (Figure 5.19a), the outlet gates may remain closed if the desired level of protection (*EF*) is 10%. For Q_0 = 20,000 cfs (Figure 5.19b), a 50% risk

of dam overtopping would be taken if the outlet gates are kept closed, and an outflow rate of 2,000 cfs would be needed to maintain the same level of protection (10%). For Q_0 = 30,000 cfs (Figure 5.19c); the risk increases to 85% and an outflow rate of 5,400 cfs would be needed to reduce it to 10%.

5.2.2.4. EOS Based on the Government Owned Land (GOL) Storage Limit

The GOL limits indicate the elevation above which residential and commercial properties are susceptible to flooding (see Section 5.1.4). Under the current emergency operation policies the possible occurrence of upstream flooding does not justify making emergency releases. Nonetheless, emergency releases may be appropriate if reservoir levels are approaching or have exceeded the GOL limits. A new set of risk-based EOS was developed by setting the maximum allowable reservoir stage at the GOL limits. In contrast to the risk-based EOS presented thus far, the *EF* value associated with these schedules does not represent the risk of dam overtopping but the risk of upstream flooding. Therefore, this operational change would allow making emergency releases based on the probability of upstream flooding. Sample EOS for *EF* = 1%, *SS* = rising, and *TY* = annual, are presented in Figure 5.21.

This modification results in a substantial reduction of the available flood storage capacity of the reservoirs. The storage capacity is reduced by 42% for Addicks and by 60% for Barker. Consequently, the transition from normal to emergency operations would occur at considerably lower stages. For instance, for Q_0 = 10,000 cfs the EOS in Figure 5.16 (same parameter values as in Figure 5.21 but based on the MSC) would dictate emergency releases if the WSE at Addicks is above 104.6 ft and above 100.1 ft at Barker, while the EOS in Figure 5.21 would dictate emergency releases if the WSE at Addicks is above 101.7 ft and above 93.4 ft at Barker; a difference of 2.9 and 6.7 ft respectively. Furthermore, while the EOS in Figure 5.16 indicates that the outlet gates may remain closed if the WSE at Addicks is below 104.6 ft and below 100.1 ft at Barker, releases of up 2,000 and 7,983 cfs would be required by the EOS in Figure 5.21 for Addicks and Barker respectively.

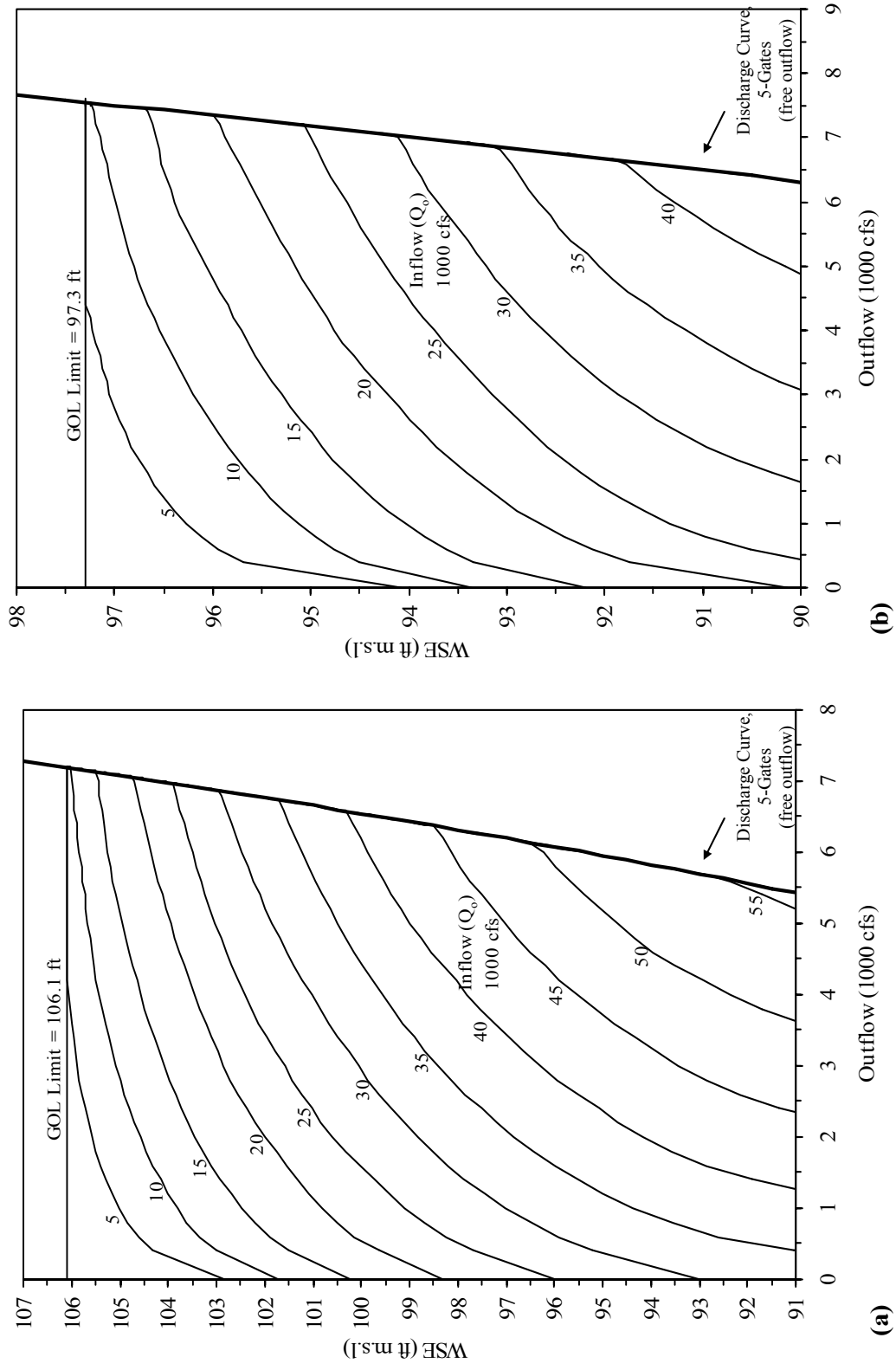

FIGURE 5.21. Risk-based EOS (EF = 1%, SS = Rising) Based on the Reservoirs GOL Limits. (a) Addicks; and (b) Barker

The operation of the reservoirs based on this alternative policy provides a greater degree of protection to upstream structures, but at the same time, it allows for a greater risk of making releases that would contribute to downstream flooding. As previously stated, this tradeoff presents a potential conflict of interests in which serious complaints or even lawsuits from downstream dwellers may arise since the policy allows emergency releases even though the reservoirs still have a significant amount of available storage capacity. In addition, the risk of upstream flooding is not as serious of a threat as it is the risk of dam overtopping. Although upstream flooding may cause severe damages, they would not be as severe as those that would result from dam overtopping. Therefore, higher risk EOS may be implemented in this case in order to reduce the possibility of excessive releases and balance the tradeoffs between upstream and downstream flooding.

CHAPTER VI

EVALUATION OF FLOOD REGULATION BASED ON ALTERNATIVE EMERGENCY OPERATION POLICIES

The EOS for the Addicks and Barker Reservoir system were developed in Chapter V using both the standard and risk-based methods. In this chapter, an existing model of the reservoirs developed for the *HEC-5 Simulation of Flood Control and Conservation Systems* (USACE 1998) computer program was updated to a *HEC-ResSim Reservoir System Simulation* (USACE 2003) model in order to test the EOS with the latest modeling capabilities. The emergency schedules were tested through a series of flood control simulations using hypothetical flood events occurring under different initial storage conditions. Rainfall data recorded from Tropical Storm Allison (TSA) was transposed over the Addicks and Barker watersheds to compute hypothetical inflow hydrographs at pertinent locations using the *HEC-HMS Hydrologic Modeling System* model (USACE 2001). The occurrence of extremely high pool levels in these reservoirs is typically attributed to the accumulation of water in storage over rainy periods rather than from a single event. Thus, in order to consider this cumulative effect, long-term simulations using historical data were used to establish the initial storage conditions at the reservoirs before the beginning of the hypothetical rainfall events. Repeated runs of the HEC-ResSim model were made using different flooding and residual storage scenarios to compare the regulation of the floods under alternative operating policies. The existing EOS for the reservoirs (USACE 1962) along with three newly developed risk-based EOS that were based on the storage capacity available within the Government Owned Land (GOL) limits were evaluated.

6.1. DEVELOPMENT OF HYPOTHETICAL RAINFALL-RUNOFF EVENTS

Flood events occurring during the life of the Addicks and Barker Reservoirs to date have not been of sufficient magnitude to require the implementation of emergency operations. However, the possibility of a storm that would produce enough runoff to trigger emergency operations is not far from reality considering the meteorology of the region. For instance, in some areas of Houston, the 5-day rainfall total that resulted from TSA during June 5 – 9, 2001, reached 35 inches (TSARP 2002b). Furthermore, at one point during the storm 28 inches of rain fell during a 12-hour period just northeast of downtown Houston. Such rainfall magnitude was estimated to be greater than the 500-yr rainfall event for this area in a 12-hr period (TSARP 2002b). This area is only about 30 and 35 miles northeast of the center of the Addicks and Barker watersheds, respectively. Due to the extreme nature of TSA and its proximity to the Addicks and Barker watersheds, it was decided that transposing the TSA rainfall pattern over the center of each watershed would provide hypothetical, but plausible, events to test the EOS.

6.1.1. Transposing TSA Over the Addicks and Barker Watersheds

The isohyetal pattern (contours of equal rainfall) for the 5-day rainfall total for TSA, the Harris County watershed boundaries, and several other data were provided in digital format (ArcView shape files) by the Harris County Flood Control District (HCFCD) along with 15-minute TSA rainfall data for several rain gages in Harris County. Figures 6.1 and 6.2 show the isohyetal pattern for TSA transposed over the center of the Addicks and Barker watersheds, respectively. The isohyetal method was applied in order to estimate the spatially averaged total rainfall depth for each watershed, including the 51 square mile watershed above the Piney Point gaging station downstream from the dams. This Buffalo Bayou sub-watershed will be referred to here as Piney Point watershed.

The total rainfall depth computations are presented in Tables 6.1 through 6.6. Each polygon in column (1) represents an equal rainfall polygon within the watershed formed by the TSA isohyetal pattern (see Figures 6.1 and 6.2). The value for the pair of

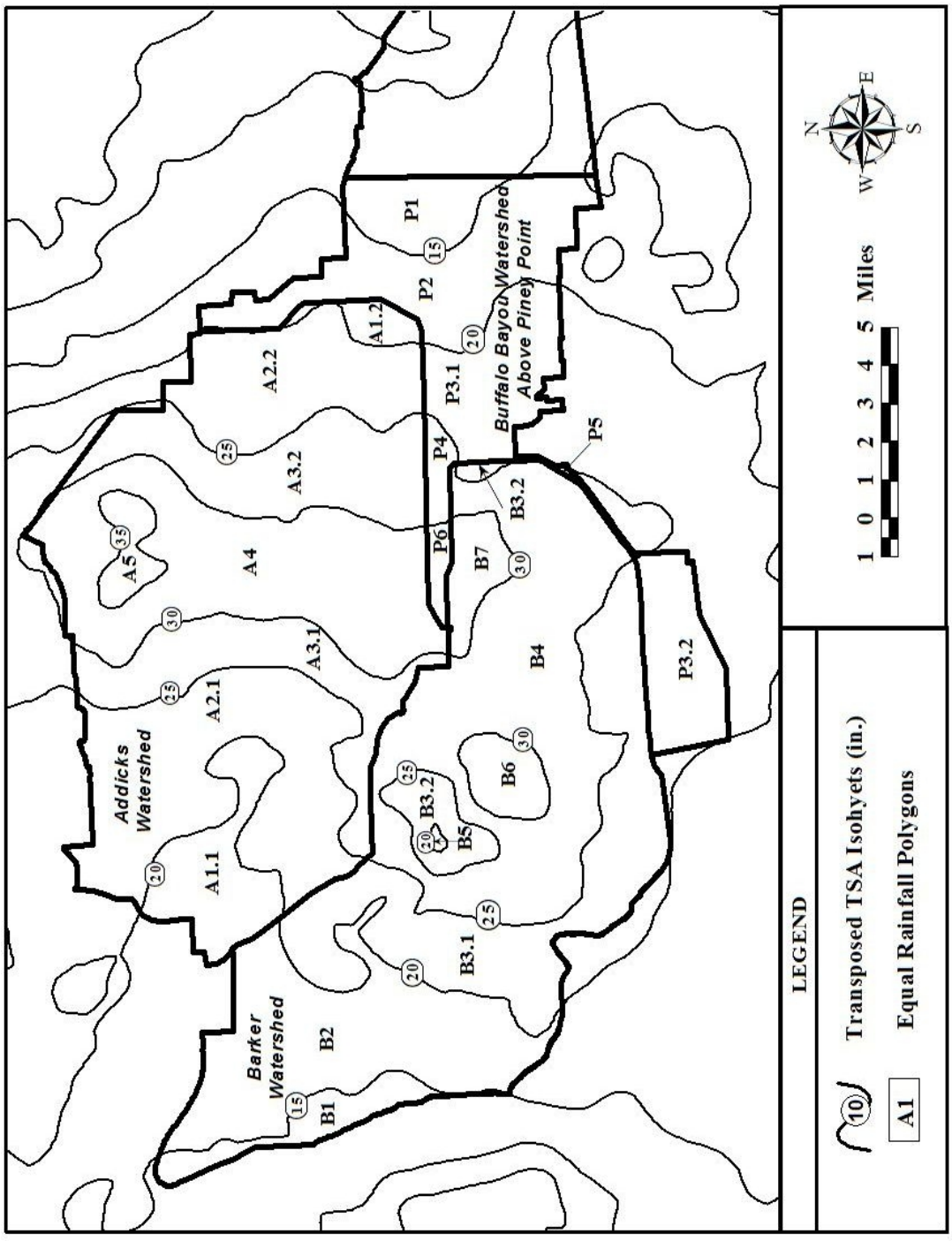

FIGURE 6.1. TSA Rainfall Distribution Transposed Over Addicks Watershed

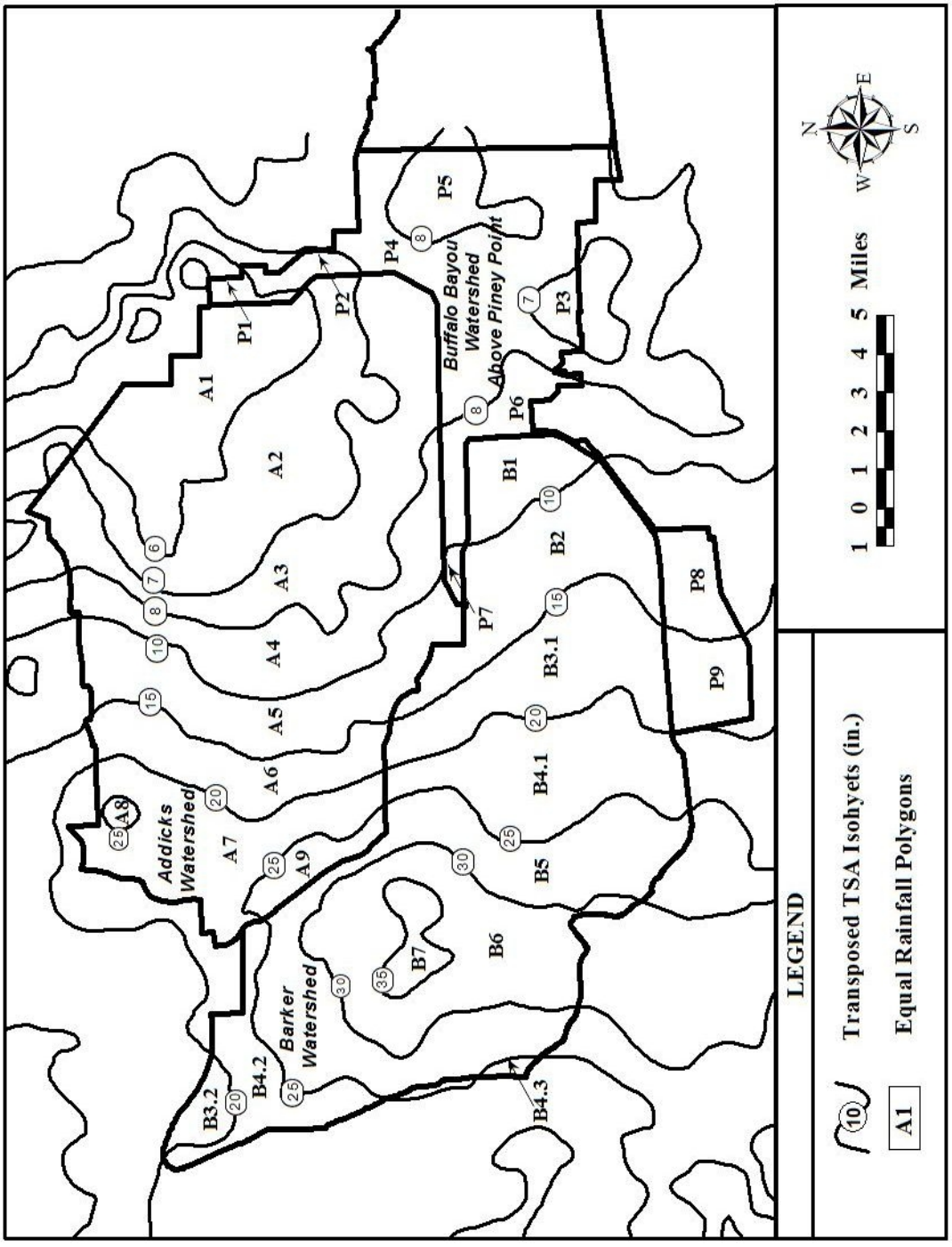

FIGURE 6.2. TSA Rainfall Distribution Transposed Over Barker Watershed

TABLE 6.1. Total Rainfall Depth for Addicks Watershed - TSA Transposed Over Addicks Watershed

Polygon ID	Isohyets Interval	Ave. Rainfall (in)	Area (mi^2)	Volume (in-mi^2)
(1)	(2)	(3)	(4)	(5)
A1.1	15 - 20	17.5	11.33	198.28
A1.2	15 - 20	17.5	2.32	40.65
A2.1	20 - 25	22.5	32.25	725.60
A2.2	20 - 25	22.5	17.38	391.07
A3.1	25 - 30	27.5	15.70	431.70
A3.2	25 - 30	27.5	18.29	502.87
A4	30 - 35	32.5	35.12	1141.53
A5	35	35	3.34	116.83
		Σ =	135.7	3548.53
		Total rainfall depth = 3548.53 / 135.7 = 26.14 in		

TABLE 6.2. Total Rainfall Depth for Barker Watershed - TSA Transposed Over Addicks Watershed

Polygon ID	Isohyets Interval	Ave. Rainfall (in)	Area (mi^2)	Volume (in-mi^2)
(1)	(2)	(3)	(4)	(5)
B1	10 - 15	12.5	5.82	72.79
B2	15 - 20	17.5	30.26	529.62
B3.1	20 - 25	22.5	32.09	721.91
B3.2	20 - 25	22.5	0.58	12.98
B4	25 - 30	27.5	49.06	1349.04
B5	20	20	0.24	4.78
B6	30	30	4.21	126.34
B7	30 - 32	31	4.31	133.61
		Σ =	126.57	2951.06
		Total rainfall depth = 2951.06 / 126.57 = 23.32 in		

TABLE 6.3. Total Rainfall Depth for Piney Point Watershed - TSA Transposed Over Addicks Watershed

Polygon ID	Isohyets Interval	Ave. Rainfall (in)	Area (mi^2)	Volume (in-mi^2)
(1)	(2)	(3)	(4)	(5)
P1	10 - 15	12.5	6.52	81.50
P2	15 - 20	17.5	19.12	334.62
P3.1	20 - 25	22.5	12.03	270.77
P3.2	20 - 25	22.5	9.65	217.01
P4	25 - 30	27.5	1.93	53.16
P5	25	25	0.34	8.48
P6	30 - 32	31	1.45	45.04
		Σ =	51.05	1010.57
		Total rainfall depth = 1010.57 / 51.05 = 19.80 in		

TABLE 6.4. Total Rainfall Depth for Addicks Watershed - TSA Transposed Over Barker Watershed

Polygon ID	Isohyets Interval	Ave. Rainfall (in)	Area (mi^2)	Volume (in-mi^2)
(1)	(2)	(3)	(4)	(5)
A1	5 - 6	5.5	17.45	95.99
A2	6 - 7	6.5	25.21	163.86
A3	7 - 8	7.5	26.01	195.05
A4	8 - 10	9	16.93	152.35
A5	10 - 15	12.5	17.60	220.03
A6	15 - 20	17.5	11.02	192.89
A7	20 - 25	22.5	17.39	391.21
A8	25	25	0.62	15.58
A9	25 - 30	27.5	3.43	94.33
		Σ =	135.7	1521.27
		Total rainfall depth = 1521.273 / 135.7 = 11.21 in		

TABLE 6.5. Total Rainfall Depth for Barker Watershed - TSA Transposed Over Barker Watershed

Polygon ID	Isohyets Interval	Ave. Rainfall (in)	Area (mi^2)	Volume (in-mi^2)
(1)	(2)	(3)	(4)	(5)
B1	8 - 10	9	6.14	55.25
B2	10 - 15	12.5	16.63	207.88
B3.1	15 - 20	17.5	16.75	293.13
B3.2	15 - 20	17.5	2.51	43.94
B4.1	20 - 25	22.5	17.78	400.05
B4.2	20 - 25	22.5	8.39	188.73
B4.3	20 - 25	22.5	0.55	12.42
B5	25 - 30	27.5	31.88	876.70
B6	30 - 35	32.5	22.83	742.07
B7	35	35	3.34	116.80
		Σ =	126.80	2936.96
		Total rainfall depth = 2936.96 / 126.8 = 23.16 in		

TABLE 6.6. Total Rainfall Depth for Piney Point Watershed - TSA Transposed Over Barker Watershed

Polygon ID	Isohyets Interval	Ave. Rainfall (in)	Area (mi^2)	Volume (in-mi^2)
(1)	(2)	(3)	(4)	(5)
P1	5 - 6	5.5	1.12	6.16
P2	6 - 7	6.5	1.85	12.03
P3	7	7	1.86	13.02
P4	7 - 8	7.5	23.79	178.43
P5	8	8	6.31	50.48
P6	8 - 10	9	5.62	50.58
P7	10 - 12	11	0.66	7.26
P8	10 - 15	12.5	4.77	59.63
P9	15 - 20	17.5	5.09	89.08
		Σ =	51.07	466.65
		Total rainfall depth = 466.65 / 51.07 = 9.14 in		

isohyets enclosing each polygon is recorded in column (2). These values are used to calculate the average rainfall for each polygon (column 3). The area of the polygons (column 4) was measured in the ArcView software package. The total rainfall depth is obtained by multiplying the average rainfall by the area of each polygon (column 5), totaling these products, and dividing it by the total watershed area. In summary, transposing TSA over Addicks watershed resulted in total rainfall depths of 26.14, 23.32, and 19.80 inches for Addicks, Barker, and Piney Point watersheds, respectively. Lower values resulted when TSA was transposed over Barker watershed, with total rainfall depths of 11.21, 23.16, and 9.14 inches respectively.

6.1.2. Development of HEC-HMS Model

The following sections present the model selection and parameter estimation for each component of the HEC-HMS model. The following hypothetical rainfall-runoff scenarios were modeled based on alternative premises regarding the location of TSA:

- Scenario (1): TSA transposed over Addicks watershed.
- Scenario (2): TSA transposed over Barker watershed.

6.1.2.1. Basin Model

A simplified basin model was developed in HEC-HMS to simulate the rainfall-runoff process of the watersheds and generate the hypothetical flood hydrographs needed to test the EOS. The basin model consists of three sub-basin elements connected to separate sinks which represent Addicks and Barker dams, and the Piney Point gaging station. No further connectivity of the elements was needed since the objective of the simulation was to obtain inflow hydrographs for each reservoir and local flows to the Piney Point gaging station.

The Soil Conservation Service (SCS), now known as the Natural Resources Conservation Service (NRCS), curve number (CN) method was selected to compute total runoff volumes. The required parameters for this method are the CN and the initial loss. The CN values representing current watershed development conditions were 70 for

Addicks and Barker, and 90 for Piney Point (Ahrens and Maidment 1999). It was assumed that the watersheds were likely to be saturated when an extreme event occurred, thus the initial loss parameter was set to zero. The optional percent imperviousness parameter was set to 5% for Addicks and Barker, and 85% for Piney Point (Ahrens and Maidment 1999).

The SCS unit hydrograph method was used for transforming excess precipitation to runoff. The only parameter required to apply this method is the SCS lag time (t_L). For this particular application, the NRCS lag equation could not be used since this equation was developed for watersheds with areas of less than about 3.1 mi^2 (Wurbs and James 2002). Instead, t_L was obtained using the empirical relationship:

$$t_L = 0.6 * t_C \tag{6.1}$$

which was also developed by the NRCS. The time of concentration (t_C) in minutes for each watershed was computed based on the Bransby-Williams empirical equation:

$$t_C = 21.3 \frac{L}{5280} \left(\frac{1}{A^{0.1} S^{0.2}} \right) \tag{6.2}$$

where L = length (ft) of flow path from the watershed divide to the outlet; A = watershed area in mi^2; and S = watershed average slope in ft/ft. The estimated L values for Addicks, Barker, and Piney Point are 111,161 ft, 162,879 ft, and 111,810 ft, respectively. These values were computed in ArcView based on the streams coverage provided by the HCFCD. The S value for Addicks and Barker is approximately 0.001 ft/ft (Doan 2000). The S value for Piney Point is about 0.00066 ft/ft. This value was also estimated using ArcView by computing the average of several slope measurements at various locations of the watershed based on a 2-foot elevation contour coverage of the area. The estimated values for t_L are 655.5, 967.1, and 791.1 minutes for Addicks, Barker, and Piney Point watersheds respectively.

Finally, it was decided that the "no baseflow" method would be used as recommended by the "Using baseflow parameters with HMS in Harris County" report (TSARP 2002c).

6.1.2.2. Meteorologic Model

Two meteorologic models were created in HEC-HMS, one for each TSA transposed location scenario. The selected precipitation method was the "User Gage Weighting" method. Three non-recording gages, or total storm gages, were created to input the total rainfall depth for each watershed (see Section 6.1.1). The temporal distribution of the storm was based on the actual 15-minute data recorded at station HC-1600 (located in Greens Bayou watershed at La Ley Road). This rain gage recorded the highest rainfall depth for TSA. One recording gage was added in order to incorporate this particular rainfall distribution into the model. Given that only one total storm gage was used for each watershed, their total storm gage weight was set to one. Similarly, a value of one was input as the temporal gage weight for each watershed.

6.1.2.3. Control Specifications

The control specifications contain the start/stop timing and calculation intervals for the simulation runs. Only one control specification was necessary for this model. The Houston area was affected by TSA from June 5 to June 9, 2001. In order for the entire watersheds to contribute to runoff, the simulation time must exceed the duration of the storm. In addition, enough time should be provided in order to capture the entire runoff volume produced by the storm. Therefore, after a series of test runs, the simulation time interval was set from the beginning of June 5 to the end of June 13 using a one hour computational time step.

6.1.3. HEC-HMS Model Results

The results for each simulation scenario are presented in Figure 6.3. As explained in Section 6.1.2.2, the temporal precipitation distribution follows the pattern of

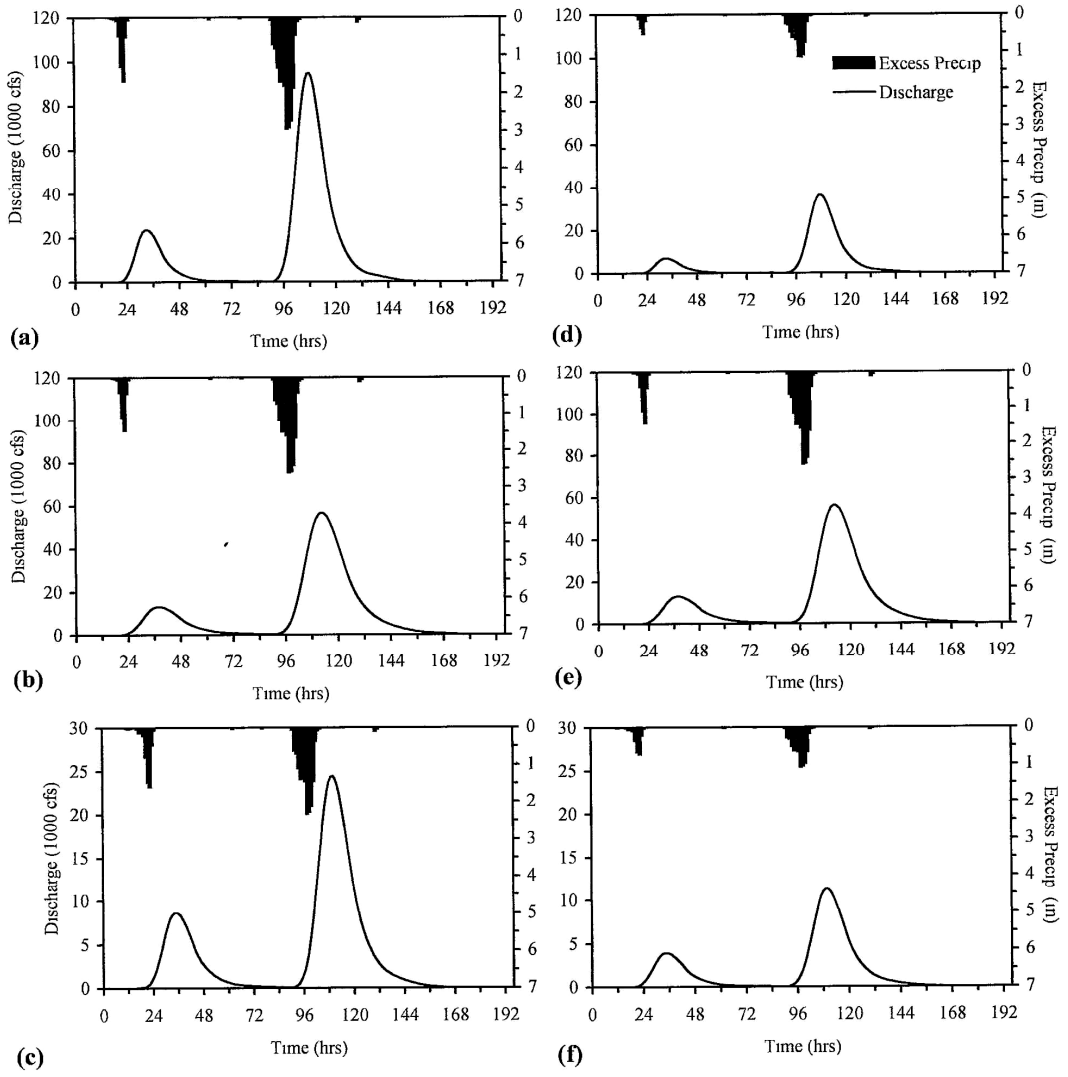

FIGURE 6.3. Computed Excess Precipitation and Flood Hydrographs for (a) Addicks; (b) Barker; and (c) Piney Point Based on Scenario (1); and for (d) Addicks; (e) Barker; and (f) Piney Point Based on Scenario (2)

TSA recorded at station HC-1600. This pattern was similar in many other rain gages. Initially, TSA passed through the Harris County area on June 5th and then continued in a northward direction. However, the storm looped back to the southwest, and on the evening of June 8th and early hours of June 9th, the re-intensified storm delivered a

second, and more intense, wave of precipitation (TSARP 2002b). Since the first wave had saturated the soils, runoff was produced immediately when the storm returned. This precipitation pattern resulted in the double-peak flood hydrographs shown in the figures.

A summary of the simulation results which includes the peak discharge and total volume of runoff produced in each simulation scenario is presented in Table 6.7.

TABLE 6.7. Summary of HEC-HMS Simulation Results

	Addicks		Barker		Piney Point	
Scenario (1)	Peak Discharge (cfs) (2)	Total Volume (ac-ft) (3)	Peak Discharge (cfs) (4)	Total Volume (ac-ft) (5)	Peak Discharge (cfs) (6)	Total Volume (ac-ft) (7)
1	94,860	163,868	56,575	134,441	24,418	53,427
2	36,334	59,814	56,151	133,384	11,231	24,457

For comparison purposes, a similar analysis performed by the TSA Recovery Project (TSARP 2002a) is introduced here. As in this study, the TSARP analysis consisted of transposing TSA over the reservoir watersheds and computing the resulting runoff hydrographs with HEC-HMS. The major difference between the models is that in the TSARP model the infiltration losses were estimated using a variable runoff coefficient which was dependent upon the amount of accumulated rainfall, while in this study; the losses were estimated using the SCS curve number method. The TSARP model computed total runoff volumes of 155,330 ac-ft for Addicks, and 130,507 ac-ft for Barker when TSA was transposed over each reservoir. The total runoff volumes computed in this study compare well with these results. The total runoff volumes for Addicks in scenario (1) (163,868 ac-ft) and for Barker in scenario (2) (133,384 ac-ft) are only 5.5% and 2.2% higher than the TSARP values. The peak discharge values were not compared since they were not included in the TSARP report.

It is important to point out here that in any scenario, the target non-damaging discharge rate of 2,000 cfs at the Piney Point gaging station would be greatly exceeded by the runoff produced in the watershed below the dams. Therefore, great flood damages would result along Buffalo Bayou even if the reservoir gates remain closed during the entire storm event.

6.2. DEVELOPMENT OF HEC-RESSIM MODEL

The HEC-ResSim program is divided into three modules: (1) watershed setup, (2) reservoir network, and (3) simulation. Streams, projects (e.g., reservoirs, levees), gage locations, impact areas, and hydrologic and hydraulic data for a specific area are defined in the watershed setup module. The river schematic is developed in the reservoir network module. Routing reaches and other network elements are added to complete the connectivity of the network schematic. Once the schematic is complete, physical and operational data for each network element are defined. The operational alternatives to be analyzed are also created in this module. The simulation module is designed to facilitate the analysis phase of reservoir modeling. For each simulation, a time window is specified for either a single alternative or a group of alternatives (USACE 2003).

6.2.1. Defining Reservoir Operations Data

The Addicks and Barker reservoirs were set to operate as a system based on controlling flows at the downstream control point representing the Piney Point gaging station. The typical balancing configuration of making releases from the reservoir with the highest percentage of its capacity occupied was adopted. One river reach was defined between the reservoirs and Piney Point. Reservoir releases were routed through this reach based on the Muskingum method with a travel time K of 15 hours and a weighting factor x of 0.25. Some of the physical data entered for each reservoir include the elevation-storage-area relationship, controlled outlets and emergency spillway characteristics, and the maximum rate of increase or decrease in reservoir releases.

A series of operation sets composed of zones, rules, and guide curves describe the operation plan upon which release decisions at each time step are based. Zones are operational subdivisions of the reservoir. Each zone is defined by a curve describing the top of the zone. Operation rules represent goals and constraints upon releases. Rules are used to describe the different factors influencing release decisions when the reservoir's water surface elevation (WSE) is within a particular zone. Rules are applied within a zone according to their relative priority. HEC-ResSim works from the lowest to the highest priority rule and adjusts releases to meet each rule. If two rules contradict each other, the higher priority rule applies (USACE 2003). Guide curves represent target elevations of the reservoir. Generally, the guide curve defines the top of the conservation pool, which effectively defines the flood control storage capacity. However, Addicks and Barker are strictly flood control reservoirs. Therefore, the adopted guide curves are simply the bottom elevation of the reservoirs. The regulation goal in each operation set is to empty the reservoir as quickly as possible within the physical constraints and operational rules described in the model.

In order to investigate the effects of allowing emergency releases based on the probability of upstream flooding, three of the risk-based emergency operation schedules (REOS) that were developed based on the GOL storage capacity were selected. These REOS correspond to exceedance frequency (*EF*) values of 1, 5, and 20%. Four operational sets were created to describe these REOS and the current emergency operations as described in the 1962 reservoir regulation manual for these reservoirs (USACE 1962). The latter operation set will be referred to here as Standard 1962. Normal operation rules were also defined in each operational set.

The reservoirs were subdivided into three zones in the Standard 1962 operation set. The lower zone ranges from the bottom of the reservoirs to an elevation below which no emergency release rules were assigned. In this zone, releases are determined based on normal operations. Three rules govern reservoir operations in this zone. A maximum release rule establishes the 2,000 cfs flow limit at the Piney Point control point, and the other rules establish the minimum and maximum rates of change of

reservoir releases under normal operations. The second zone defines the portion of the reservoir pool where emergency operations might be triggered. Releases in this zone are dictated by two rules. The first rule sets releases in accordance to the flow limit at Piney Point. The second rule, which has a higher priority, is an induced surcharge rule. This type of rule allows creating an EOS using the standard method. This is the only type of rule that allows making releases based on two model variables (i.e. WSE and inflows). This rule was used to approximate the 1962 EOS. When inflows are large enough, this rule is used to determine the appropriate emergency releases. The third zone represents elevations above the reservoirs' maximum WSE. If the WSE reaches this zone, a maximum release rule is implemented which is governed by the reservoirs' elevation versus outflow capacity relationship. In addition, uncontrolled releases would occur in this zone through the reservoirs' emergency spillways.

The operation sets describing the REOS rules were developed as follows. The lower zone and the zone above the maximum WSE are identical to the ones in the Standard 1962 operation set. The REOS determine releases as function of inflows and WSE. However, save for the induced surcharge rule, HEC-ResSim only allows establishing releases as a function of one model variable. Therefore, a series of elevation zones were established between these two zones at intervals of 0.2 ft. For each zone, the REOS were entered as two release function rules, one for rising and one for receding streamflow conditions. These rules determine releases as a function of the previous 24-hr inflow average. In this manner, the model was able to determine emergency releases as a function of both WSE (i.e. each zone) and inflows (i.e. release rules). Each zone also considers the maximum flow rule at Piney Point. However, the REOS rules have a higher priority, reflecting the change in operational policy under emergency conditions. In addition, the minimum and maximum rates of change of reservoir releases under normal operations (120 cfs/hr for Addicks and 114 cfs/hr for Barker, approximately 1-foot gate opening per hour) are overridden under emergency conditions and the model follows the larger rates of change established in the reservoirs' physical data (1,000 cfs/hr).

6.2.2. Defining Flood Regulation Simulations

As explained in section 6.1.2, two precipitation scenarios where adopted to test the operation of the reservoirs under emergency conditions. The regulation of the resulting flood hydrographs was simulated under two alternative initial storage (IS) conditions. For the first IS condition (IS1), the reservoirs were assumed to be empty, replicating the actual storage conditions at the beginning of TSA. For the second IS condition (IS2), the reservoirs were assumed to be partially filled. The historic record was used to find a scenario in which the storage was gradually reduced by a sequence of relatively small flood events before the occurrence of a major flood event. An excellent example of this ratcheting effect was the series of floods that occurred in the spring of 1992. The storage levels for IS2 reflect the accumulated storage up to March 4, 1992 (Addicks 25% full, and Barker 28% full). On that date, up to 10 inches of rain fell in portions of western Houston causing the reservoirs to reach record storage levels (USACE 1995). In summary, a total of four simulation scenarios were analyzed using the four alternative operating policies:

- Scenario (F1IS1) – Regulation of flood hydrographs resulting from transposing TSA over Addicks with full storage capacity available.
- Scenario (F2IS1) – Regulation of flood hydrographs resulting from transposing TSA over Barker with full storage capacity available.
- Scenario (F1IS2) – Regulation of flood hydrographs resulting from transposing TSA over Addicks with storage capacity partially full (Mar-4-1992 storage levels).
- Scenario (F2IS2) – Regulation of flood hydrographs resulting from transposing TSA over Barker with storage capacity partially full (Mar-4-1992 storage levels).

6.2.3. HEC-ResSim Simulation Results

The simulation analyses served to evaluate the four operational alternatives based on the following criteria: maximum WSE (upstream flooding), reservoir releases, and downstream flooding. Results are presented in Figures 6.4 – 6.11 and summarized in Table 6.8. The figures depict WSE traces, reservoir releases, and downstream flooding

TABLE 6.8. HEC-ResSim Simulation Results for Alternative Emergency Reservoir Regulation Policies

		Addicks				Barker				Piney Point	
Simulation Scenario	Regulation Policy	Peak WSE (ft)	Over GOL† (ft)	Flooded over GOL‡ (mi^2)	Peak Release (cfs)	Peak WSE (ft)	Over GOL† (ft)	Flooded over GOL‡ (mi^2)	Peak Release (cfs)	Peak Discharge (cfs)	Periods over 2,000 cfs
(1)	(2)	(3)	(4)	(5)	(6)	(7)	(8)	(9)	(10)	(11)	(12)
F1IS1	Standard 1962	108.8	2.7	2.5	7,219	101.2	3.9	3.4	79	24,686	111
	REOS 1%	108.0	1.9	1.7	7,392	99.5	2.2	2.1	7,887	24,418	151
	REOS 5%	108.0	1.9	1.8	7,396	99.5	2.2	2.1	7,892	24,418	151
	REOS 20%	108.1	2.0	1.8	7,400	99.5	2.2	2.1	7,897	24,488	151
F1IS2	Standard 1962	111.7	5.6	5.9	7,704	104.4	7.1	6.0	6,570	24,790	134
	REOS 1%	111.2	5.1	5.3	7,706	102.5	5.2	4.3	8,329	27,933	196
	REOS 5%	111.2	5.1	5.3	7,711	102.6	5.3	4.4	8,347	27,407	196
	REOS 20%	111.3	5.2	5.4	7,715	102.7	5.4	4.5	8,362	27,022	193
F2IS1	Standard 1962	100.8	-5.3	0.0	244	100.3	3.0	2.8	2,173	11,962	94
	REOS 1%	100.7	-5.4	0.0	1,155	98.9	1.6	1.6	7,804	11,878	144
	REOS 5%	100.8	-5.3	0.0	330	98.9	1.6	1.6	7,808	11,962	144
	REOS 20%	100.8	-5.3	0.0	244	99.0	1.7	1.7	7,815	11,962	144
F2IS2	Standard 1962	105.7	-0.4	0.0	0	103.7	6.4	5.3	4,908	11,964	113
	REOS 1%	104.8	-1.3	0.0	6,945	102.2	4.9	4.0	8,289	13,903	189
	REOS 5%	104.9	-1.2	0.0	6,621	102.3	5.0	4.1	8,300	13,311	176
	REOS 20%	105.1	-1.1	0.0	5,502	102.4	5.1	4.2	8,312	12,073	151

Notes: † Refers to the water surface elevation above the GOL limits.

‡ Flooded area beyond GOL limits.

(a)

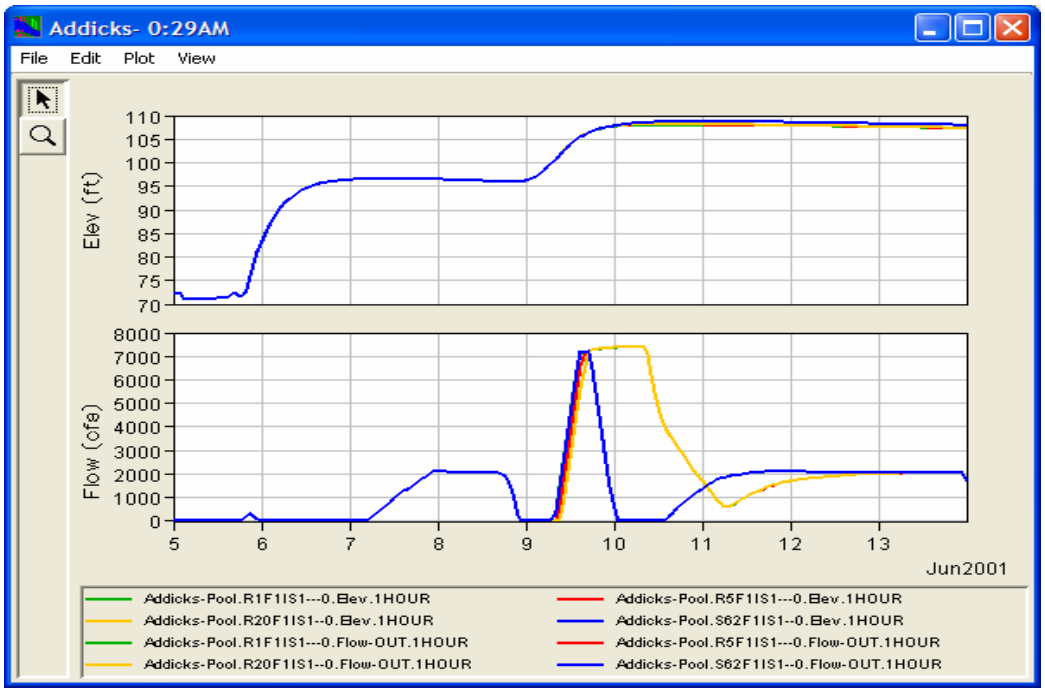

(b)

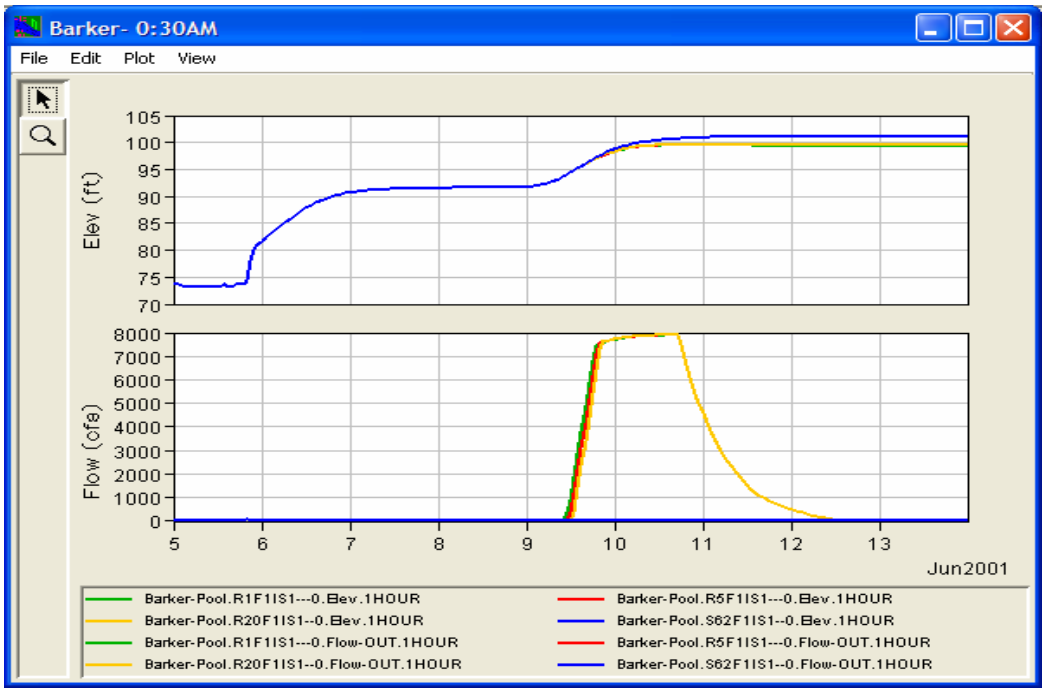

FIGURE 6.4. Water Surface Elevation Traces and Reservoir Releases for a) Addicks; and b) Barker; Based on Simulation F1IS1

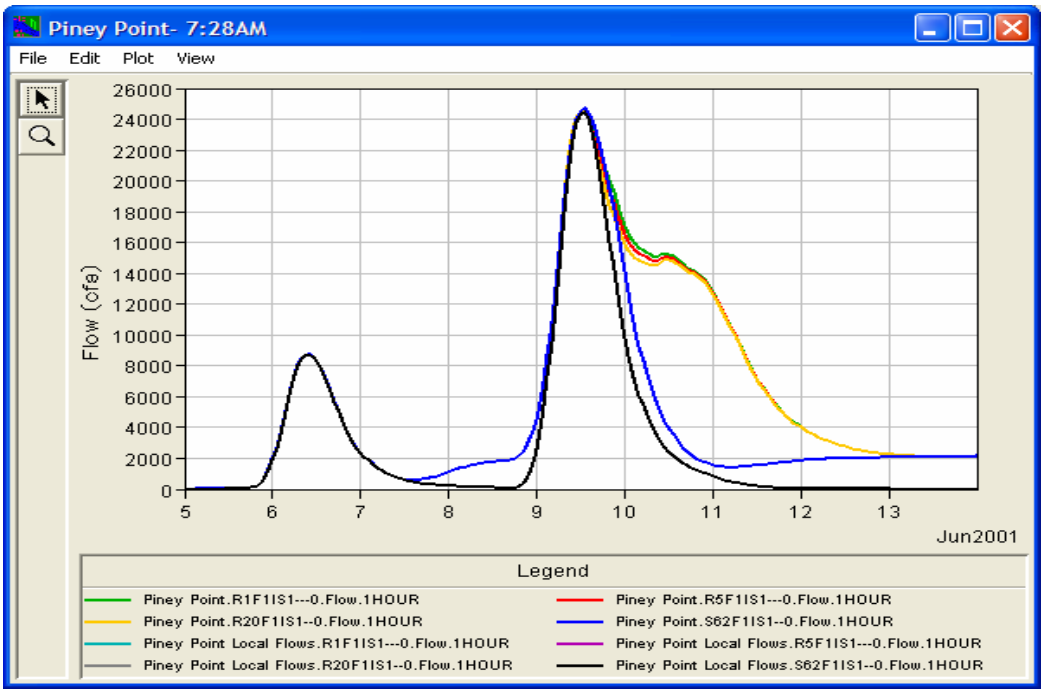

FIGURE 6.5. Flooding Conditions at Piney Point Based on Simulation F1IS1

conditions for the hypothetical period of June 5–13, 2001. The results for the alternative operation sets are color-coded as follows: blue for Standard 1962, green for REOS *EF*=1%, red for REOS *EF*=5%, and yellow for REOS *EF*=20%. The black line in the Piney Point plots represents local uncontrolled inflows. The F1IS1 simulation results for Addicks (Figure 6.4) show that the risk-based releases are very similar and continue for a longer period than those dictated by Standard 1962. However, as shown in Table 6.8, the maximum difference in peak WSE between Standard 1962 and the REOS alternatives is only 0.8 ft. In the case of Barker, emergency releases were only dictated by the REOS policies, resulting in lower peak WSE's (1.7 ft lower) (Table 6.8). Although the local uncontrolled runoff at Piney Point greatly exceeds the 2,000 cfs limit, emergency releases after June 10 further increased downstream flooding. While differences in peak discharge among alternatives are not significant, higher flows are sustained for a significantly longer period. Moreover, between days 10 and 11 there are

instances were the flows resulting from the REOS alternatives are up to three times higher than those of Standard 1962. This increase in downstream flooding is the result of making emergency releases to protect the areas above the GOL limits. However, the magnitude of TSA is such that even when the reservoirs are releasing water at maximum capacity, upstream flooding could not be prevented. The benefit of making emergency releases was minimal in terms of the area that was protected from flooding (less than 1 mi^2 for Addicks and 1.3 mi^2 for Barker) (Table 6.8).

Similar observations were made from the F2IS1 simulation (Figures 6.6 – 6.7). In this case, the inflows into Addicks are significantly smaller (Table 6.7), and thus emergency releases were only dictated by the REOS *EF*=1% and *EF*=5% policies. These releases, however, were relatively small and the difference in peak WSE's was minimal. Emergency releases in Barker were only dictated by the REOS policies, resulting in lower peak WSE's (1.3 ft lower) (Table 6.8). Once again, there is no significant difference in peak flows at Piney Point, and the same scenario of having higher flows for a longer period was observed. The effect of following a lower risk REOS is better observed here. Although only a small difference was observed in the emergency releases for Barker, the higher release rates dictated by the REOS *EF*=1% and *EF*=5% policies in Addicks resulted in higher discharge values at the Piney Point gage during the June 10–11 period. Also, the WSE at Addicks never reach the GOL limits, but this was not the case for Barker. Following Standard 1962, the peak WSE at Barker was 3 ft over the GOL limits, covering an area of 2.8 mi^2. Once again, the REOS policies failed to significantly reduce flooding beyond the GOL limits as compared to the Standard 1962 policy (Table 6.8).

Scenarios F1IS2 and F2IS2 (Figures 6.8 – 6.11) provide better examples for observing the variability in emergency releases as a function of risk. As with most of the previous simulations, the flood that occurs between June 9 and 10 triggers the emergency operations, but the magnitude of flood is such that even making reservoir releases at maximum capacity cannot offset the amount of water that is entering the reservoirs in such a short time and the WSE quickly exceeds the GOL limits. However,

(a)

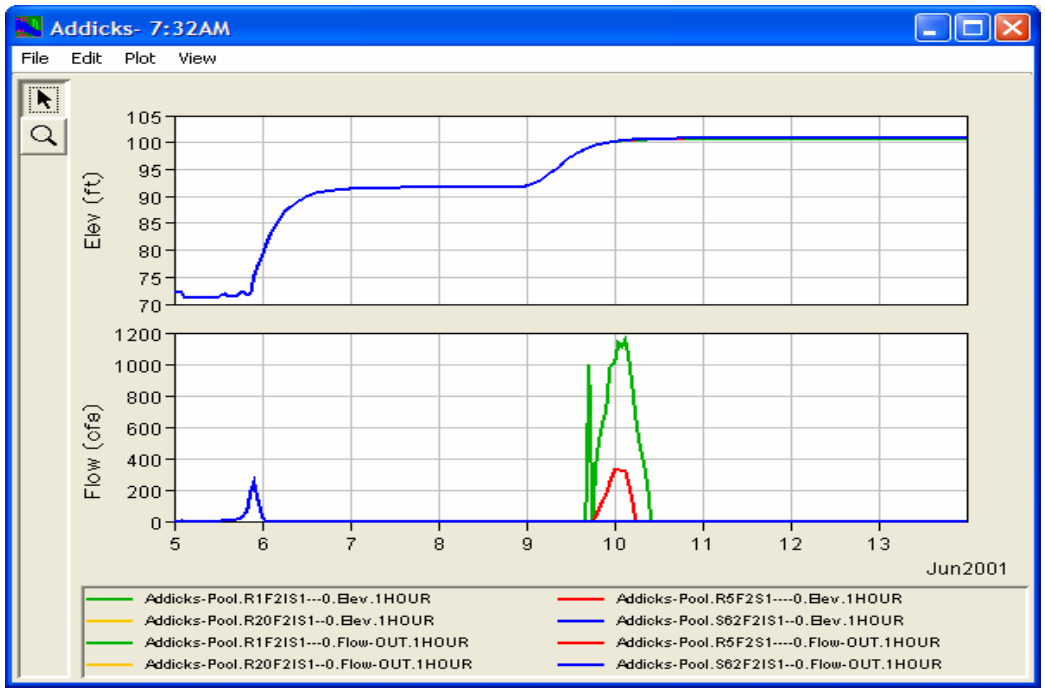

(b)

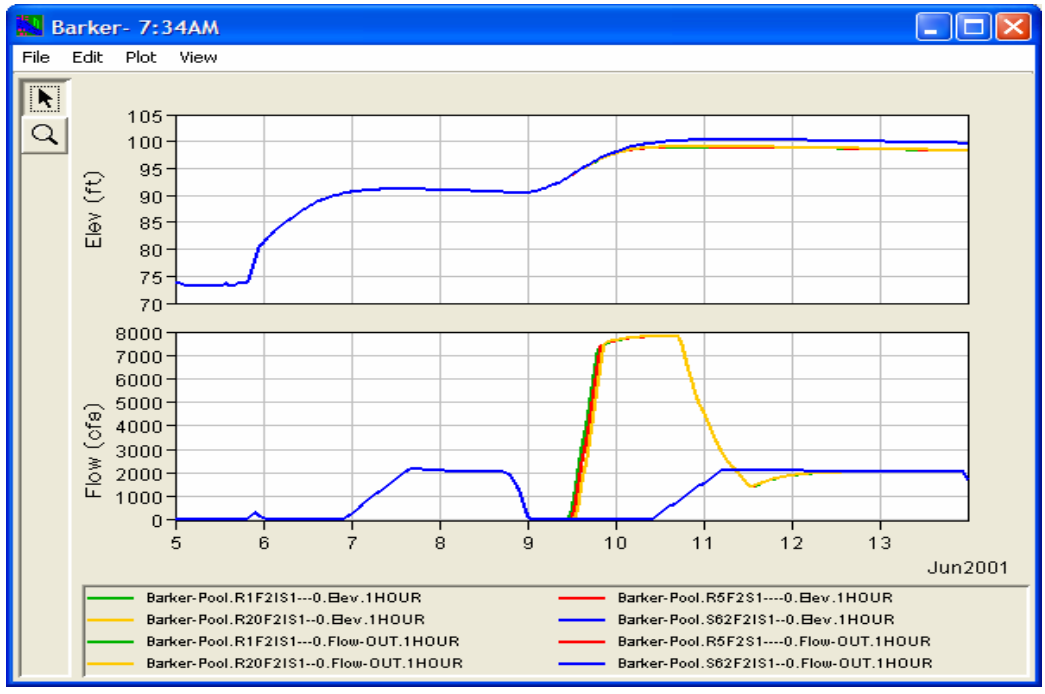

FIGURE 6.6. Water Surface Elevation Traces and Reservoir Releases for a) Addicks; and b) Barker; Based on Simulation F2IS1

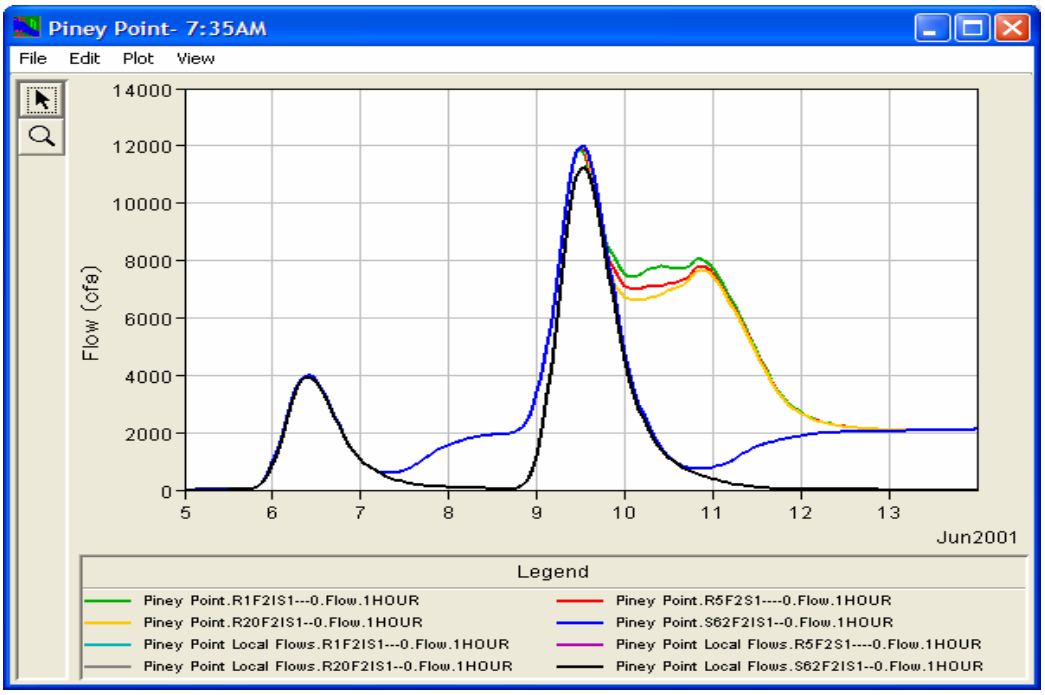

FIGURE 6.7. Flooding Conditions at Piney Point Based on Simulation F2IS1

the risk-based emergency releases were able to consistently maintain the WSE at lower levels than the Standard 1962 policy. For instance, the peak WSE for Barker in scenario F1IS2 was 1.9 ft lower with the REOS EF=1% policy. For this reason, the examination of these scenarios will be focused on the first portion of the flood event (before June 9). The Standard 1962 policy does not dictate any emergency releases in this period. The REOS policies, however, dictate releases since the initial storage conditions are close to the GOL limits, especially at Barker. Notice that these releases provide more protection to the areas above the GOL, but they resulted in exceeding the flow limit at Piney Point, except for REOS EF=20% in scenario F2IS2. However, this increase in flood levels is not very significant. Although the Standard 1962 policy was able to manage this portion of the flood successfully, it can be argued that for these particular scenarios the REOS EF=20% policy provides the better combination of providing a higher degree of protection to upstream lands without significantly affecting downstream flooding conditions.

(a)

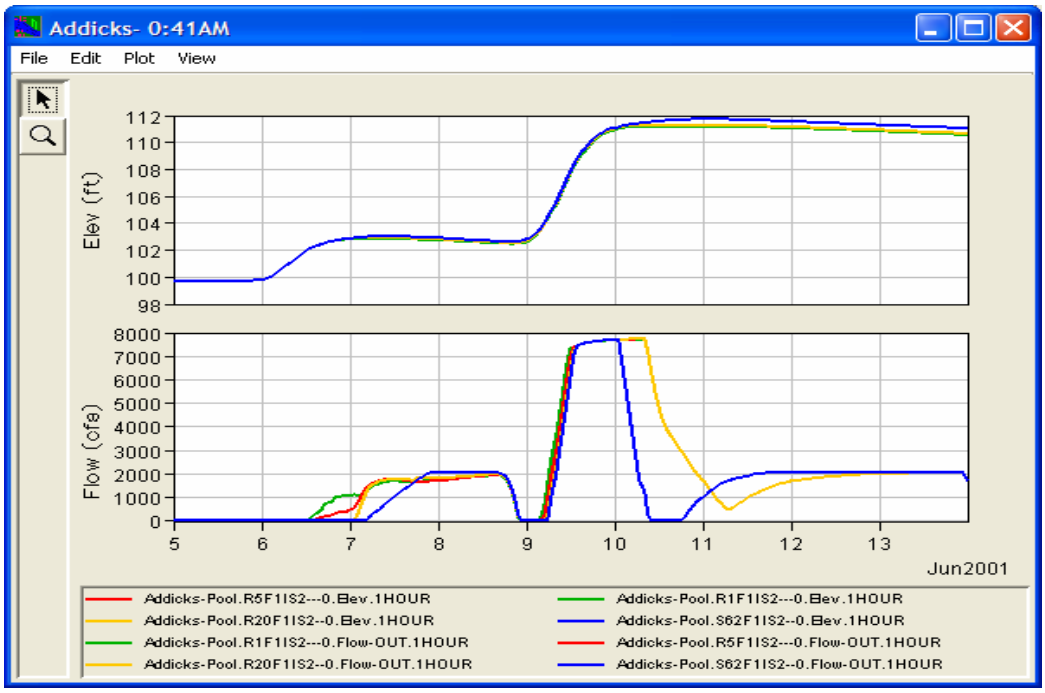

(b)

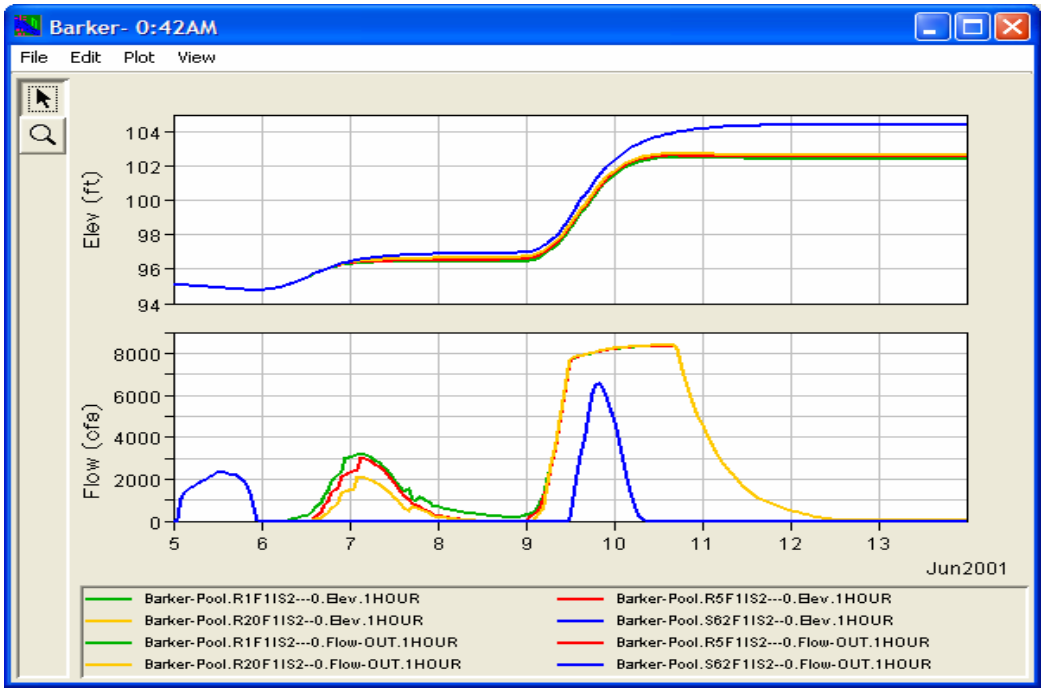

FIGURE 6.8. Water Surface Elevation Traces and Reservoir Releases for a) Addicks; and b) Barker; Based on Simulation F1IS2

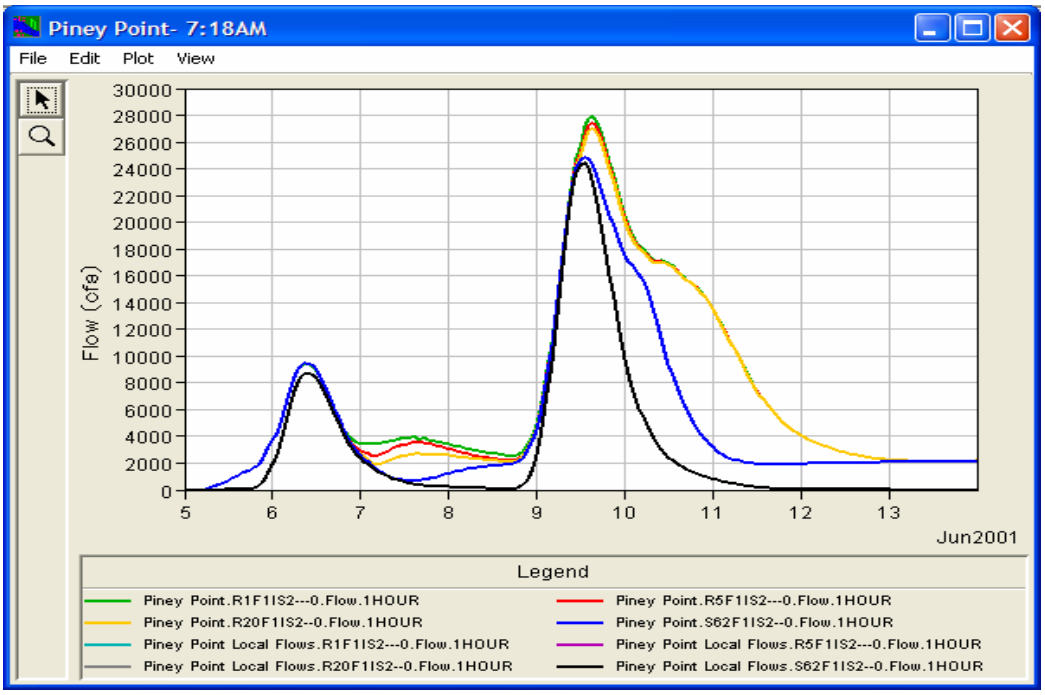

FIGURE 6.9. Flooding Conditions at Piney Point Based on Simulation F1IS2

(a)

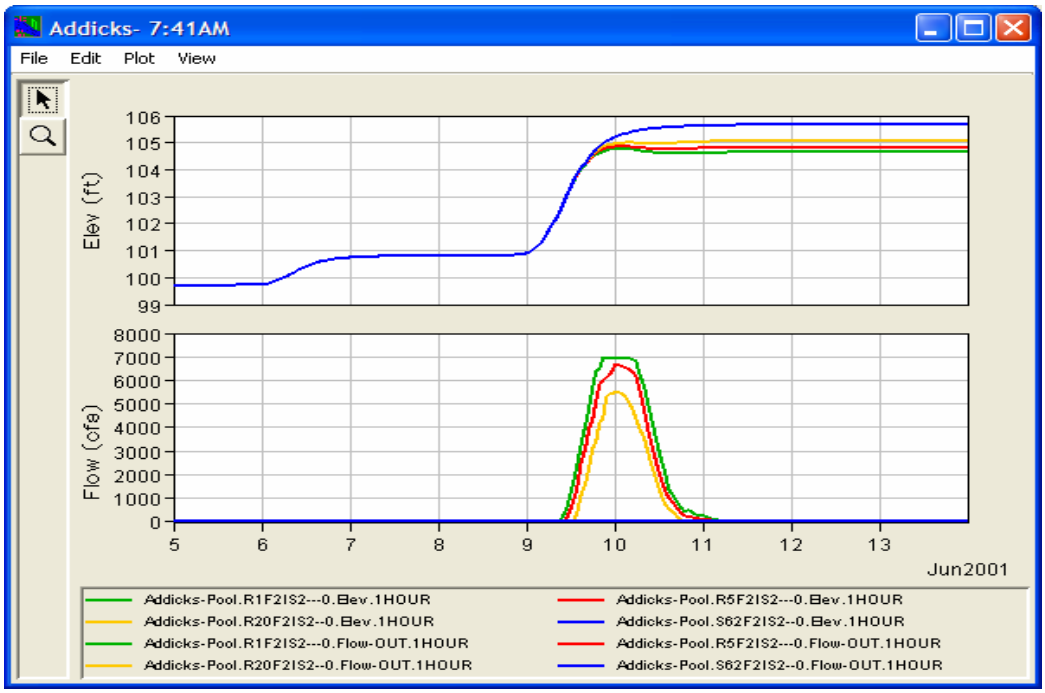

(b)

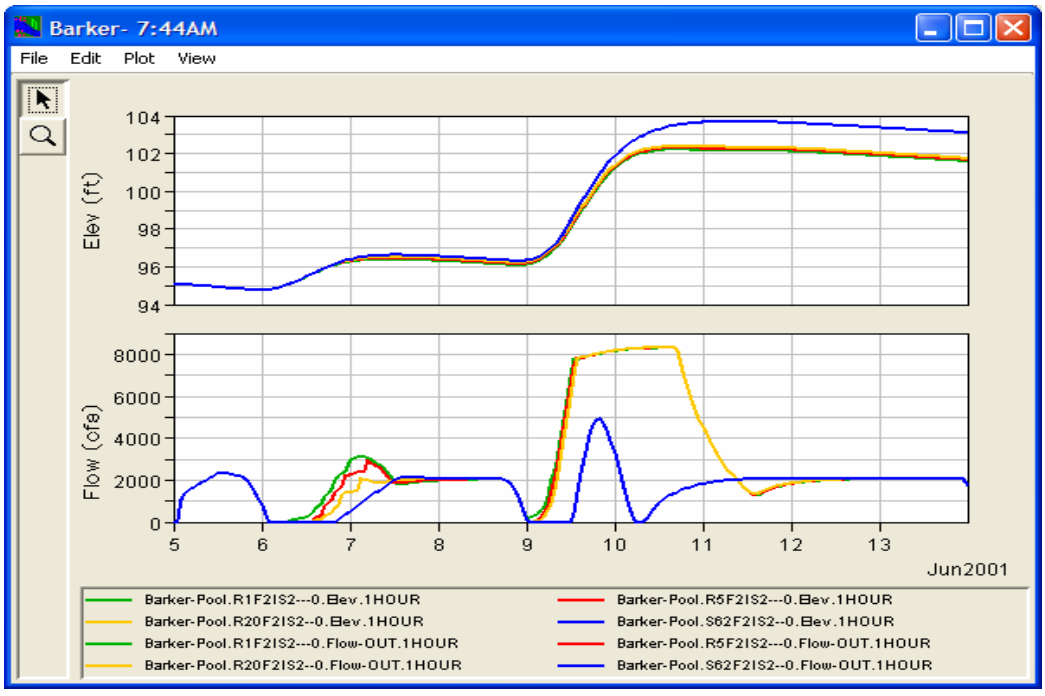

FIGURE 6.10. Water Surface Elevation Traces and Reservoir Releases for a) Addicks; and b) Barker; Based on Simulation F2IS2

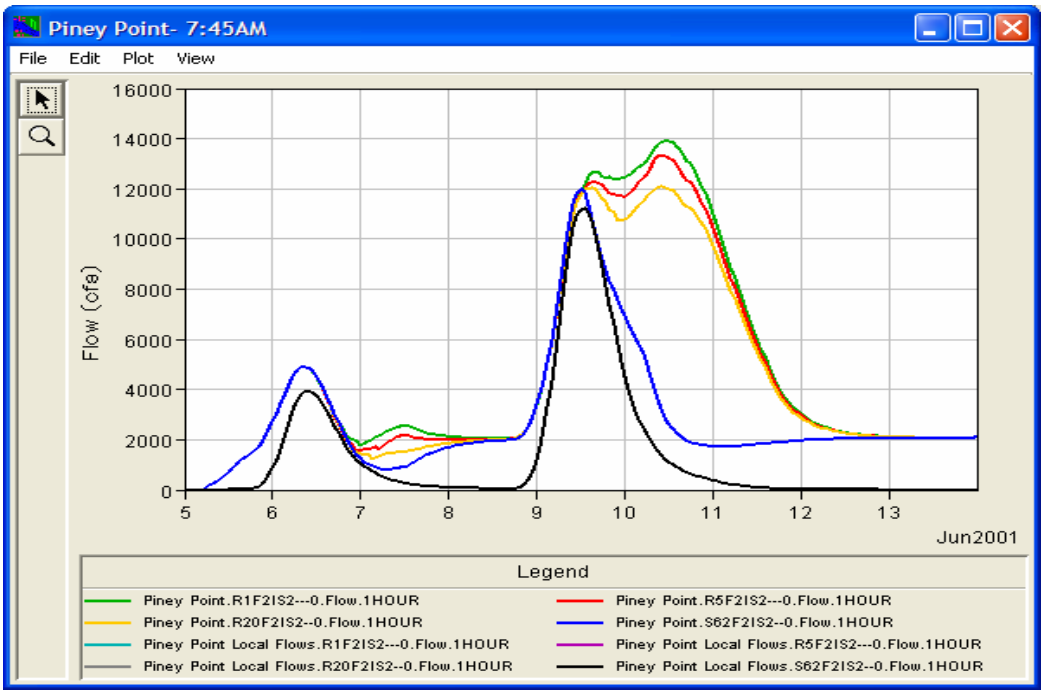

FIGURE 6.11. Flooding Conditions at Piney Point Based on Simulation F2IS2

6.2.4. Conclusions

The series of flood control simulations performed in HEC-ResSim provided several insights regarding the operation of the reservoirs under emergency conditions. Emergency releases under the Standard 1962 policy are based on preventing the storage levels from exceeding the reservoir's maximum capacity. Thus, the resulting WSE traces were always higher than those resulting from the operation of the reservoirs according to the risk-based schedules. However, differences in peak WSE's were not very significant. For the most part, the lower WSE's were obtained at the expense of making much larger releases that contributed greatly to downstream flooding. Even though in some instances the REOS policies provided a greater degree of protection against upstream flooding without causing excessive flows at Piney Point, it appears that after the GOL limits are exceeded large releases would be needed for extended periods of time in order to provide a minimal protection upstream. Further investigations are needed to evaluate in more detail

the tradeoff between increasing flooding downstream in order to reduce upstream flooding.

The variation in emergency releases as a function of risk was also investigated. In general, it was observed that the larger releases dictated by the lower risk schedules do not have a considerable effect in terms of WSE. Larger releases, however, have a significant effect on downstream flooding. It was also observed that in several occasions the emergency releases were nearly identical. A review of the release decision report generated in HEC-ResSim revealed that though the lower risk schedules did required much higher releases, they were constrained by the maximum allowable rate of change of reservoir releases. Although this hindered the ability to observe the differences in release decisions, this rule is needed in order to avoid the creation of a flood wave with rapid changes in stage.

Even though emergency releases were made in most of the simulations, for the most part, WSE's exceeded the GOL limits in both reservoirs. This highlights the magnitude of the TSA event. A storm like TSA, if centered over either of the reservoir watersheds, would cause extensive damages downstream regardless of the emergency policy adopted. It is important to point out here that in any scenario, the flow limit at Piney Point would be greatly exceeded by the uncontrolled runoff produced in the watershed below the dams. Therefore, great flood damages would result along Buffalo Bayou even if the reservoir gates remain closed during the entire storm event.

CHAPTER VII

QUANTIFYING THE PROBABILITY OF UPSTREAM FLOODING FOR THE ADDICKS AND BARKER RESERVOIR SYSTEM

The exceedance frequency (*EF*) associated with the risk-based emergency operations schedules (REOS) that were developed based on the storage capacity available up to the reservoir's Government Owned Land (GOL) limits represents the probability of exceeding the GOL given that a flood event that would trigger emergency operations takes place. In other words, *EF* reflects a conditional probability of upstream flooding that is only applicable if the reservoirs are under emergency conditions. The objective of the analyses presented in this chapter is to provide an estimate of the joint probability of having an event that would trigger emergency operations and that this event would result in upstream flooding even if emergency releases are made. A stage-frequency analysis was performed in order to estimate the probability of an event that would result in stages that would equal or exceed the GOL limits under normal operations. This event represents the smallest magnitude event that would result in upstream flooding if emergency releases are not made. The joint probability of upstream flooding was then estimated by multiplying the exceedance probability of this event by the *EF* (expressed as an exceedance probability) associated with a particular REOS. This joint probability provides a more lucid measure of the actual probability of upstream flooding.

7.1 STAGE-FREQUENCY ANALYSIS

Stage-frequency relations were developed for the Addicks and Barker reservoirs by applying the log-Pearson type III probability distribution to the following alternative sequences of annual peak water surface elevations:

- Maximum annual stages computed with HEC-5 (1945 – 1968)
- Historical record of observed annual stages (1969 – 2002)

The log-Pearson type III probability distribution is recommended in Bulletin 17B of the Interagency Advisory Committee on Water Data (1982), which outlines the flood flow frequency analysis procedures followed by federal water agencies. The USACE Hydrologic Engineering Center *Flood Frequency Analysis* program (HEC-FFA) was used to perform the analysis (USACE 1992). HEC-FFA performs the frequency analysis procedures for peak annual streamflows as outlined in Bulletin 17B. The same frequency analysis methods may also be applied to annual peak reservoir stages (Wurbs and James 2002).

Direct use of observed stages in the frequency analysis is advantageous from the perspective of reflecting actual release decisions made by reservoir operators and eliminating modeling premises and approximations (Wurbs 2002). In this case, however, the historical record also reflects changes in the reservoirs outlet structure capacity and operating policies. Therefore, a HEC-5 model of the reservoirs, developed by Wurbs (2002), was used to simulate reservoir operations over the period that does not reflect the current outlet works characteristics and operating policies (1945–1968). This simulation allowed obtaining peak annual stages for this period based on a constant operating policy that approximates the current one. The HEC-5 model was selected over the HEC-ResSim model because the current practice of closing the reservoir gates in anticipation of a flood even if downstream flows are below the 2,000 cfs limit can be better approximated in HEC-5. Emergency operations have never been implemented in these reservoirs, and they were not defined in the HEC-5 model. Therefore, the computed and historical annual peak stages (58 observations) presented in Table 7.1 represent the maximum stages that resulted from operating the reservoirs under the current normal policy.

The parameters of the log-Pearson type III probability distribution are the mean, standard deviation, and skew coefficient. These values are computed from the input data. However, since the skew coefficient is very sensitive to sample size, Bulletin 17B provides generalized skew coefficients as a function of geographic location. HEC-FFA can combine the computed and the generalized skew coefficients to form a better estimate of the skew for a given watershed (see Bulletin 17B page 12). The adopted generalized skew coefficient for both Addicks and Barker watersheds was -0.3.

TABLE 7.1. Maximum Annual Stage Data

Year	Addicks (ft)	Barker (ft)	Year	Addicks (ft)	Barker (ft)
(1)	(2)	(3)	(4)	(5)	(6)
1945	103.04	94.42	1974	95.48	91.77
1946	98.09	91.81	1975	93.90	91.42
1947	93.80	88.40	1976	92.90	90.48
1948	81.71	82.15	1977	89.67	87.03
1949	93.29	88.17	1978	91.88	90.00
1950	92.69	87.50	1979	98.16	94.16
1951	84.39	82.74	1980	95.04	91.79
1952	89.51	84.59	1981	97.37	92.37
1953	94.70	89.97	1982	93.46	89.10
1954	93.58	85.49	1983	95.70	90.56
1955	88.43	87.43	1984	95.50	90.16
1956	84.03	82.45	1985	93.85	90.02
1957	92.48	89.55	1986	94.03	91.13
1958	90.60	87.27	1987	94.87	91.34
1959	94.57	90.64	1988	87.62	86.20
1960	98.72	98.87	1989	93.00	89.32
1961	95.64	90.68	1990	90.29	86.32
1962	87.65	85.10	1991	96.78	93.63
1963	88.86	86.12	1992	100.58	95.89
1964	90.19	87.82	1993	96.88	92.92
1965	87.67	86.95	1994	98.75	92.78
1966	92.06	89.68	1995	92.13	89.09
1967	87.36	84.04	1996	91.03	87.41
1968	101.82	93.95	1997	96.75	92.88
1969	95.48	92.05	1998	94.19	90.97
1970	94.40	90.58	1999	89.09	87.37
1971	96.69	91.82	2000	90.07	87.60
1972	97.10	93.72	2001	94.29	90.53
1973	97.76	93.88	2002	99.57	95.53

A plotting position formula is required to plot observed stages versus exceedance probability. Plotting position formulas provide a visual display of how close the analytical distribution fits the observed data. HEC-FFA was set to use the Weibull plotting position formula,

$$P = \frac{m}{N+1} \tag{7.1}$$

where P is the exceedance probability, N is the number of years of observations, and m is the rank of the event in order of magnitude, with the largest event having $m = 1$. The exceedance probability may be expressed as an exceedance frequency in percent by multiplying P by 100 percent. The exceedance probabilities computed with the Weibull formula are shown in Tables 7.2 and 7.3 for Addicks and Barker, respectively. Notice that there are only 57 events in Table 7.2 instead of 58. HEC-FFA performs outlier tests prior to computing the final results. These tests are equivalent to one-sided outlier tests at the 10% level of significance (see Bulletin 17B page 17). The program identified one outlier in the Addicks data below the computed threshold value of 81.8 ft, and thus it was not included in the computations.

The stage-frequency relations for Addicks and Barker are presented graphically in Figures 7.1 and 7.2. The computational procedures used to obtain these results are based on a limited sample size and they represent a median stage-frequency relation. This means that there is an equal 50% chance of the true stage for a given exceedance frequency being either above or below the estimated value. However, HEC-FFA also computes confidence limits that provide a measure of uncertainty of the estimated stages. The dashed lines in the figures enclose a 90% confidence band (i.e. there is a 90% probability that the true value lies within this band). The lower limit indicates that there is a 5% chance that the true stage values are below this line. Similarly, the upper limit indicates that there is 5% chance that the true stage values are above this line. It can be observed from the figures that the analytical distribution (solid line) fits well the observed data (plotted based on the empirical Weibull formula) for both reservoirs.

TABLE 7.2. Addicks Stages in Ranked Order With *P* From Weibull Formula

Rank	Year	Stage (ft)	*P*	Rank	Year	Stage (ft)	*P*
(1)	(2)	(3)	(4)	(5)	(6)	(7)	(8)
1	1945	103.04	0.02	30	1985	93.85	0.52
2	1968	101.82	0.03	31	1947	93.80	0.53
3	1992	100.58	0.05	32	1954	93.58	0.55
4	2002	99.57	0.07	33	1982	93.46	0.57
5	1994	98.75	0.09	34	1949	93.29	0.59
6	1960	98.72	0.10	35	1989	93.00	0.60
7	1979	98.16	0.12	36	1976	92.90	0.62
8	1946	98.09	0.14	37	1950	92.69	0.64
9	1973	97.76	0.16	38	1957	92.48	0.66
10	1981	97.37	0.17	39	1995	92.13	0.67
11	1972	97.10	0.19	40	1966	92.06	0.69
12	1993	96.88	0.21	41	1978	91.88	0.71
13	1991	96.78	0.22	42	1996	91.03	0.72
14	1997	96.75	0.24	43	1958	90.60	0.74
15	1971	96.69	0.26	44	1990	90.29	0.76
16	1983	95.70	0.28	45	1964	90.19	0.78
17	1961	95.64	0.29	46	2000	90.07	0.79
18	1984	95.50	0.31	47	1977	89.67	0.81
19	1969	95.48	0.33	48	1952	89.51	0.83
20	1974	95.48	0.34	49	1999	89.09	0.84
21	1980	95.04	0.36	50	1963	88.86	0.86
22	1987	94.87	0.38	51	1955	88.43	0.88
23	1953	94.70	0.40	52	1965	87.67	0.90
24	1959	94.57	0.41	53	1962	87.65	0.91
25	1970	94.40	0.43	54	1988	87.62	0.93
26	2001	94.29	0.45	55	1967	87.36	0.95
27	1998	94.19	0.47	56	1951	84.39	0.97
28	1986	94.03	0.48	57	1956	84.03	0.98
29	1975	93.90	0.50				

TABLE 7.3. Barker Stages in Ranked Order With *P* From Weibull Formula

Rank	Year	Stage (ft)	*P*	Rank	Year	Stage (ft)	*P*
(1)	(2)	(3)	(4)	(5)	(6)	(7)	(8)
1	1960	98.87	0.02	30	1985	90.02	0.51
2	1992	95.89	0.03	31	1978	90.00	0.53
3	2002	95.53	0.05	32	1953	89.97	0.54
4	1945	94.42	0.07	33	1966	89.68	0.56
5	1979	94.16	0.08	34	1957	89.55	0.58
6	1968	93.95	0.10	35	1989	89.32	0.59
7	1973	93.88	0.12	36	1982	89.10	0.61
8	1972	93.72	0.14	37	1995	89.09	0.63
9	1991	93.63	0.15	38	1947	88.40	0.64
10	1993	92.92	0.17	39	1949	88.17	0.66
11	1997	92.88	0.19	40	1964	87.82	0.68
12	1994	92.78	0.20	41	2000	87.60	0.69
13	1981	92.37	0.22	42	1950	87.50	0.71
14	1969	92.05	0.24	43	1955	87.43	0.73
15	1971	91.82	0.25	44	1996	87.41	0.75
16	1946	91.81	0.27	45	1999	87.37	0.76
17	1980	91.79	0.29	46	1958	87.27	0.78
18	1974	91.77	0.31	47	1977	87.03	0.80
19	1975	91.42	0.32	48	1965	86.95	0.81
20	1987	91.34	0.34	49	1990	86.32	0.83
21	1986	91.13	0.36	50	1988	86.20	0.85
22	1998	90.97	0.37	51	1963	86.12	0.86
23	1961	90.68	0.39	52	1954	85.49	0.88
24	1959	90.64	0.41	53	1962	85.10	0.90
25	1970	90.58	0.42	54	1952	84.59	0.92
26	1983	90.56	0.44	55	1967	84.04	0.93
27	2001	90.53	0.46	56	1951	82.74	0.95
28	1976	90.48	0.47	57	1956	82.45	0.97
29	1984	90.16	0.49	58	1948	82.15	0.98

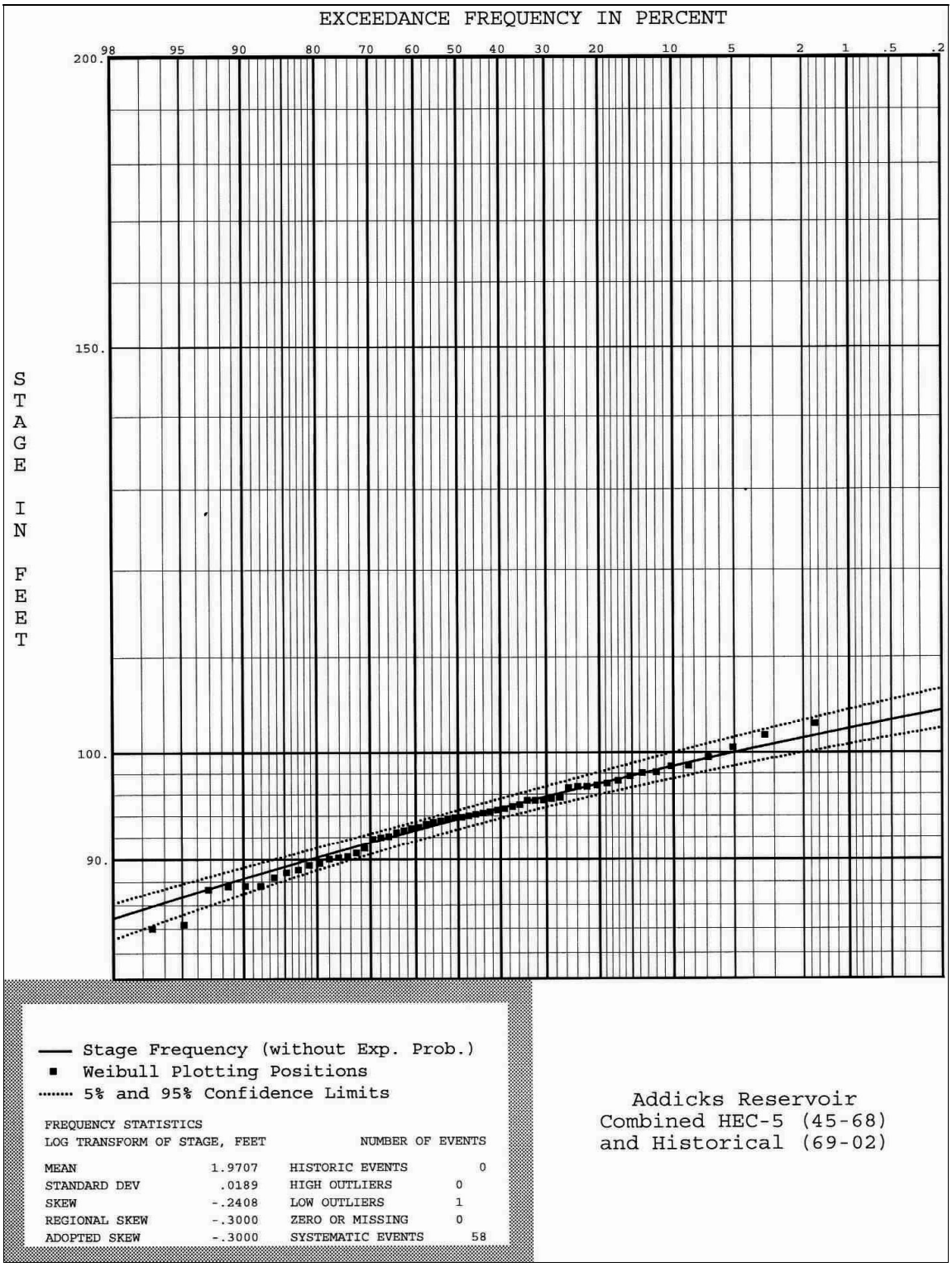

FIGURE 7.1. Stage-Frequency Relation for Addicks Reservoir

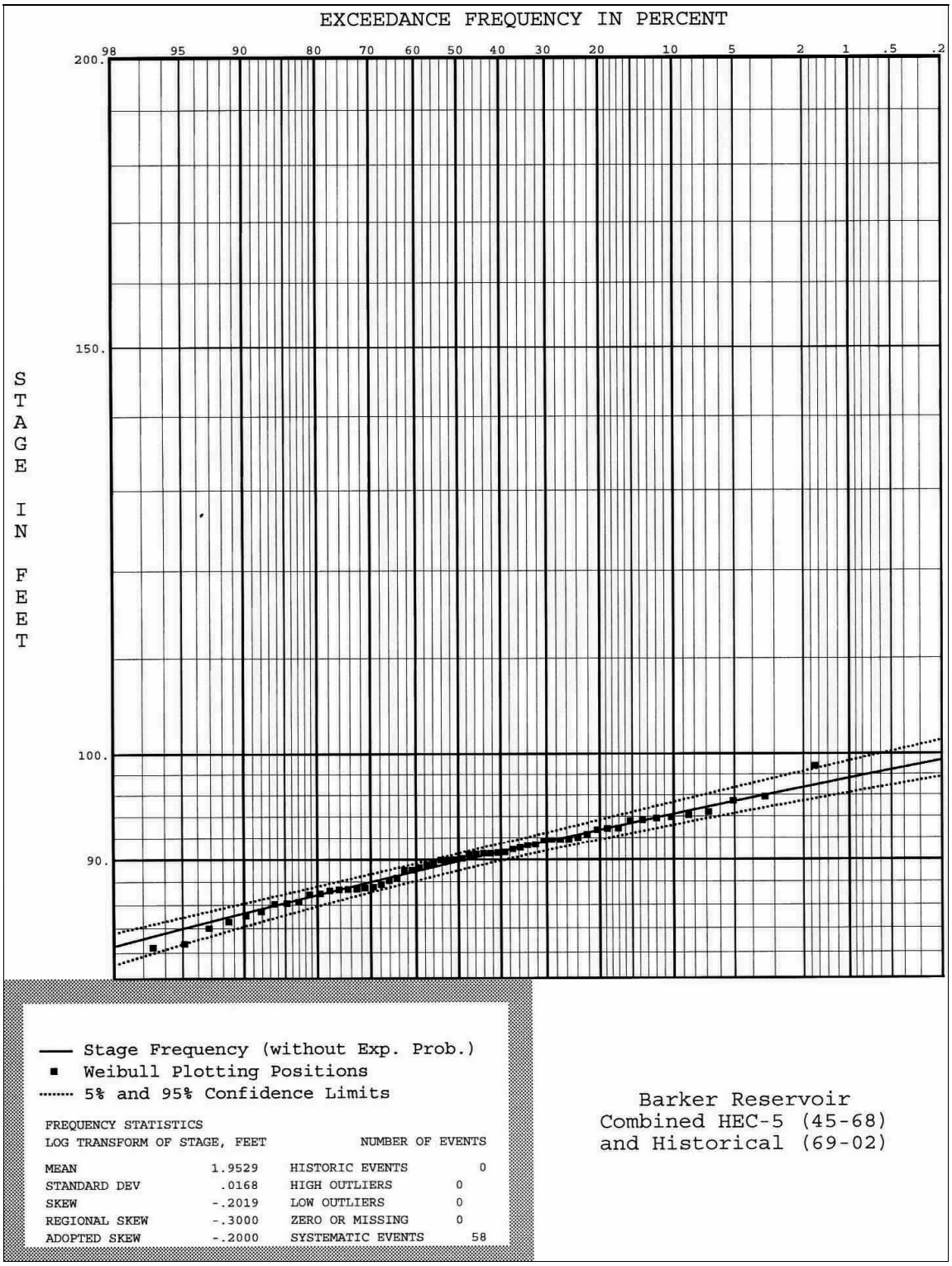

FIGURE 7.2. Stage-Frequency Relation for Barker Reservoir

The main objective of the stage-frequency analysis was to estimate the probability of the flood event that would result in equaling or exceeding the GOL under normal operations. However, the GOL stage is beyond the range of values observed for Addicks and near the high end (low probability events) of the values for Barker. The empirical relation (Weibull formula) provides reasonably accurate estimates of probabilities of frequent events well within the range covered by the observations. Yet, the estimates of exceedance probability assigned to the largest floods in the observed data may be highly inaccurate, and thus, plots of the observed data should not be extrapolated (Wurbs and James 2002). Instead, the analytical distribution should be used to extrapolate up to the exceedance probability associated with the GOL stage for each reservoir. The exceedance frequency values used in HEC-FFA to define the analytical curve may be set by the user in the input file. One of these values was changed iteratively until its associated stage would match the GOL. The results of this analysis are shown in Tables 7.4 and 7.5. The recurrence interval (RI) for each event is also included in the table. This value is the average interval, in years, between successive occurrences of events equaling or exceeding the specified stage. The RI is obtained dividing 100 by the exceedance frequency. The analysis showed that the GOL stages for Addicks (106.1 ft) and Barker (97.3 ft) are associated with exceedance frequencies of 0.03% (3,333-yr RI) and 1.3% (77-yr RI), respectively. Evidently, the risk of upstream flooding at Barker is much greater than at Addicks. Notice, however, that as the exceedance frequency decreases, the confidence band becomes wider (i.e. increased uncertainty). Therefore, care should be taken with the result for Addicks because the extrapolation goes well beyond the observed data and the confidence band for that exceedance frequency extends from 104.1 to 108.8 ft (4.71 ft wide). Yet, the 0.03% exceedance frequency does serve as an indication that an event of much greater magnitude needs to occur in order to exceed the GOL in Addicks under normal operations. This disparity in upstream flooding risk levels has prompted suggestions to modify the balancing configuration of reservoir releases. For example, in a USACE reconnaissance report of the reservoirs (USACE 1995) one of the proposed operational

TABLE 7.4. Stage-frequency Relation for Addicks Reservoir

Exceedance frequency (%) (1)	Recurrence Interval (years) (2)	Computed stage (ft) (3)	Confidence limits Upper (ft) (4)	Lower (ft) (5)
0.03	3333.3	106.09	108.80	104.09
0.05	2000	105.65	108.28	103.71
0.1	1000	105.01	107.51	103.15
0.2	500	104.32	106.69	102.55
0.4	250	103.56	105.79	101.89
0.5	200	103.31	105.49	101.67
1	100	102.46	104.48	100.92
2	50	101.50	103.36	100.08
5	20	100.04	101.65	98.78
10	10	98.69	100.10	97.57
20	5	97.02	98.20	96.03
50	2	93.68	94.59	92.80
90	1.1	88.30	89.34	87.03

TABLE 7.5. Stage-frequency Relation for Barker Reservoir

Exceedance frequency (%) (1)	Recurrence Interval (years) (2)	Computed stage (ft) (3)	Confidence limits Upper (ft) (4)	Lower (ft) (5)
0.2	500	99.38	101.45	97.82
0.5	200	98.42	100.32	96.99
0.8	125	97.89	99.69	96.52
1	100	97.63	99.38	96.29
1.25	80	97.35	99.06	96.05
1.3	76.9	97.30	99.00	96.01
1.6	62.5	97.04	98.69	95.78
2	50	96.75	98.35	95.52
5	20	95.41	96.79	94.33
10	10	94.20	95.40	93.24
20	5	92.72	93.73	91.88
50	2	89.84	90.60	89.08
90	1.1	85.31	86.20	84.22

changes was to make releases based on the percent occupancy of GOL storage of the reservoirs instead of the percent occupancy of their full capacity. This would utilize a greater portion of the larger GOL storage in Addicks and reduce the use of the GOL storage in Barker. Based on the findings of this report, this change in operational policy would result in lowering the exceedance frequency of the event that would reach the GOL in Barker from 1.43% (70-yr RI) to approximately 1% (100-yr RI).

7.2. JOINT PROBABILITY ANALYSIS

The stage-frequency analysis allowed estimating the probability of a flood event that would result in equaling or exceeding the GOL under normal operations. This event will be referred to as event A and its estimated probability as $P(A)$. Event A is the smallest magnitude event that would result in upstream flooding if emergency operations are not implemented. The goal of emergency operations is to avoid exceeding a specified critical water surface elevation (WSE). Therefore, it is assumed here that if the emergency policies for Addicks and Barker were modified to allow emergency releases in order to avoid upstream flooding, then event A would trigger emergency operations before the WSE reaches the GOL.

Now, let event B be the occurrence of upstream flooding (exceeding the GOL limits) even if emergency operations are implemented. Clearly, the occurrence of event B is dependent upon the occurrence of event A. Thus, the probability of event B may be expressed as the conditional probability $P(B|A)$, that is, the probability that event B occurs given that event A has occurred. If event A does not occur, then $P(B|A)$ is zero. If event A does occur, then $P(B|A)$, within the context of this study, is given by the EF (expressed as an exceedance probability) associated with a particular REOS. In general, the probability of an event can be approximated by the relative frequency, or proportion of times that the event occurs. EF is the relative frequency with which event B would occur provided that emergency operations have been triggered. This relative frequency was considered a good estimate of the true probability since it was computed based on a sample of 10,000 equally likely inflow sequences (see Chapter III, section 3.3.3).

The combination of events A and B may be called a composite event. The probability of the composite event may be interpreted as the actual probability of upstream flooding, as it considers both the occurrence of a flood that if regulated following normal operations would reach or exceed the GOL and the risk of failing to avoid upstream flooding even if emergency releases were made. The probability of the composite event is given by the multiplication law,

$$P(A \cap B) = P(A) * P(B \mid A) \tag{7.2}$$

where $P(A \cap B)$ is the joint probability that both events A and B (the composite event) occur (Berry and Lindgren 1996). The joint probability of the composite event based on various EF values (expressed as exceedance probabilities) is presented in Table 7.6.

TABLE 7.6. Joint Probability of Upstream Flooding

Addicks				Barker			
$P(A)$	$P(B\|A)$	$P(A \cap B)$	$P(A \cap B)$ (%)	$P(A)$	$P(B\|A)$	$P(A \cap B)$	$P(A \cap B)$ (%)
(1)	(2)	(3)	(4)	(5)	(6)	(7)	(8)
0.0003	0.01	0.000003	0.0003	0.013	0.01	0.000130	0.0130
0.0003	0.05	0.000015	0.0015	0.013	0.05	0.000650	0.0650
0.0003	0.10	0.000030	0.0030	0.013	0.10	0.001300	0.1300
0.0003	0.20	0.000060	0.0060	0.013	0.20	0.002600	0.2600
0.0003	0.25	0.000075	0.0075	0.013	0.25	0.003250	0.3250
0.0003	0.50	0.000150	0.0150	0.013	0.50	0.006500	0.6500

The values in columns (1) and (5) show the probability of event A for each reservoir as computed in section 7.1 (Tables 7.4 and 7.5). Columns (2) and (6) show selected exceedance probabilities associated with different REOS (EF = 1, 5, 10, 20, 25, and 50%). The joint probabilities computed in columns (3) and (7) are also expressed as a percentage in columns (4) and (8). Evidently, the probability of upstream flooding would be greatly

reduced if the emergency operation schedules were based on protecting the fringe areas between the upper limits of the GOL and the maximum pool levels. Based on the premises of this analysis, this operational change would reduce the probability of upstream flooding at Addicks from 0.03% to 0.015% or less, and at Barker from 1.3% to 0.65% or less.

The much smaller joint probabilities for Addicks reiterate the fact that an event of much greater magnitude needs to take place in order to exceed the GOL in Addicks. However, recall that the $P(A)$ for Addicks is an extrapolated value which is highly uncertain. The stage-frequency analysis showed that events of lesser magnitude may also reach the GOL if we take into account that the true stages may be higher than the computed stages (Tables 7.4 and 7.5). For example, the upper confidence limit for the 0.2% exceedance frequency stage (500-yr RI) at Addicks is 106.69 ft (0.59 ft above the GOL stage). Hence, it is possible that $P(A)$ is actually 0.002 and not 0.0003. This increase in $P(A)$ would result in joint probabilities of 0.1% or less, instead of 0.015% or less. Even though the $P(A)$ value for Barker is more reliable than for Addicks, the same reasoning may be applied. The upper confidence limit for the 2% exceedance frequency stage (50-yr RI) at Barker is 98.35 ft (1.05 ft above the GOL stage). In this case, the joint probabilities would be 1% or less, instead of 0.65% or less.

The joint probability analysis can provide a more lucid measure of the actual probability of upstream flooding as opposed to just using the probabilities of event A and B individually. The analysis clearly shows that the fringe areas at Barker are at a much greater risk of being flooded than at Addicks. The potential changes in the emergency operation policies that have been evaluated in this study would result in an increased degree of protection against upstream flooding. However, as it was pointed out in Chapter VI, this increased protection would be accomplished at the expense of increasing the magnitude and the duration of flood stages downstream from the dams. Further investigations are needed to evaluate in more detail the tradeoff between increasing flooding downstream in order to reduce upstream flooding.

CHAPTER VIII

SUMMARY AND CONCLUSIONS

8.1 RESEARCH SUMMARY

Emergency operation schedules (EOS) are decision tools that provide guidance to reservoir operators in charge of making real-time release decisions during major flood events. The standard methodology that has been used to develop the EOS for most USACE reservoir projects dates to the 1950's. In this research study, an innovative methodology was devised for developing risk-based EOS in which emergency releases are based on the probability that the expected flood volume would exceed the reservoir's maximum storage capacity or any other critical storage level. As opposed to the deterministic USACE approach, this methodology deals with uncertainties regarding future inflows by considering them as a stochastic process. Stochastic streamflow generation models provided the capability of analyzing statistical probabilities of the expected inflow volumes conditional to the current streamflow conditions. The final product of the methodology is a series of alternative risk-based EOS in which the reservoir releases are associated with certain risk of failing to attain the emergency operations objectives. An annual regulation schedule may be developed based on the expected flows succeeding an initial condition that is evaluated at different times of the year. Alternatively, monthly regulation schedules may be defined if the initial condition is always evaluated in the same month. The assumption is that once emergency operations are triggered by a flood event, the risk associated with a particular EOS reflects the probability of exceeding the critical storage level given that the same EOS is followed throughout the event. This provides reservoir operators a mechanism for evaluating the potential consequences of their release decisions.

A computer program named REOS was created to perform the computations to develop risk-based EOS. The computational algorithm in REOS is divided in three major components: (1) synthetic streamflow generation, (2) mass balance computations,

and (3) frequency analysis. Stochastic streamflow generation models are used in REOS to create a large number of inflow sequences with a recurrent initial condition defined by the initial inflow rate Q_0 and the streamflow state *SS* (i.e. rising, receding). REOS then determines the required storage to precisely accommodate each inflow sequence using a mass balance equation that relates cumulative inflows and outflows to storage changes. The maximum cumulative storage change (SC_{max}) represents the maximum volume to be stored in a reservoir for a given inflow sequence and constant outflow rate (O_c). REOS determines SC_{max} values for each inflow sequence using various O_c values. This computation is then repeated for all Q_0 of interest and both *SS* categories. The result is an array of equally likely SC_{max} realizations for a given system condition which is defined by Q_0, O_c, and *SS*. The SC_{max} array is then ranked in order of magnitude and relative exceedance frequencies (*EF*'s) are assigned to each value. Alternative regulation schedules may then be developed based on the SC_{max} values corresponding to a specific *EF*. SC_{max} is subtracted from the maximum allowable storage level to determine the initial reservoir storage. This initial storage is then expressed as an initial water surface elevation (WSE_I). The family of regulation curves forming the EOS for a selected *EF* and *SS* can be developed by plotting the WSE_I corresponding to a continuous set of O_c values using Q_0 as a parameter.

Emergency schedules using both the standard and the risk-based methods were developed for the Addicks and Barker Reservoir system. The operational complexities and current flooding hazards of this reservoir system provided an ideal case study for testing the applicability of the risk-based EOS. In particular, these reservoirs present the operational challenge of having to manage the tradeoffs between flooding risks upstream and downstream from the dams. One of the main features of the risk-based EOS is that they provide a means for considering these risks in the release decision process. The potential for upstream flooding is a major concern due to the growing development adjacent to the Government Owned Lands (GOL). The GOL limit is the key elevation above which residential and commercial properties are susceptible to flooding, however, the occurrence of upstream flooding does not justify making emergency releases under

the current policy. Although extreme flood events are infrequent, the historical rainfall events that have occurred in the vicinity of these reservoirs have demonstrated that there is a realistic threat for flooding conditions involving stages that could approach or exceed the GOL limits, especially at Barker.

The emergency schedules were tested through a series of flood control simulations using hypothetical flood events occurring under different initial storage conditions. Rainfall data recorded from Tropical Storm Allison (TSA) was transposed over the Addicks and Barker watersheds to compute hypothetical inflow hydrographs using HEC-HMS. The occurrence of extremely high pool levels in these reservoirs is typically attributed to the accumulation of water in storage over rainy periods rather than from a single event. Therefore, long-term simulations using historical data were used to establish the initial storage conditions at the reservoirs before the beginning of the hypothetical rainfall events. Repeated runs of the HEC-ResSim model were made using different flooding and residual storage scenarios to compare the regulation of the floods under alternative operating policies. The existing EOS for the reservoirs along with three newly developed risk-based EOS that were based on the storage capacity available within the GOL limits were evaluated. These risk-based EOS represented a change in operational policy that would allow making emergency releases based on the probability of upstream flooding.

An alternative application of the risk-based EOS in which their risk parameter (*EF*) was used to help quantify the actual probability of upstream flooding in Addicks and Barker Reservoirs was also presented. The objective of this application was to provide an estimate of the joint probability of having an event that would trigger emergency operations and that this event would result in upstream flooding even if emergency releases are made. A stage-frequency analysis was performed to estimate the probability of an event that would result in stages that would equal or exceed the GOL limits under normal operations. The joint probability of upstream flooding was then estimated by multiplying the exceedance probability of this event by the *EF* (expressed

as an exceedance probability) associated with a particular REOS. This joint probability provided a more lucid measure of the actual probability of upstream flooding.

8.2 RESEARCH FINDINGS AND CONCLUSIONS

8.2.1 Fundamental Distinctions Between the Standard and Risk-based Methods

The deterministic nature of the standard USACE method allows it to be a straightforward approach for developing EOS. However, two major shortcomings were identified in this study. First, the method relies on a series of simplifying assumptions regarding future flows. The method assumes that the current inflow rate corresponds to the peak discharge of the flood and that inflows will continue a receding trend. The flood volume computations only reflect the input of this single event, disregarding the possibility that inflows may continue to increase or that the recession may be interrupted by a subsequent event. Due to the inherent variability of streamflows, infinite possibilities exist for sequencing of future flows. Therefore, formulating an EOS assuming that a single sequence of streamflows is adequate to describe all future conditions is rather limited. Second, the method does not provide a mechanism for evaluating the potential risks associated with release decisions. These schedules only provide a rigid and conservative set of rules that are assumed to be appropriate under all flooding conditions.

The REOS method defines the regulation schedules based on probability considerations. The assumptions of the standard method regarding future flows are removed in this method by using stochastic streamflow generation models to create the inflow sequences. Although the computations in the REOS method are more complex, the resulting schedules provide a wider and more flexible decision framework for reservoir operators. The risk-based EOS provide a set of rules that reflect the risk of making an operational error in terms of making insufficient releases that would result in dam overtopping and/or upstream flooding, or making excessive releases that would contribute unnecessarily to downstream flooding. Reservoir operators may use the risk

parameter as a means to evaluate the tradeoffs and the potential consequences of their release decisions. One major limitation, though, is that the REOS computer program is not a generalized program and can only be used to derive the emergency schedules for Addicks and Barker Reservoirs. However, the source code of the program may be modified, with some effort and ingenuity, in order to make it applicable for other reservoirs.

8.2.2 Appropriateness of the Stochastic Streamflow Generation Models

A critical aspect of the REOS approach is the proper generation of synthetic streamflow data. The fractional autoregressive integrated moving average (FARIMA) models were selected because of their ability to simulate both the short- and long-term characteristics of daily streamflows. The final model incorporated in the REOS program was a composition of 12 models with periodical parameters. The models were able to reproduce streamflow sequences with statistical properties similar to those of the observed data with the exception of the standard deviation (SD). The SD of the observed data was greatly influenced by the peak discharge values. The observed peak discharges were not well reproduced by the FARIMA models, causing the SD of the synthetic series to be much lower than the SD of the observed series. This discrepancy was not considered a major limitation for this particular study since in the REOS methodology high flows are introduced into the streamflow sequences as a recurrent initial condition, and thus, the models need not to reproduce high flows in order to develop the EOS for such conditions.

Additional statistical tests were performed to further evaluate the appropriateness of the selected models. The cumulative frequency of the observed and the generated daily streamflows for each month was found to be in good agreement. The two-sample Kolmogorov-Smirnov test, which formally tests the hypothesis of statistical similarity between the observed and the generated data, was applied to the data for each month and for the composite annual data. In both instances, the test results were favorable.

The estimated FARIMA models required up to three assumed values to initialize their recursive computations. The first of these values is Q_0, which is the recurrent streamflow value in every simulation. Because of the strong correlation between succeeding flows, the values preceding Q_0 were estimated using a backward generation process using autoregressive lag-1 models. These models were only tested in terms of their ability to reproduce the lag-1 autocorrelation coefficient $\rho(1)$ for each month. The results indicated that the models were able to reproduce the observed $\rho(1)$ satisfactorily.

8.2.3 Variation in Emergency Release Policies

The emergency releases dictated by an EOS depend on the parameters that were selected to formulate the schedules. In the case of the standard method, the shape of the EOS curves for a particular reservoir depends upon the selected value of the recession constant T_s. Three EOS were developed for Addicks and Barker in order to evaluate their sensitivity to changes in T_s. Significant changes in emergency release rates resulted from relatively small variations in T_s. It was also found that these changes were more pronounced as the reservoir conditions worsen (i.e. higher water surface elevation (WSE) and/or higher inflows). The critical decision of making emergency releases that would contribute to downstream flooding and the magnitude of such releases are greatly affected by the selection of T_s, and thus, caution should be taken in the computation of this value.

In addition to Q_0, the risk-based EOS also incorporate *SS* and the time of year as parameters in the schedules. These parameters are regarded as predictor variables of the potential inflow volumes. The scheduled releases are a function of the residual storage capacity and the information provided by these parameters. The risk parameter (*EF*) associated with each schedule may be regarded as a measure of the degree of protection that the schedules provide against exceeding the selected critical storage level; lower *EF*'s provide greater protection.

Several risk-based EOS were developed and compared in order to evaluate the variation in emergency release policies as a function of these parameters. In terms of *SS*, it was found that for a given initial condition (i.e. Q_0 and WSE) the EOS curves for *SS* = rising were below their counterparts for *SS* = receding. This indicates that for rising streamflow conditions the transition from normal to emergency operations would occur at lower stages and that a larger outflow rate would be required for any given initial condition. This was an expected result since streamflows usually exhibit a strong tendency to continue their current trend. The inflow volume following Q_0 will typically be greater for rising conditions than for receding conditions, and thus, greater outflow rates would be needed to accommodate the remainder of a flood. Evidently, this streamflow tendency was well-reproduced by the stochastic streamflow generation models and its anticipated effects were reflected in the schedules.

The FARIMA models were capable of capturing the particular autocorrelation structure of each month and reflecting it in the resulting monthly schedules for Addicks and Barker. The position of the EOS curves shifted downward or upward as a reflection of the magnitude of the typical inflow volumes that can be expected for each month as described by the FARIMA models. Significant differences were observed among the monthly risk-based EOS. Emergency releases may be drastically different depending upon the time of year at which emergency conditions are encountered. In several instances, the difference in outflow rates for successive months was very significant. Although the monthly schedules were not tested in the simulation study, it is clear that such differences would present an operational challenge when regulating floods occurring near the end of a month that is followed by a month with a significantly different EOS. This situation would create a degree of uncertainty in terms of which EOS would be more appropriate to regulate the flood. A decision needs to be made as to which EOS to follow, considering that even if the flood started in a particular month the incoming streamflows may reflect the characteristics of the next month. This is a critical decision especially because each EOS may establish the transition from normal to emergency operations at significantly different reservoir stages.

A series of 21 annual risk-based EOS (*SS* = rising) were developed with different *EF* values to evaluate the variation in release policies as a function of risk. It was found that for *EF* values above 20%, significant increases in the level of protection can be obtained with relatively small increases in outflow rates. However, for *EF* values below 20% greater changes in outflow rates are required in order to increase the level of protection by the same amount. It was also observed that for a given Q_0 the outflow rate required to maintain the same level of protection (constant *EF*) increases considerably with relatively minor reductions in residual storage. Moreover, for a given WSE greater outflow rates are required to maintain the same level of protection as Q_0 increases.

8.2.4 Evaluation of Emergency Policies for the Addicks and Barker Reservoir System

The original EOS for Addicks and Barker were based on ensuring that the dams are never overtopped, not on avoiding upstream flooding. Modifications to the current regulation policies that would allow emergency releases based on the probability of upstream flooding were investigated. Three risk-based EOS (*EF* = 1, 5, and 20%) that were developed based on the GOL storage capacity were selected to test this operational change. The flood hydrographs used to test the schedules were based on the rainfall depths produced by TSA. Transposing the TSA rainfall pattern over the center of the reservoir watersheds resulted in flood hydrographs that reflected the extreme rainfall events that are possible in this area.

The series of flood control simulations performed in HEC-ResSim provided several insights regarding the operation of the reservoirs under emergency conditions. Four operational sets were created in HEC-ResSim describing the risk-based EOS and the current emergency operations as described in the 1962 reservoir regulation manual. HEC-ResSim provided flexible capabilities for modeling the river/reservoir system and evaluating the alternative operating policies. As expected, the WSE traces resulting from regulating the floods based on the 1962 policy were always higher than those resulting from the operation of the reservoirs according to the selected risk-based schedules. However, differences in peak WSE's were not very significant. For the most

part, the lower WSE's were obtained at the expense of making much larger releases that contributed greatly to downstream flooding. It is important to point out here that in any scenario, the target non-damaging discharge rate of 2,000 cfs at Piney Point would be greatly exceeded by the runoff produced in the watershed below the dams. Therefore, great flood damages would result downstream even if the reservoir gates remain closed during the entire storm event.

The variation in emergency releases as a function of risk was also investigated. In general, it was observed that the larger releases dictated by the lower risk schedules did not have a considerable impact in terms of lowering the WSE. Larger releases, however, did have a significant effect on downstream flooding, with larger flows being sustained for longer periods. It was also observed that in several occasions the emergency releases were nearly identical. A review of the release decision report generated in HEC-ResSim revealed that though the lower risk schedules did required much higher releases, they were constrained by the maximum allowable rate of change of reservoir releases. Although this hindered the ability to observe the differences in release decisions, this rule was needed to avoid the creation of a flood wave with rapid changes in stage.

Even though in some instances the risk-based policies provided a greater degree of protection against upstream flooding without causing excessive flows downstream, it appears that after the GOL limits are exceeded large releases would be needed for extended periods of time in order to provide a minimal protection upstream. However, other studies have suggested that making releases that would exceed the 2,000 cfs limit at Piney Point only on rare occasions may be justified based on the relatively higher benefits that downstream areas have obtained over the life of the project compared to upstream structures (USACE 1995). Estimating the extent of the inundated areas downstream, the amount of households that would be flooded, the time span of flood stages, and the magnitude of the economic losses that would result from avoiding upstream flooding was beyond the scope of this study. However, these factors and other legal considerations need to be carefully evaluated in order to make a decision in terms of the feasibility of making this operational change.

The stage-frequency analysis, which was easily performed with HEC-FFA, showed that the GOL stages for Addicks and Barker are associated with exceedance frequencies of 0.03% (3,333-yr RI) and 1.3% (77-yr RI), respectively. This probability of upstream flooding would be greatly reduced if the emergency operation schedules were based on protecting the areas above the GOL limits. Based on the joint probability analysis, this operational change would reduce the probability of upstream flooding at Addicks from 0.03% to less than 0.015%, and at Barker from 1.3% to less than 0.65%. The much smaller joint probabilities for Addicks reiterate the fact that an event of much greater magnitude needs to take place in order to exceed the GOL in Addicks. This disparity in upstream flooding risk levels has prompted suggestions to modify the balancing configuration of reservoir releases under normal operations in which releases would based on the percent occupancy of GOL storage of the reservoirs instead of the percent occupancy of their full capacity (USACE 1995). This would utilize a greater portion of the larger GOL storage in Addicks and reduce the use of the GOL storage in Barker. Although not investigated in this study, another potential solution would be to implement a low risk EOS for Barker and a high risk EOS for Addicks. This could result in a more efficient use of the combined flood storage capacity under emergency conditions. Yet, the selection of the acceptable levels of risk would still need to be evaluated before the implementation of such operational change.

8.3 SUGGESTED AREAS OF FUTURE RESEARCH

The risk-based EOS provide a new approach of making release decisions under emergency conditions. The flood simulation study described in Chapter VI presented an application of the schedules and compared the results for selected values of *EF*. In actual operations, only one schedule is typically followed. Formulating methodologies for establishing the acceptable level of risk (*EF*) as a function of certain hydrologic and operational factors is a necessary extension to this study if the new schedules are to be implemented. Also, evaluating the effects of implementing EOS with different levels of risk

to provide a more efficient use of the available flood storage in the context of multi-reservoir system operations could also be a valuable contribution.

Another related study is to evaluate the benefits of following a more complex flood regulation approach in which multiple regulation schedules could be implemented during a single flood event. In this manner, as a flood event progresses and the flood control storage of the reservoir is diminished, lower risk schedules could be implemented. In this approach, the selection of the EOS would depend upon a pre-established relationship describing the acceptable risk at different storage levels and the required outflow rates would be adjusted accordingly.

As previously mentioned, significant differences were observed among the monthly risk-based EOS. Formulating methodologies for the proper application of this type of schedules and evaluating their feasibility could contribute to a better regulation of the reservoirs. The HEC-ResSim model could also be used in this effort since it provides the option of incorporating release rules that vary according to the time of year.

Finally, as previously discussed, a comprehensive study considering the hydrological, socio-economical, and legal aspects of flood regulation is needed to properly evaluate the tradeoffs between increasing flooding risks downstream in order to reduce the risk of upstream flooding and to establish the feasibility of this major operational change.

REFERENCES

Ahrens, S. R., and Maidment, D. R. (1999). "Flood forecasting for the Buffalo Bayou using CRWR-PrePro and HEC-HMS." *CRWR Online Report 99-6*, Center for Research in Water Resources, Austin, Texas. <http://crwr.utexas.edu/online.html> (Jun. 12, 2004).

Aksoy, H. (2003). "Markov chain-based modeling techniques for stochastic generation of daily intermittent streamflows." *Advances in Water Resources*, 26(6), 663–671.

Andrade, M. G., Fragoso, M. D., and Carneiro, A. A. F. M. (2001). "A stochastic approach to the flood control problem." *Applied Mathematical Modelling*, 25(6), 499–511.

Arnold, J. L. (1988). "The Flood Control Act of 1936: A study in politics, planning, and ideology." *The flood control challenge: past, present, and future*, H. Rosen and M. Reuss, eds., Public Works Historical Society, Chicago, Illinois.

Beard, L. R. (1963). "Flood control operation of reservoirs." *Journal of the Hydraulics Division, ASCE*, 89(HY1), 1–23.

Beard, L. R. (1967). "Simulation of daily streamflow." *Proceedings, The International Hydrology Symposium*, Fort Collins, Colorado, 624–632.

Beard, L. R., and Chang, S. (1979). "Optimizing flood operation rules." *Report CRWR-166*, Center for Research in Water Resources: Bureau of Engineering Research, University of Texas, Austin, Texas.

Beran, J. (1994). *Statistics for long-memory processes*, Chapman & Hall, New York.

Bernard Johnson, Inc. (1995). "Addicks Reservoir watershed management study." *BJI J.O. 90049-01*, prepared for the Harris County Flood Control District.

Berry, D. A., and Lindgren, B. W. (1996). *Statistics: Theory and Methods*, Second Edition, Duxbury Press, Belmont, California.

Box, G. E. P., and Jenkins, G. M. (1976). *Time series analysis: forecasting and control*, Holden-Day, Oakland, California.

Brockwell, P. J., and Davis, R. A. (1987). *Time series: theory and methods*, Springer-Verlag, New York.

Brockwell, P. J., and Davis, R. A. (1996). *Introduction to time series and forecasting*, Springer-Verlag, New York.

Chang, F-J., and Chen, L. (1998). "Real-coded genetic algorithm for rule-based flood control reservoir management." *Water Resources Management*, 12, 185–198.

Cheng, C., and Chau, K. W. (2001). "Fuzzy iteration methodology for reservoir flood control operation." *Journal of the American Water Resources Association*, 37(5), 1381–1388.

Costello, Inc. (2000). "Feasibility study for improvements to Addicks and Barker Reservoirs." *CI Job No. 19-96083-04*, prepared for the Harris County Flood Control District.

Cowpertwait, P. S. P., and O'Connell, P. E. (1992). "Naymann-Scott shot noise model for the generation of daily streamflow time series." *Advances in theoretical hydrology – A tribute to James Dooge,* J. P. O'Kane, ed., Elsevier Science, New York.

Cruise, J. F., and Singh, V. P. (1996). "A stochastic model for reservoir flood operation." *Civil Engineering Systems*, 13(2), 141–155.

Doan, J. H. (2000). "Hydrologic model of the Buffalo Bayou using GIS." *Hydrologic and hydraulic modeling support with geographic information systems,* D. R. Maidment, and D. Djokic, eds., ESRI Press, Redlands, California, 113–143.

Feldman, A. D. (1992). "Systems analysis applications at the Hydrologic Engineering Center." *Journal of Water Resources Planning and Management*, 118(3), 249–261.

Gan, T., and Beard, L. R. (1980). "Reliability of stochastic models generating hydrologic series." *Report CRWR-168*, Center for Research in Water Resources: Bureau of Engineering Research, University of Texas, Austin, Texas.

Giraitis, L., and Leipus, R. (1995). "A generalized fractionally differencing approach in long-memory modelling." *Lithuanian Mathematical Journal*, 35(1), 53–65.

Granger, C. W. J., and Joyeux, R. (1980). "An introduction to long-range time series models and fractional differencing." *Journal of Time Series Analysis*, 1, 15–30.

Green, N. M. D. (1973). "A synthetic model for daily streamflow." *Journal of Hydrology*, 20, 351–364.

Gupta, R. S. (1995). *Hydrology and hydraulic systems*, Waveland Press, Prospect Heights, Illinois.

Hasebe, M., and Nagayama, Y. (2002). "Reservoir operation using the neural network and fuzzy systems for dam control and operation support." *Advances in Engineering Software*, 33, 245–260.

Hosking, J. R. M. (1981). "Fractional differencing." *Biometrika*, 68, 165-176.

Hosking, J. R. M. (1984). "Modeling persistence in hydrological time series using fractional differencing." *Water Resources Research*, 20(12), 1898–1908.

Interagency Advisory Committee on Water Data. (1982). *Guidelines for determining flood flow frequency*, Bulletin 17B of the Hydrology Subcommittee, Office of Water Data Coordination, U.S. Geological Survey, Reston, Virginia.

Jain, S. K., Goel, M. K., and Agarwal, P. K. (1998). "Reservoir operation studies of Sabarmati System, India." *Journal of Water Resources Planning and Management*, 124(1), 31–38.

Jain, S. K., Yoganarasimhan, G. N., and Seth, S. M. (1992). "A risk-based approach for flood control operation of a multipurpose reservoir." *Water Resources Bulletin*, 28(6), 1037–1043.

Kelman, J. (1977). "Stochastic modeling of hydrologic intermittent daily processes." *Hydrology Paper No. 89*, Colorado State University, Fort Collins, Colorado.

Kelman, J. (1980). "A stochastic model for daily streamflow." *Journal of Hydrology*, 47(1– 4), 235–249.

Kokoszka, P., and Taqqu, M. S. (1996). "Parameter estimation for infinite variance fractional ARIMA." *The Annals of Statistics*, 24(5), 1880–1913.

Kottegoda, N. T. (1970). "Statistical methods for river flow synthesis for water resources assessment, with discussion." *Proceedings of the Institution of Civil Engineers*, paper 7339S, suppl. XVIII, 415–442.

Kottegoda, N. T. (1972). "Stochastic five daily stream flow model." *Journal of the Hydraulics Division*, *ASCE*, 98(HY9), 1469–1485.

Kottegoda, N. T. (1980). *Stochastic water resources technology*, John Wiley & Sons, New York.

Kron, W., Plate, E. J., and Ihringer, J. (1990). "A model for the generation of simultaneous daily discharges of two rivers at their point of confluence." *Stochastic Hydrology and Hydraulics*, 4(4), 255–276.

Krzysztofowicz, R. (2001). "The case for probabilistic forecasting in hydrology." *Journal of Hydrology*, 249(1 – 4), 2–9.

Labadie, J. W. (1997). "Reservoir system optimization models." *Water Resources Update*, 108, 83–110.

Levin, O. (1969). "Optimal control of a storage reservoir during a flood season." *Automatica*, 5, 27–34.

Ljung, G. M., and Box, G. E. P. (1978). "On a measure of lack of fit in time series models." *Biometrika*, 65, 297–303.

Marien, J. L., Damázio, J. M., and Costa, F. S. (1994). "Building flood control rule curves for multipurpose multireservoir systems using controllability conditions." *Water Resources Research*, 30(4), 1135–1144.

Matalas, N. C. (1967). "Mathematical assessment of synthetic hydrology." *Water Resources Research*, 3(4), 937–945.

Montanari, A., Longoni, M., and Rosso, R. (1999). "A seasonal long-memory stochastic model for the simulation of daily river flows." *Physics and Chemistry of the Earth (B)*, 24(4), 319–324.

Montanari, A., Rosso, R., and Taqqu, M. S. (1997). "Fractionally differenced ARIMA models applied to hydrologic time series: Identification, estimation, and simulation." *Water Resources Research*, 33(5), 1035–1044.

Murrone, F., Rossi, F., and Claps, P. (1997). "Conceptually-based shot noise modeling of streamflows at short time interval." *Stochastic Hydrology and Hydraulics*, 11(6), 483–510.

Philbrick, C. R., and Kitanidis, P. K. (1999). "Limitations of deterministic optimization applied to reservoir operations." *Journal of Water Resources Planning and Management*, ASCE, 125(3), 135–142.

Rivera-Ramírez, H. D., Warner, G. S., and Scatena, F. N. (2002). "Prediction of master recession curves and baseflow recessions in the Luquillo Mountains of Puerto Rico." *Journal of the American Water Resources Association*, 38(3), 693–704.

Salas, J. D. (1993). "Analysis and modeling of hydrologic time series." *Handbook of hydrology*, D. R. Maidment, ed., McGraw-Hill, New York.

Samorodnitsky, G., and Taqqu, M. S. (1994). *Stable non-gaussian random processes, stochastic models with infinite variance*, Chapman & Hall, New York.

Shrestha, B. P., Duckstein, L., and Stakhiv, E. Z. (1996). "Fuzzy rule-based modeling of reservoir operation." *Journal of Water Resources Planning and Management*, 122(4), 262–269.

Taqqu, M. S., and Teverovsky, V. (1998). "On estimating the intensity of long-range dependence in finite and infinite variance time series." *A practical guide to heavy tails: statistical techniques and applications*, R. Adler, R. Feldman and M. S. Taqqu, eds., Birkhäuser, Boston, 177–217.

Treiber, B., and Plate, E. J. (1977). "A stochastic model for the simulation of daily flows." *Hydrologic Science Bulletin*, 22(1), 175–192.

Tropical Storm Allison Recovery Project (TSARP). (2002a). "Tropical Storm Allison event analysis technical report: Vol. 1." <http://www.tsarp.org/tsarp_doc/index.html> (Mar. 27, 2004).

Tropical Storm Allison Recovery Project (TSARP). (2002b). "Tropical Storm Allison public report." <http://www.tsarp.org/tsarp_doc/index.html> (Mar. 27, 2004).

Tropical Storm Allison Recovery Project (TSARP). (2002c). "Using baseflow parameters with HMS in Harris County." <http://www.tsarp.org/tsarp_doc/index.html> (Mar. 27, 2004).

U.S. Army Corps of Engineers (USACE). (1959). "Reservoir regulation." *EM 1110-2-3600*, Washington, D.C.

U.S. Army Corps of Engineers (USACE). (1962). "Reservoir regulation manual for Addicks and Barker reservoirs, Buffalo Bayou watershed." USACE, Galveston District, Texas.

U.S. Army Corps of Engineers (USACE). (1977). "Hydrology, Addicks and Barker reservoirs, Buffalo Bayou and tributaries, Texas." USACE, Galveston District, Texas.

U.S. Army Corps of Engineers (USACE). (1986). "Master plan update, Addicks and Barker reservoirs, Buffalo Bayou watershed, Houston, Texas." USACE, Wilmington District, North Carolina.

U.S. Army Corps of Engineers (USACE). (1987). "Management of water control systems." *EM 1110-2-3600*, Washington, D.C.

U.S. Army Corps of Engineers (USACE). (1992). *HEC-FFA flood frequency analysis. User's manual*. Hydrologic Engineering Center, Davis, California.

U.S. Army Corps of Engineers (USACE). (1995). "Reconnaissance report, Section 216 study, Addicks and Barker reservoirs, Houston, Texas." USACE, Galveston District, Texas.

U.S. Army Corps of Engineers (USACE). (1998). *HEC-5 Simulation of flood control and conservation systems. User's manual*. Hydrologic Engineering Center, Davis, California.

U.S. Army Corps of Engineers (USACE). (2001). *HEC-HMS hydrologic modeling system. User's manual*. Hydrologic Engineering Center, Davis, California.

U.S. Army Corps of Engineers (USACE). (2003). *HEC-ResSim reservoir system simulation. User's manual*. Hydrologic Engineering Center, Davis, California.

Valdes, J. B., and Marco, J. B. (1995). "Managing reservoirs for flood control." *U.S. – Italy Research Workshop on the Hydrometeorology, Impacts, and Management of Extreme Floods*, Perugia, Italy, 1 – 13. <http://iranrivers.com/TrainandResearch/Pdf/Rivers/43valdes.pdf> (Jul. 14, 2003)

Valencia, R. D., and Schaake, J. C. (1973). "Disaggregation processes in stochastic hydrology." *Water Resources Research*, 9(3), 580–585.

Viessman, W., and Lewis, G. L. (1996). *Introduction to hydrology*, Harper Collins, New York.

Wasimi, S. A., and Kitanidis, P. K. (1983). "Real-time forecasting and daily operation of a multireservoir system during floods by linear quadratic Gaussian control." *Water Resources Research*, 19(6), 1511–1522.

Weiss, G. (1977). "Shot noise models for synthetic generation of multisite daily streamflow data." *Water Resources Research*, 13(1), 101–108.

Willis, R., Finney, B. A., and Chu, W. (1984). "Monte Carlo optimization for reservoir operation." *Water Resources Research*, 20(9), 1177–1182.

Windsor, J. S. (1973). "Optimization model for the operation of flood control systems." *Water Resources Research*, 9(5), 1219–1226.

Wurbs, R. A. (1993). "Reservoir-system simulation and optimization models." *Journal of Water Resources Planning and Management*, 119(4), 455–472.

Wurbs, R. A. (1996). *Modeling and analysis of reservoir system operations*, Prentice Hall PTR, Upper Saddle River, New Jersey.

Wurbs, R. A. (2002). "State-frequency analyses for urban flood control reservoirs." *Journal of Hydrologic Engineering*, 7(1), 35–42.

Wurbs, R. A., and James, W. P. (2002). *Water resources engineering*, Prentice Hall, Upper Saddle River, New Jersey.

Wurbs, R. A., Tibbets, M. N., Cabezas, L. M., and Roy, L. C. (1985). "State-of-the-art review and annotated bibliography of systems analysis techniques applied to reservoir operation." *Technical Report 136*, Texas Water Resources Institute, College Station, Texas.

Xu, Z., X., Schumann, A., and Brass, C. (2001a). "Markov autocorrelation pulse model for two sites daily streamflow." *Journal of Hydrologic Engineering*, 6(3), 189–195.

Xu, Z. X., Schumann, A., Brass, C., Li, J., and Ito, K. (2001b). "Chain-dependent Markov correlation pulse model for daily streamflow generation." *Advances in Water Resources*, 24(5), 551–564.

Xu, Z. X., Schumann, A., and Li, J. (2003). "Markov cross-correlation pulse model for daily streamflow generation at multiple sites." *Advances in Water Resources*, 26(3), 325–335.

Yeh, W. W-G. (1985). "Reservoir management and operations models: A state-of-the-art review." *Water Resources Research*, 21(12), 1797–1818.

VITA

HECTOR DAVID RIVERA RAMIREZ

Urb. Casamia
5116 Calle Zorzal
Ponce, P.R. 00728-3404

EDUCATION

Ph.D., Civil Engineering. Texas A&M University, College Station, Texas. (December 2004)

M.S., Natural Resources Management: Land, Water and Air. University of Connecticut, Storrs, Connecticut. (May 1999)

B.S., Environmental Science. Universidad de Puerto Rico, Rio Piedras, Puerto Rico. (May 1997)

WORK EXPERIENCE

Lockwood, Andrews, and Newnam, Inc., Houston, Texas. Civil Engineer (May 2004 – Present)

Texas A&M University, College Station, Texas. Research Assistant (1999 – 2004)

University of Connecticut, Storrs, Connecticut. Research Assistant (1997 – 1999)

U.S. Bureau of Reclamation, Boulder City, Nevada. Intern (January – May 1997)

U.S. Bureau of Reclamation, Billings, Montana. Intern (June – August 1996)

PUBLICATIONS

- Rivera-Ramírez, H. D., Warner, G. S., and Scatena, F. N. (2002). "Prediction of master recession curves and baseflow recessions in the Luquillo Mountains of Puerto Rico." *Journal of the American Water Resources Association*, 38(3), 693–704
- Rivera-Ramírez, H. D., and Wurbs, R. A. (2004). "Flood control reservoir operations for conditions of limited storage capacity." *Proceedings of Fall 2004 Conference*, Texas Section, American Society of Civil Engineers, Houston, Texas.